Summer 2022

APPLICATION OF MOLECULAR TOOLS TO ASSESS TOXICITY IN INDUSTRIAL WASTEWATER AND TRACK VIRAL PATHOGENS IN MUNICIPAL WASTEWATERS

Mina Aghababaei Shahrestani
University of New Hampshire

APPLICATION OF MOLECULAR TOOLS TO ASSESS TOXICITY IN INDUSTRIAL WASTEWATER AND TRACK VIRAL PATHOGENS IN MUNICIPAL WASTEWATERS

BY

MINA AGHABABAEI SHAHRESTANI

B.Sc. Isfahan University of Technology, 2010

M.Sc. Shahid Beheshti University, 2013

DISSERTATION

Submitted to the University of New Hampshire

in Partial Fulfillment of

the Requirements for the Degree of

Doctor of Philosophy

In

Civil and Environmental Engineering

September, 2022

This dissertation has been examined and approved in partial fulfillment of the requirements for the degree of Doctor of Philosophy in Civil and Environmental Engineering by:

Dissertation Director, Dr. Paula J. Mouser
Associate Professor of Civil and Environmental Engineering

Dr. James P. Malley Jr.
Professor of Civil and Environmental Engineering

Dr. Nancy E. Kinner
Professor of Civil and Environmental Engineering

Dr. Louis Tisa
Professor of Microbiology and Genetics

Dr. Jenna L. Luek
Chemist at Portsmouth Naval Shipyard

On June 23th, 2022

Original approval signatures are on file with the University of New Hampshire Graduate School.

To my parents, Zohreh and Ali, for their endless love, support and encouragements.

To my sister, Maryam, for her wisdom, patience and love.

To my brother, Mohammad, for his advice, support and love.

"*Never give up, for that is just the place and time that the tide will turn.*"

- Harriet Beecher Stowe

Acknowledgements

I would like to express my sincere gratitude to my dissertation advisor, Dr. Paula J. Mouser for the continuous support, guidance, and dedication. She supported my doctoral research and molded me into the researcher I am today. My appreciation and respect for her are unquantifiable. I would like to acknowledge my committee members, Dr. James P. Malley, Dr. Nancy E. Kinner, Dr. Louis Tisa and Dr. Jenna L. Luek for their valuable time, encouragement, insightful comments which helped me to improve the quality of my dissertation research.

I would like to extend my appreciation to Dr. Jishnu Adhikari, Dr. Fabrizio Colosimo and Dr. Jenna L. Luek for their continued support and encouragement. I cannot express my gratitude enough for dedicating your time to advise me throughout my doctoral research. Thank you to my friends and colleagues who supported this dissertation research: Chika Ugwuodo, Sydney Adams, Carmela Antonellis, Alexandria Hidrovo, Katie Morsefield, Cassidy Yates, Taler Bixler, Emily Wilcox, Aaron Kearnan, Dr. Melissa Gloekler, Dr. Rachel Coleman and Dr. Radhika Bartaula. Thank you for your continuous support and constantly reminding me of the bigger picture. I would like to also thank Kellen Sawyer whose support helped me endure even the toughest times in my doctoral research.

Additionally, I would like to thank my friends specially Dr. Shokoufeh Zargar, Dr. Pegah Jarast, Hoda Vakili and Nella Jahan for their understanding, encouragement and friendship in my many moments of crisis. Your friendship makes my life a wonderful experience.

Lastly, I would like to express my deepest gratitude and appreciation to my phenomenal family for providing me the much needed support, love and encouragement, to pursue my dreams and to complete this challenging endeavor.

Funding for this research was provided by the National Science Foundation (CBET award no. 1823069), New Hampshire Sea Grant Development Funds and a Summer Teaching Assistant Fellowship (STAF) from the Graduate School at the University of New Hampshire.

Abstract

Wastewater is a complex matrix containing a wide range of microorganisms and chemical compounds. For public health purposes, it is critical to monitor for harmful microorganisms and evaluate the toxicity of chemicals present in industrial and municipal wastewaters on human and ecosystem health. Over the past decade, sophisticated technologies such as high-throughput sequencing have enabled the development of molecular tools, which are now widely employed for tracking pathogens and assessing toxicity of municipal and industrial wastewaters. Molecular tools for biomonitoring of wastewater are designed to target specific microbial biomarkers including nucleic acids, proteins and antigens. Accordingly, this dissertation applied molecular tools to characterize water quality and assess the occurrence of pathogens for improved management of industrial and municipal wastewater.

Chapter 2 quantifies toxicity of wastewater generated from hydraulically fractured natural gas wells**.** My research involved adapting two toxicity microassays, a broad spectrum BioLuminescence Inhibition Assay (BLIA) employing the halotolerant bacterium *Aliivibrio fischeri,* and a specific cytotoxicity N-acetylcysteine (NAC) thiol reactivity assay to quantify toxicity of flowback and produced water (FPW) after hydraulic fracturing. My results suggested that both acute toxicity and thiol reactivity diminished with time after fracturing and were influenced by specific chemical additives in the wastewater, as opposed to sample fraction (solids vs liquid), or shale formation.

In Chapter 3, I assessed concentrations of SARS-CoV-2 genetic material (N1 and N2) in both liquid and solids wastewater samples from seven coastal New England treatment facilities. My work shows that municipal wastewater treatment facilities efficiently remove SARS-CoV-2 from

effluent, with the greatest removal from the liquid phase after secondary clarification. Viral particles were found at lower levels in wastewater sampled post-secondary treatment and were below detection after disinfection, compared to the primary-treated wastewater. Sludge samples had the highest concentrations, suggesting affinity of the viral genetic material toward the solids.

In Chapter 4, I compared temporal trends of SARS-CoV-2 RNA biomarker signals on a small university campus (UNH Durham) versus biomarker signals for the broader Durham community before, during, and post-vaccination. My results revealed that COVID-19 vaccine administration resulted in a significant decrease in SARS-CoV-2 biomarker concentrations in wastewater concurrent with decreasing number of COVID-19 infections in the community. When new variants emerged, a significant increase in SARS-CoV-2 biomarker concentration occurred in the wastewater parallel with increasing number of COVID-19 infections in the UNH community.

Taken together, this dissertation demonstrates that molecular tools optimized for wastewater from both municipal and industrial sources can effectively be used for assessing temporal trends in toxicity and pathogen prevalence to provide early detection and mitigate human health risks.

Table of Contents

List of Tables

List of Figures

Chapter 1: Introduction

1.1 Molecular tools for industrial and municipal wastewater

For public health purposes, it is important to monitor the microbial composition and abundance in industrial and municipal wastewater before discharge into the environment or reuse. Wastewater is typically a complex matrix containing diverse array of microorganisms including bacteria, fungi and viruses. Some of these microbes often found in wastewater are plant, animal and human pathogens. Untreated wastewater could, therefore, be a vehicle for the transmission of these pathogens. Several decades ago, culture-based techniques were predominantly used for wastewater biomonitoring. However, with the advent and advancement of sophisticated technology, such as high-throughput sequencing, molecular tools have taken over since they are more accurate and less time consuming.

Molecular tools are technologies which are applied to target certain biomarkers to characterize microbial community composition and processes relevant to the environment of interest (Rastogi and Sani, 2011). Commonly targeted biomarkers include nucleic acid sequences, proteins, peptides and lipids as well as bacteria. Depending on the biomarker of interest, several molecular tools have been devised, most of which have been applied to monitor industrial and municipal wastewater at different scales (Malik et al., 2008). A few of these will be described in this section and fall under major categories including techniques for microbial community fingerprinting, nucleic acid hybridization-based tools, and toxicity assays.

1.1.1 Techniques for microbial community fingerprinting

Fingerprinting is the targeting and amplification of a particular genomic region, mostly for microbial identification. Fingerprinting-based techniques make it possible to know what microbes are present in the wastewater, enabling easy identification of pathogens of interest. The most commonly used amplification technique is the polymerase chain reaction (PCR) a method used to produce multiple copies of a given segment of nucleic acid (Rahman et al., 2013). Some of the PCR-based fingerprinting tools include random amplification of polymorphic DNA (RAPD), denaturing or temperature gradient gel electrophoresis (DGGE or TGGE), amplified ribosomal DNA restriction analysis (ARDRA), terminal restriction fragment length polymorphism (T-RFLP), ribosomal intergenic spacer analysis (RISA) and single-strand conformation polymorphism (SSCP) (Urrea-Valencia et al., 2021). Urrea-Valencia et al., (2021) provide a detailed review of these approaches. All of these techniques have been applied to biomonitoring of both municipal and industrial wastewaters.

Each of these tools have their advantages and disadvantages. For instance, amplified ribosomal DNA restriction analysis (ARDRA) is fast, simple and accurate (Błaszczyk et al., 2011;Sarti et al., 2012;Princy et al., 2020), but has lower discriminatory power compared to other techniques such as denaturing gradient gel electrophoresis (DDGE) (Silveira et al., 2021) and single-strand conformation polymorphism (SSCP) (Braun et al., 2011). In addition, while random amplification of polymorphic DNA (RAPD) is cheap and does not require prior knowledge, it is not the most reproducible and demands stringent PCR standardizations (Urrea-Valencia et al., 2021).

1.1.2 Nucleic-acid hybridization-based tools

Hybridization involves the interaction between labelled single-stranded nucleic probes and their complementary targets. This enables the accurate detection and quantification of specific sequences on nucleic acids, including gene abundance (mRNAs). Hybridization-based tools which have been applied to the monitoring of industrial and municipal wastewater include fluorescent in situ hybridization (FISH), microarray and quantitative PCR (Urrea-Valencia et al., 2021). Approaches used for these techniques vary, but the end product is similar including detection and possible quantification of specific gene targets. FISH involves the hybridization of a complementary probe to a target gene (e.g. ammonia oxidizers), for taxon-resolved identification of active microbial community members (Amann et al., 1995;Felske et al., 1998). Microarray technologies make it possible to track gene expression and abundance (DNA or RNA) in microbes in wastewater for easy functional characterization (Lucchini et al., 2001).

Quantitative PCR targets and counts the number of copies of a particular nucleic acid sequence (biomarker) present in the wastewater (Smith and Osborn, 2009). Quantitative PCR technologies have evolved over the years. Regular qPCR makes use of an intercalating dye to count oligonucleotide incorporation for amplicon synthesis (Taylor et al., 2010). However, newer quantitative PCR technologies have emerged, including the digital droplet PCR (ddPCR). ddPCR combines microfluidics and surfactant chemistries to very accurately count the copies of specific biomarkers in wastewater or other matrices (Suo et al., 2020). Its accuracy lies in the droplet generation step, whereby the samples are divided into several tiny water-in-oil droplets amplified via PCR, the implication of which is greater detection of target genes. ddPCR has been the standard

(CDC-recommended) technique since the COVID-19 pandemic for quantifying SARS-CoV-2 RNA biomarkers in municipal wastewater (Suo et al., 2020).

To detect and quantify pathogens in municipal and industrial wastewaters, certain biomarkers are targeted by molecular tools, some of which were reviewed above. Most of the molecular tools and approaches target nucleic acid materials (DNA or RNA). Other less targeted biomarkers for pathogens include proteins and antigens (Cui et al., 2021). For microbial community composition analysis, the 16S rRNA gene is often targeted by sequencing-based methods (fingerprinting). This biomarker is ideal for microbial identification being a conserved region in the microbial genome. By targeting the 16S rRNA gene, it is possible to characterize the microbial community (bacteria and archaea) present in municipal and industrial wastewaters (Guo et al., 2013). Pathogens in wastewater are also identified by targeting antibiotic resistance DNA or RNA biomarkers. There are a growing number of antibiotic resistance (AR) genes targeted in pathogens (Hong et al., 2018). In some cases, these genes are carried on mobile genetic elements (MGEs) such as plasmids (Rahube and Yost, 2010). Several tools are designed to meet specific pathogen biomonitoring needs.

For SARS-CoV-2, the new coronavirus responsible for the current global pandemic, the biomarkers targeted by CDC-approved molecular approaches are the N1 and N2 regions of viral genome. Both genes are segments of the viral RNA coding the synthesis of nucleocapsid proteins. Using hybridization-based molecular tools, such as digital droplet PCR (ddPCR), it is possible to precisely and accurately count copies of these biomarkers in wastewater (Suo et al., 2020).

1.1.3 Toxicity assessment of wastewater

In addition to microorganisms, industrial and municipal wastewaters contain a diverse array of chemical compounds, some of which are toxic to plants, animals and humans. The toxicity of wastewater depends on a number of factors including source and environmental conditions. For instance, wastewater from pharmaceutical industries will considerably differ in chemical composition and toxicity from effluents generated by a textile manufacturing plant. Similarly, the constituents of municipal wastewater will depend on several demographic factors and the sewer system design. However, in general, toxic compounds commonly found in wastewaters include organic chemicals (including antibiotics and pharmaceutical care products) (Hena et al., 2021) and inorganic trace elements (including heavy metals and radioactive compounds) (Linstedt et al., 1971). Wastewater from a hydraulically fractured shale well contains a number of toxic compounds including dissolved organic carbon, salinity, solids content, heavy metals as well as radioactive elements (Vengosh et al., 2014;Lauer et al., 2016;He et al., 2018).

There are tools and techniques devised to assess the physicochemical properties and toxicity of municipal and industrial wastewaters. These techniques could fall under two broad categories, whole-organism assay and *ex-vivo* approaches. Several whole organisms assays include microbes and aquatic species that are used to assess adverse outcomes of toxic chemicals. One very common whole-organism approach is Bioluminescence Inhibition Assay (BLIA) using the marine bacterium, *Allivibrio fischeri*. In this technique, the ability of wastewater samples to inhibit bioluminescence is evaluated (Hull et al., 2018;Aghababaei et al., 2021). In principle, the toxicity of wastewater is positively correlated to bioluminescence inhibition. The *ex-vivo* approaches do not involve the use of whole-organisms. A notable example is the N-acetyl cysteine (NAC) thiol

reactivity assay which assess the interaction between toxic compounds and biological thiol compounds. This assay increasingly has been employed to detect the toxicants that are reactive with biological thiols in the series of water and wastewater samples (Dong et al., 2018b;Dong et al., 2019;Aghababaei et al., 2021).

Using these molecular tools, this dissertation sought to characterize toxicity and pathogen prevalence in two types of wastewater. The first system studied was wastewaters generated from hydraulically fractured natural gas wells across a range of complex and variable flowback and produced water (FPW) matrices. The second system was municipal wastewaters to assess concentrations of SARS-CoV-2 genetic material (N1 and N2) in both liquid and solid phases of wastewater samples. These systems and our approach are described below.

1.2 Hydraulic fracturing wastewater

There is a growing environmental concern regarding the effects of hydraulic fracturing processes on the environment (Boudet et al., 2014;Theodori et al., 2014;Gehman et al., 2016). Highly pressurized fluids (<69000 kPa) are pumped into wells during hydraulic fracturing to release hydrocarbons from geologic formations (Figure 1.1) (Burden et al., 2016). The composition of the injected fluid is complex and specific to each well. Injected fluids are generally composed of proppants (sand/ceramic beads), biocides, gelling and foaming agents, pH adjustors, clay stabilizers, and surfactants (Arthur et al., 2009;Elsner and Hoelzer, 2016). The mixtures eventually return to the surface, where they are referred to as flowback and produced water. This unconventional natural gas wastewater consists of the initially injected fluid (30-80% by volume) (Alessi et al., 2017) and formation-derived brine. Flowback generally refers to the injected fluid

that returns within the first few days, whereas produced water returns after spending several weeks to months within the shale formation, taking on characteristics of brine (King, 2012;Barbot et al., 2013). It is estimated that 5200-25,870 m^3 of FPW per horizontal well are generally produced during shale gas extraction (Kondash and Vengosh, 2015), resulting in a large volume of industrial wastewater requiring management.

Spills of FPW can result in surface and groundwater contamination that negatively affect freshwater invertebrate and fish populations. This results in long-term environmental pollution issues within the aquatic ecosystem (Vidic et al., 2013;Warner et al., 2013). Millions of gallons of

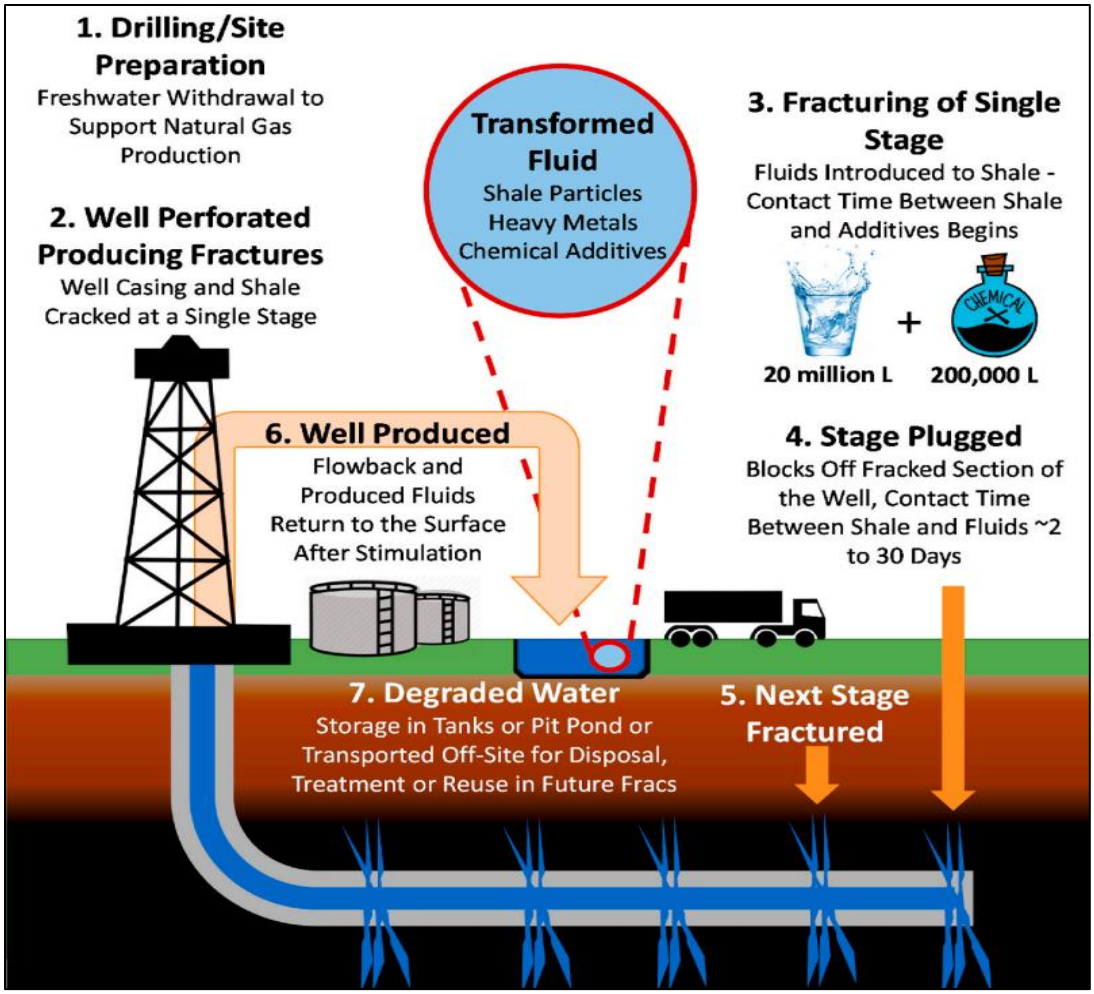

Figure 1.1. Schematic of the hydraulic fracturing process (Manz et al., 2021).

FPW have been accidentally released into the environment due to well integrity issues, on-site fluid handling accidents, or spills during transportation to disposal wells in the United States and Canada (Warner et al., 2013;Patterson et al., 2017).

A study on the potential risk for contamination associated with wastewater disposal from hydraulic fracturing in the Marcellus Shale revealed that municipal wastewater treatment plants lack the capacity to deal with the composition and large volume of the wastewater produced (Rozell and Reaven, 2012). Assessing the toxicity of hydraulic fracturing wastewater is challenging due to its highly complex organic carbon and saline matrix.

1.2.1 Toxicity of hydraulic fracturing wastewater

As the practice of hydraulic fracturing for oil and gas extraction continues to grow, the potential of environmental contamination from FPW release events will also increase (Entrekin et al., 2011;Goss et al., 2015;Alessi et al., 2017). Several recent studies have reported a range of toxicological effects of the complex FPW mixture on vertebrates, invertebrates, fishes and human cells including liver and kidney cells (Kassotis et al., 2014;Payne et al., 2014;Kassotis et al., 2016b;Chen and Carter, 2017;Crosby et al., 2018), rat (Ishikawa et al., 2016), mice (Kassotis et al., 2016a), Daphnia (Blewett et al., 2017a;Delompré et al., 2019a), rainbow trout (Blewett et al., 2017b;He et al., 2017b;Delompré et al., 2019b) and zebrafish (Christen et al., 2017;Folkerts et al., 2017a;He et al., 2017a;Majumdar et al., 2018). Many of these toxicological effects have been associated with the sediment and organic chemical constituents present in FPW. The above referenced studies have determined that organic compounds (e.g., polycyclic aromatic hydrocarbons (PAHs)), are one of the main contributors to the toxicity observed in each species exposed to FPW samples. However, to date, knowledge is very limited regarding the possible

toxicological impact of FPW spills on human and ecosystem health. There is, therefore, a need to investigate the toxicity of field collected FPW samples on human and ecosystem health.

It is necessary to investigate the environmental impact of different FPW samples with various physicochemical characteristics that result from varying target geologic formations and considering the FPW sampling time from the wellhead with respect to the flowback start time. Freshwater organisms serve as an important exposure toxicological model for human and environmental health (Folkerts et al., 2017a;b). The prominent finding of the recent studies on FPW toxicity is that the salinity component of the hydraulic fracturing wastewater is a primary mechanistic mode of toxicity for exposed freshwater organisms compared to other potentially harmful chemical compounds. The salt content of FPW samples (up to 240 ppt) can be far beyond the salinity of seawater (~33 ppt), and hence, represents a significant challenge to freshwater organisms. The high salt content of FPW can disrupt the optimal ionic balance in the freshwater organism, quickly leading to toxicity (Blewett et al., 2017a;Blewett et al., 2017b;Delompré et al., 2019a).

The high salt content of FPW samples (up to 240 ppt) (He et al., 2017a) necessitates the selection of an appropriate bioassay for determining other inhibitory effects beyond salinity without excessive dilution. One such bioassay previously reported is the *Aliivibrio fischeri* (*A. fischeri*) bioluminescence assay (Hull et al., 2018;Parmaki et al., 2018;Aghababaei et al., 2021). This has the advantage of high sensitivity to a broad range of environmental contaminants. Another important factor for toxicity studies of complex FPW samples is the identification of additive toxicants which might adversely affect human and ecological health. The N-acetyl-L-cysteine (NAC) thiol reactivity assay has been previously employed to detect the toxicants that are reactive with biological thiols in a series of water and wastewater samples (Pals et al., 2016;Dong et al.,

2018a;Dong et al., 2018b;Dong et al., 2019;Aghababaei et al., 2021). Employing these analytical biological assays could provide direct comparison of composite toxicity through time or across geographic sampling locations.

1.3 SARS-CoV-2 viral RNA in wastewater treatment plants

SARS-CoV-2, the virus that causes COVID-19 disease, is shed in human stool from infected individuals. Within the framework of the COVID-19 pandemic, an early warning and surveillance system using a Wastewater-Based Epidemiology (WBE) approach has helped advance our understanding of the emergence and epidemiology of COVID-19 virus around the world. Increasing prevalence of COVID-19 in the population, therefore, increases the viral load in wastewater treatment plants (WWTPs) serving communities. Several studies have reported the detection of SARS-CoV-2 in wastewater around the world (Kumar et al., 2021;Mohan et al., 2021;Westhaus et al., 2021;Wurtzer et al., 2021). However, the fate of the virus in the treatment train is unknown. Thus, there is a critical need to collect information about the efficacy of our engineered facilities to remove this novel coronavirus, especially considering that a varied spectrum of removal is expected depending on population infection rate, the treatment facility design, and the disinfection approach. Confirmation that viral genetic material is removed prior to effluent discharge and further knowledge on potential sinks of the virus within the treatment train (e.g., sludge, liquids) is critical to minimize routes of exposure, and to inform public health responses. It is important to investigate the impact of solids content and the presence of micropollutants on the stability and survival of COVID-19 virus when present in primary-treated wastewater compared to secondary-treated wastewater.

To date, only a few studies have assessed viral RNA removal during the key treatment stages of a wastewater treatment process (Figure 1.2) (Haramoto et al., 2020;Randazzo et al., 2020;Sherchan et al., 2020). Furthermore, there is scarce data available regarding the decay of SARS-CoV-2 RNA present during the sludge treatment process (e.g., activated sludge, waste activated sludge, digested sludge) (Kocamemi et al., 2020;Abu Ali et al., 2021;Balboa et al., 2021;Bhattarai et al., 2021;Serra-Compte et al., 2021;Westhaus et al., 2021).

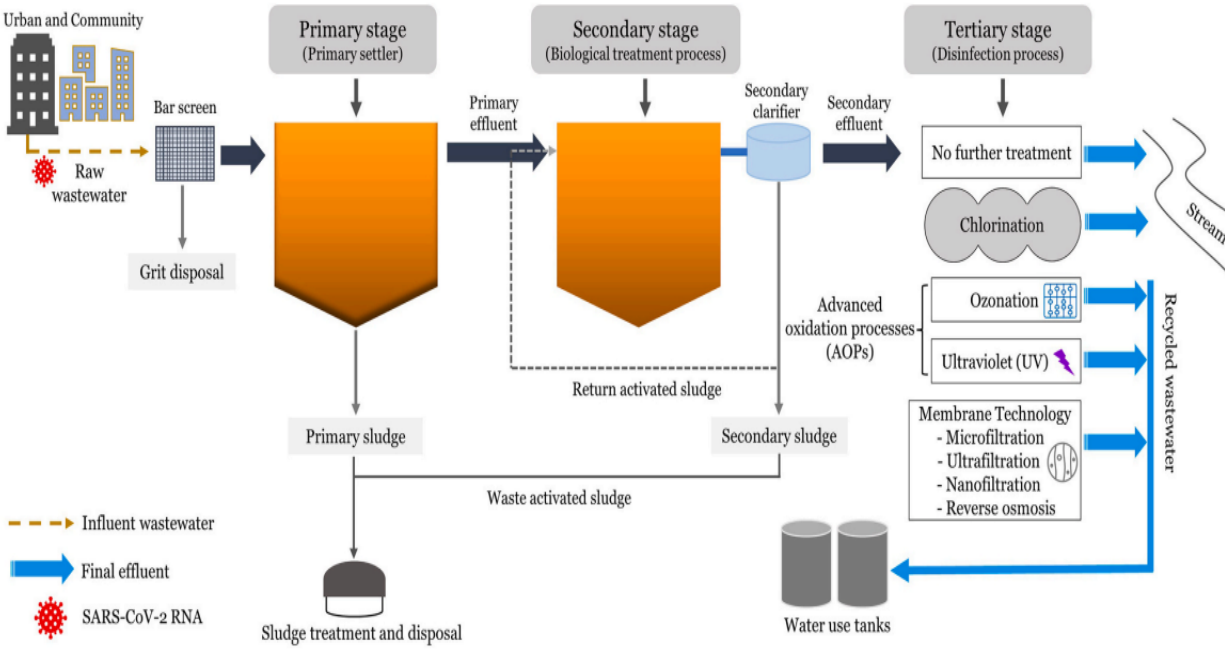

Figure 1.2. Schematics of wastewater treatment stages in WWTPs (Sangkham, 2021).

The majority of the existing studies are focused on comparison of SARS-CoV-2 genetic material loads in the liquid phase and very little attention has been paid to their fate in the solid phase of wastewater (Kocamemi et al., 2020;Peccia et al., 2020).

There is a long history of the practice of environmental surveillance to monitor the circulation of a wide range of viruses such as rotavirus, norovirus, adenovirus, hepatitis A virus as well as wild and vaccine strains of poliovirus in human populations (Metcalf et al., 1995;Matthijnssens et al., 2009;Blanco Fernández et al., 2012;Hovi et al., 2012;Lodder et al., 2012;Battistone et al., 2014;Majumdar et al., 2018;Wang et al., 2020). These studies indicated that with the introduction of vaccines, the total number of hospitalizations due to viral infections (e.g. rotavirus, norovirus, adenovirus, poliovirus, hepatitis A virus) and the biomarker signals in wastewater were significantly diminished (Matthijnssens et al., 2009;Blanco Fernández et al., 2012;Hovi et al., 2012;Lodder et al., 2012;Battistone et al., 2014;Majumdar et al., 2018;Wang et al., 2020). Additionally, these studies demonstrated a large fluctuation in the strain distribution of viruses from different geographical locations, years after the introduction of vaccines (Fumian et al., 2011;Bucardo and Nordgren, 2015). This necessitates studies to use WBE to evaluate the efficacy of vaccines and to detect new strains of viruses circulating in the community through wastewater-based epidemiology.

Importantly, the effectiveness of vaccines on the shedding of SARS-CoV-2 RNA, including the mRNA vaccines (e.g., Pfizer-BioNTech, Moderna), remains unknown and difficult to predict. Therefore, it is necessary to consider a long-term environmental surveillance plan for SARS CoV-2 RNA in untreated sewage to identify the effects of the vaccination program on viral shedding.

Recent literature demonstrated that SARS-CoV-2 RNA concentrations in wastewater predict the COVID-19 case trends by as much as a week (Medema et al., 2020;McClary-Gutierrez et al., 2021). Prior to the COVID-19 pandemic, WBE had been applied at university campuses to detect illicit drugs in various settings (Zuccato et al., 2017;Lemas et al., 2021;Montgomery et al., 2021). As universities started reopening for the 2020-2021 academic year; wastewater surveillance was

primarily used to manage COVID-19 at university campuses (Figure 1.3) across the United States (Betancourt et al., 2021;Corchis-Scott et al., 2021;Gibas et al., 2021;Harris-Lovett et al., 2021;Scott et al., 2021;Fahrenfeld et al., 2022;Sweetapple et al., 2022) including the University of New Hampshire (UNH).

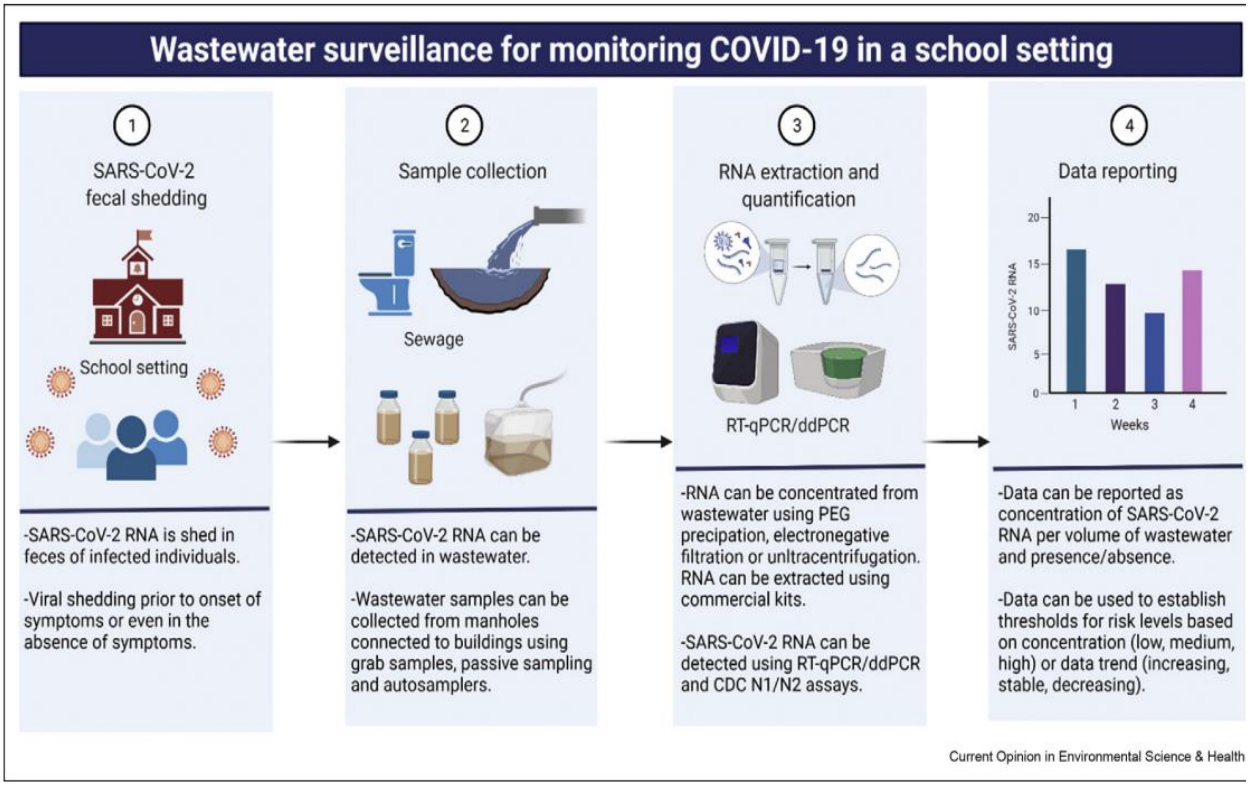

Figure 1.3. Technical framework for COVID-19 wastewater surveillance in a university campus setting (Kapoor et al., 2022).

As universities re-opened their campuses to in-person education, there was a critical need to consider a long-term environmental surveillance plan for SARS CoV-2 in untreated sewage to identify the effects of the vaccination program on circulating strains among local communities. To date, there is only one study that looked at temporal changes in SARS-CoV-2 biomarker load before and after introduction of vaccines in the untreated sewage (Bivins and Bibby, 2021).

1.4 Research objectives

My dissertation applies molecular tools to characterize water quality and pathogens for improved management of industrial and municipal wastewaters.

There are three research objectives in this dissertation:

1. Quantify toxicity of wastewaters generated from hydraulically fractured natural gas wells across a range of dissolved organic carbon concentrations, salinity, and solids content using BioLuminescence Inhibition Assay (BLIA) employing the halotolerant bacterium *Aliivibrio fischeri* for broad spectrum toxicity assessment, and utilizing a N-acetylcysteine (NAC) thiol reactivity assay for specific human cytotoxicity assessment;
2. Assessing removal efficacy of SARS-CoV-2 in New England wastewater treatment plants that differ in their treatment processes using the CDC SARS-CoV-2 assay to target two regions of the SARS-CoV-2 nucleocapsid (N) gene (N1 and N2), and the human RP gene (RP);
3. Studying the temporal trends of SARS-CoV-2 biomarker presence at Durham WWTP as a function of changes in community size and membership in a longer duration study to understand the actual effect of mass-scale vaccination, the seasonal variation of SARS-CoV-2 virus and the new strains in untreated sewage using the CDC SARS-CoV-2 assay.

These objectives are addressed in Chapters 2, 3 and 4, respectively. Chapter 5 summarizes the major findings of my work and provides suggestions on future work in these areas.

1.5 References

Abu Ali, H., Yaniv, K., Bar-Zeev, E., Chaudhury, S., Shagan, M., Lakkakula, S., Ronen, Z., Kushmaro, A., and Nir, O. (2021). Tracking SARS-CoV-2 RNA through the wastewater treatment process. *ACS ES&T Water* 1**,** 1161-1167.

Aghababaei, M., Luek, J.L., Ziemkiewicz, P.F., and Mouser, P.J. (2021). Toxicity of hydraulic fracturing wastewater from black shale natural-gas wells influenced by well maturity and chemical additives. *Environmental Science: Processes & Impacts* 23**,** 621-632.

Alessi, D.S., Zolfaghari, A., Kletke, S., Gehman, J., Allen, D.M., and Goss, G.G. (2017). Comparative analysis of hydraulic fracturing wastewater practices in unconventional shale development: Water sourcing, treatment and disposal practices. *Canadian Water Resources Journal/Revue canadienne des ressources hydriques* 42**,** 105-121.

Amann, R.I., Ludwig, W., and Schleifer, K.-H. (1995). Phylogenetic identification and in situ detection of individual microbial cells without cultivation. *Microbiological reviews* 59**,** 143-169.

Arthur, J.D., Bohm, B.K., and Cornue, D. (Year). "Environmental considerations of modern shale gas development", in: *SPE annual technical conference and exhibition*: OnePetro).

Balboa, S., Mauricio-Iglesias, M., Rodriguez, S., Martínez-Lamas, L., Vasallo, F.J., Regueiro, B., and Lema, J.M. (2021). The fate of SARS-COV-2 in WWTPS points out the sludge line as a suitable spot for detection of COVID-19. *Science of the Total Environment* 772**,** 145268.

Barbot, E., Vidic, N.S., Gregory, K.B., and Vidic, R.D. (2013). Spatial and temporal correlation of water quality parameters of produced waters from Devonian-age shale following hydraulic fracturing. *Environmental science & technology* 47**,** 2562-2569.

Battistone, A., Buttinelli, G., Fiore, S., Amato, C., Bonomo, P., Patti, A.M., Vulcano, A., Barbi, M., Binda, S., and Pellegrinelli, L. (2014). Sporadic isolation of Sabin-like polioviruses and high-level detection of non-polio enteroviruses during sewage surveillance in seven Italian cities, after several years of inactivated poliovirus vaccination. *Applied and environmental microbiology* 80**,** 4491-4501.

Betancourt, W.Q., Schmitz, B.W., Innes, G.K., Prasek, S.M., Brown, K.M.P., Stark, E.R., Foster, A.R., Sprissler, R.S., Harris, D.T., and Sherchan, S.P. (2021). COVID-19 containment on

a college campus via wastewater-based epidemiology, targeted clinical testing and an intervention. *Science of The Total Environment* 779**,** 146408.

Bhattarai, B., Sahulka, S.Q., Podder, A., Hong, S., Li, H., Gilcrease, E., Beams, A., Steed, R., and Goel, R. (2021). Prevalence of SARS-CoV-2 genes in water reclamation facilities: From influent to anaerobic digester. *Science of the Total Environment* 796**,** 148905.

Bivins, A., and Bibby, K. (2021). Wastewater surveillance during mass COVID-19 vaccination on a college campus. *Environmental Science & Technology Letters* 8**,** 792-798.

Blanco Fernández, M., Torres, C., Riviello-López, G., Poma, H., Rajal, V., Nates, S., Cisterna, D., Campos, R., and Mbayed, V. (2012). Analysis of the circulation of hepatitis A virus in Argentina since vaccine introduction. *Clinical Microbiology and Infection* 18**,** E548-E551.

Błaszczyk, D., Bednarek, I., Machnik, G., Sypniewski, D., Sołtysik, D., Loch, T., and Gałka, S. (2011). Amplified ribosomal DNA restriction analysis (ARDRA) as a screening method for normal and bulking activated sludge sample differentiation. *Polish J Environ Stud* 20**,** 29-36.

Blewett, T.A., Delompré, P.L., He, Y., Folkerts, E.J., Flynn, S.L., Alessi, D.S., and Goss, G.G. (2017a). Sublethal and reproductive effects of acute and chronic exposure to flowback and produced water from hydraulic fracturing on the water flea Daphnia magna. *Environmental science & technology* 51**,** 3032-3039.

Blewett, T.A., Weinrauch, A.M., Delompré, P.L., and Goss, G.G. (2017b). The effect of hydraulic flowback and produced water on gill morphology, oxidative stress and antioxidant response in rainbow trout (Oncorhynchus mykiss). *Scientific reports* 7**,** 1-11.

Boudet, H., Clarke, C., Bugden, D., Maibach, E., Roser-Renouf, C., and Leiserowitz, A. (2014). "Fracking" controversy and communication: Using national survey data to understand public perceptions of hydraulic fracturing. *Energy Policy* 65**,** 57-67.

Braun, F., Hamelin, J., Gévaudan, G., and Patureau, D. (2011). Development and application of an enzymatic and cell flotation treatment for the recovery of viable microbial cells from environmental matrices such as anaerobic sludge. *Applied and environmental microbiology* 77**,** 8487-8493.

Bucardo, F., and Nordgren, J. (2015). Impact of vaccination on the molecular epidemiology and evolution of group A rotaviruses in Latin America and factors affecting vaccine efficacy. *Infection, Genetics and Evolution* 34**,** 106-113.

Burden, S., Fleming, M., Frithsen, J., Hills, L., Klewicki, K., and Knightes, C. (2016). Hydraulic fracturing for oil and gas: Impacts from the hydraulic fracturing water cycle on drinking water resources in the United States. *Washington, DC: US EPA.*

Chen, H., and Carter, K.E. (2017). Modeling potential occupational inhalation exposures and associated risks of toxic organics from chemical storage tanks used in hydraulic fracturing using AERMOD. *Environmental Pollution* 224**,** 300-309.

Christen, V., Faltermann, S., Brun, N.R., Kunz, P.Y., and Fent, K. (2017). Cytotoxicity and molecular effects of biocidal disinfectants (quaternary ammonia, glutaraldehyde, poly (hexamethylene biguanide) hydrochloride PHMB) and their mixtures in vitro and in zebrafish eleuthero-embryos. *Science of the Total Environment* 586**,** 1204-1218.

Corchis-Scott, R., Geng, Q., Seth, R., Ray, R., Beg, M., Biswas, N., Charron, L., Drouillard, K.D., D'souza, R., and Heath, D.D. (2021). Averting an Outbreak of SARS-CoV-2 in a University Residence Hall through Wastewater Surveillance. *Microbiology spectrum* 9**,** e00792-00721.

Crosby, L., Tatu, C.A., Varonka, M., Charles, K.M., and Orem, W.H. (2018). Toxicological and chemical studies of wastewater from hydraulic fracture and conventional shale gas wells. *Environmental toxicology and chemistry* 37**,** 2098-2111.

Cui, L., Li, H.-Z., Yang, K., Zhu, L.-J., Xu, F., and Zhu, Y.-G. (2021). Raman biosensor and molecular tools for integrated monitoring of pathogens and antimicrobial resistance in wastewater. *TrAC Trends in Analytical Chemistry* 143**,** 116415.

Delompré, P., Blewett, T., Goss, G., and Glover, C. (2019a). Shedding light on the effects of hydraulic fracturing flowback and produced water on phototactic behavior in Daphnia magna. *Ecotoxicology and environmental safety* 174**,** 315-323.

Delompré, P., Blewett, T., Snihur, K., Flynn, S., Alessi, D., Glover, C., and Goss, G. (2019b). The osmotic effect of hyper-saline hydraulic fracturing fluid on rainbow trout, Oncorhynchus mykiss. *Aquatic Toxicology* 211**,** 1-10.

Dong, S., Massalha, N., Plewa, M.J., and Nguyen, T.H. (2018a). The impact of disinfection Ct values on cytotoxicity of agricultural wastewaters: ozonation vs. chlorination. *Water research* 144**,** 482-490.

Dong, S., Page, M.A., Massalha, N., Hur, A., Hur, K., Bokenkamp, K., Wagner, E.D., and Plewa, M.J. (2019). Toxicological comparison of water, wastewaters, and processed wastewaters. *Environmental science & technology* 53**,** 9139-9147.

Dong, S., Page, M.A., Wagner, E.D., and Plewa, M.J. (2018b). Thiol reactivity analyses to predict mammalian cell cytotoxicity of water samples. *Environmental science & technology* 52**,** 8822-8829.

Elsner, M., and Hoelzer, K. (2016). Quantitative survey and structural classification of hydraulic fracturing chemicals reported in unconventional gas production. *Environmental science & technology* 50**,** 3290-3314.

Entrekin, S., Evans-White, M., Johnson, B., and Hagenbuch, E. (2011). Rapid expansion of natural gas development poses a threat to surface waters. *Frontiers in Ecology and the Environment* 9**,** 503-511.

Fahrenfeld, N., Medina, W.R.M., D'elia, S., Modica, M., Ruiz, A., and Mclane, M. (2022). Comparison of residential dormitory COVID-19 monitoring via weekly saliva testing and sewage monitoring. *Science of The Total Environment* 814**,** 151947.

Felske, A., Akkermans, A.D., and De Vos, W.M. (1998). In situ detection of an uncultured predominant Bacillus in Dutch grassland soils. *Applied and environmental microbiology* 64**,** 4588-4590.

Folkerts, E.J., Blewett, T.A., He, Y., and Goss, G.G. (2017a). Alterations to juvenile zebrafish (Danio rerio) swim performance after acute embryonic exposure to sub-lethal exposures of hydraulic fracturing flowback and produced water. *Aquatic Toxicology* 193**,** 50-59.

Folkerts, E.J., Blewett, T.A., He, Y., and Goss, G.G. (2017b). Cardio-respirometry disruption in zebrafish (Danio rerio) embryos exposed to hydraulic fracturing flowback and produced water. *Environmental Pollution* 231**,** 1477-1487.

Fumian, T.M., Leite, J.P.G., Rose, T.L., Prado, T., and Miagostovich, M.P. (2011). One year environmental surveillance of rotavirus specie A (RVA) genotypes in circulation after the introduction of the Rotarix® vaccine in Rio de Janeiro, Brazil. *Water Research* 45**,** 5755-5763.

Gehman, J., Thompson, D.Y., Alessi, D.S., Allen, D.M., and Goss, G.G. (2016). Comparative analysis of hydraulic fracturing wastewater practices in unconventional shale development:

Newspaper coverage of stakeholder concerns and social license to operate. *Sustainability* 8**,** 912.

Gibas, C., Lambirth, K., Mittal, N., Juel, M.a.I., Barua, V.B., Brazell, L.R., Hinton, K., Lontai, J., Stark, N., and Young, I. (2021). Implementing building-level SARS-CoV-2 wastewater surveillance on a university campus. *Science of The Total Environment* 782**,** 146749.

Goss, G., Alessi, D., Allen, D., Gehman, J., Brisbois, J., Kletke, S., Zolfaghari, A., Notte, C., Thompson, Y., and Hong, K. (2015). Unconventional wastewater management: a comparative review and analysis of hydraulic fracturing wastewater management practices across four North American basins. *Canadian Water Network*.

Guo, F., Ju, F., Cai, L., and Zhang, T. (2013). Taxonomic precision of different hypervariable regions of 16S rRNA gene and annotation methods for functional bacterial groups in biological wastewater treatment. *PloS one* 8**,** e76185.

Haramoto, E., Malla, B., Thakali, O., and Kitajima, M. (2020). First environmental surveillance for the presence of SARS-CoV-2 RNA in wastewater and river water in Japan. *Science of the Total Environment* 737**,** 140405.

Harris-Lovett, S., Nelson, K.L., Beamer, P., Bischel, H.N., Bivins, A., Bruder, A., Butler, C., Camenisch, T.D., De Long, S.K., and Karthikeyan, S. (2021). Wastewater surveillance for SARS-CoV-2 on college campuses: initial efforts, lessons learned, and research needs. *International journal of environmental research and public health* 18**,** 4455.

He, Y., Flynn, S.L., Folkerts, E.J., Zhang, Y., Ruan, D., Alessi, D.S., Martin, J.W., and Goss, G.G. (2017a). Chemical and toxicological characterizations of hydraulic fracturing flowback and produced water. *Water research* 114**,** 78-87.

He, Y., Folkerts, E.J., Zhang, Y., Martin, J.W., Alessi, D.S., and Goss, G.G. (2017b). Effects on biotransformation, oxidative stress, and endocrine disruption in rainbow trout (Oncorhynchus mykiss) exposed to hydraulic fracturing flowback and produced water. *Environmental science & technology* 51**,** 940-947.

He, Y., Zhang, Y., Martin, J.W., Alessi, D.S., Giesy, J.P., and Goss, G.G. (2018). In vitro assessment of endocrine disrupting potential of organic fractions extracted from hydraulic fracturing flowback and produced water (HF-FPW). *Environment international* 121**,** 824-831.

Hena, S., Gutierrez, L., and Croué, J.-P. (2021). Removal of pharmaceutical and personal care products (PPCPs) from wastewater using microalgae: A review. *Journal of hazardous materials* 403**,** 124041.

Hong, P.-Y., Julian, T.R., Pype, M.-L., Jiang, S.C., Nelson, K.L., Graham, D., Pruden, A., and Manaia, C.M. (2018). Reusing treated wastewater: consideration of the safety aspects associated with antibiotic-resistant bacteria and antibiotic resistance genes. *Water* 10**,** 244.

Hovi, T., Shulman, L., Van Der Avoort, H., Deshpande, J., Roivainen, M., and De Gourville, E. (2012). Role of environmental poliovirus surveillance in global polio eradication and beyond. *Epidemiology & Infection* 140**,** 1-13.

Hull, N.M., Rosenblum, J.S., Robertson, C.E., Harris, J.K., and Linden, K.G. (2018). Succession of toxicity and microbiota in hydraulic fracturing flowback and produced water in the Denver–Julesburg Basin. *Science of the total environment* 644**,** 183-192.

Ishikawa, M., Muraguchi, R., Azuma, A., Nawata, S., Miya, M., Katsuura, T., Naito, T., and Oyama, Y. (2016). Cytotoxic actions of 2, 2-dibromo-3-nitrilopropionamide, a biocide in hydraulic fracturing fluids, on rat thymocytes. *Toxicology Research* 5**,** 1329-1334.

Kapoor, V., Al-Duroobi, H., Phan, D.C., Palekar, R.S., Blount, B., and Rambhia, K.J. (2022). Wastewater Surveillance for SARS-CoV-2 to Support Return to Campus: Methodological Considerations and Data Interpretation. *Current Opinion in Environmental Science & Health***,** 100362.

Kassotis, C.D., Bromfield, J.J., Klemp, K.C., Meng, C.-X., Wolfe, A., Zoeller, R.T., Balise, V.D., Isiguzo, C.J., Tillitt, D.E., and Nagel, S.C. (2016a). Adverse reproductive and developmental health outcomes following prenatal exposure to a hydraulic fracturing chemical mixture in female C57Bl/6 mice. *Endocrinology* 157**,** 3469-3481.

Kassotis, C.D., Iwanowicz, L.R., Akob, D.M., Cozzarelli, I.M., Mumford, A.C., Orem, W.H., and Nagel, S.C. (2016b). Endocrine disrupting activities of surface water associated with a West Virginia oil and gas industry wastewater disposal site. *Science of The Total Environment* 557**,** 901-910.

Kassotis, C.D., Tillitt, D.E., Davis, J.W., Hormann, A.M., and Nagel, S.C. (2014). Estrogen and androgen receptor activities of hydraulic fracturing chemicals and surface and ground water in a drilling-dense region. *Endocrinology* 155**,** 897-907.

King, G.E. (Year). "Hydraulic fracturing 101: What every representative, environmentalist, regulator, reporter, investor, university researcher, neighbor and engineer should know about estimating frac risk and improving frac performance in unconventional gas and oil wells", in: *SPE hydraulic fracturing technology conference*: OnePetro).

Kocamemi, B.A., Kurt, H., Sait, A., Sarac, F., Saatci, A.M., and Pakdemirli, B. (2020). SARS-CoV-2 detection in Istanbul wastewater treatment plant sludges. *MedRxiv*.

Kondash, A., and Vengosh, A. (2015). Water footprint of hydraulic fracturing. *Environmental Science & Technology Letters* 2**,** 276-280.

Kumar, M., Kuroda, K., Patel, A.K., Patel, N., Bhattacharya, P., Joshi, M., and Joshi, C.G. (2021). Decay of SARS-CoV-2 RNA along the wastewater treatment outfitted with Upflow Anaerobic Sludge Blanket (UASB) system evaluated through two sample concentration techniques. *Science of the Total Environment* 754**,** 142329.

Lauer, N.E., Harkness, J.S., and Vengosh, A. (2016). Brine spills associated with unconventional oil development in North Dakota. *Environmental science & technology* 50**,** 5389-5397.

Lemas, D.J., Loop, M.S., Duong, M., Schleffer, A., Collins, C., Bowden, J.A., Du, X., Patel, K., Ciesielski, A.L., and Ridge, Z. (2021). Estimating drug consumption during a college sporting event from wastewater using liquid chromatography mass spectrometry. *Science of the total environment* 764**,** 143963.

Linstedt, K.D., Houck, C.P., and O'connor, J.T. (1971). Trace element removals in advanced wastewater treatment processes. *Journal (Water Pollution Control Federation)***,** 1507-1513.

Lodder, W., Buisman, A., Rutjes, S., Heijne, J., Teunis, P., and De Roda Husman, A. (2012). Feasibility of quantitative environmental surveillance in poliovirus eradication strategies. *Applied and environmental microbiology* 78**,** 3800-3805.

Lucchini, S., Thompson, A., and Hinton, J.D. (2001). Microarrays for microbiologists. *Microbiology* 147**,** 1403-1414.

Majumdar, M., Klapsa, D., Wilton, T., Akello, J., Anscombe, C., Allen, D., Mee, E.T., Minor, P.D., and Martin, J. (2018). Isolation of vaccine-like poliovirus strains in sewage samples from the United Kingdom. *The Journal of Infectious Diseases* 217**,** 1222-1230.

Malik, S., Beer, M., Megharaj, M., and Naidu, R. (2008). The use of molecular techniques to characterize the microbial communities in contaminated soil and water. *Environment international* 34**,** 265-276.

Manz, K.E., Palomino, A.M., Cyr, H., and Carter, K.E. (2021). Shale particle interactions with organic and inorganic hydraulic fracturing additives. *Applied Geochemistry* 127**,** 104901.

Matthijnssens, J., Bilcke, J., Ciarlet, M., Martella, V., Bányai, K., Rahman, M., Zeller, M., Beutels, P., Van Damme, P., and Van Ranst, M. (2009). Rotavirus disease and vaccination: impact on genotype diversity. *Future microbiology* 4**,** 1303-1316.

Mcclary-Gutierrez, J., Mattioli, M., Marcenac, P., Silverman, A., Boehm, A., Bibby, K., Balliet, M., De Los Reyes Iii, F., Gerrity, D., and Griffith, J. (2021). Sars-Cov-2 Wastewater Surveillance for Public Health Action: Connecting Perspectives From Wastewater Researchers and Public Health Officials During a Global Pandemic.

Medema, G., Heijnen, L., Elsinga, G., Italiaander, R., and Brouwer, A. (2020). Presence of SARS-Coronavirus-2 RNA in sewage and correlation with reported COVID-19 prevalence in the early stage of the epidemic in the Netherlands. *Environmental Science & Technology Letters* 7**,** 511-516.

Metcalf, T., Melnick, J., and Estes, M. (1995). Environmental virology: from detection of virus in sewage and water by isolation to identification by molecular biology—a trip of over 50 years. *Annual review of microbiology* 49**,** 461-487.

Mohan, S.V., Hemalatha, M., Kopperi, H., Ranjith, I., and Kumar, A.K. (2021). SARS-CoV-2 in environmental perspective: Occurrence, persistence, surveillance, inactivation and challenges. *Chemical Engineering Journal* 405**,** 126893.

Montgomery, A.B., O'rourke, C.E., and Subedi, B. (2021). Basketball and drugs: wastewater-based epidemiological estimation of discharged drugs during basketball games in Kentucky. *Science of the total environment* 752**,** 141712.

Pals, J.A., Wagner, E.D., and Plewa, M.J. (2016). Energy of the lowest unoccupied molecular orbital, thiol reactivity, and toxicity of three monobrominated water disinfection byproducts. *Environmental science & technology* 50**,** 3215-3221.

Parmaki, S., Vyrides, I., Vasquez, M.I., Hartman, V., Zacharia, I., Hadjiadamou, I., Barbeitos, C.B., Ferreira, F.C., Afonso, C.A., and Drouza, C. (2018). Bioconversion of alkaloids to

high-value chemicals: Comparative analysis of newly isolated lupanine degrading strains. *Chemosphere* 193**,** 50-59.

Patterson, L.A., Konschnik, K.E., Wiseman, H., Fargione, J., Maloney, K.O., Kiesecker, J., Nicot, J.-P., Baruch-Mordo, S., Entrekin, S., and Trainor, A. (2017). Unconventional oil and gas spills: risks, mitigation priorities, and state reporting requirements. *Environmental Science & Technology* 51**,** 2563-2573.

Payne, M.E., Chapman, H.F., Cumming, J., and Leusch, F.D. (2014). In vitro cytotoxicity assessment of a hydraulic fracturing fluid. *Environmental Chemistry* 12**,** 286-292.

Peccia, J., Zulli, A., Brackney, D.E., Grubaugh, N.D., Kaplan, E.H., Casanovas-Massana, A., Ko, A.I., Malik, A.A., Wang, D., and Wang, M. (2020). Measurement of SARS-CoV-2 RNA in wastewater tracks community infection dynamics. *Nature biotechnology* 38**,** 1164-1167.

Princy, S., Sathish, S.S., Cibichakravarthy, B., and Prabagaran, S.R. (2020). Hexavalent chromium reduction by Morganella morganii (1Ab1) isolated from tannery effluent contaminated sites of Tamil Nadu, India. *Biocatalysis and Agricultural Biotechnology* 23**,** 101469.

Rahman, M.T., Uddin, M.S., Sultana, R., Moue, A., and Setu, M. (2013). Polymerase chain reaction (PCR): a short review. *Anwer Khan Modern Medical College Journal* 4**,** 30-36.

Rahube, T.O., and Yost, C.K. (2010). Antibiotic resistance plasmids in wastewater treatment plants and their possible dissemination into the environment. *African Journal of Biotechnology* 9**,** 9183-9190.

Randazzo, W., Truchado, P., Cuevas-Ferrando, E., Simón, P., Allende, A., and Sánchez, G. (2020). SARS-CoV-2 RNA in wastewater anticipated COVID-19 occurrence in a low prevalence area. *Water research* 181**,** 115942.

Rastogi, G., and Sani, R.K. (2011). "Molecular techniques to assess microbial community structure, function, and dynamics in the environment," in *Microbes and microbial technology*. Springer), 29-57.

Rozell, D.J., and Reaven, S.J. (2012). Water pollution risk associated with natural gas extraction from the Marcellus Shale. *Risk Analysis: An International Journal* 32**,** 1382-1393.

Sangkham, S. (2021). A review on detection of SARS-CoV-2 RNA in wastewater in light of the current knowledge of treatment process for removal of viral fragments. *Journal of Environmental Management* 299**,** 113563.

Sarti, A., Pozzi, E., and Zaiat, M. (2012). Characterization of immobilized biomass by amplified rDNA restriction analysis (ARDRA) in an anaerobic sequencing-batch biofilm reactor (ASBBR) for the treatment of industrial wastewater. *Brazilian Archives of Biology and Technology* 55**,** 623-629.

Scott, L.C., Aubee, A., Babahaji, L., Vigil, K., Tims, S., and Aw, T.G. (2021). Targeted wastewater surveillance of SARS-CoV-2 on a university campus for COVID-19 outbreak detection and mitigation. *Environmental research* 200**,** 111374.

Serra-Compte, A., González, S., Arnaldos, M., Berlendis, S., Courtois, S., Loret, J.F., Schlosser, O., Yáñez, A.M., Soria-Soria, E., and Fittipaldi, M. (2021). Elimination of SARS-CoV-2 along wastewater and sludge treatment processes. *Water research* 202**,** 117435.

Sherchan, S.P., Shahin, S., Ward, L.M., Tandukar, S., Aw, T.G., Schmitz, B., Ahmed, W., and Kitajima, M. (2020). First detection of SARS-CoV-2 RNA in wastewater in North America: a study in Louisiana, USA. *Science of The Total Environment* 743**,** 140621.

Silveira, D., Filho, P.B., Philippi, L., Cantão, M., Foulquier, A., Bayle, S., Delforno, T., and Molle, P. (2021). In-depth assessment of microbial communities in the full-scale vertical flow treatment wetlands fed with raw domestic wastewater. *Environmental Technology* 42**,** 3106-3121.

Smith, C.J., and Osborn, A.M. (2009). Advantages and limitations of quantitative PCR (Q-PCR)-based approaches in microbial ecology. *FEMS microbiology ecology* 67**,** 6-20.

Suo, T., Liu, X., Feng, J., Guo, M., Hu, W., Guo, D., Ullah, H., Yang, Y., Zhang, Q., and Wang, X. (2020). ddPCR: a more accurate tool for SARS-CoV-2 detection in low viral load specimens. *Emerging microbes & infections* 9**,** 1259-1268.

Sweetapple, C., Melville-Shreeve, P., Chen, A.S., Grimsley, J.M., Bunce, J.T., Gaze, W., Fielding, S., and Wade, M.J. (2022). Building knowledge of university campus population dynamics to enhance near-to-source sewage surveillance for SARS-CoV-2 detection. *Science of the Total Environment* 806**,** 150406.

Taylor, S., Wakem, M., Dijkman, G., Alsarraj, M., and Nguyen, M. (2010). A practical approach to RT-qPCR—publishing data that conform to the MIQE guidelines. *Methods* 50**,** S1-S5.

Theodori, G.L., Luloff, A., Willits, F.K., and Burnett, D.B. (2014). Hydraulic fracturing and the management, disposal, and reuse of frac flowback waters: Views from the public in the Marcellus Shale. *Energy Research & Social Science* 2**,** 66-74.

Urrea-Valencia, S., Melo, A.L.D.A., Gonçalves, D.R.P., Galvão, C.W., and Etto, R.M. (2021). Molecular Techniques to Study Microbial Wastewater Communities. *Brazilian Archives of Biology and Technology* 64.

Vengosh, A., Jackson, R.B., Warner, N., Darrah, T.H., and Kondash, A. (2014). A critical review of the risks to water resources from unconventional shale gas development and hydraulic fracturing in the United States. *Environmental science & technology* 48**,** 8334-8348.

Vidic, R.D., Brantley, S.L., Vandenbossche, J.M., Yoxtheimer, D., and Abad, J.D. (2013). Impact of shale gas development on regional water quality. *science* 340**,** 1235009.

Wang, H., Neyvaldt, J., Enache, L., Sikora, P., Mattsson, A., Johansson, A., Lindh, M., Bergstedt, O., and Norder, H. (2020). Variations among viruses in influent water and effluent water at a wastewater plant over one year as assessed by quantitative PCR and metagenomics. *Applied and environmental microbiology* 86**,** e02073-02020.

Warner, N.R., Christie, C.A., Jackson, R.B., and Vengosh, A. (2013). Impacts of shale gas wastewater disposal on water quality in western Pennsylvania. *Environmental science & technology* 47**,** 11849-11857.

Westhaus, S., Weber, F.-A., Schiwy, S., Linnemann, V., Brinkmann, M., Widera, M., Greve, C., Janke, A., Hollert, H., and Wintgens, T. (2021). Detection of SARS-CoV-2 in raw and treated wastewater in Germany–suitability for COVID-19 surveillance and potential transmission risks. *Science of The Total Environment* 751**,** 141750.

Wurtzer, S., Waldman, P., Ferrier-Rembert, A., Frenois-Veyrat, G., Mouchel, J.-M., Boni, M., Maday, Y., Marechal, V., and Moulin, L. (2021). Several forms of SARS-CoV-2 RNA can be detected in wastewaters: implication for wastewater-based epidemiology and risk assessment. *Water Research* 198**,** 117183.

Zuccato, E., Gracia-Lor, E., Rousis, N.I., Parabiaghi, A., Senta, I., Riva, F., and Castiglioni, S. (2017). Illicit drug consumption in school populations measured by wastewater analysis. *Drug and alcohol dependence* 178**,** 285-290.

Chapter 2. Toxicity of Hydraulic Fracturing Wastewater from Black Shale Natural-Gas Wells Influenced by Well Maturity and Chemical Additives

This chapter has been published in the following form:

Aghababaei, M., Luek, J.L., Ziemkiewicz, P.F., Mouser, P.J. (2021). Toxicity of Hydraulic Fracturing Wastewater from Black Shale Natural-Gas Wells Influenced by Well Maturity and Chemical Additives. *Environmental Science: Processes & Impacts* 23 (4), 621-632. DOI: 10.1039/D1EM00023C

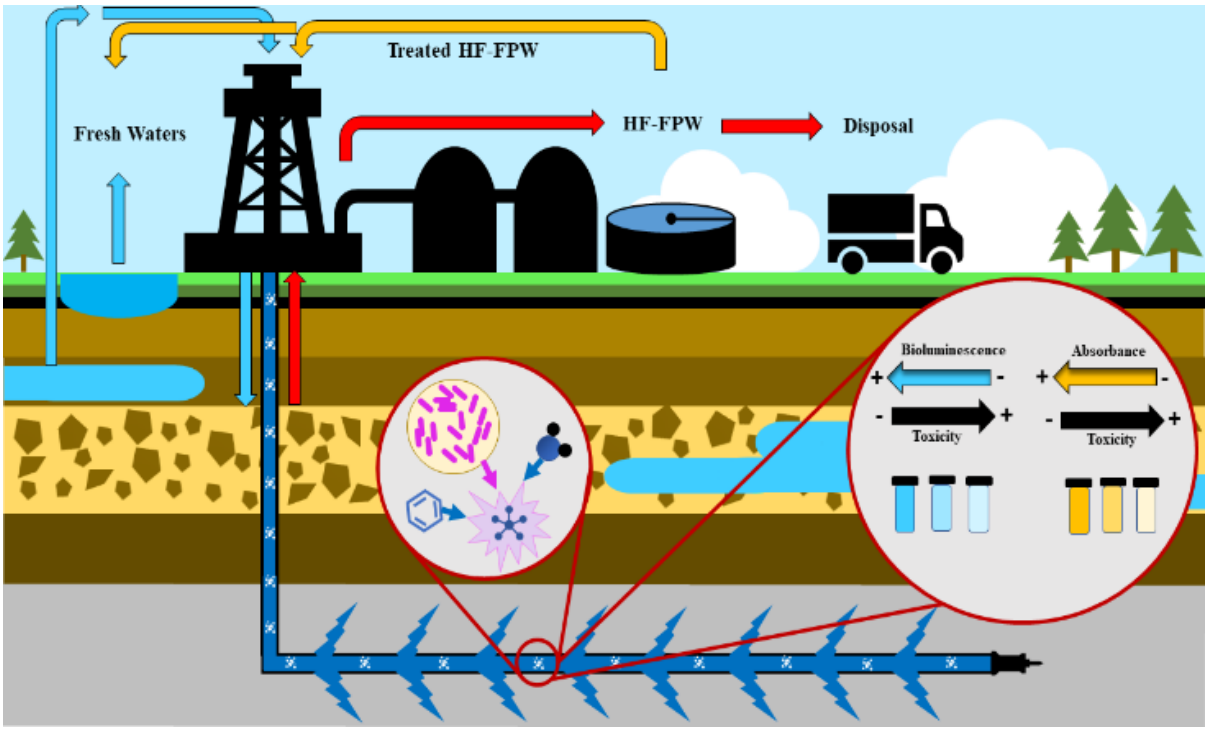

Abstract

Hydraulic fracturing of deep shale formations generates large volumes of wastewater that must be managed through treatment, reuse, or disposal. Produced wastewater liberates formation-derived radionuclides and contains previously uncharacterized organohalides thought to be generated within the shale well, both posing unknown toxicity to human and ecological health. Here, we assess the toxicity of 42 input media and produced fluid samples collected from four wells in the Utica Formation and Marcellus Shale using two distinct endpoint screening assays. Broad spectrum acute toxicity was assessed using a BioLuminescence Inhibition Assay employing the halotolerant bacterium *Aliivibrio fischeri*, while predictive mammalian cytotoxicity was evaluated using a N-acetylcysteine (NAC) thiol reactivity assay. The acute toxicity and thiol reactivity of early-stage flowback was higher than later produced fluids, with levels diminishing through time as the natural gas wells matured. Acute toxicity of early stage flowback and drilling muds were on par with the positive control, 3,5-dichlorophenol (6.8 mg/L). Differences in both acute toxicity and thiol reactivity between paired natural gas well samples were associated with specific chemical additives. Samples from wells containing a larger diversity and concentration of organic additives resulted in higher acute toxicity, while samples from a well applying a higher composition of ammonium persulfate, a strong oxidizer, showed greater thiol reactivity, predictive of higher mammalian toxicity. Both acute toxicity and thiol reactivity are consistently detected in produced waters, in some cases present up to nine months after hydraulic fracturing. These results support that specific chemical additives, the reactions generated by the additives, or the constituents liberated from the formation by the additives contribute to the toxicity of hydraulic fracturing produced waters and reinforces the need for careful consideration of early produced fluid management.

Environmental Significance

Hydraulic fracturing stimulates the release of natural gas and other hydrocarbons from low permeability shale formations. We identified temporal shifts from higher to lower acute toxicity and predictive mammalian cytotoxicity as four shale gas wells matured. Our findings add to the growing body of work quantifying the toxic effects of hydraulic fracturing waste fluids, and links higher toxicities by these end points with chemical composition. As the volume of hydraulic fracturing waste fluids produced increases year after year, it is imperative to utilize information regarding their composition and toxicity to inform safe and effective wastewater management.

2.1 Introduction

The process of extracting hydrocarbon resources from low permeability formations, such as black shales using horizontal drilling and hydraulic fracturing techniques, remains a growing practice in the oil and gas industry, especially in North America (EIA 2013). During hydraulic fracturing, a large-volume (up to 20 million L or more (Alessi, Zolfaghari et al. 2017, Kondash, Lauer et al. 2018)) of a water-based fluid is injected into the well at a high pressure (up to 69 MPa (EPA 2016)), generating new fractures in the formation to enhance the release of hydrocarbons. Injected fluids are primarily water(~90%) combined with proppants such as ceramic beads or sand (~9%), and a short list of chemical modifiers (~1%), commonly including biocides, gelling or foaming agents, pH adjustors, clay stabilizers, and surfactants (Arthur, Bohm et al. 2009, Stringfellow, Domen et al. 2014, Elsner and Hoelzer 2016), with the fluid chemistry designed specifically for the conditions of each well. Additionally, the composition of the flowback fluid (generated during the first few weeks after well completion) and produced water (generated once the well transitions

into production), collectively abbreviated as FPW, are highly variable and depend on the fracture fluid chemistry, formation-specific geogenic constituents, chemicals formed *in situ* by industry design, or those generated through unanticipated subsurface reactions (Stringfellow, Domen et al. 2014, Lester, Ferrer et al. 2015, DiGiulio and Jackson 2016, Kim, Omur-Ozbek et al. 2016, McAdams, Carter et al. 2019). Well age exerts the greatest influence over major ion concentrations in FPW (Ziemkiewicz and He 2015).

Despite the wide-spread application of these technologies in unconventional oil and gas formations, there remain substantial environmental concerns surrounding water resource use, management, and pollution (Johnson and Johnson 2012, Barbot, Vidic et al. 2013, Kondash and Vengosh 2015, Alessi, Zolfaghari et al. 2017, Kondash, Patino-Echeverri et al. 2019). One major water resource challenge is the management of large volumes of wastewater containing elevated levels of dissolved solids (Warner, Christie et al. 2013), salts, radionuclides (Rowan, Engle et al. 2011, Barbot, Vidic et al. 2013), bromide (Ziemkiewicz and He 2015), and iodide (Harkness, Dwyer et al. 2015, Liberatore, Plewa et al. 2017), which are difficult to treat using conventional treatment processes (Sun, Wang et al. 2019). Treatment of FPW fluids has also been associated with the generation of toxins resulting from disinfection byproducts, including organoiodides and brominated sulfonates. Additionally, accidental release of hydraulic fracturing fluids, flowback fluids, and produced waters during well integrity issues, on-site fluid handling and transportation to disposal wells has resulted in contamination of surface water and groundwater (Vengosh, Jackson et al. 2014). Spills have been shown to negatively affect freshwater invertebrate and fish species, highlighting the potential for both short and long-term environmental impacts to downstream aquatic ecosystems (Blewett, Delompré et al. 2017, He, Sun et al. 2018) and water resource users (McLaughlin, Borch et al. 2020).

As the practice of hydraulic fracturing in oil and gas extraction continues to grow, the need for research evaluating FPW toxicity also increases. In a recent review, Danforth and coauthors summarized toxicity information for individual produced water constituents, finding ecological or human health risk values for only 14% of identified chemicals (Danforth, Chiu et al. 2020). Moreover, interaction effects between fracture fluid chemicals and the FPW itself on toxicity remains poorly understood. The salt content of FPW samples (up to 400 g/L (He, Flynn et al. 2017)) can be far beyond the salinity of seawater (~33 g/L(He, Flynn et al. 2017)), representing a significant physiological challenge to freshwater and estuarine organisms. As a result, the high salt content alone of FPW can disrupt organism ionic balance, leading to toxicity (Blewett, Delompré et al. 2017, Delompré, Blewett et al. 2019); aquatic invertebrate acute toxicity has primarily attributed to the high salinity from Duvernay Basin and Appalachian Basin produced waters (Blewett, Delompré et al. 2017, Tasker, Burgos et al. 2018, Mehler, Nagel et al. 2020). FPW toxicity beyond acute salinity effects have been observed in several model aquatic organisms (Blewett, Delompré et al. 2017, Blewett, Weinrauch et al. 2017, He, Flynn et al. 2017, Delompré, Blewett et al. 2019), with some toxicity endpoints linked to higher organic compound concentrations(Folkerts, Blewett et al. 2019) as well as the solid phase, which may concentrate some toxicants (e.g., polycyclic aromatic hydrocarbons) relative to the dissolved phase (He, Folkerts et al. 2017).

Whole organism studies are invaluable in linking adverse outcomes of chemicals on organisms and their receptors, and can be used to assess both individual and synergistic effects. However, whole organism toxicity tests are frequently time consuming to perform, may require large fluid volumes, and FPW salinity may mask a range of additional adverse effects. Toxicity screening assays provide a complimentary tool to whole organism tests to quickly assess toxic bioactivity

across a large number of environmental samples. The *Aliivibrio fischeri* (*A. fischeri*) bioluminescence assay (Shemer and Linden 2007, Hull, Rosenblum et al. 2018, Parmaki, Vyrides et al. 2018) is a widely employed acute toxicity screening test that is sensitive across a wide range of organic and inorganic contaminants and effective in an array of complex waste matrices (Cotou, Papathanassiou et al. 2002, Rigol, Latorre et al. 2004). Hull and coauthors (Hull, Rosenblum et al. 2018) applied this approach to track acute toxicity over 220 days in produced fluids from a Denver-Julesberg Basin (Colorado) shale well, finding BioLuminescence Inhibition Assay (BLIA) inhibition stabilized in the 4 months after hydraulic fracturing. Biological assays have also identified the induction of mutagenicity (Hull, Rosenblum et al. 2018), estrogenicity (He, Zhang et al. 2018), and specific cellular pathways indicative of xenobiotic toxicity response (including pregnane-X receptor, aryl hydrocarbon receptor) (He, Zhang et al. 2018, Tasker, Burgos et al. 2018) to compounds concentrated in the organic fraction of shale gas flowback and produced waters. Halogenated organic compounds identified in the organic fraction have the potential to cause a biological response by inducing cysteine thiol in glutathione as a reductant, which can lead to adverse effects including an immunotoxicity reaction (Meister and Anderson 1983, Townsend, Tew et al. 2003). The NAC thiol reactivity assay has recently been applied to environmental samples to detect interactions between organic chemical constituents and biological thiols (Dong, Page et al. 2018, Dong, Page et al. 2019), and can be utilized on FPW extracts previously characterized to include a diverse array of halogenated organic compounds (Luek, Harir et al. 2018). Although these two screening assays are not capable of characterizing specific toxicity effects at the whole organism level, they provide a rapid, high throughput measure of broad acute toxicity (BLIA) to thiol reactive toxicity (NAC thiol) that can be applied to complex and variable FPW samples.

Although the health effects of some disclosed chemicals used in hydraulic fracturing are known (Sun, Wang et al. 2019), many gaps remain (Elliott, Ettinger et al. 2017), and toxicity studies evaluating synergetic effects between compounds is relatively unexplored. With the exception of the aforementioned temporal toxicity study for a shale well in the Denver-Julesberg Basin (Hull, Rosenblum et al. 2018), long term assessment of temporal toxicity for FPW also remains limited. Barriers to such studies include gaining continuing access and coordinating sampling with operators at well pads, obtaining and transporting sufficient sample volume for toxicity studies, and sample matrix shifts that occur during well maturation, possibly influencing toxicity results. Among the existing studies, toxicity of flowback collected from a shale well in the Canadian Duvernay formation was highest among most aquatic species at the earliest time (Folkerts, Blewett et al. 2019) while a second study from this same formation noted an inverse relationships through time in toxicity of FPW organic extracts for two different endocrine disrupting assays (He, Zhang et al. 2018).

Given the continued need to better understand the character and possible environmental impacts from unconventional oil and gas wastewaters, the goal of this work was to compare and track temporal changes in toxicity for input media and produced fluid samples from multiple hydraulically fractured natural-gas wells in the northern Appalachian Basin using two high throughput screening assays (Pals, Wagner et al. 2016, Pals, Wagner et al. 2017). We hypothesized that toxicity would decrease through time after fracturing and that both geological formation and chemical additive components would play an important role in toxicity differences. We were also interested in assessing the toxicity of specific sample fractions to better understand the source of toxicity through time. Results from this study improve our understanding of the toxicity of hydraulic fracture wastewaters and its variability through time in the Appalachian Basin to better

inform monitoring and risk assessment efforts in these and other formations slated for future hydraulic fracturing development.

2.2 Material and Methods

2.2.1 Fluid Sampling and Processing

Hydraulic fracturing fluids were collected and processed as previously described (Daly, Borton et al. 2016, Borton, Hoyt et al. 2018, Evans, Panescu et al. 2018, Luek, Harir et al. 2018). Toxicity analyses were conducted on input media and produced fluid samples from four hydraulically fractured natural-gas wells in the northern Appalachian Basin: two from the Marcellus Shale (M-4 and M-5) and two from the Utica-Point Pleasant Formation (U-6 and U-7). Field samples were collected as part of several large scale, multi-university collaborative efforts to characterize a diverse array of geological, chemical, and biological parameters; access to fluid samples was contingent upon operator and collaborative research plans. Although not all wells were sampled at the same time intervals, the wide array of related data available for analyzed samples is a unique advantage of these multiyear datasets. A total of 42 samples (see Table A2) were collected from drilling equipment, holding tanks, drill muds, or from gas-fluid separators, including: M-4 (n=10 flowback and produced water (FPW), 1 “kill” fluid (a high density fluid pumped into a well to temporarily stop gas flow for maintenance purposes), 1 drill mud, and 1 sidewall mud), M-5 (n= 8 FPW), U-6 (n= 9 FPW, 2 freshwater tank, 1 produced water additive, and 1 recycled produced water additive (make-up water from recycled produced water)), and U-7 (n= 8 FPW) for acute

toxicity (bioluminescence assay) and were immediately stored at -20ºC until analysis (see Figure A1 for field experimental details).

Samples for predictive mammalian cell cytotoxicity (NAC thiol assay) were pre-processed using solid phase extraction (SPE) as previously described (Luek, Harir et al. 2018), then stored at -20ºC until analysis (see Table A3). SPE is important for reducing interferences for the NAC thiol assay and enables increased sensitivity and detection of thiol reactivity by concentrating larger volume samples. Briefly, a 200 mL sample was filtered (0.7 mm glass fiber filter (Whatman GF/F)) and acidified to pH 2 with concentrated HCl to increase extraction efficiency for organic acids and phenols (Dittmar, Koch et al. 2008). SPE cartridges (Agilent Bond Elut PPL SPE cartridges (1 g, 3 mL)) were pre-conditioned with methanol (HPLC grade, Fisher Scientific) then rinsed with 0.1% formic acid (Acros Organics). Samples were applied to the SPE resin at a flow rate of ~5-10 mL/min before rinsing the resin with 10 mL 0.1% formic acid and cleaning the cartridge exterior with Milli-Q water to remove sample impurities. SPE cartridges were dried under vacuum before eluting the concentrated and de-salted sample using 10 mL methanol.

2.2.2 Bioluminescence Inhibition Assay

Acute toxicity for 42 field samples (35 FPW and 7 drill muds/input fluids) was assessed using an *A. fischeri* (NRRL B11177) bioluminescence inhibition microassay (BLIA) (Lumoplate Ultimate Matrix kit, EBPI, Mississauga, ON, Canada). Briefly, lyophilized bacteria were reconstituted into a background diluent (supplied by the manufacturer) for 30 minutes at 4ºC, followed by 30 minutes at 15ºC to activate the *A. fischeri* reagent. Next, samples (200 µL) were added to the plate and serially diluted (1:2) throughout the microplate column. The *A. fischeri* reagent (100 µL) was then

dispensed into microplate wells. Luminescence was measured at 1, 5, 15, and 30 minutes of sample exposure using a Synergy HTX microplate reader (BioTek, Winooski, VT, USA) located in an environmental growth chamber held at 15ºC. Orbital shaking of the plates occurred every one second between measurements.

Samples were analyzed in duplicate and fractionated as described below, and positive (3,5-dichlorophenol (Sigma-Aldrich)) and negative controls (background diluent) were included on every plate. A salt control (SW) was analyzed containing Na, Mg, K, Ca and Cl, typical of Appalachian shale FPW (Table A1). To separate toxicity effects between solid (particles) and aqueous (dissolved) phases, field samples were fractioned into a sediment-containing sample (S) and a sediment-free (SF) portion. Sediment-containing fractions were raw and unprocessed fluids or muds, while sediment-free fractions contained the supernatant after centrifugation (9.6x*g* for 10 minutes) that also passed through a 0.2 μm pore size polyethersulfone (PES) filter. When samples were outside of a circumneutral range, the pH was adjusted to 7.0±0.2 using 1.0 M NaOH or HCl solutions for the samples shown in Table A2. Considering the high concentration of chloride (g/L) present in flowback and produced water samples, hydrochloric acid addition to adjust sample pH is not expected to produce halogenated toxicants. The total dissolved solids (TDS) concentration was adjusted to 20 g/L with MilliQ water for all samples per standard procedure for optimal *A. fischeri* growth (ISO 21338:2010 standard); dilution factors ranged from 3 to 7 for FPW samples (see Table A2).

The percentage of bioluminescence inhibition (INH%) was determined by comparing sample bioluminescence (I_s) and background control (I_c) as follows (Eq. 1):

$$INH\% = 100\text{-}100 \times (I_{S30} / KF) \times I_{S1}) \quad (1)$$

where KF is the correction factor ($KF= I_{C30}/ I_{C1}$), I_{C1} is the control luminescence intensity at one minute, I_{C30} is the control luminescence intensity after 30 minutes, I_{S1} is the sample luminescence intensity at one minute, and I_{S30} is the sample luminescence intensity after 30 minutes. The concentration that inhibited 50% of the population (EC_{50}) was determined from bioluminescence results using EBPI toxicity calculation software following ISO standard 21338. A Toxicity Unit (TU_{50}) was then calculated as $100/EC_{50}$. Based on the TU_{50} values, samples were classified as non-toxic ($TU_{50}= 0$), slightly toxic ($0 < TU_{50} < 1$), toxic ($1 < TU_{50} < 10$), very toxic ($11 < TU_{50} <100$), and extremely toxic ($TU_{50} >100$) (Persoone, Goyvaerts et al. 1993).

2.2.3 N-Acetylcysteine Thiol Reactivity Assay

The toxicity of SPE extracts for 18 FPW and 4 input fluid samples from M-4 and M-5 were analyzed using the NAC thiol reactivity assay (Table A3), which is a predictor of reactive cytotoxicity for mammalian cells (Pals, Wagner et al. 2016, Pals, Wagner et al. 2017, Dong, Page et al. 2018). The NAC thiol assay quantifies the availability of cysteine thiol groups on N-acetylcysteine as a surrogate for glutathione, a biomolecule that defends against reactive toxins in biological systems (Timbrell 2008). In this assay, 2-nitro-5-thiobenzoate (NTB) is produced and measured from a reaction between Ellman's reagent (5,5'-dithiobis-(2-nitrobenzoic acid) or DTNB) (Ellman 1959) with unreacted thiol groups on NAC after sample exposure. A dilution series of four replicate sample extracts in Tris buffer (1M, pH 8.0, Thermofisher) (40 µL volume) was incubated with 4 mM NAC (10 µL) at room temperature in the dark for 20 min with linear shaking. Next, 50 µL of Ellman's reagent (1 mM DTNB in 100 mM potassium phosphate buffer and 0.1 mM EDTA at pH 8.0) was added to the assay to react with any remaining NAC during 10

seconds of linear shaking. The produced NTB was immediately quantified by measuring absorbance at 412 nm using the Synergy HTX microplate reader. In addition to sample extracts and their corresponding blanks (extract, Tris buffer, and Ellman's reagent), each plate contained a negative control (NAC, Tris buffer and Ellman's reagent), and a positive control (NAC, Tris buffer, Ellman's reagent, and 10 mM maleimide (2,5-Pyrroledione, Sigma-Aldrich)). The percent of concurrent negative control was defined by averaging blank-corrected negative control data and dividing these estimates into individual absorbance value measured at 412 nm for each FPW sample. The data were reported as the percentage of the concurrent negative control.

2.2.4 Geochemical and Organic Analyses

Total dissolved solids (TDS) were estimated based on measured electrical conductivity on unfiltered samples using Orion star field probes (ThermoFisher Scientific, Waltham, MA). Samples for geochemical and organic analysis were collected in high density polyethylene or glass containers with no headspace and stored at 4°C until analysis within 48 hours. Samples for total dissolved carbon (DOC) were filtered (0.22 µm pore size PES filters, EMD Millipore, Burlington, MA) and measured as non-purgeable organic carbon by combustion using a TOC/TN analyzer equipped with autosampler (TOC-V CSN/TNM-1/ASI-V, Shimadzu, Kyoto, Japan). During the M-4 and M-5 sampling campaigns, samples were also collected for BTEX (inc. benzene, toluene, ethylbenzene, total xylene, m,p-xylene, o-xylene) and surfactants (methylene blue active substances [MBAS]). Samples for BTEX were preserved using hydrochloric acid (pH <2) and analyzed using GC-MS using EPA SW-846 8260B while the methylene blue active substances assay was performed per EPA SM5540C. Comparisons are also made against a previously

published chemical dataset of iodinated organic ions detected in the same produced fluid solid phase extracts utilized for the thiol reactivity assay (Luek, Harir et al. 2018).

2.2.5 Statistical analyses

All statistical analyses were conducted using SigmaPlot version 14.0 (Systat Software Inc., San Jose, CA, USA). Data were first tested for normality (Shapiro-Wilk test) and homogeneity of variance (Levene's test). Data that failed these tests were transformed or analyzed using nonparametric statistical approaches (e.g. Wilcoxon Signed Ranked test). Positive bioluminescence inhibition of the sediment-containing and sediment-free samples were compared using a Kruskal-Wallis One Way Analysis of Variance on Ranks, while interactions between BLIA, NAC-thiol reactivity, geochemical parameters, organic chemical parameters, and halogenated organic compounds were investigated by regression analyses. Differences were considered statistically significant at $p \leq 0.05$.

2.3 Results

2.3.1 Acute toxicity persists in some shale wells up to nine months after hydraulic fracturing

We first investigated changes in acute toxicity on halotolerant bacteria for FPW samples (diluted to 20 g/L TDS) collected up to 764 days post-stimulation from two Marcellus shale natural gas wells using the *A. fischeri* assay. We expected a decrease in toxicity with time after hydraulic fracturing as the injected fluid additives reacted with each other and with the shale matrix and were diluted by formation brines before returning to the surface as FPW. Our results support decreased

toxicity as Marcellus natural-gas wells mature, with acute toxicity of early-stage flowback measuring higher than that of later FPW for both sediment-containing and sediment-free fractions in both wells (Figure 2.1). Toxicity of FPW in M-4 remained high for more than 9 months (280 days) after flowback began, then declined in subsequent months for both fractions (Figure 2.1a). A similar temporal trend was observed in M-5, although toxicity diminished at an earlier time, by 4 months post-stimulation (Figure 2.1b). Negative INH% was measured in FPW samples from both M-4 and M-5 after nine months production (from 406 to 764 days), indicating the halotolerant bacteria *A. fischeri* was actually stimulated by the geochemistry of later produced fluid samples above that of the negative control, which only contained cells and background diluent (Figure 2.1a, 2.1b). Although we cannot pinpoint an explanation for this effect based on our collected data, one possibility is that constituents present in these fluids might serve as additional carbon, nutrient, or energy sources for this taxon, stimulating its growth. Compared with the two Marcellus wells, FPW acute toxicity from Utica-Point Pleasant Formation natural gas well samples decreased very quickly. Samples from U-6 diminished in toxicity within 30 days, while samples from U-7 showed no acute toxicity regardless of time sampled for both sediment-containing and sediment free fractions (Figure 2.1c and d). To put these acute toxicity values in perspective, we calculated their half maximal effective concentration (EC_{50}), then applied the classification scheme developed by Persoone et al (Persoone, Goyvaerts et al. 1993), which categorically ranks values from non-toxic to extremely toxic. Early flowback samples in M-4, M-5, and U-6 ranged from slightly toxic to toxic, with the highest classified toxicity in days 2, 9 and 119 of flowback in M-5. Using this criteria, FPW samples that were collected from mature wells, or wells producing natural gas for greater than one year, were classified as non-toxic (Figure 2.1).

Based on previous studies (Blewett, Delompré et al. 2017, Folkerts, Blewett et al. 2017, Folkerts, Blewett et al. 2017, He, Folkerts et al. 2017), we expected the removal of sediments and associated metals and/or hydrophobic organic matter to decrease toxicity in FPW samples. However, for samples measuring positive toxicity in the two Marcellus and one Utica well (280 days or less, M-4; 119 days or less, M-5; 22 days or less, U-6), we detected no significant difference between sediment-containing and sediment-free fractions for individual wells (Figure 2.2a). We observed samples from one Marcellus well (M-5) contained average higher toxicity than the other on the same well pad (M-4) for both sediment-containing and sediment-free fractions ($p<0.05$). However, average acute toxicities for the Utica well samples (U-6) did not significantly differ from sediment-containing or sediment-free fractions in either M-4 or M-5 indicating that the toxins are primarily dissolved. Altogether, these data suggest acute toxicity of FPW samples from these four natural gas wells as measured using the *A. fischeri* BLIA assay is primarily influenced by sample timing and specific well additives, as opposed to sample fraction or Appalachian shale formation.

2.3.2 Input media containing additives show high toxicity

In samples showing positive acute toxicity, the average INH% of both sediment-containing fractions (M-4 and M-5) and sediment free the undiluted toxicity of M-5 and U-6 samples would likely be similar to or considerably higher than the positive control during the first few months of flowback assuming extrapolation of the acute toxicity response within this dilution range. We verified that the assay response was not solely due to major ions by analyzing the toxicity of a salt control. The average INH% of acute toxicity in the salt control was on par with the negative toxicities measured in all four mature wells studied (Figure 2.2b), which is unsurprising given that *A. fischeri* is a moderate halophile (Gallardo, Candia et al. 2016). Among the media tested for

toxicity from these sites, input muds and fluids (drill mud, sidewall mud, and kill fluid) exhibited the highest INH%, while produced water and recycled produced water additives exhibited lower INH% (Figure 2.2c).

Unsurprisingly, negative inhibition was measured in the freshwater used as the source fluid in U-6 and U-7 (Figure 2.2c). Importantly, the dilution factors for these media varied considerably, ranging from 1 to 7 for all except the drill mud, which required a 70-fold dilution (see Table A2).

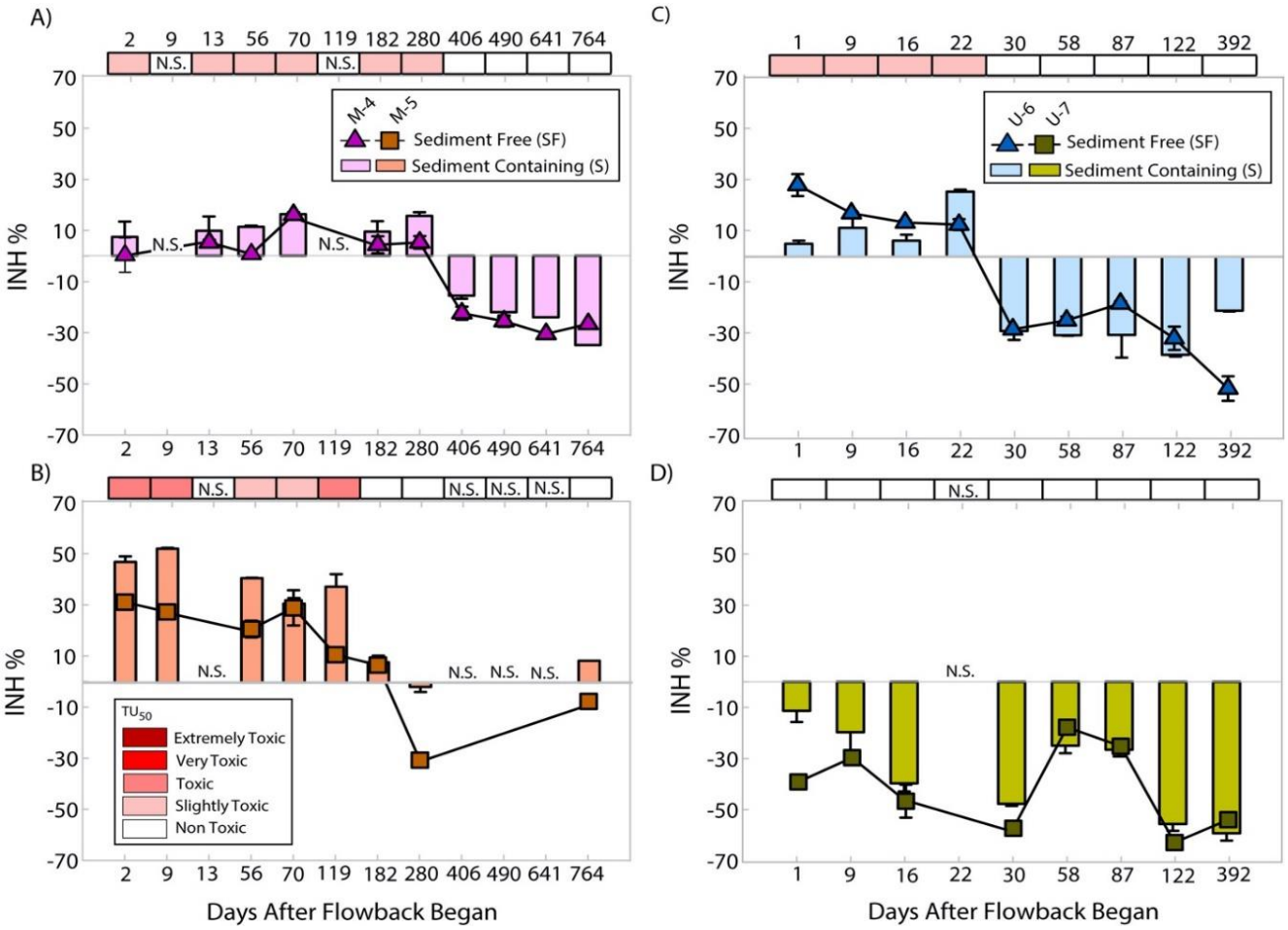

Figure 2.1 Acute toxicity of flowback and produced water measured using the *A. fischeri* BLIA assay from Marcellus Shale natural-gas wells M-4 (A) and M-5 (B), and Utica natural gas wells U-6 (C) and U-7 (D). Sediment containing fractions are depicted as bars while sediment-free fractions are shown as lines with markers. Boxes above each figure represents toxicity classification (TU_{50}) based on EC_{50} values determined from assay concentrations of sediment containing samples; N.S. indicates no sample was analyzed at that time point.

The Marcellus drill mud and sidewall mud were categorized as toxic while the kill fluid was classified as very toxic based on classification of half maximal effective concentration values (EC_{50}).

2.3.3 NAC thiol reactivity persists in Marcellus wells months after hydraulic fracturing

To further understand the specific pathways that may contribute to the acute toxicity measured using the *A. fischeri* assay, we applied a high-throughput NAC-based thiol reactivity assay that quantified a toxicity pathway predictive of mammalian cells for FPW samples collected up to 764 days post-stimulation from M-4 and M-5. Based on our acute toxicity results, we expected a decrease in thiol reactivity with time after hydraulic fracturing. Our results supported this hypothesis, as the thiol reactivity of early flowback was higher than that of mature produced fluids (Figure 2.3a). Although M-5 showed higher acute toxicity, its thiol reactivity diminished quickly, within 70 days post-stimulation. In contrast, M-4 had higher sustained NAC thiol reactivity

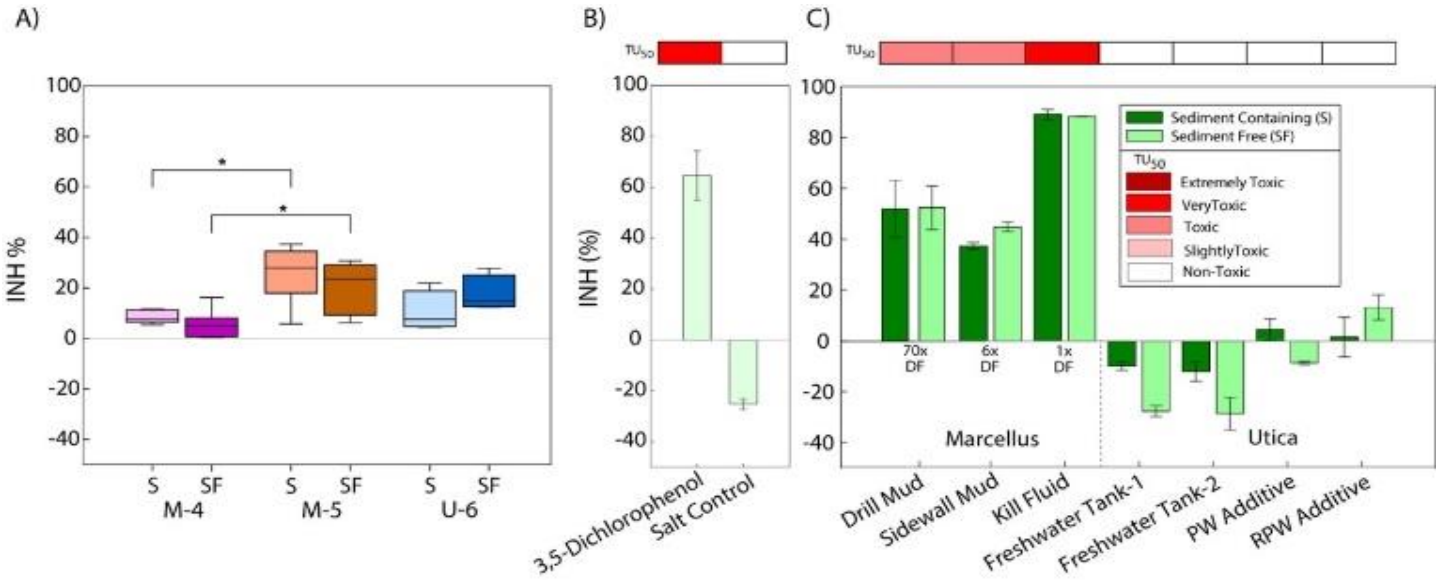

Figure 2.2 Average acute toxicity as measured using the *A. fischeri* BLIA assay of (A) FPW samples (*indicates statistical significance at $p<0.05$), (B) positive control (3,5-Dichlorophenol, 6.8 mg/l) and salt control and (C) input media from the Marcellus and Utica well pads.

through 182 days of flowback, with values on average 1.3 fold higher than M-5 (Figure 2.3b). Although we were unable to apply the NAC thiol reactivity to all input media used in the acute toxicity assay, we tested four input media samples that were processed using SPE: two fracture fluids and two input river fluids. The M-4 fracture fluid had higher NAC thiol reactivity response than the fracture fluid used in M-5, which is consistent with early FPW samples from these wells (Figure 2.3c). Recognizing sample concentration factors (CF) were 8 times higher for FPW samples (200x CF) compared with fracture fluids (25x CF, limited by SPE clogging from fracture fluid additives), measured fracture fluid NAC thiol toxicity was comparable to that of early FPW samples (Figure 2.3c), indicating injected fluids likely contained considerably higher thiol reactivity if differences in concentration factors were accounted for. Due to the non-linearity of thiol reactivity response, responses of less concentrated injected fluids were not extrapolated. Additionally, the composition of the fracture fluid before and after breaker addition (in well) could also influence the measured toxicity (e.g., possible formation of organohalides following breaker addition (Sumner and Plata 2019)). Interestingly, input river samples (200x CF) measured thiol

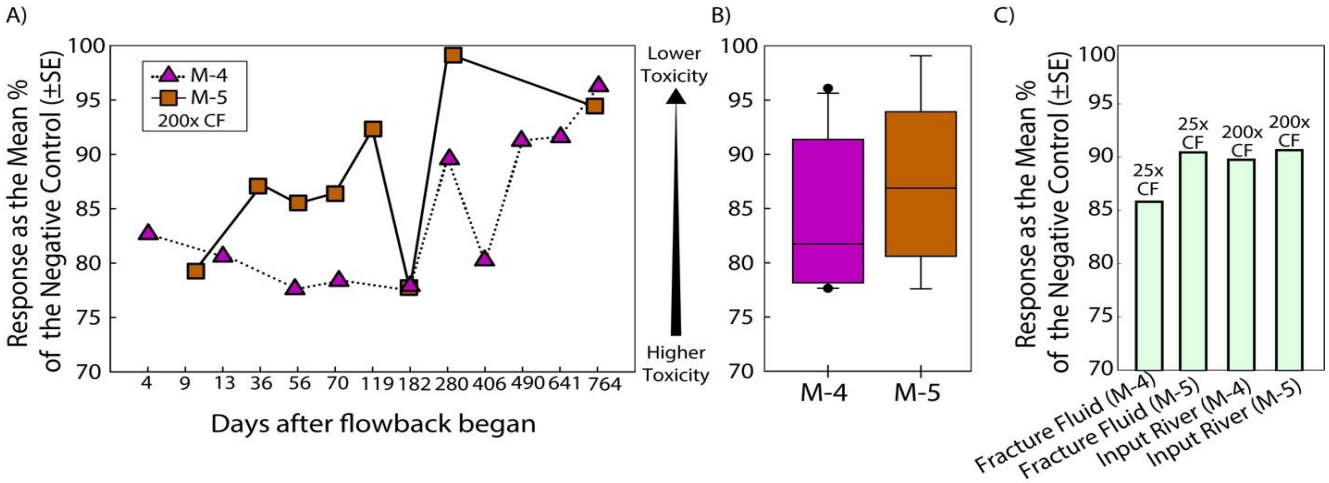

Figure 2.3 (A) NAC thiol reactivity for flowback and produced water from Marcellus Shale natural-gas wells M-4 and M-5. Average NAC thiol reactivity of (B) FPW samples and (C) input media from the Marcellus well pad samples.

reactivity response similar to that in later time points for both M-4 and M-5 (200x CF). These findings further support fracturing fluid additives as the source of toxicity in early FPW samples, with diminished toxicity as the natural gas well matures.

To further explore how results from the whole effluent acute toxicity assay (BLIA) related to the NAC thiol assay, which targeted electrophilic and redox reactive compounds in organic extracts, we compared their responses (Figure 2.4). These two toxicity assays were significantly inversely correlated to each other ($p<0.0001$), indicating high acute toxicity was associated with higher thiol reactivity. Moreover, the NAC thiol reactivity explained only about half the acute toxicity measured via the *A. fischeri* assay (Figure 2.4), which is not surprising, considering the BLIA is sensitive to a broad range of chemical compounds while NAC thiol is measuring a specific reaction between DNTB and NAC thiol groups. The NAC thiol reaction involves the nucleophilic attack of the thiolate on an electrophile (Ferrer-Sueta, Manta et al. 2011) and therefore its response would not include other forms of toxicity derived from the diverse chemical additives, products, and radionuclides commonly present in FPW samples.

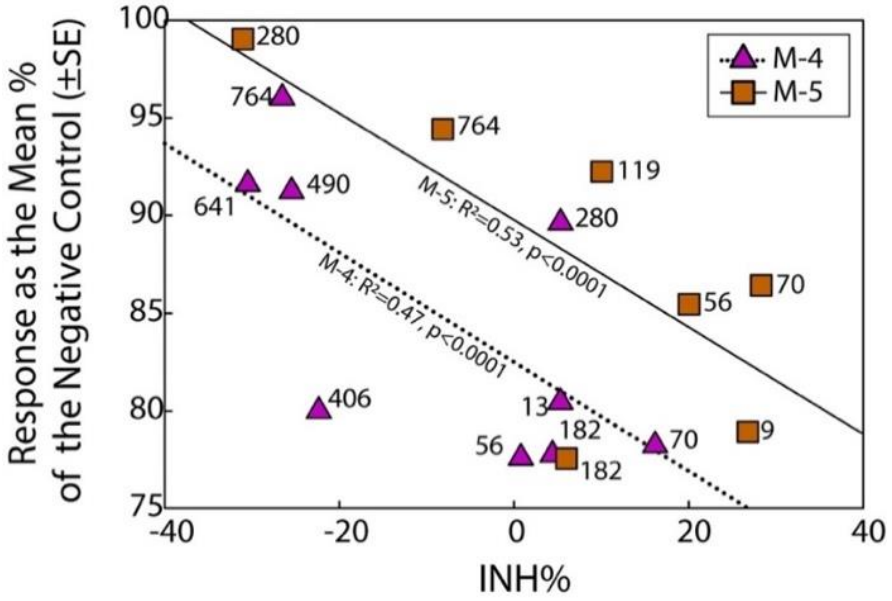

Figure 2.4 Comparison between the *A. fischeri* acute toxicity assay and the NAC thiol reactivity response for all FPW samples from M-4 and M-5.

2.3.4 Differences in toxicity are associated with variations in fracture fluid chemical additives

Since the samples from these four natural gas wells represent two well pairs on two different pads, we had the opportunity to examine differences in geochemistry and specific chemical additives that might influence the toxicity of input media and resulting FPW. Interestingly, the fracture fluid composition in M-5 had 18 additives added at 1.1 to 2.7 times higher concentration than M-4, while only 5 additives were higher in M-4 (Table A4 & A5). Moreover, a larger overall fraction of organic chemical additives were present in M-5, including the biocide C_{12}-C_{16} alkyl dimethylbenzyl ammonium chloride, breaker ethylene glycol, and the corrosion inhibitor methanol. These compounds are associated with oral acute toxicity (Yost, Stanek et al. 2016) identified by the EPA's Human Health Benchmarks for Pesticides and the EPA's Integrated Risk Information System database, which may in part explain the higher acute toxicity measured in M-5 through time. In contrast, M-4 fracture fluid contained 2.7 times higher concentration of guar gum (a gelling agent), 6.5 times higher polyacrylamide-co-acrylic acid and alcohol ethoxylates (friction reducers), and 74 times higher ammonium persulfate (an oxidative radical initiator) than M-5.

Although Hull et. al suggested labile organics (e.g., organic acids, guar gum) may mask toxicity of other additives (Hull, Rosenblum et al. 2018), our results show that M-4, which contained 2.7 times higher concentrations of guar gum than M-5, had lower acute toxicity but higher thiol reactivity. The combination of organic additives in M-5 likely contributed to its higher acute toxicity, while specific reactions initiated by ammonium persulfate (Sumner and Plata 2018, Sumner and Plata 2019) may explain the higher thiol reactivity in M-4 as compared to M-5. Halides compete with the intended radical reaction initiated by ammonium persulfate (Peyton

1993) and unsurprisingly ammonium persulfate has been shown to initiate halogenation of fracturing chemicals including cinnamaldehyde (Sumner and Plata 2018, Sumner and Plata 2019). Although these samples were desalted prior to analysis, organohalides generated through halogenation reactions would still be present in the extract, as evidenced by Luek et al (Luek, Harir et al. 2018).

In a similar capacity, we compared the disclosed chemical additives in U-6 and U-7, finding that six constituents were added at 1.1 to 1.5 higher concentration in U-6, including petroleum distillates, n-Alkyl dimethyl benzyl ammonium chloride and methanol (Table A6 & A7). These minor differences in overall chemical additive composition could partially explain differences in acute toxicity for U-6 well as compared to U-7. The n-Alkyl dimethyl benzyl ammonium chloride and methanol are associated with oral acute toxicity (Yost, Stanek et al. 2016, Hu, Liu et al. 2018) while certain petroleum distillates may not be readily biodegraded by the bacteria used in this assay.

2.3.5 Toxicity correlated with organic chemical concentrations

Based on these disclosed differences in organic chemical compositions, we further explored the relationship between BLIA acute and NAC thiol toxicity results and organic chemical measurements. A general trend in hydraulically fractured Appalachian Basin shales is a decrease in dissolved organic carbon concentration (DOC) with time after hydraulic fracturing (Cluff, Hartsock et al. 2014, Folkerts, Blewett et al. 2019). Consistent with studies of other well sites, DOC decreased through time in each of these four wells. Toxicity also decreased with time, therefore we identified a significant positive correlation between DOC and acute toxicity in the

Table 2.1 Hydraulic fracturing fluid additives of (A) Marcellus Shale natural-gas wells M-4 and M-5, and (B) Utica Point Pleasant Formation natural gas wells U-6 and U-7, as disclosed in the FracFocus database. Disclosed information was used to calculate fold differences in wells on the same pad. The intensity of box shading represents the fold difference in mass fractions for hydraulic fracturing fluid additives for wells from the same well pad and formation. Specific mass fractions for additives listed here are provided in Tables A4-A7. Dark grey shading indicates additive absent/fold difference not calculated due to the lack of information.

a)

CAS RNs	Ingredient	Fold difference in max concentration	
		M-4	M-5
14808-60-7	Quartz, Crystalline silica		
7647-01-0	Hydrochloric acid		
7783-20-2	Ammonium sulfate		
9000-30-0	Guar gum		
38193-60-1	Acrylamide[a]		
111-30-8	Glutaraldehyde		
68171-29-9	Sodium salt[b]		
7727-54-0	Diammonium peroxidisulphate		
136793-29-8	Methyl acrylate[c]		
68424-85-1	Alkyl (c12-16) DAC[d]		
6381-77-7	Sodium erythorbate		
7601-54-9	Trisodium ortho phosphate		
57-13-6	Urea		
25322-69-4	Polypropylene glycol		
67-56-1	Methanol		
61790-12-3	Fatty acids, tall-oil		
68527-49-1	Thiourea, polymer[e]		
107-21-1	Ethylene Glycol		
7631-86-9	Non-crystalline silica		
25038-72-6	Halogenated polymers[f]		
7757-82-6	Sodium sulfate		
68951-67-7	Alcohols, alkoxylated[g]		
64-17-5	Ethanol		
107-19-7	Propargyl alcohol		
79-06-1	2-Propenamid (impurity)		
629-73-2	Hexadec-1-ene		
112-88-9	1-Octadecene (C18)		
63148-62-9	Silicones[h]		
64-02-8	TSEDT		
67762-90-7	Silica[i]		
556-67-2	Octamethylcyclotetrasiloxane		
9002-84-0	Poly (tetrafluoroethylene)		
50-00-0	Formaldehyde		
541-02-6	Decamethyl cyclopentasiloxane		
14807-96-6	Magnesium silicate hydrate		
9003-06-9	Polyacrylamide-co-acrylic acid		
7647-14-5	Sodium Chloride		
Trade	Alcohol Ethoxylate Surfactants		
64742-47-8	Petroleum Distillate		

[a]Acrylamide, 2-acrylamido-2-methylpropanesulfonic acid, sodium salt polymer

[b]Ethanol, 2,2',2''-nitrilotris-, 1,1',1''-tris (dihydrogen phosphate), sodium salt

[c] Polymer of 2-acrylamido-2-methylpropanesulfonic acid sodium salt and methyl acrylate

[d] Alkyl (c12-16) dimethylbenzyl ammonium chloride

[e] Thiourea, polymer with formaldehyde and 1-phenylethanone

[f]Halogenated polymers: Vinylidene chloride/methylacrylate copolymer

[g] Alcohols, C14-15, ethoxylated (7EO)

[h] Dimethyl siloxanes and silicones

[i] Siloxanes and silicones, dimethyl, reaction products with silica

b)

CAS RNs	Ingredient	Fold difference in max concentration	
		U-6	U-7
14808-60-7	Sand		
7647-01-0	Hydrogen chloride		
69418-26-4	Acrylamide[a]		
Proprietary	Proprietary		
64742-47-8	Petroleum Distillate		
84133-50-6	Alcohol – alkoxylated[b]		
124-04-9	Adipic acid		
111-30-8	Glutaraldehyde		
7173-51-5	DD ammonium chloride[c]		
68424-85-1	n-Alkyl dimethyl BAC[d]		
64-17-5	Ethanol		
7722-84-1	Hydrogen Peroxide		
Proprietary	Sodium Polyacrylate		
9000-30-0	Guar Gum		
64742-47-8	Light petroleum distillates[e]		
Proprietary	Organophylic Clay		
34398-01-1	Alcohol ethoxylate		
14808-60-7	Crystalline Silica		
67-56-1	Methanol		

[a]Ethanaminium, N,N,N-trimethyl-2-[(1-oxo-2-propenyl)oxy]-, -chloride, polymer with 2-propenamide

[b] Alcohols, C12-14-secondary, ethoxylated

[c] Didecyl dimethyl ammonium chloride

[d] n-Alkyl dimethyl benzyl ammonium chloride

[e] Distillate (petroleum), hydrotreated light

Legend

10-100

5-10

1-5

0-1

No Data

sediment free fraction (SF) of M-5 and sediment containing fraction (S) of M-4 ($p<0.05$). In addition, a weak correlation between DOC and BLIA acute toxicity was observed for U-6 ($R^2=0.5$) and U-7 ($R^2=0.54$). No significant correlation was found between DOC concentrations and thiol reactivity for either M-4 or M-5. Samples from M-4 and M-5 were also analyzed for several organic constituents (BTEX, MBAS, oil and grease (O&G), Table A8) frequently detected in produced waters (Coalition and Hayes 2009, Lester, Ferrer et al. 2015, Ziemkiewicz and He 2015, Hoelzer, Sumner et al. 2016, Khan, Engle et al. 2016, Rosenblum, Thurman et al. 2017). Like bulk DOC, the concentration of BTEX, MBAS, and O&G generally decreased in M-4 and M-5 natural-gas wells as they matured (Figure A2A-Figure A2C). Benzene and toluene were found in all FPW samples, with the highest benzene (14 µg/L, day 8) and toluene (53 µg/L, 42 days) measured in M-5 (Figure A2A). Similarly, MBAS and O&G were present in all FPW samples, with M-5 containing higher MBAS (3mg/L, 402 days) and O&G concentrations (500 mg/L, 56 days) (Figure A2A and A2B). MBAS concentrations were positively correlated with acute toxicity ($p<0.05$) for both S and SF fractions from M-4 and for SF fractions from M-5. Ethylbenzene, total xylenes, m,p-xylene, and o-xylene varied through time from non-detect to 31 µg/L in the two Marcellus wells (Figure A2B and A2C). Both benzene and toluene were positively correlated to acute toxicity ($p<0.05$) in M-4 for both S and SF fractions, as well as the SF fractions in M-5.

The M-4 and M-5 samples analyzed here were also assessed for halogenated organic ions characterized in a previous study using the non-target mass spectrometry approach FT-ICR-MS(Luek, Harir et al. 2018). Luek and coauthers (Luek, Harir et al. 2018) identified dozens of previously uncharacterized iodinated organic ions (Table A9) and suggested the compounds could be associated with toxicological effects based on previously characterized species (e.g. disinfection byproducts) (Dong, Masalha et al. 2017, Dong, Massalha et al. 2018, Dong, Page et al. 2018, Dong,

Page et al. 2019). A recent study demonstrated enhanced mammalian cell cytotoxicity due to the generation of iodinated organic compounds that formed during chloramination of oil and gas wastewaters (Liberatore, Plewa et al. 2017). Here, we found a significant correlation between acute toxicity measurements and the number of detected iodinated ions ($p<0.05$) for both S and SF fractions from M-5. However, a similar correlation was not seen in M-4 samples, potentially due to the overall lower acute toxicity level measured therein. Lastly, we investigated the relationship between NAC thiol reactivity and specific organic chemical concentrations (*inc.*, BTEX, MBAS, O&G, and iodinated organic ions). Only benzene and toluene were positively correlated to NAC thiol reactivity in M-5 ($p<0.05$) while the concentration of all other constituents were statistically unrelated.

2.4 Conclusion

In this work, we sought to investigate how toxicity of hydraulic fracturing media differed across formations and through time. We also aimed to separate toxicity effects from inorganic salts versus organic constituents, and constituents associated with solids as opposed to those in the dissolved phase. The high salinity of hydraulic fracturing wastewater is a primary mechanism of toxicity for freshwater organisms, but other potentially harmful chemical compounds are present (Blewett, Delompré et al. 2017, He, Sun et al. 2018, Delompré, Blewett et al. 2019). Here, our application of a BLIA screening assay employing a halotolerant bacterium identified acute toxicity of FPW beyond salinity that is broadly associated with changes in dissolved constituents. Although distinguishing between toxicity effects for specific chemical additives, for compounds generated by these chemical additives within the formation, or for other constituents liberated by these additives outside of salinity (e.g., radionuclides) was beyond the scope of this study, the results

from our acute screening assay is in agreement with recent whole organism toxicity studies reporting toxicity and other adverse effects derived from organic compounds in FPW (Blewett, Delompré et al. 2018), (He, Flynn et al. 2017, He, Sun et al. 2018). In contrast to previous work that identified toxicity in higher order organisms is associated with solid fractions (He, Flynn et al. 2017, He, Folkerts et al. 2017), here we found no significant difference in acute toxicity for sediment-containing versus filtered fractions of wastewater, indicating the halotolerant bacteria used in the BLIA assay are more sensitive to dissolved constituents.

Our work shows the acute toxicity and NAC thiol reactivity of FPW is highest during initial flowback and diminishes as the natural gas well matures. Importantly, toxicity as measured by these assays was associated with the dissolved sample fraction and was correlated to bulk organic carbon concentrations, specific organic constituents (MBAS, benzene, toluene), and the number of iodinated compounds in these wells. Higher toxicity in early flowback samples is in agreement with a study tracking acute toxicity of FPW samples in the Denver–Julesburg Basin (Hull, Rosenblum et al. 2018) although our data provides a broader assessment of these trends through time, utilizes replicate wells on a pad, and encompasses two shale formations that differ considerably in depth and geological characteristics from Denver-Julesburg Basin. Moreover, our work is consistent with that of Folkerts et al (Folkerts, Blewett et al. 2019), who show earlier FPW samples to be more toxic to *Daphnia magna*, *Lumbriculus variegatus*, *Danio rerio*, and *Oncorhynchus mykiss*. The chemical additives highlighted here could pose toxicity in their original form, via the compounds they generate through abiotic or biotic mechanisms before or after injection, or through the chemicals they liberate from the formation (Sumner and Plata 2018, Evans, Sumner et al. 2019, Sumner and Plata 2019). Although difficult to quantify, our work suggests toxicity for the measured endpoints is higher for FPW samples when larger quantities of

specific chemical additives are applied, including oxidative radical initiators, biocides and surfactants. Moreover, we also observed that samples with the highest NAC thiol reactivity derived from well samples utilizing injected fluids that specifically contained a higher amount of oxidative radical chemicals. This finding is consistent with related studies quantifying NAC thiol reactivity in water and wastewater samples receiving higher oxidative inputs from disinfection processes (Dong, Massalha et al. 2018, Dong, Page et al. 2018, Massalha, Plewa et al. 2020), which are thought to initiate the biological thiol-specific detoxification mechanism and suggests that similar reactions may occur in the fractured shale system.

Our results support the need for careful management of wastewater from hydraulically fractured shale wells, particularly during the handling of injection fluids and fluids initially returning from the well after hydraulic fracturing in order to reduce their release to the environment. Higher acute toxicity in early flowback is particularly problematic for wastewater management in "tight" hydraulically fractured formations, such as shale gas, as the largest volume of water is produced during initial flowback. Our findings further highlight the need for additional testing of multiple toxicity end points to better characterize differences in FPW toxicity that vary through time and geologic formation as well as assess potential interactions between chemical additives.

Acknowledgements

This research was supported by funding from the National Science Foundation Chemical Biological and Environmental Transport (CBET) grant number 1823069. We thank the Department of Energy National Energy Technology Laboratory through the Marcellus Shale Energy and Environmental Laboratory (project #DE-FE0024297, PI Timothy Carr) and two industry partners for site access and sample support. The authors would like to thank Dr. Michael Gonsior for providing samples, and Dr. Michael Plewa for considerable assistance in modifying the NAC thiol reactivity for these samples, and his constructive feedback on the manuscript.

2.5 References

Alessi, D. S., A. Zolfaghari, S. Kletke, J. Gehman, D. M. Allen and G. G. Goss (2017). "Comparative analysis of hydraulic fracturing wastewater practices in unconventional shale development: Water sourcing, treatment and disposal practices." Canadian Water Resources Journal/Revue canadienne des ressources hydriques **42**(2): 105-121.

Arthur, J. D., B. K. Bohm and D. Cornue (2009). Environmental considerations of modern shale gas development. SPE annual technical conference and exhibition, Society of Petroleum Engineers.

Barbot, E., N. S. Vidic, K. B. Gregory and R. D. Vidic (2013). "Spatial and temporal correlation of water quality parameters of produced waters from Devonian-age shale following hydraulic fracturing." Environmental Science & Technology **47**(6): 2562-2569.

Blewett, T. A., P. L. Delompré, C. N. Glover and G. G. Goss (2018). "Physical immobility as a sensitive indicator of hydraulic fracturing fluid toxicity towards Daphnia magna." Science of The Total Environment **635**: 639-643.

Blewett, T. A., P. L. Delompré, Y. He, E. J. Folkerts, S. L. Flynn, D. S. Alessi and G. G. Goss (2017). "Sublethal and reproductive effects of acute and chronic exposure to flowback and produced water from hydraulic fracturing on the water flea Daphnia magna." Environmental Science & Technology **51**(5): 3032-3039.

Blewett, T. A., A. M. Weinrauch, P. L. Delompré and G. G. Goss (2017). "The effect of hydraulic flowback and produced water on gill morphology, oxidative stress and antioxidant response in rainbow trout (Oncorhynchus mykiss)." Scientific Reports **7**: 46582.

Borton, M. A., D. W. Hoyt, S. Roux, R. A. Daly, S. A. Welch, C. D. Nicora, S. Purvine, E. K. Eder, A. J. Hanson and J. M. Sheets (2018). "Coupled laboratory and field investigations resolve microbial interactions that underpin persistence in hydraulically fractured shales." Proceedings of the National Academy of Sciences **115**(28): E6585-E6594.

Cluff, M. A., A. Hartsock, J. D. MacRae, K. Carter and P. J. Mouser (2014). "Temporal changes in microbial ecology and geochemistry in produced water from hydraulically fractured Marcellus shale gas wells." Environmental Science & Technology **48**(11): 6508-6517.

Coalition, M. S. and T. Hayes (2009). "Sampling and Analysis of Water Streams Associated with the Development of Marcellus Shale Gas."

Cotou, E., E. Papathanassiou and C. Tsangaris (2002). "Assessing the quality of marine coastal environments: comparison of scope for growth and Microtox® bioassay results of pollution gradient areas in eastern Mediterranean (Greece)." Environmental Pollution **119**(2): 141-149.

Daly, R. A., M. A. Borton, M. J. Wilkins, D. W. Hoyt, D. J. Kountz, R. A. Wolfe, S. A. Welch, D. N. Marcus, R. V. Trexler and J. D. MacRae (2016). "Microbial metabolisms in a 2.5-km-deep ecosystem created by hydraulic fracturing in shales." Nature Microbiology **1**(10): 1-9.

Danforth, C., W. A. Chiu, I. Rusyn, K. Schultz, A. Bolden, C. Kwiatkowski and E. Craft (2020). "An integrative method for identification and prioritization of constituents of concern in produced water from onshore oil and gas extraction." Environment International **134**: 105280.

Delompré, P., T. Blewett, G. Goss and C. Glover (2019). "Shedding light on the effects of hydraulic fracturing flowback and produced water on phototactic behavior in Daphnia magna." Ecotoxicology and Environmental Safety **174**: 315-323.

DiGiulio, D. C. and R. B. Jackson (2016). "Impact to underground sources of drinking water and domestic wells from production well stimulation and completion practices in the Pavillion, Wyoming, field." Environmental Science & Technology **50**(8): 4524-4536.

Dittmar, T., B. Koch, N. Hertkorn and G. Kattner (2008). "A simple and efficient method for the solid-phase extraction of dissolved organic matter (SPE-DOM) from seawater." Limnology and Oceanography: Methods **6**(6): 230-235.

Dong, S., N. Masalha, M. J. Plewa and T. H. Nguyen (2017). "Toxicity of wastewater with elevated bromide and iodide after chlorination, chloramination, or ozonation disinfection." Environmental Science & Technology **51**(16): 9297-9304.

Dong, S., N. Massalha, M. J. Plewa and T. H. Nguyen (2018). "The impact of disinfection Ct values on cytotoxicity of agricultural wastewaters: Ozonation vs. chlorination." Water Research **144**: 482-490.

Dong, S., M. A. Page, N. Massalha, A. Hur, K. Hur, K. Bokenkamp, E. D. Wagner and M. J. Plewa (2019). "Toxicological comparison of water, wastewaters, and processed wastewaters." Environmental science & technology **53**(15): 9139-9147.

Dong, S., M. A. Page, E. D. Wagner and M. J. Plewa (2018). "Thiol reactivity analyses to predict mammalian cell cytotoxicity of water samples." Environmental Science & Technology **52**(15): 8822-8829.

EIA (2013). Technically Recoverable Shale Oil and Shale Gas Resources. **10:** 2013.

Elliott, E. G., A. S. Ettinger, B. P. Leaderer, M. B. Bracken and N. C. Deziel (2017). "A systematic evaluation of chemicals in hydraulic-fracturing fluids and wastewater for reproductive and developmental toxicity." Journal of Exposure Science & Environmental Epidemiology **27**(1): 90-99.

Ellman, G. L. (1959). "Tissue sulfhydryl groups." Archives of biochemistry and biophysics **82**(1): 70-77.

Elsner, M. and K. Hoelzer (2016). "Quantitative survey and structural classification of hydraulic fracturing chemicals reported in unconventional gas production." Environmental Science & Technology **50**(7): 3290-3314.

EPA, U. (2016). Hydraulic fracturing for oil and gas: Impacts from the hydraulic fracturing water cycle on drinking water resources in the united states. Washington, DC: US Environmental Protection Agency, EPA/600/R-16.

Evans, M. V., J. Panescu, A. J. Hanson, S. A. Welch, J. M. Sheets, N. Nastasi, R. A. Daly, D. R. Cole, T. H. Darrah and M. J. Wilkins (2018). "Members of Marinobacter and Arcobacter influence system biogeochemistry during early production of hydraulically fractured natural gas wells in the Appalachian basin." Frontiers in microbiology **9**: 2646.

Evans, M. V., A. J. Sumner, R. A. Daly, J. L. Luek, D. L. Plata, K. C. Wrighton and P. J. Mouser (2019). "Hydraulically fractured natural-gas well microbial communities contain genomic halogenation and dehalogenation potential." Environmental Science & Technology Letters **6**(10): 585-591.

Ferrer-Sueta, G., B. Manta, H. Botti, R. Radi, M. Trujillo and A. Denicola (2011). "Factors affecting protein thiol reactivity and specificity in peroxide reduction." Chemical Research in Toxicology **24**(4): 434-450.

Folkerts, E. J., T. A. Blewett, P. Delompré, W. T. Mehler, S. L. Flynn, C. Sun, Y. Zhang, J. W. Martin, D. S. Alessi and G. G. Goss (2019). "Toxicity in aquatic model species exposed to a temporal series of three different flowback and produced water samples collected

from a horizontal hydraulically fractured well." Ecotoxicology and Environmental Safety **180**: 600-609.

Folkerts, E. J., T. A. Blewett, Y. He and G. G. Goss (2017). "Alterations to Juvenile Zebrafish (Danio rerio) swim performance after acute embryonic exposure to sub-lethal exposures of hydraulic fracturing flowback and produced water." Aquatic Toxicology **193**: 50-59.

Folkerts, E. J., T. A. Blewett, Y. He and G. G. Goss (2017). "Cardio-respirometry disruption in zebrafish (Danio rerio) embryos exposed to hydraulic fracturing flowback and produced water." Environmental Pollution **231**: 1477-1487.

Gallardo, K., J. E. Candia, F. Remonsellez, L. V. Escudero and C. S. Demergasso (2016). "The ecological coherence of temperature and salinity tolerance interaction and pigmentation in a non-marine Vibrio isolated from Salar de Atacama." Frontiers in Microbiology **7**: 1943.

Harkness, J. S., G. S. Dwyer, N. R. Warner, K. M. Parker, W. A. Mitch and A. Vengosh (2015). "Iodide, bromide, and ammonium in hydraulic fracturing and oil and gas wastewaters: environmental implications." Environmental Science & Technology **49**(3): 1955-1963.

He, Y., S. L. Flynn, E. J. Folkerts, Y. Zhang, D. Ruan, D. S. Alessi, J. W. Martin and G. G. Goss (2017). "Chemical and toxicological characterizations of hydraulic fracturing flowback and produced water." Water Research **114**: 78-87.

He, Y., E. J. Folkerts, Y. Zhang, J. W. Martin, D. S. Alessi and G. G. Goss (2017). "Effects on biotransformation, oxidative stress, and endocrine disruption in rainbow trout (Oncorhynchus mykiss) exposed to hydraulic fracturing flowback and produced water." Environmental science & technology **51**(2): 940-947.

He, Y., C. Sun, Y. Zhang, E. J. Folkerts, J. W. Martin and G. G. Goss (2018). "Developmental toxicity of the organic fraction from hydraulic fracturing flowback and produced waters to early life stages of Zebrafish (Danio rerio)." Environmental Science & Technology **52**(6): 3820-3830.

He, Y., Y. Zhang, J. W. Martin, D. S. Alessi, J. P. Giesy and G. G. Goss (2018). "In vitro assessment of endocrine disrupting potential of organic fractions extracted from hydraulic fracturing flowback and produced water (HF-FPW)." Environment International **121**: 824-831.

Hoelzer, K., A. J. Sumner, O. Karatum, R. K. Nelson, B. D. Drollette, M. P. O'Connor, E. L. D'Ambro, G. J. Getzinger, P. L. Ferguson and C. M. Reddy (2016). "Indications of transformation products from hydraulic fracturing additives in shale-gas wastewater." Environmental Science & Technology **50**(15): 8036-8048.

Hu, G., T. Liu, J. Hager, K. Hewage and R. Sadiq (2018). "Hazard assessment of hydraulic fracturing chemicals using an indexing method." Science of the Total Environment **619**: 281-290.

Hull, N. M., J. S. Rosenblum, C. E. Robertson, J. K. Harris and K. G. Linden (2018). "Succession of toxicity and microbiota in hydraulic fracturing flowback and produced water in the Denver–Julesburg Basin." Science of the Total Environment **644**: 183-192.

Johnson, E. G. and L. A. Johnson (2012). "Hydraulic fracture water usage in northeast British Columbia: Locations, volumes and trends." Geoscience Reports **2012**: 41-63.

Khan, N. A., M. Engle, B. Dungan, F. O. Holguin, P. Xu and K. C. Carroll (2016). "Volatile-organic molecular characterization of shale-oil produced water from the Permian Basin." Chemosphere **148**: 126-136.

Kim, S., P. Omur-Ozbek, A. Dhanasekar, A. Prior and K. Carlson (2016). "Temporal analysis of flowback and produced water composition from shale oil and gas operations: Impact of frac fluid characteristics." Journal of Petroleum Science and Engineering **147**: 202-210.

Kondash, A. and A. Vengosh (2015). "Water footprint of hydraulic fracturing." Environmental Science & Technology Letters **2**(10): 276-280.

Kondash, A. J., N. E. Lauer and A. Vengosh (2018). "The intensification of the water footprint of hydraulic fracturing." Science Advances **4**(8): eaar5982.

Kondash, A. J., D. Patino-Echeverri and A. Vengosh (2019). "Quantification of the water-use reduction associated with the transition from coal to natural gas in the US electricity sector." Environmental Research Letters **14**(12): 124028.

Lester, Y., I. Ferrer, E. M. Thurman, K. A. Sitterley, J. A. Korak, G. Aiken and K. G. Linden (2015). "Characterization of hydraulic fracturing flowback water in Colorado: implications for water treatment." Science of the Total Environment **512**: 637-644.

Liberatore, H. K., M. J. Plewa, E. D. Wagner, J. M. VanBriesen, D. B. Burnett, L. H. Cizmas and S. D. Richardson (2017). "Identification and comparative mammalian cell cytotoxicity

of new iodo-phenolic disinfection byproducts in chloraminated oil and gas wastewaters." Environmental Science & Technology Letters **4**(11): 475-480.

Luek, J. L., M. Harir, P. Schmitt-Kopplin, P. J. Mouser and M. Gonsior (2018). "Temporal dynamics of halogenated organic compounds in Marcellus Shale flowback." Water Research **136**: 200-206.

Massalha, N., M. J. Plewa, T. H. Nguyen and S. Dong (2020). "Influence of Anaerobic Mesophilic and Thermophilic Digestion on Cytotoxicity of Swine Wastewaters." Environmental Science & Technology **54**(5): 3032-3038.

McAdams, B. C., K. E. Carter, J. Blotevogel, T. Borch and J. A. Hakala (2019). "In situ transformation of hydraulic fracturing surfactants from well injection to produced water." Environmental Science: Processes & Impacts **21**(10): 1777-1786.

McLaughlin, M. C., T. Borch, B. McDevitt, N. R. Warner and J. Blotevogel (2020). "Water quality assessment downstream of oil and gas produced water discharges intended for beneficial reuse in arid regions." Science of The Total Environment **713**: 136607.

Mehler, W. T., A. Nagel, S. Flynn, Y. Zhang, C. Sun, J. Martin, D. Alessi and G. G. Goss (2020). "Understanding the effects of hydraulic fracturing flowback and produced water (FPW) to the aquatic invertebrate, Lumbriculus variegatus under various exposure regimes." Environmental Pollution: 113889.

Meister, A. and M. E. Anderson (1983). "Glutathione." Annual review of biochemistry **52**(1): 711-760.

Pals, J. A., E. D. Wagner and M. J. Plewa (2016). "Energy of the lowest unoccupied molecular orbital, thiol reactivity, and toxicity of three monobrominated water disinfection byproducts." Environmental Science & Technology **50**(6): 3215-3221.

Pals, J. A., E. D. Wagner, M. J. Plewa, M. Xia and M. S. Attene-Ramos (2017). "Monohalogenated acetamide-induced cellular stress and genotoxicity are related to electrophilic softness and thiol/thiolate reactivity." Journal of Environmental Sciences **58**: 224-230.

Parmaki, S., I. Vyrides, M. I. Vasquez, V. Hartman, I. Zacharia, I. Hadjiadamou, C. B. Barbeitos, F. C. Ferreira, C. A. Afonso and C. Drouza (2018). "Bioconversion of alkaloids to high-value chemicals: Comparative analysis of newly isolated lupanine degrading strains." Chemosphere **193**: 50-59.

Persoone, G., M. Goyvaerts, C. Janssen, W. De Coen and M. Vangheluwe (1993). "Cost-effective acute hazard monitoring of polluted waters and waste dumps with the aid of Toxkits." Final Report EEC, Contract ACE **89**.

Peyton, G. R. (1993). "The free-radical chemistry of persulfate-based total organic carbon analyzers." Marine Chemistry **41**(1-3): 91-103.

Rigol, A., A. Latorre, S. Lacorte and D. Barceló (2004). "Bioluminescence inhibition assays for toxicity screening of wood extractives and biocides in paper mill process waters." Environmental Toxicology and Chemistry: An International Journal **23**(2): 339-347.

Rosenblum, J., E. M. Thurman, I. Ferrer, G. Aiken and K. G. Linden (2017). "Organic chemical characterization and mass balance of a hydraulically fractured well: From fracturing fluid to produced water over 405 days." Environmental Science & Technology **51**(23): 14006-14015.

Rowan, E., M. Engle, C. Kirby and T. Kraemer (2011). "Radium content of oil-and gas-field produced waters in the Northern Appalachian Basin (USA): Summary and discussion of data." US Geological Survey Scientific Investigations Report **5135**(2011): 31.

Shemer, H. and K. G. Linden (2007). "Photolysis, oxidation and subsequent toxicity of a mixture of polycyclic aromatic hydrocarbons in natural waters." Journal of Photochemistry and Photobiology A: Chemistry **187**(2-3): 186-195.

Stringfellow, W. T., J. K. Domen, M. K. Camarillo, W. L. Sandelin and S. Borglin (2014). "Physical, chemical, and biological characteristics of compounds used in hydraulic fracturing." Journal of Hazardous Materials **275**: 37-54.

Sumner, A. J. and D. L. Plata (2018). "Halogenation chemistry of hydraulic fracturing additives under highly saline simulated subsurface conditions." Environmental science & technology **52**(16): 9097-9107.

Sumner, A. J. and D. L. Plata (2019). "Oxidative Breakers Can Stimulate Halogenation and Competitive Oxidation in Guar-Gelled Hydraulic Fracturing Fluids." Environmental science & technology **53**(14): 8216-8226.

Sun, Y., D. Wang, D. C. Tsang, L. Wang, Y. S. Ok and Y. Feng (2019). "A critical review of risks, characteristics, and treatment strategies for potentially toxic elements in wastewater from shale gas extraction." Environment International **125**: 452-469.

Tasker, T., W. D. Burgos, P. Piotrowski, L. Castillo-Meza, T. Blewett, K. Ganow, A. Stallworth, P. Delompré, G. Goss and L. B. Fowler (2018). "Environmental and human health impacts of spreading oil and gas wastewater on roads." Environmental science & technology **52**(12): 7081-7091.

Timbrell, J. A. (2008). Principles of Biochemical Toxicology. Boca Raton, CRC Press.

Townsend, D. M., K. D. Tew and H. Tapiero (2003). "The importance of glutathione in human disease." Biomedicine & pharmacotherapy **57**(3-4): 145-155.

Vengosh, A., R. B. Jackson, N. Warner, T. H. Darrah and A. Kondash (2014). "A critical review of the risks to water resources from unconventional shale gas development and hydraulic fracturing in the United States." Environmental Science & Technology **48**(15): 8334-8348.

Warner, N. R., C. A. Christie, R. B. Jackson and A. Vengosh (2013). "Impacts of shale gas wastewater disposal on water quality in western Pennsylvania." Environmental Science & Technology **47**(20): 11849-11857.

Yost, E. E., J. Stanek, R. S. DeWoskin and L. D. Burgoon (2016). "Overview of chronic oral toxicity values for chemicals present in hydraulic fracturing fluids, flowback, and produced waters." Environmental Science & Technology **50**(9): 4788-4797.

Ziemkiewicz, P. F. and Y. T. He (2015). "Evolution of water chemistry during Marcellus Shale gas development: A case study in West Virginia." Chemosphere **134**: 224-231.

Chapter 3. The Fate of SARS-CoV-2 Viral RNA in Coastal New England Wastewater Treatment Plants

This chapter has been submitted for publication in the following form:

Aghababaei, M., Colosimo, F., Malley, J.P., Mouser, P.J. (2022). The Fate of SARS-CoV-2 Viral RNA in Coastal New England Wastewater Treatment Plants. *ACS ES&T Water*

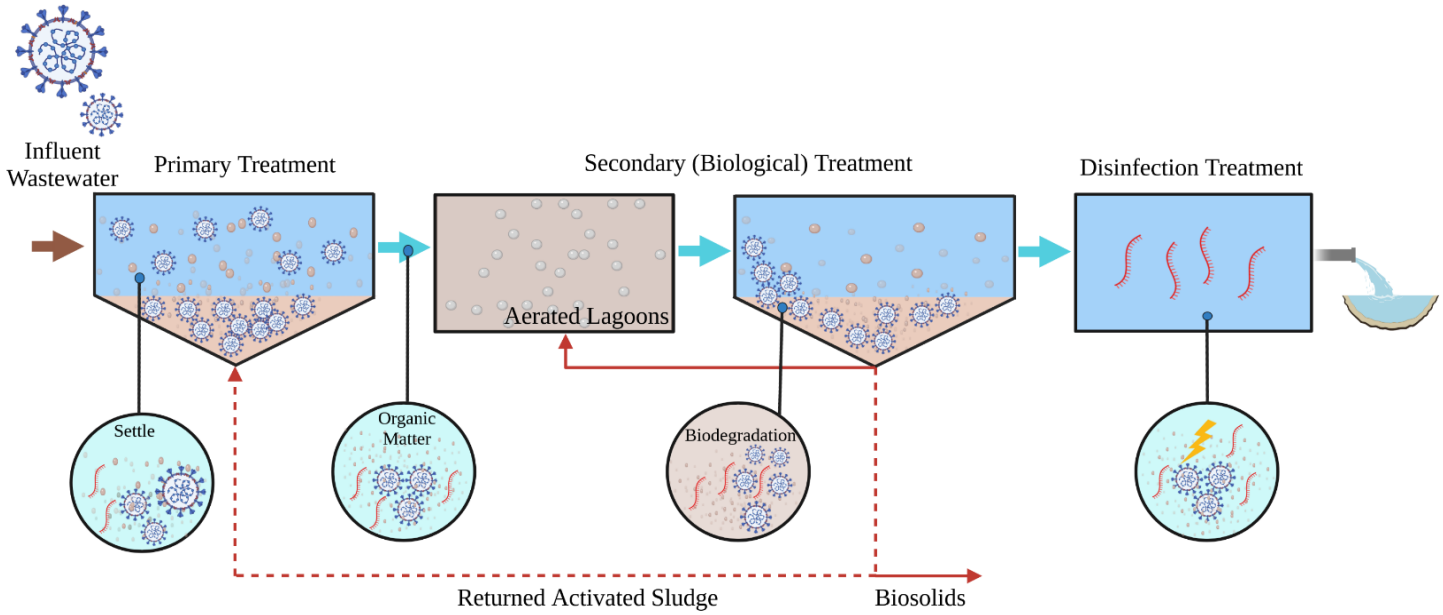

Abstract

Municipal sewage carries SARS-CoV-2 viruses shed in the human stool by infected individuals to wastewater treatment plants (WWTPs). It is well established that increasing prevalence of COVID-19 in a community increases the viral load in its WWTPs. Despite the fact that wastewater treatment facilities serve a critical role in protecting downstream human and environmental health through removal or inactivation of the virus, little is known about the fate of the virus along the treatment train. To assess the efficacy of differing WWTP size and treatment processes in viral RNA removal we quantified two SARS-CoV-2 nucleocapsid (N) biomarkers (N1 and N2) in both liquid and solids phases for multiple treatment train locations from seven coastal New England WWTPs. SARS-CoV-2 biomarkers were commonly detected in the influent, primary treated, and sludge samples (returned activated sludge, waste activated sludge, and digested sludge), and not detected after secondary clarification processes or disinfection. Solid fractions had 470 to 3700-fold higher concentrations of viral biomarkers than liquid fractions, suggesting considerably higher affinity of the virus for the solid phase. Our findings indicate that a variety of wastewater treatment designs are efficient at achieving high removal of SARS CoV-2 from effluent; however, quantifiable viral RNA was commonly detected in wastewater solids at various points in the facility, and represents an important human health risk. This study supports the important role municipal wastewater treatment facilities serve in reducing the discharge of SARS-CoV-2 viral fragments to the environment and highlights the need to better understand the fate of this virus in wastewater solids.

3.1 Introduction

For more than a decade, wastewater surveillance has been used to track chemical markers of human activity, such as illicit drugs, pharmaceuticals, tobacco and alcohol (Causanilles et al., 2017;Choi et al., 2018;Mercan et al., 2019;Estévez-Danta et al., 2022), as well as pathogens including enteric viruses (Bisseux et al., 2018), Poliovirus (Hovi et al., 2012), Hepatitis A Virus and Norovirus (Hellmér et al., 2014). Between January and March 2020, the early detection of the new human coronavirus (SARS-CoV-2) in the stool of confirmed COVID-19 patients (Wu et al., 2020) and in sewage samples (Medema et al., 2020) suggested wastewater surveillance could also be useful in monitoring the spread of COVID-19. Since that time, SARS-CoV-2 has been found in stool samples of both symptomatic and asymptomatic individuals (Amirian, 2020;Mizumoto et al., 2020;Nishiura et al., 2020) and in community wastewater systems across the globe (Ahmed et al., 2020a). It is clear that increasing prevalence of COVID-19 in the population increases the viral load in community wastewater treatment plants (WWTPs) (Amoah et al., 2020;Bogler et al., 2020;Paul et al., 2021).

Wastewater treatment personnel may come in contact with wastewater media (liquids, solids, aerosols) during sampling or system maintenance; therefore, there was early concern of SARS-CoV-2 exposure to personnel at treatment facilities (Ghernaout and Elboughdiri, 2020;Oliver et al., 2020;Shutler et al., 2020). However, several studies have shown the risk of COVID-19 transmission during wastewater treatment to be limited (Arora et al., 2020;Kitajima et al., 2020). Nevertheless, only a few studies have assessed the fate of SARS-CoV-2 in wastewater systems including their discharge to freshwater bodies (Kumar et al., 2021;Mohan et al., 2021;Westhaus et al., 2021;Wurtzer et al., 2021). Bivins et al., (2020) documented 90% reduction of SARS-CoV-2 viability after only 1.5 days in wastewater, which is longer than the hydraulic residence time in a

sewage network and considerably shorter than the typical hydraulic residence time in treatment facilities (Xing et al., 2021). Recent studies showed that SARS-CoV-2 RNA was detected in hospital wastewater (Gonçalves et al., 2021;Pourakbar et al., 2021), WWTP influents (Sherchan et al., 2020;Hata et al., 2021) and effluents (Nasseri et al., 2021;Westhaus et al., 2021), as well as in water bodies receiving the treated wastewater (Naddeo and Liu, 2020), indicating a potential downstream human and environmental health risk via the fecal-oral and fecal- aerosol infection routes (Lewis, 2020;Gholipour et al., 2021). For instance, Pourakbar et al., (2021) reported the presence of SARS-CoV-2 RNA in aerosols released due to active aeration in the biological treatment reactors that could be a potential threat to the personnel.

Like other enteric pathogens present in human sewage, the fate of SARS-CoV-2 in wastewater treatment facilities is likely to be influenced by facility design and operational factors. Recent studies have suggested that the efficiency of our engineered facilities in eliminating enteric virus such as SARS-CoV-2 or neutralizing its infectivity depends on population infection rate, the treatment facility design (Wigginton et al., 2015), the disinfection approach (Arslan et al., 2020;Bogler et al., 2020) and environmental factors such as temperature, pH, organic matter, oxidizing agents and presence of antagonistic bacteria (Gundy et al., 2009). Therefore, assessing the viability of SARS-CoV-2 in wastewater is complicated by multiple factors, even though recent studies suggest that SARS-CoV-2 particles in treated wastewater are not infective (Kitajima et al., 2020;Rimoldi et al., 2020). Due to this uncertainty, there is a critical need to collect information about the occurrence and fate of SARS-CoV-2 at the outlets, as well as along wastewater treatment process stages.

To date, only a few studies have assessed SARS-CoV-2 biomarker removal during the key stages of a wastewater treatment process (Haramoto et al., 2020;Randazzo et al., 2020;Sherchan et al.,

2020). Furthermore, there is limited data available regarding the removal or decay of SARS-CoV-2 present in sludge after treatment (Kocamemi et al., 2020;Abu Ali et al., 2021;Balboa et al., 2021;Bhattarai et al., 2021;Serra-Compte et al., 2021;Westhaus et al., 2021). These studies suggest that the virus particles are mostly diverted to the sludge, and that RNA degradation may also contribute to their absence in the liquid phase after secondary treatment. The majority of existing studies are focused on the comparison of SARS-CoV-2 genetic material loads in the liquid phase and very little attention has been paid to their fate in the solid phase of wastewater (Kocamemi et al., 2020;Peccia et al., 2020). It is known that enteric viruses such as SARS-CoV-2 can adsorb to solid and/or colloidal particles due to the presence of a lipid bilayer surrounding the protein capsid, via electrostatic and hydrophobic interactions (Arraj et al., 2005;Verbyla and Mihelcic, 2015). Balbola et al., (2021) also found SARS-CoV-2 genetic material to have high affinity to primary sludge and sludge thickened solids.

Here, we set out to document how SARS-CoV-2 genetic material moves through seven coastal New England wastewater treatment facilities. Our three objectives were: 1) to track changes in SARS-CoV-2 RNA biomarkers along the treatment train and assess viral RNA removal before discharge; 2) to evaluate the fate of SARS-CoV-2 within the facility, specifically its partitioning between the liquid and solid phases; and 3) to compare the log removal and adsorption–desorption distribution coefficient (K_D) of SARS-CoV-2 to other well studied viruses in wastewater systems. This study demonstrates the important role played by municipal wastewater treatment facilities in collecting, concentrating, and removing SARS-CoV-2 in sewage systems before discharge to the environment, and highlights the need to better understand the fate of this virus in wastewater solids.

3.2 Materials and Methods

3.2.1 Collection of Wastewater Samples

Samples were collected between October 2020 and February 2021 from seven WWTPs located within 25 miles in three coastal New England states: New Hampshire, Maine and Massachusetts. The WWTPs differ considerably by flow, population served, treatment train used, and estimated infection rates at the time of sampling (Table B1 in Supporting Information). WWTPs are referenced in this manuscript based on their location (e.g., NH-1), secondary treatment process (Bard=multi-stage Bardenpho or AS=Activated Sludge) and their disinfection system (CD=chlorination/dechlorination or UV=UV disinfection). A total of 45 samples were collected in duplicate from the seven WWTPs, including untreated wastewater (n=9), primary treated (n=4), secondary treated (n=13), solids/sludge including return activated sludge, waste activated sludge, and digested sludge (n=12), and final effluent (after disinfection, n=7). Samples were collected from locations from the beginning to the end of the facility, designated as BP=Before Primary, AP=After Primary, AL=Aerated Lagoon, AS=After Secondary, ASC=After Secondary Clarifier, RAS=Returned Activated Sludge, WAS=Waste Activated Sludge, CD=After Chlorination/Dechlorination, and UV=After UV Disinfection (Figure S1). Samples were collected in sterile 1-L RNase/DNase free polystyrene containers in the morning (between 10:00 am to 12:00 noon) and immediately transported on ice to the University of New Hampshire, where they were processed within 24 hours.

3.2.2 Extraction and quantification of SARS-CoV-2 viral RNA

Viral RNA was extracted separately from solid and liquid fractions and quantified (Figure B2). Of the 45 samples, 33 were fractionated into solid and liquid fractions, with the remaining 12 solely analyzed for liquids because of insufficient solids generated during centrifugation. The solid fraction was collected from the pre-centrifuge step, where subsamples were centrifuged at 5000×g for 30 min in order to pellet suspended solids including microbial cells and associated viral particles (Ahmed et al., 2020b). Nucleic acids were extracted from 0.25 g of the pelleted solids using the Allprep PowerViral DNA/RNA Kit (Qiagen, Hilden, Germany) and a QIAcube Connect (Qiagen, Hilden, Germany). The supernatant generated from the pre-centrifuge step, representing the liquid fraction, was subsequently transferred into a sterile 50 mL conical tube containing 10% (w/v) Polyethylene Glycol 8000 (PEG) (Millipore Sigma) and 2.25% (w/v) NaCl (0.3 M, Millipore Sigma) (Bibby and Peccia, 2013;Ahmed et al., 2020b). The liquid fraction viral genetic material was concentrated with PEG/NaCl by centrifugation at 12,000 ×g for 2 hours. After the supernatant was removed, the resulting liquid fraction pellet was resuspended in 400 µL of RNAse free dH2O. Nucleic acids were extracted from the liquid fraction pellet suspension using the Allprep PowerViral DNA/RNA Kit (Qiagen, Hilden, Germany) and a QIAcube Connect (Qiagen, Hilden, Germany). Viral RNA for both fractions (solids and liquids) were each eluted into a 50 uL final volume RNase free dH_2O for quantification.

Two SARS-CoV-2 viral nucleocapsid biomarkers (N1 and N2) and a biomarker for the human RNase P gene (RP) (CDC, 2020) were quantified in RNA extracts using reverse transcriptase droplet digital PCR (RT-ddPCR). Each RT-ddPCR reaction was performed in 22 µL final volume containing 5.5 µL 1×one-step RT-ddPCR Supermix (Bio-Rad), 2.2 µL reverse transcriptase (Bio-Rad), 1.1 µL 300 mM DTT (BioRad), 1.1 µL forward and reverse primer and probe mixture (2019-

nCoV CDC ddPCR Triplex Probe Assay (20x); BioRad), 6.6 µL RNase-free water, and 5.5 µL eluted template RNA. Droplets were generated by adding 70 µL of droplet generation oil to the PCR mixture on a QX200 AutoDG Droplet Digital PCR System (Bio-Rad Laboratories, Hercules, CA). RT-ddPCR was performed using a Bio-Rad C1000Touch Thermal Cycler. See Supporting Information for thermocycling parameters and Table S2 for primer and probes used in this study. Droplets were read using a QX200 droplet reader with positive droplets called manually and quantification performed using QX Manager Standard Edition software (Bio-Rad, Hercules, CA). All RT-ddPCR reactions were performed in triplicates, and each plate included a no template control and a positive control (catalog no. COV019; Exact Diagnostics, Fort Worth, TX). Although quantified RNA was not adjusted based on percent recovered, we determined the recovery of SARS-CoV-2 RNA from both solid and liquid fractions by spiking synthetic SARS-CoV-2 RNA quantified control (catalog no. COV019; Exact Diagnostics, Fort Worth, TX) into sterilized wastewater at two concentrations. Recovered concentrations were converted to percent recovery by dividing by the total spiked concentration. An average 58% to 54% recovery of N1 and N2 biomarkers in liquid fractions and average of 37% to 31% recovery of N1 and N2 biomarkers in solid fractions was observed. These recoveries are comparable with those obtained by similar studies using the electronegative filtration method (Gonzalez et al., 2020;Sherchan et al., 2020).

3.2.3 Field and Wastewater Physicochemical Parameters Analyses

In addition to collecting samples for SARS-CoV-2 RNA quantification, we collected parallel samples into 1L HDPE sterile bottles for analyses of total suspended solids (TSS), total dissolved solids (TDS), volatile suspended solids (VSS), and chemical oxygen demand (COD). TDS, TSS,

and VSS were determined within 24 hours of sampling following EPA methods 2540-C, 2540-D and 2540-E, respectively. COD analysis was conducted on unfiltered samples within two days of sample collection using a spectrophotometer (DR6000, Hach, USA), following Method 8000 TNT Plus 821/822. Field measurements were collected at each sample location for electrical conductivity (EC), pH, dissolved oxygen (DO), and redox potential using a Thermo Scientific Orion Star A329 meter (ThermoFisher Scientific, Waltham, MA) calibrated before each sampling event.

3.2.4 Data normalization and statistical analyses

Differences between SARS-CoV-2 RNA concentrations before and after each treatment stage were evaluated using a paired t-test ($p \leq 0.05$), while associations between viral RNA concentrations and physicochemical parameters were evaluated with Pearson's correlation coefficient in SigmaPlot version 14.5 (Systat Software Inc., San Jose, CA, USA). Viral RNA concentrations that were below method detection limits (LODs) were treated as half of the LOD value in our statistical comparisons.

To elucidate sorption behavior of SARS-CoV-2 viral particles in wastewater, we calculated adsorption–desorption distribution coefficient (K_D in L/kg) at different stages of treatment based on viral RNA biomarker concentrations measured in the solid and liquid fractions. The K_D was obtained by dividing viral biomarker concentration in the solids fraction (copies/Kg of wet weight solid) by the biomarker concentration in the liquid fraction (copies/L).

Log removal of SARS-CoV-2 biomarkers between influent and effluent samples for each treatment stage was calculated as follows:

Log removal= $Log_{10} \frac{Influent\ concentration}{Effluent\ concentration}$

Influent concentration refers to the SARS-CoV-2 RNA concentration of the influent (both liquid and solid phase) of each WWTP, while effluent concentration refers to SARS-CoV-2 RNA concentration (liquid and solid phase) of the effluent from the corresponding treatment stage.

Liquid-solid partitioning (%abundance) was calculated using the fraction of SARS-CoV-2 biomarkers mean loadings discharged in liquid or sludge, where the loadings were calculated from SARS-CoV-2 biomarker concentrations per respective volume (for liquid samples) or wet weighted mass load (for sludge samples) (see table B7 in the Supplementary material).

3.3 Results and discussion

3.3.1 SARS-CoV-2 viral RNA is removed from effluent during wastewater treatment

To investigate the efficiency of SARS-CoV-2 viral RNA removal in WWTPs differing in size and treatment processes, we quantified two biomarkers (N1 and N2), and the human RNase P gene (RP), in both liquid and solid phases of wastewater samples from seven coastal New England WWTPs. The average daily flow of the WWTPs studied ranged from <1 million gallons per day (MGD) to >1,000 MGD, representing small towns (1,062 persons) to a major metropolitan area (greater than 3 million persons) with estimated positivity (based on 7-day average) that ranged from 3.6 to 9.9 at the time of sampling, respectively (Table B1). Despite significant differences in population size and percent positivity during sampling, SARS-CoV-2 viral biomarkers N1 and N2

were consistently quantified at concentrations <2,200 copies/100 ml in the liquid phase and <16,000 copies/g in the solid phase of the influent wastewater samples. Specifically, viral biomarker concentrations ranged from 1.07×10^3 to 2.2×10^3 copies/100 mL for N1, and 9.1×10^2 to 2.1×10^3 copies/100 mL for N2 in raw (untreated) wastewater (Figure 3.1 and Table B3), values in line with those reported by Sherchan and coauthors in raw wastewater samples from WWTPs in Louisiana, USA (Sherchan et al., 2020). Levels of viral biomarkers N1 and N2 were below detection after disinfection for all facilities sampled, highlighting the efficiency of these

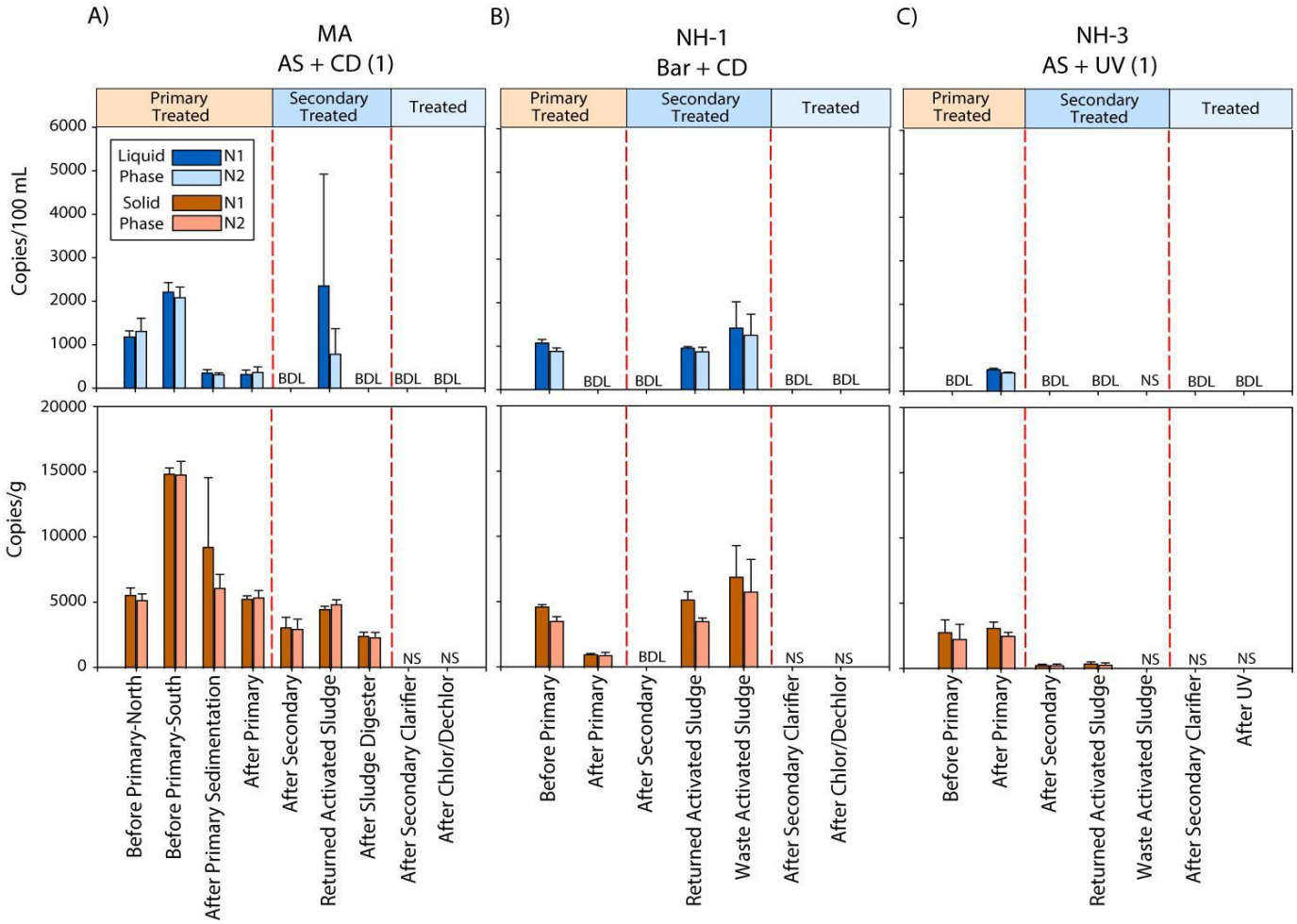

Figure 3.1. Concentrations of two SARS-CoV-2 RNA biomarkers (N1 and N2) measured using RT-ddPCR in the liquid and solid phases of untreated and treated wastewater samples from three coastal New England WWTPs. Liquid phase concentrations are shown as blue bars, while solid phase concentrations are shown in brown. N.S. indicates no sample was analyzed due to limited solids recovery. BDL represents concentrations below the limit of detection of the instrument.

WWTPs in removing viral particles during treatment (Figure 3.1a-c and Table B3). In all WWTPs sampled, viral biomarkers N1 and N2 decreased in the liquid phase from the influent until after the secondary clarifier. However, N1 and N2 biomarker concentrations in the liquid phase of return activated sludge (RAS) and/or waste activated sludge (WAS) were on par with and sometimes larger than liquid phase biomarker concentrations before primary treatment. Similarly, viral biomarkers in the solids fraction also decreased from the influent until after the secondary treatment, with N1 and N2 biomarkers concentrated in the RAS and/or WAS at levels similar to before primary treatment (Figure 3.1 and Table B3). Interestingly, we found relatively high SARS-CoV-2 RNA concentrations in waste activated sludge samples (up to 5.4×10^3 copies/g) from the three smallest WWTPs (NH-1, NH-5 and ME) where the sludge is only treated by volume reduction methods. Similarly, SARS-CoV-2 biomarkers were detected in the solid phase of digested sludge samples (up to 2.6×10^3 copies/g) where waste activated sludge discharge into the anaerobic sludge digester (MA WWTP). These data are in line with recent studies conducted in Spain, France, Iran, rural Canada, and Utah (USA) documenting the removal of SARS-CoV-2 RNA during wastewater treatment (Balboa et al., 2021;Bhattarai et al., 2021;D'Aoust et al., 2021;Pourakbar et al., 2021;Serra-Compte et al., 2021).

We observed that primary treatment (n=5) resulted in a log removal of 0.25 to 0.27 for N1 and N2 biomarkers, respectively, from the liquid phase of the effluents collected from WWTPs after this stage. Viral particle removal during secondary treatment processes showed a similar range. However, we observed differences in removal depending on the type of secondary treatment process. In WWTPs with AS systems (NH-3, NH-4, NH-5, MA and ME), which used aeration to enhance biological degradation of suspended and dissolved solids, an average 0.17 to 0.19 log reduction of N1 and N2 biomarkers was observed (Table B4). In contrast, wastewater systems

designed with Bard (NH-1 and NH-2) had 0.5 to 0.53 log reduction in SARS-CoV-2 biomarkers. Higher virus adsorption to suspended particles in the Bard system may accelerate SARS-CoV-2 RNA removal and support the higher log removal observed compared to the AS system. Additionally, enhanced nutrient and suspended solids removal in the Bard system than in other secondary treatment processes may improve viral particle removal (Schmitz et al., 2016). Finally, no viral RNA was detected after the secondary clarifier stage, resulting in 1.39 log reduction or higher (Table B4). These results provide evidence that secondary treatment and the subsequent clarification processes effectively remove the majority of detectable SARS- CoV-2 genetic material from the liquid phase during wastewater treatment.

The presence of SARS-CoV-2 RNA in the solid phase of seven investigated WWTPs was also evaluated. We detected N1 and N2 biomarkers in sample solids from influent wastewater through secondary treatment (at concentrations up to 3.56×10^3 copies/g). Primary treatment (n=5) resulted in a log removal of 0.25 to 0.26 for N1 and N2 biomarkers from the solid phase of the effluents (Table B4). Viral particle removal during secondary treatment processes showed a similar range. In WWTPs with AS systems (NH-3, NH-4, NH-5, MA and ME), an average of 0.2 to 0.23 log reduction was observed (Table B4). Interestingly, wastewater systems designed with advanced Bardenpho process (NH-1 and NH-2) had 0.5 to 0.45 log reduction in SARS-CoV-2 biomarkers (N1 and N2) which is higher than facilities using conventional processes. We were unable to quantify log removal for solids after secondary clarification because insufficient mass was recovered for viral extraction. Results of SARS-CoV-2 log removal for both solid and liquid phases reported here (Table B4 and Figure 3.1) demonstrated that only a portion of viral genetic material present in the influent is removed during the first stage of wastewater treatment, through physical procedures like gravitational precipitation of suspended colloids or settling of organic matter

(Saawarn and Hait, 2021;Sangkham, 2021). Consequently, secondary treatment and/or disinfection is necessary for complete removal of SARS-CoV-2.

3.3.2 Solids carry a sizeable portion of SARS-CoV-2 viral RNA in wastewater

Balboa and coauthors (2021) showed SARS-CoV-2 was preferentially associated with wastewater sludge. To further assess the affinity of SARS-CoV-2 genetic material for wastewater solids, we estimated adsorption-desorption distribution coefficients (K_D in L/kg) for different stages of treatment based on N1 and N2 concentrations measured in liquid and solid phases (Table B5). In general, log K_D increased with higher solids content of wastewater samples along the treatment train. For instance, the mean log K_D for the N1 biomarker increased from 2.7 L/kg in the influent, to 3.2 L/kg after-primary, and 3.6 L/kg after-secondary (MA) (Table B5). These estimates indicated SARS-CoV-2 is approximately 470 to 3700x more concentrated in the solids as compared the liquid phase. Moreover, despite solids making up only a small fraction of the sample (solids content ~0.02%), the majority of SARS-CoV-2 genetic material is associated with the solids fraction.

Based on these differences in the adsorption-desorption distribution constant, we further explored sample partitioning at three facilities (MA, NH-1 and NH-2) by considering the percent solids in each sample. We assumed in our calculation that the majority of solids were separated and extracted in our wet weighted solids fraction, with the remaining sample volume extracted as liquid phase. Using a straight water density conversion (1g=1mL), we calculated the portion of biomarkers associated with each phase (Table B7). N1 ratios ranged from 51 to 81% in raw wastewater, 60 to 89% after primary treatment, then 66 to 90% after secondary treatment (Figure 3.2 and Table B7).

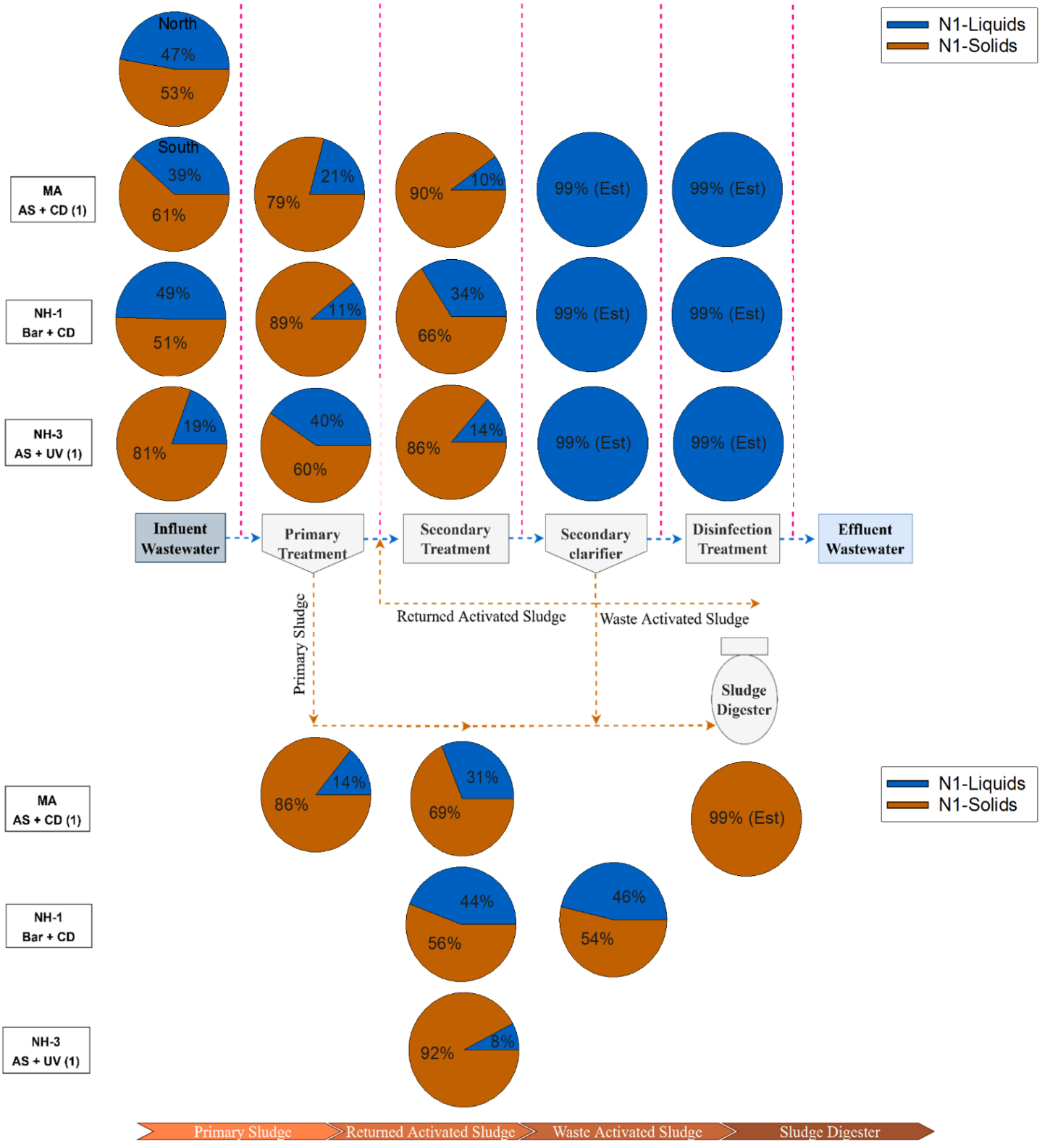

Figure 3.2: Percentage abundance of SARS-CoV-2 biomarkers across treatment stages in three different wastewater treatment plants in coastal New England area.

RAS and WAS samples showed a similar range (54 to 92%). These values indicated that the majority of viral particles in wastewater samples prior to the secondary clarifier are associated with the solids, which in turn represents a very small mass fraction of the sample. This is supported by limited data reported by others (Balboa et al., 2021;Serra-Compte et al., 2021).

The WWTPs sampled in this work vary in several aspects that may influence the liquid - solid partitioning of SARS-CoV-2 RNA. Influent total suspended solids (TSS) concentrations differed 20-fold between the seven WWTPs (104 to 3050 mg/L), which may have affected SARS-CoV-2 RNA partitioning. Similarly, influent organic matter percentage (VSS/TSS) varied from 11 to 98%, indicating that in some cases the TSS was comprised primarily of inorganic content (MA, NH-2) as compared to organics (NH-1, NH-3, NH-5, ME). Furthermore, the average removal rates of TSS measured after secondary treatment were higher in MA and NH-1 (93% and 99.5% respectively) WWTPs than those measured in NH-2, NH-3, NH-4, NH-5 and ME (60 %, 81.9 %, 16 %, 86% and 81.6% respectively) WWTPs. This potentially affected the removal rate of viral RNA attached to the suspended solids during this treatment step.

In order to determine whether EC, TSS, TDS, VSS, or COD concentrations were predictive of SARS-CoV-2 viral biomarker concentrations, we next assessed the relationship between these parameters using Pearson's correlation coefficient. No significant correlation ($p>0.05$) was found between TSS, TDS, VSS, pH, redox and COD and SARS-CoV-2 biomarkers N1 and N2 in either the liquid or solid wastewater fractions (Figure B3 and Figure B4). Interestingly, SARS-CoV-2 biomarkers were strongly associated with EC values in both liquid and solid phases (Table B8). Electrical conductivity, which is a measure of the ability of water to conduct an electrical current, depends on the concentration of conductive ions (cations and ions) in the water (Liu et al., 2020). One possible explanation for this correlation is that high cation content disrupts floc structures,

reducing its settleability (Kara et al., 2008) and enhancing adsorption sites for viruses (Wong et al., 2013). The presence of cations can also reduce the electrostatic double layer, altering charge structure on solids (Nasser et al., 1993;Wong et al., 2012;Yang et al., 2022).

3.4 Discussion

In this work, we sought to investigate changes in concentrations of SARS-CoV-2 RNA biomarkers along the wastewater treatment train and assess viral RNA removal before discharge. We also aimed to evaluate the fate of SARS-CoV-2 within the facility, specifically its partitioning between the liquid and solid phases. Our work indicates that primary and secondary treatments achieves variable but consistent removal of SARS-CoV-2 RNA biomarkers from wastewater liquids across all investigated WWTPs. This finding is consistent with related studies assessing viral RNA removal during the key stages of a wastewater treatment process (Haramoto et al., 2020;Randazzo et al., 2020;Sherchan et al., 2020). In contrast to previous work that analyzed samples from several WWTPs in Germany on the same day and reported detectable viral RNA in both the influent and treated sewage (Westhaus et al., 2021), here we found no quantifiable viral RNA after the secondary clarification process, showing the effectiveness of several different wastewater treatment sizes and designs in removing SARS-CoV-2 RNA before discharge to receiving water bodies.

It is known that enteric viruses can adsorb to solid and/or colloidal particles due to the presence of a lipid bilayer surrounding the protein capsid, via electrostatic and hydrophobic interactions (Arraj et al., 2005;Verbyla and Mihelcic, 2015). Here, our analyses showed measurable levels of SARS-CoV-2 biomarkers in primary, secondary and anaerobic digested sludge samples, supporting

evidence that this enveloped virus may have a higher affinity toward solids. Importantly, almost 70% of measured SARS-CoV-2 biomarkers left the treatment system in the solids, demonstrating the importance of this wastewater media in concentrating viral particles during treatment. Our results are in agreement with recent studies reporting that solids are responsible for sorptive protection of viral particles, suggesting that the SARS-CoV-2 RNA biomarkers are mostly diverted to the sludge (Kocamemi et al., 2020;Balboa et al., 2021;Serra-Compte et al., 2021). Moreover, our work is consistent with those of Serra-Compte et al., (2021), who reported the presence of SARS-CoV-2 genetic material in anaerobic digester sludge indicating that viral biomarkers may continue to partition into the solids fraction of samples and are not inactivated by the anaerobic condition of the digester (Zhang et al., 2017). Similarly, previous studies with other human coronaviruses reported the occurrence of viral particles in sludge samples after anaerobic digestion (Bibby et al., 2011;Bibby and Peccia, 2013). Although PCR-based molecular tools do not indicate infectious SARS-CoV-2 virus is present, biomarker concentrations are useful for monitoring the prevalence and fate of viruses in wastewater treatment media, especially when treated sludge is reused for beneficial purposes such as soil amendment (Wigginton et al., 2015). Recent studies indicated that biosolids containing detectable SARS-CoV-2 genetic material may leach into the surrounding soils (Li et al., 2020;Yang et al., 2020). Therefore, further studies assessing the viability of viral particles in biosolids would inform our understanding of any public health risks associated with their handling.

Acknowledgements

We are grateful for financial support from the New Hampshire Sea Grant (NHSG) Development funds and a UNH STAF fellowship. We also thank Kellen Sawyer and wastewater treatment personnel for assisting with facility sampling. We are also grateful to Dr. Jenna L. Luek for her constructive feedback which greatly improved the manuscript.

Conflict of Interest Disclosure

The authors have no conflicts of interest to disclose.

3.5 References

Abu Ali, H., Yaniv, K., Bar-Zeev, E., Chaudhury, S., Shagan, M., Lakkakula, S., Ronen, Z., Kushmaro, A., and Nir, O. (2021). Tracking SARS-CoV-2 RNA through the wastewater treatment process. *ACS ES&T Water* 1**,** 1161-1167.

Ahmed, W., Angel, N., Edson, J., Bibby, K., Bivins, A., O'brien, J.W., Choi, P.M., Kitajima, M., Simpson, S.L., and Li, J. (2020a). First confirmed detection of SARS-CoV-2 in untreated wastewater in Australia: a proof of concept for the wastewater surveillance of COVID-19 in the community. *Science of the Total Environment* 728**,** 138764.

Ahmed, W., Bertsch, P.M., Bivins, A., Bibby, K., Farkas, K., Gathercole, A., Haramoto, E., Gyawali, P., Korajkic, A., and Mcminn, B.R. (2020b). Comparison of virus concentration methods for the RT-qPCR-based recovery of murine hepatitis virus, a surrogate for SARS-CoV-2 from untreated wastewater. *Science of the Total Environment* 739**,** 139960.

Amirian, E.S. (2020). Potential fecal transmission of SARS-CoV-2: Current evidence and implications for public health. *International Journal of Infectious Diseases*.

Amoah, I.D., Kumari, S., and Bux, F. (2020). Coronaviruses in wastewater processes: source, fate and potential risks. *Environment international* 143**,** 105962.

Arora, S., Nag, A., Sethi, J., Rajvanshi, J., Saxena, S., Shrivastava, S.K., and Gupta, A.B. (2020). Sewage surveillance for the presence of SARS-CoV-2 genome as a useful wastewater based epidemiology (WBE) tracking tool in India. *Water Science and Technology* 82**,** 2823-2836.

Arraj, A., Bohatier, J., Laveran, H., and Traore, O. (2005). Comparison of bacteriophage and enteric virus removal in pilot scale activated sludge plants. *Journal of Applied Microbiology* 98**,** 516-524.

Arslan, M., Xu, B., and El-Din, M.G. (2020). Transmission of SARS-CoV-2 via fecal-oral and aerosols–borne routes: Environmental dynamics and implications for wastewater management in underprivileged societies. *Science of the Total Environment* 743**,** 140709.

Balboa, S., Mauricio-Iglesias, M., Rodriguez, S., Martínez-Lamas, L., Vasallo, F.J., Regueiro, B., and Lema, J.M. (2021). The fate of SARS-COV-2 in WWTPS points out the sludge line as a suitable spot for detection of COVID-19. *Science of The Total Environment* 772**,** 145268.

Bhattarai, B., Sahulka, S.Q., Podder, A., Hong, S., Li, H., Gilcrease, E., Beams, A., Steed, R., and Goel, R. (2021). Prevalence of SARS-CoV-2 genes in water reclamation facilities: From influent to anaerobic digester. *Science of The Total Environment***,** 148905.

Bibby, K., and Peccia, J. (2013). Identification of viral pathogen diversity in sewage sludge by metagenome analysis. *Environmental science & technology* 47**,** 1945-1951.

Bibby, K., Viau, E., and Peccia, J. (2011). Viral metagenome analysis to guide human pathogen monitoring in environmental samples. *Letters in applied microbiology* 52**,** 386-392.

Bisseux, M., Colombet, J., Mirand, A., Roque-Afonso, A.-M., Abravanel, F., Izopet, J., Archimbaud, C., Peigue-Lafeuille, H., Debroas, D., and Bailly, J.-L. (2018). Monitoring human enteric viruses in wastewater and relevance to infections encountered in the clinical setting: a one-year experiment in central France, 2014 to 2015. *Eurosurveillance* 23**,** 17-00237.

Bogler, A., Packman, A., Furman, A., Gross, A., Kushmaro, A., Ronen, A., Dagot, C., Hill, C., Vaizel-Ohayon, D., and Morgenroth, E. (2020). Rethinking wastewater risks and monitoring in light of the COVID-19 pandemic. *Nature Sustainability* 3**,** 981-990.

Causanilles, A., Ruepert, C., Ibáñez, M., Emke, E., Hernández, F., and De Voogt, P. (2017). Occurrence and fate of illicit drugs and pharmaceuticals in wastewater from two wastewater treatment plants in Costa Rica. *Science of the Total Environment* 599**,** 98-107.

Cdc (2020). 2019-novel coronavirus (2019-nCoV) real-time RT-PCR primer and probe information.

Choi, P.M., Tscharke, B.J., Donner, E., O'brien, J.W., Grant, S.C., Kaserzon, S.L., Mackie, R., O'malley, E., Crosbie, N.D., and Thomas, K.V. (2018). Wastewater-based epidemiology biomarkers: past, present and future. *TrAC Trends in Analytical Chemistry* 105**,** 453-469.

D'aoust, P.M., Towhid, S.T., Mercier, É., Hegazy, N., Tian, X., Bhatnagar, K., Zhang, Z., Naughton, C.C., Mackenzie, A.E., and Graber, T.E. (2021). COVID-19 wastewater surveillance in rural communities: Comparison of lagoon and pumping station samples. *Science of the Total Environment* 801**,** 149618.

Estévez-Danta, A., Bijlsma, L., Capela, R., Cela, R., Celma, A., Hernández, F., Lertxundi, U., Matias, J., Montes, R., and Orive, G. (2022). Use of illicit drugs, alcohol and tobacco in Spain and Portugal during the COVID-19 crisis in 2020 as measured by wastewater-based epidemiology. *Science of The Total Environment***,** 155697.

Ghernaout, D., and Elboughdiri, N. (2020). Antibiotics resistance in water mediums: background, facts, and trends. *Applied Engineering* 4**,** 1-6.

Gholipour, S., Mohammadi, F., Nikaeen, M., Shamsizadeh, Z., Khazeni, A., Sahbaei, Z., Mousavi, S.M., Ghobadian, M., and Mirhendi, H. (2021). COVID-19 infection risk from exposure to aerosols of wastewater treatment plants. *Chemosphere* 273**,** 129701.

Gonçalves, J., Koritnik, T., Mioč, V., Trkov, M., Bolješič, M., Berginc, N., Prosenc, K., Kotar, T., and Paragi, M. (2021). Detection of SARS-CoV-2 RNA in hospital wastewater from a low COVID-19 disease prevalence area. *Science of The Total Environment* 755**,** 143226.

Gonzalez, R., Curtis, K., Bivins, A., Bibby, K., Weir, M.H., Yetka, K., Thompson, H., Keeling, D., Mitchell, J., and Gonzalez, D. (2020). COVID-19 surveillance in Southeastern Virginia using wastewater-based epidemiology. *Water research* 186**,** 116296.

Gundy, P.M., Gerba, C.P., and Pepper, I.L. (2009). Survival of coronaviruses in water and wastewater. *Food and Environmental Virology* 1**,** 10-14.

Haramoto, E., Malla, B., Thakali, O., and Kitajima, M. (2020). First environmental surveillance for the presence of SARS-CoV-2 RNA in wastewater and river water in Japan. *Science of the Total Environment* 737**,** 140405.

Hata, A., Hara-Yamamura, H., Meuchi, Y., Imai, S., and Honda, R. (2021). Detection of SARS-CoV-2 in wastewater in Japan during a COVID-19 outbreak. *Science of The Total Environment* 758**,** 143578.

Hellmér, M., Paxéus, N., Magnius, L., Enache, L., Arnholm, B., Johansson, A., Bergström, T., and Norder, H. (2014). Detection of pathogenic viruses in sewage provided early warnings of hepatitis A virus and norovirus outbreaks. *Applied and environmental microbiology* 80**,** 6771-6781.

Hovi, T., Shulman, L., Van Der Avoort, H., Deshpande, J., Roivainen, M., and De Gourville, E. (2012). Role of environmental poliovirus surveillance in global polio eradication and beyond. *Epidemiology & Infection* 140**,** 1-13.

Kara, F., Gurakan, G., and Sanin, F.D. (2008). Monovalent cations and their influence on activated sludge floc chemistry, structure, and physical characteristics. *Biotechnology and bioengineering* 100**,** 231-239.

Kitajima, M., Ahmed, W., Bibby, K., Carducci, A., Gerba, C.P., Hamilton, K.A., Haramoto, E., and Rose, J.B. (2020). SARS-CoV-2 in wastewater: State of the knowledge and research needs. *Science of The Total Environment* 739**,** 139076.

Kocamemi, B., Kurt, H., Sait, A., Sarac, F., Saatci, A., and Pakdemirli, B. (2020). "SARS-CoV-2 Detection in Istanbul Wastewater Treatment Plant Sludges. medRxiv 2020.05. 12.20099358".).

Kumar, M., Kuroda, K., Patel, A.K., Patel, N., Bhattacharya, P., Joshi, M., and Joshi, C.G. (2021). Decay of SARS-CoV-2 RNA along the wastewater treatment outfitted with Upflow Anaerobic Sludge Blanket (UASB) system evaluated through two sample concentration techniques. *Science of the Total Environment* 754**,** 142329.

Lewis, D. (2020). Mounting evidence suggests coronavirus is airborne—but health advice has not caught up. *Nature* 583**,** 510-513.

Li, M., Yang, Y., Lu, Y., Zhang, D., Liu, Y., Cui, X., Yang, L., Liu, R., Liu, J., and Li, G. (2020). Natural host–environmental media–human: A new potential pathway of COVID-19 outbreak. *Engineering* 6**,** 1085-1098.

Liu, J., Yang, P., and Yang, Z.J. (2020). Electrical properties of frozen saline clay and their relationship with unfrozen water content. *Cold Regions Science and Technology* 178**,** 103127.

Medema, G., Heijnen, L., Elsinga, G., Italiaander, R., and Brouwer, A. (2020). Presence of SARS-Coronavirus-2 in sewage. medRxiv. *Published online July*.

Mercan, S., Kuloglu, M., and Asicioglu, F. (2019). Monitoring of illicit drug consumption via wastewater: development, challenges, and future aspects. *Current Opinion in Environmental Science & Health* 9**,** 64-72.

Mizumoto, K., Kagaya, K., Zarebski, A., and Chowell, G. (2020). Estimating the asymptomatic proportion of coronavirus disease 2019 (COVID-19) cases on board the Diamond Princess cruise ship, Yokohama, Japan, 2020. *Eurosurveillance* 25**,** 2000180.

Mohan, S.V., Hemalatha, M., Kopperi, H., Ranjith, I., and Kumar, A.K. (2021). SARS-CoV-2 in environmental perspective: Occurrence, persistence, surveillance, inactivation and challenges. *Chemical Engineering Journal* 405**,** 126893.

Naddeo, V., and Liu, H. (2020). Editorial Perspectives: 2019 novel coronavirus (SARS-CoV-2): what is its fate in urban water cycle and how can the water research community respond? *Environmental Science: Water Research & Technology* 6**,** 1213-1216.

Nasser, A., Adin, A., and Fattal, B. (1993). Adsorption of poliovirus 1 and F+ bacteriophages onto sand. *Water Science and Technology* 27**,** 331-338.

Nasseri, S., Yavarian, J., Baghani, A.N., Azad, T.M., Nejati, A., Nabizadeh, R., Hadi, M., Jandaghi, N.Z.S., Vakili, B., and Vaghefi, S.K.A. (2021). The presence of SARS-CoV-2 in raw and treated wastewater in 3 cities of Iran: Tehran, Qom and Anzali during coronavirus disease 2019 (COVID-19) outbreak. *Journal of Environmental Health Science and Engineering* 19**,** 573-584.

Nishiura, H., Kobayashi, T., Miyama, T., Suzuki, A., Jung, S.-M., Hayashi, K., Kinoshita, R., Yang, Y., Yuan, B., and Akhmetzhanov, A.R. (2020). Estimation of the asymptomatic ratio of novel coronavirus infections (COVID-19). *International journal of infectious diseases* 94**,** 154.

Oliver, M.M.H., Hewa, G.A., Pezzaniti, D., Haque, M.A., Haque, S., Haque, M.M., Moniruzzaman, M., Rahman, M.M., Saha, K.K., and Kadir, M.N. (2020). COVID-19 and recycled wastewater irrigation: a review of implications.

Paul, D., Kolar, P., and Hall, S.G. (2021). A review of the impact of environmental factors on the fate and transport of coronaviruses in aqueous environments. *npj Clean Water* 4**,** 1-13.

Peccia, J., Zulli, A., Brackney, D.E., Grubaugh, N.D., Kaplan, E.H., Casanovas-Massana, A., Ko, A.I., Malik, A.A., Wang, D., and Wang, M. (2020). Measurement of SARS-CoV-2 RNA in wastewater tracks community infection dynamics. *Nature Biotechnology* 38**,** 1164-1167.

Pourakbar, M., Abdolahnejad, A., Raeghi, S., Ghayourdoost, F., Yousefi, R., and Behnami, A. (2021). Comprehensive investigation of SARS-CoV-2 fate in wastewater and finding the virus transfer and destruction route through conventional activated sludge and sequencing batch reactor. *Science of The Total Environment***,** 151391.

Randazzo, W., Truchado, P., Cuevas-Ferrando, E., Simón, P., Allende, A., and Sánchez, G. (2020). SARS-CoV-2 RNA in wastewater anticipated COVID-19 occurrence in a low prevalence area. *Water research* 181**,** 115942.

Rimoldi, S.G., Stefani, F., Gigantiello, A., Polesello, S., Comandatore, F., Mileto, D., Maresca, M., Longobardi, C., Mancon, A., and Romeri, F. (2020). Presence and infectivity of SARS-CoV-2 virus in wastewaters and rivers. *Science of the Total Environment* 744**,** 140911.

Saawarn, B., and Hait, S. (2021). Occurrence, fate and removal of SARS-CoV-2 in wastewater: Current knowledge and future perspectives. *Journal of Environmental Chemical Engineering* 9**,** 104870.

Sangkham, S. (2021). A review on detection of SARS-CoV-2 RNA in wastewater in light of the current knowledge of treatment process for removal of viral particles. *Journal of Environmental Management***,** 113563.

Schmitz, B.W., Kitajima, M., Campillo, M.E., Gerba, C.P., and Pepper, I.L. (2016). Virus reduction during advanced bardenpho and conventional wastewater treatment processes. *Environmental science & technology* 50**,** 9524-9532.

Serra-Compte, A., González, S., Arnaldos, M., Berlendis, S., Courtois, S., Loret, J.F., Schlosser, O., Yáñez, A.M., Soria-Soria, E., and Fittipaldi, M. (2021). Elimination of SARS-CoV-2 along wastewater and sludge treatment processes. *Water research* 202**,** 117435.

Sherchan, S.P., Shahin, S., Ward, L.M., Tandukar, S., Aw, T.G., Schmitz, B., Ahmed, W., and Kitajima, M. (2020). First detection of SARS-CoV-2 RNA in wastewater in North America: a study in Louisiana, USA. *Science of The Total Environment* 743**,** 140621.

Shutler, J., Zaraska, K., Holding, T., Machnik, M., Uppuluri, K., Ashton, I., Migdał, Ł., and Dahiya, R. (2020). Risk of SARS-CoV-2 infection from contaminated water systems. *MedRxiv*.

Verbyla, M.E., and Mihelcic, J.R. (2015). A review of virus removal in wastewater treatment pond systems. *Water Research* 71**,** 107-124.

Westhaus, S., Weber, F.-A., Schiwy, S., Linnemann, V., Brinkmann, M., Widera, M., Greve, C., Janke, A., Hollert, H., and Wintgens, T. (2021). Detection of SARS-CoV-2 in raw and treated wastewater in Germany–suitability for COVID-19 surveillance and potential transmission risks. *Science of The Total Environment* 751**,** 141750.

Wigginton, K., Ye, Y., and Ellenberg, R. (2015). Emerging investigators series: the source and fate of pandemic viruses in the urban water cycle. *Environmental Science: Water Research & Technology* 1**,** 735-746.

Wong, K., Mukherjee, B., Kahler, A.M., Zepp, R., and Molina, M. (2012). Influence of inorganic ions on aggregation and adsorption behaviors of human adenovirus. *Environmental science & technology* 46**,** 11145-11153.

Wong, K., Voice, T.C., and Xagoraraki, I. (2013). Effect of organic carbon on sorption of human adenovirus to soil particles and laboratory containers. *water research* 47**,** 3339-3346.

Wu, Y., Guo, C., Tang, L., Hong, Z., Zhou, J., Dong, X., Yin, H., Xiao, Q., Tang, Y., and Qu, X. (2020). Prolonged presence of SARS-CoV-2 viral RNA in faecal samples. *The lancet Gastroenterology & hepatology* 5**,** 434-435.

Wurtzer, S., Waldman, P., Ferrier-Rembert, A., Frenois-Veyrat, G., Mouchel, J.-M., Boni, M., Maday, Y., Marechal, V., and Moulin, L. (2021). Several forms of SARS-CoV-2 RNA can be detected in wastewaters: implication for wastewater-based epidemiology and risk assessment. *Water Research* 198**,** 117183.

Xing, Y., Wang, S.-P., Zhang, Z.-Q., Liu, X., and Lu, J.-S. (2021). Effect of minocycline on the changes in the sewage chemical index and microbial communities in sewage pipes. *Journal of Hazardous Materials* 402**,** 123792.

Yang, W., Cai, C., and Dai, X. (2020). The potential exposure and transmission risk of SARS-CoV-2 through sludge treatment and disposal. *Resources, Conservation, and Recycling* 162**,** 105043.

Yang, W., Cai, C., and Dai, X. (2022). Interactions between virus surrogates and sewage sludge vary by viral analyte: Recovery, persistence, and sorption. *Water research* 210**,** 117995.

Zhang, J., Gao, Q., Zhang, Q., Wang, T., Yue, H., Wu, L., Shi, J., Qin, Z., Zhou, J., and Zuo, J. (2017). Bacteriophage–prokaryote dynamics and interaction within anaerobic digestion processes across time and space. *Microbiome* 5**,** 1-10.

Chapter 4. Comparison of Sewershed and Subsewershed SARS-CoV-2 Wastewater Surveillance before and after Mass COVID-19 Vaccination

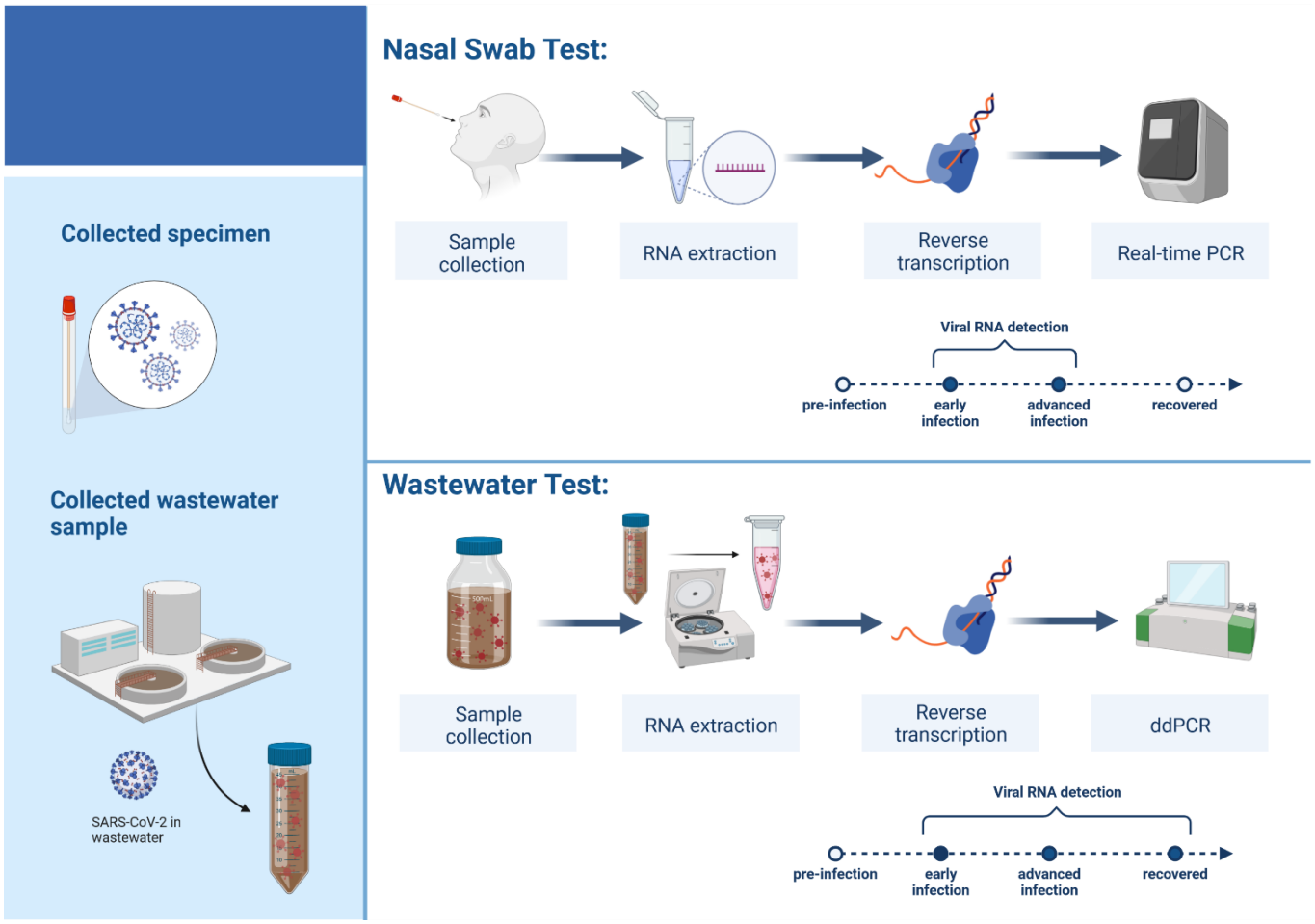

Abstract

Studies around the world conducted during the pandemic demonstrated that tracking SARS-CoV-2 viral biomarkers in wastewater could provide information about the spread of SARS-CoV-2 in the population served by a wastewater treatment plant. The effectiveness of mass scale vaccination on the detection of the SARS-CoV-2 RNA in wastewater remains unknown and difficult to predict. At the University of New Hampshire, we conducted a SARS-CoV-2 wastewater surveillance before, during and after university mass scale vaccination campaign and compared the results with COVID-19 clinical tests at both sewershed and subsewershed levels. SARS-CoV-2 RNA concentrations in wastewater liquids positively correlated with the 7-day average of COVID-19 cases from 0 to 8 days with 2 and 4 days lag showed the highest correlations for the sewershed level (ρ= 0.72−0.74; p <0.0001). The presence of SARS-CoV-2 RNA biomarkers in wastewater liquid samples at subsewershed level were positively correlated with the current COVID-19 cases when wastewater data was lagged 2 days (ρ= 0.47; p=0.027). COVID-19 vaccine administration resulted in a significant decrease in SARS-CoV-2 RNA concentration in wastewater concurrent with decreasing number of COVID-19 infections. Interestingly, emergence of the new variants that might not be covered by existing vaccines resulted in a significant increase in SARS-CoV-2 RNA concentration in wastewater liquids and solids parallel with increasing number of COVID-19 infections in the UNH community after the mass-scale vaccination campaign. During Fall 2021 semester, SARS-CoV-2 RNA concentrations in wastewater solids positively correlated with the 7-day average of COVID-19 cases when wastewater data was lagged zero day (ρ= 0.47; p<0.05) at sewershed level. The result of this study suggested the efficacy and sensitivity of wastewater liquids and solids to evaluate SARS-CoV-2 RNA biomarker concentration at the sewershed level, even after mass-scale vaccinations. These results highlight the need to further evaluate the changes

in SARS-CoV-2 RNA biomarker signal with the introduction of new COVID-19 variants and as vaccines wane to monitor and support public health.

4.1 Introduction

The new human coronavirus (SARS-CoV-2) has been detected in the feces of COVID-19 patients including asymptomatic individuals (Amirian, 2020;Mizumoto et al., 2020;Nishiura et al., 2020), which are collected in domestic wastewater systems. This provides the opportunity to track SARS-CoV-2 genetic material in wastewater to assess the prevalence of the disease. Wastewater-Based Epidemiology (WBE) is an emerging field in environmental engineering that uses molecular tools to quantify biomarkers in wastewater samples to understand public health trends within the "pooled" population. There is a long history of the use of environmental surveillance to compare the presence of RNA/DNA biomarkers from a wide range of viruses such as rotavirus, norovirus, adenovirus, poliovirus, hepatitis A virus in wastewater into the infected populations in a community (Matthijnssens et al., 2009;Blanco Fernández et al., 2012;Hovi et al., 2012;Lodder et al., 2012;Battistone et al., 2014;Majumdar et al., 2018;Wang et al., 2020). Importantly, the effectiveness of vaccines, including the mRNA vaccines (e.g., Pfizer-BioNTech, Moderna), on the shedding of SARS-CoV-2 RNA, remains unknown and difficult to predict.

The concentration of SARS-CoV-2 biomarkers in wastewater is particularly useful to estimate the number of infected persons in a community, hence justifying the use of WBE as an appropriate tool to understand the spread of SARS-CoV-2 in the population served by a wastewater treatment plant (Ahmed et al., 2020a;Gonzalez et al., 2020;Wurtzer et al., 2020;Gerrity et al., 2021). Recent literature demonstrated that SARS-CoV-2 RNA concentration in wastewater led the COVID-19 case trends by 2–7 days (Medema et al., 2020). Wastewater surveillance has also been used to

assist in tracking and minimizing the spread of the COVID-19 within the university campuses across the United States (Corchis-Scott et al., 2021;Fahrenfeld et al., 2021;Harris-Lovett et al., 2021;Anderson-Coughlin et al., 2022;Sweetapple et al., 2022) including the University of New Hampshire (UNH). Many colleges have initiated wastewater surveillance programs to monitor for potential infections on campus and to help university decision makers respond to possible future outbreaks. University campus wastewater surveillance is recognized as predictive of cases infected with SARS-CoV-2, including asymptomatic individuals, where individual testing is less frequent and wastewater surveillance is more frequent (Betancourt et al., 2021;Gibas et al., 2021;Karthikeyan et al., 2021;Scott et al., 2021). On the other hand, however, when individual testing is more frequent wastewater is a lagging indicator (Bivins and Bibby, 2021).

While, many university campuses apply wastewater surveillance as part of their monitoring programs (Betancourt et al., 2021;Corchis-Scott et al., 2021;Fahrenfeld et al., 2021;Gibas et al., 2021;Karthikeyan et al., 2021;Scott et al., 2021), to date, only one study examined temporal changes in SARS-CoV-2 biomarker load in untreated sewage before and after introduction of vaccines (Bivins and Bibby, 2021). This is particularly important to assess whether SARS-CoV-2 viral genetic material slows down in response to vaccines. Further studies are needed to investigate trends in SARS-CoV-2 RNA biomarkers in WWTPs in the context of vaccinations, using current and cumulative infection data and the number of people getting vaccinated.

In this study, we examined the SARS-CoV-2 RNA biomarker signals in wastewater from the UNH campus, and the larger Durham community sewershed before, during, and post-vaccination. To investigate the effect of mass-scale vaccination on viral RNA concentrations, we used the CDC SARS-CoV-2 assay to target two regions of the SARS-CoV-2 nucleocapsid (N) gene (N1 and N2), and the human RP gene (RP) in each wastewater sample. We focused on three major objectives:

1) compare the SARS-CoV-2 RNA concentration in wastewater to the current COVID-19 cases at both sewershed and subsewershed levels; 2) determine if mass-scale vaccination affects the SARS-CoV-2 RNA signal in wastewater; and 3) compare the SARS-CoV-2 RNA concentration in the liquid and solid phase of the wastewater samples during Fall 2021 semester and after the mass-scale vaccination campaign. A combination of SARS-CoV-2 RNA biomarker concentration analyses and frequent nasal swab tests in a longer duration study was a unique approach to determining the actual effect of mass-scale vaccination and the seasonal variation of SARS-CoV-2 RNA concentration in untreated sewage.

4.2 Materials and Methods

4.2.1 Collection of Wastewater Samples

4.2.1.1 Durham WWTP

To assess temporal trends in SARS-CoV-2 RNA concentrations in wastewater at the sewershed community level, we collected 24-hour composite samples from the Durham WWTP throughout the Spring and Fall 2021 semesters on 2× or 3× weekly basis. Samples were collected before primary treatment without solids removal. All wastewater samples were collected from 7–12 am in 250 mL RNase/DNase-free polystyrene containers (CELLTREAT Scientific Products), transported on ice and stored at 4°C until further analyses. All samples were aliquoted in three subsamples of 45 mL each into 50 mL RNase/DNase-free polystyrene containers (CELLTREAT Scientific Products) and processed within 24 hours of sampling.

4.2.1.2 UNH Central Campus

To assess temporal trends in SARS-CoV-2 RNA concentrations in wastewater at subsewershed level, samples were collected from August 2020 to December 2021, from the sewage manholes of north Durham located at the UNH campus. Between January and July 2021, grab samples were collected from the manhole. In August 2021, modified Moore swab samples (Rafiee et al., 2021) were deployed for two or three day windows in the manhole. The swabs were made of 12 layers of Band-Aid® Cushion-Care gauze pads sewn together with 18" of Power Pro® 30-pound test fishing line. These pads were immersed in the manhole with a fishing swivel at the terminal end and a concrete screw as an anchor point near the lid for easy retrieval. The swabs were collected at 48- and 72-hour intervals and stored in Whirl-Pak® bags and delivered to the laboratory on ice.

4.2.2 Viral RNA concentration, extraction, and quantification

Grab, composite and swab samples were pre-processed and extracted differently. Composite and grab samples were collected and extracted as follows. Bacterial cells and debris were removed from the three 45 mL subsamples (liquid fraction) of raw wastewater by centrifugation at 5000 ×g for 30 min. Exactly 35 mL of the resulting supernatant was transferred into a sterile 50 mL tube. Polyethylene Glycol 8000 (PEG) (10% w/v) (Millipore Sigma) and 2.25% (w/v) NaCl (0.3 M, Millipore Sigma) were added to the 50 mL tube to concentrate the supernatant (Bibby and Peccia, 2013;Ahmed et al., 2020b). Thereafter, the tube was centrifuged at 12000 ×g for 2 hours. The supernatant was discarded and the concentrated pellet (containing viral particles) was resuspended in 400 µL of RNase free dH_2O. RNA was extracted from the pellet, using the the RNA PowerMicrobiome Kit (Qiagen, Hilden, Germany) on the QIAcube Connect automated extraction

platform for liquid phase of the wastewater samples during Spring and Summer 2021 semesters (Qiagen, Hilden, Germany).

Viral RNA was extracted from the solid fraction of Durham WWTP samples obtained following the pre-centrifugation step. Briefly, 0.25 g of solid was weighed into a clean tube. Then RNA was extracted using the Allprep PowerViral DNA/RNA kit (Qiagen, Hilden, Germany) following the manufacturer's instructions. All RNA samples were preserved by storage in a -80°C refrigerator until further use.

In August 2021, the extraction method for composite and swab samples was modified as follows. Swabs were washed using 40 mL of Dulbecco's Phosphate Buffered Saline (PBS) (Gibco, 21600-044) and agitated for 60 seconds. Then, 50 mL of the resultant solution was poured into 50 mL RNase/DNase-free conical tube and the swab was squeezed to harvest all the trapped liquid. The solution was centrifuged at 8500 ×g for two minutes to remove bacterial cells and large aggregates. In the next step, 40 mL of supernatant was poured into a 50 mL RNase-free conical tube with minimal disturbance of the sediment pellet. For composite samples, 40 mL were poured into conical tubes and centrifuged for two minutes. Following this step, 600 µL of Nanotrap® particles (Ceres Nanosciences, Manassas, VA) were added to the sample and gently inverted two times to distribute the nanoparticles. The samples incubated for 10 minutes, were inverted again two times, followed by another 10-minute reaction period. In the next step, samples were placed for 10 minutes on a 3-D printed rack with 48 pound pull magnets (Applied Magnets, NB054-2) mounted on one side for separation. Then, the liquid was decanted and any remaining sample fluid removed with a pipette. The nanoparticles coated in viral material were washed off the side of the conical tube and suspended in 500 µL of Fisher Scientific Lysis Buffer. The remaining solution was put on circular magnets with 22.5 lbs pull (Master Magnetics, Castle Rock, CO) to separate the

nanoparticles from the solution. 400 µL were placed in the sample plate with 42 µL of Proteinase-K for 10 minutes following manufacturer's instructions. The ThermoFisher® KingFisher® was used for extraction according to the manufacturer's instructions. All samples were analyzed within 24 hours of collection and SARS-CoV-2 RNA was quantified with reverse transcription droplet digital PCR (RT-ddPCR) using CDC diagnostic panel assays (Lu et al., 2020).

To quantify the amount of SARS-CoV-2 RNA biomarkers present in each sample, reverse transcription droplet digital PCR (RT-ddPCR) was employed according to CDC diagnostic panel assay protocols (Lu et al., 2020). Table 2 of the Supporting Information provides details on primers and probes used. Briefly, targeted regions on the SARS-CoV-2 RNA were amplified using a C1000Touch Thermal Cycler (Bio-Rad Laboratories). Each RT-ddPCR reaction mixture (22 µL total volume) contained: 5.5 µL viral RNA, 5.5 µL 1 x one-step RT-ddPCR Supermix (Bio-Rad), 2.2 µL reverse transcriptase (Bio-Rad), 1.1 µL 300 mM dithiothreitol (BioRad), 1.1 µL forward and reverse primers and probes (2019-nCoV CDC ddPCR Triplex Probe Assay (20x); BioRad), and 6.6 µL RNase-free water. A negative (nuclease-free deionized water) and a positive control (catalog no. COV019; Exact Diagnostics, Fort Worth, TX) were also prepared. The QX200 AutoDG Droplex Digital PCR System was used to generate droplets from the PCR mixture to which 70 µL of droplet generation oil had been added. The Thermal Cycler operational settings were as follows: reverse transcription at 50°C for 60 min (1 cycle); enzyme activation at 95°C for 10 min (1 cycle); denaturation at 94°C for 30 seconds (40 cycles); annealing/extension at 55°C for 1 min (40 cycles at a ramp rate of 2°C per second); enzyme deactivation at 98°C for 10 min (1 cycle); and droplet stabilization at 4°C for 30 min. At the end of RT-ddPCR, reaction plates were inserted into a QX200 droplet reader (Bio-Rad, Hercules, CA). Positive droplets were manually identified. Absolute quantification of biomarker concentration was achieved using a QX Manager

Standard Edition software (Bio-Rad, Hercules, CA). All RT-ddPCR reactions were done in triplicate.

4.2.3 Ancillary Data – Infections, Vaccinations & Demographic Information

The current and cumulative infection data were collected from the New Hampshire Department of Health and Human Services (DHHS) dashboard for the Spring, Summer and Fall 2021 semesters. DHHS tracks COVID-19 infections on a dashboard with regular updates (https://www.covid19.nh.gov/dashboard/case-summary) since March 29, 2020. This data was used to check for correlation between SARS-CoV-2 biomarker concentrations in wastewater and the number of COVID-19 cases in the Durham community (sewershed level).

The current infection data, average daily total test, testing results by population, and fully vaccinated counts by population for the UNH Durham campus (subsewershed level) were obtained from UNH COVID-19 lab testing dashboard. All clinical testing results and vaccination information are publicly available and updated daily on the UNH COVID-19 lab testing dashboard (https://www.unh.edu/coronavirus/dashboard) beginning on August 22, 2020.

4.2.4 Data normalization and statistical analyses

Quantitative comparisons between SARS-CoV-2 RNA concentrations in wastewater before and during each phase of the vaccination campaign were conducted using SigmaPlot version 14.5 (Systat Software Inc., San Jose, CA, USA). Correlation between SARS-CoV-2 RNA concentrations and current COVID-19 infections were evaluated using Pearson's correlation. Differences were considered statistically significant at $p \leq 0.05$.

4.3 Results and discussion

4.3.1 First mass vaccination significantly decreased wastewater biomarker signal

The incidence of COVID-19 cases and consequently SARS-CoV-2 RNA biomarker signal in wastewater decreased initially in response to vaccination during the Spring 2021 semester (Figure 4.1 and Figure 4.2). During the first dose of the mass-scale vaccination period (April 7−26, 2021), an average of 3010 daily total COVID-19 clinical tests were conducted per day. The incidence of COVID-19 decreased from a 7-day average of 96 cases (positivity rate of 0.45%) on April 7 to 30 cases (positivity rate of 0.14%) by April 26. During the second dose of mass-scale vaccine administration (April 28 to May 21, 2021), the 7-day average of positive COVID-19 tests decreased from 30 cases (positivity rate of 0.14%) on April 28 to 7 cases (positivity rate of 0.05%) by May 21. The 7-day average of COVID-19 incidence reached zero on June 6, 2021, and remained ≤4 cases throughout Summer 2021 (Figure 4.3A&B). The daily total COVID-19 clinical tests decreased to 522 at the end of Spring 2021 semester (May 30) and with the start of Summer since fully vaccinated students who worked on campus were no longer required to participate in mandatory weekly clinical testing.

The SARS-CoV-2 B.1.1.7 (Alpha) variant was identified for the first time on February 12, 2021 in New Hampshire and several cases associated with the delta (B.1.617.2) variant were reported in late August (DHHS, 2021). Although sequencing data were not available from campus, two SARS-CoV-2 variants of concern, alpha (B.1.1.7) and delta (B.1.617.2) that are extremely infectious and highly transmissible were not likely to represent a large proportion of COVID-19 cases on UNH campus during the Spring 2021 semester as they were implicated in only a few cases in the state of New Hampshire.

Wastewater signal during the mass-scale vaccination period was measured via its positivity for SARS-CoV-2 RNA at the sewershed level (Durham WWTP). During the first dose of the mass-scale vaccination period (April 7−26, 2021), SARS-CoV-2 RNA was detected in wastewater liquids on 7 of 9 sampling days. Interestingly, during the second dose of mass-scale vaccination administration (April 28 to May 21, 2021), SARS-CoV-2 RNA was detected in wastewater liquids on only 3 of 11 sampling days.

During the same period, a similar decrease in signal detection was observed in subsewershed level results (UNH Central campus). During the first dose (April 7−26, 2021), SARS-CoV-2 RNA was measured in wastewater liquids on 6 of 9 sampling days. During the second dose of mass-scale vaccination administration (April 28 to May 21, 2021), until the end of the semester, SARS-CoV-2 RNA was not detected in any of wastewater liquids samples collected from central campus.

Commencement (May 21-22, 2021) brought visitors and likely infected individuals to campus. During the closing days of the spring semester, SARS-CoV-2 RNA concentration in wastewater liquids increased to >600 copies/100 mL on Friday, May 21, the first day of commencement despite, daily positive tests among the UNH community remained ≤ 2. SARS-CoV-2 RNA biomarkers were detected before, during and after the commencement weekend, suggesting that infected guests contributed to increased prevalence and viral shedding in the Durham community wastewater system.

4.3.2 Correlation between SARS-CoV-2 biomarkers in wastewater and current infections

During Spring 2021 semester, at the sewershed level (Durham WWTP), the N1 SARS-CoV-2 biomarker concentration was positively correlated with current COVID-19 cases from 0 to 8 days.

Correlation increased from a lag of zero days (ρ= 0.62; p<0.0001), to 2 days (ρ= 0.74; p<0.0001), decreasing again at day 4 (ρ= 0.72; p<0.0001), 6 (ρ= 0.61; p<0.0001), and 8 (ρ= 0.43; p= 0.002) (Table C2). Similarly, we observed that N2 SARS-CoV-2 biomarkers were positively correlated from zero (ρ= 0.66; p<0.0001), 2 (ρ= 0.78; p<0.0001), 4 (ρ= 0.77; p<0.0001), 6 (ρ= 0.66; p<0.0001), and 8 days (ρ= 0.45; p= 0.0016) with 2 and 4 days lag showed the highest correlations for the sewershed level (Table C3). Interestingly, N2 biomarker concentration showed a slightly better correlation with current COVID-19 cases when wastewater data was lagged at sewershed level.

The presence of SARS-CoV-2 RNA biomarkers (N1 and N2) in wastewater liquid samples collected from a manhole at subsewershed level (central campus) which was receiving wastewater from several locations in North Durham, was also evaluated. During Spring 2021 semester, N1 SARS-CoV-2 biomarkers were positively correlated with the current COVID-19 cases when wastewater data was lagged 2 days (ρ= 0.47; p=0.027) (Table C4).

The differences in results between the sewershed and subsewershed levels could be attributed to greater variation at the subsewershed level and the sampling technique. At the subsewershed level, we obtained grab samples in contrast to composite sampling at Durham WWTP. Additionally, climate and environmental factors including rainfall, the relative proportions of domestic effluent and the community water usage could potentially influence the differences observed in SARS-CoV-2 RNA concentrations in wastewater.

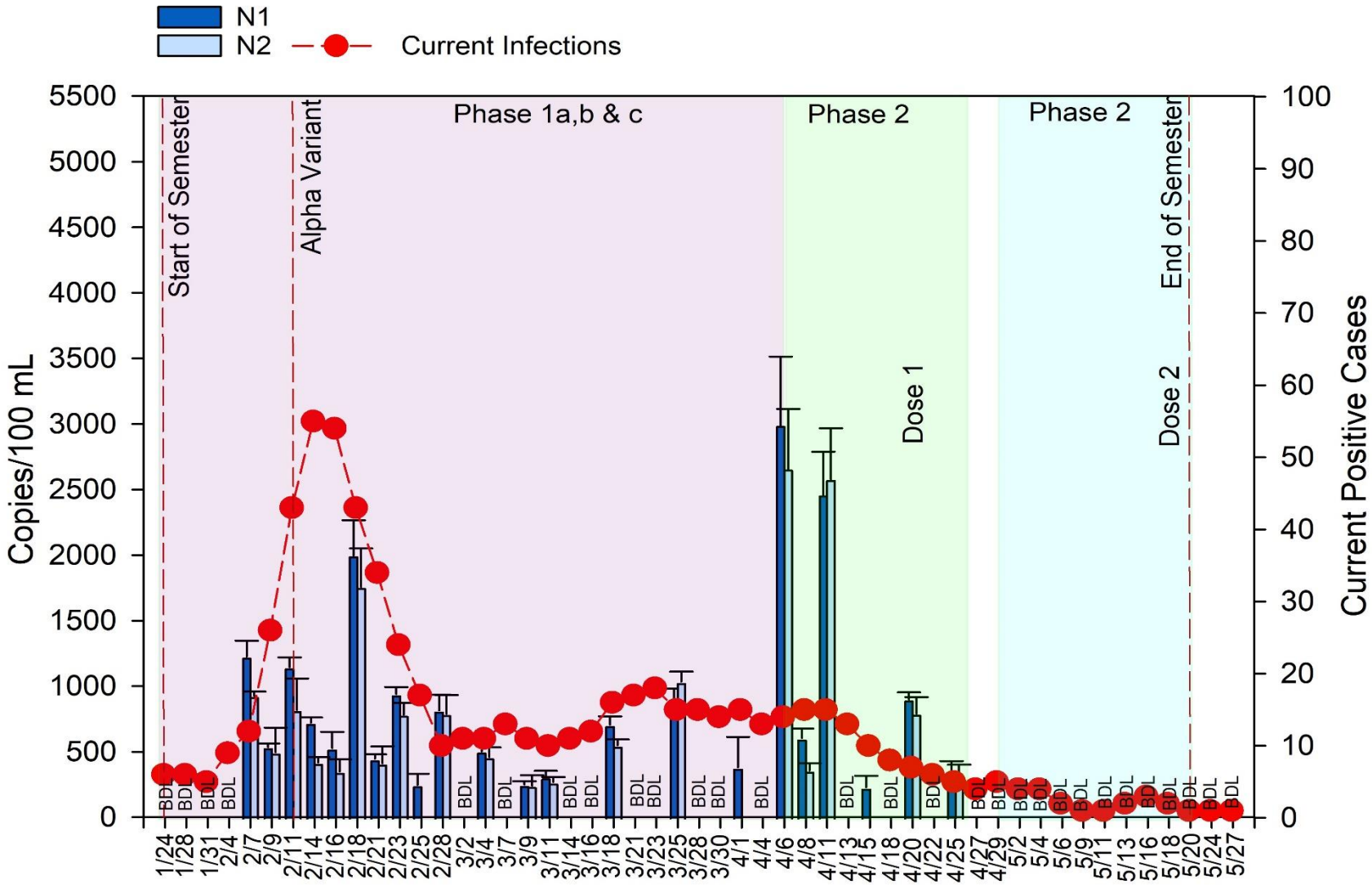

Figure 4.1. SARS-CoV-2 RNA in raw wastewater liquids (N1 & N2 copies per 100 mL) as measured by RT-ddPCR before and during the administration of COVID-19 mass-scale vaccination campaign (Spring 2021 semester) at UNH central campus. BDL represents samples below limit of detection.

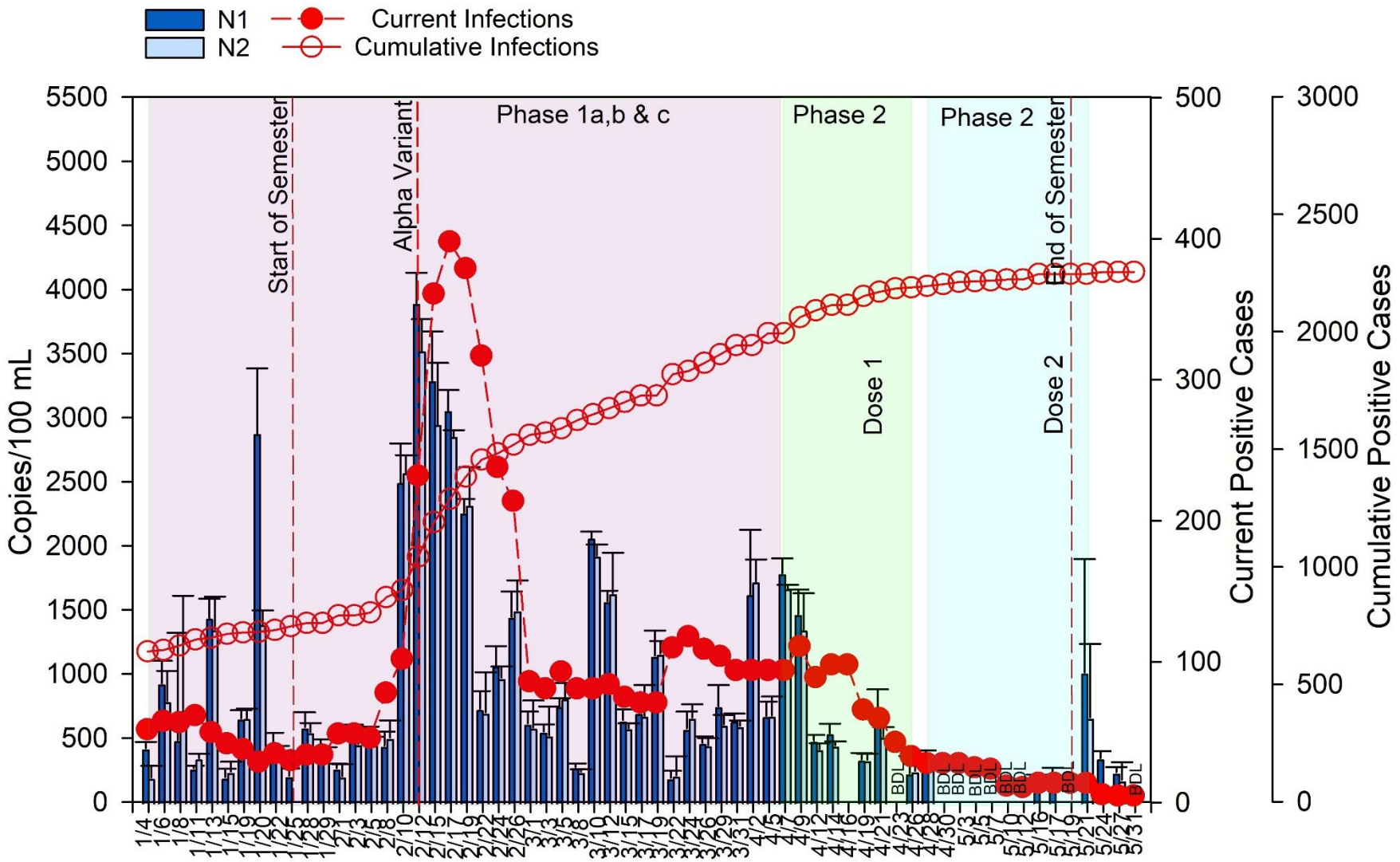

Figure 4.2. SARS-CoV-2 RNA in raw wastewater liquids (N1 & N2 copies per 100 mL) as measured by RT-ddPCR before and during the administration of COVID-19 mass-scale vaccination campaign (Spring 2021 semester) at Durham WWTP. BDL represents samples below limit of detection.

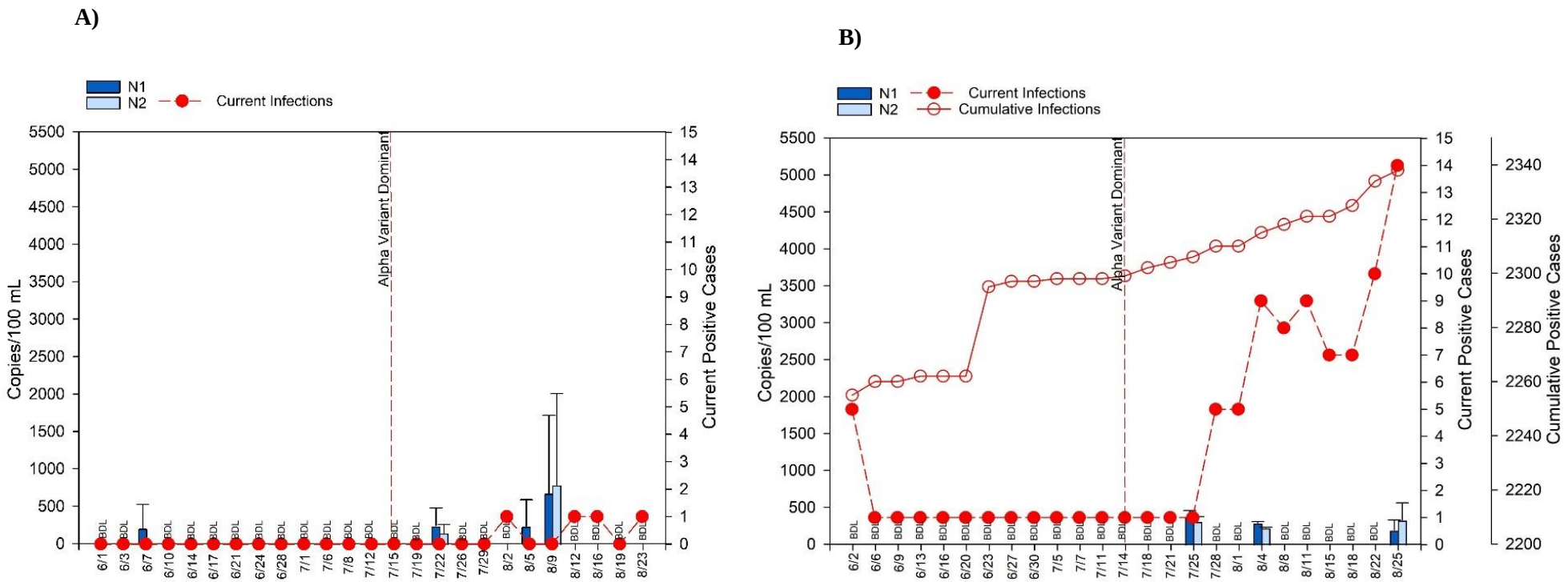

Figure 4.3. SARS-CoV-2 RNA in raw wastewater liquids (N1 & N2 copies per 100 mL) after the COVID-19 mass-scale vaccination (Summer 2021 semester) at UNH central campus (A), and Durham WWTP (B). BDL represents samples below limit of detection.

4.3.3 University trends as new variants are introduced and vaccines wane

We continued wastewater surveillance during Fall 2021 semester to better understand the effects of mass-scale vaccinations on the spread of the virus in the population. The incidence of COVID-19 cases and consequently SARS-CoV-2 RNA biomarker signal in wastewater steadily increased throughout the Fall 2021 semester, apparently due to the emergence of new COVID-19 variants that might not have been covered by existing vaccines (Figure 4.4A&B). UNH students returned to campus in Fall 2021 semester after traveling (internally or internationally) and considerable interactions with outside community members. Beginning Fall 2021, there was a total of 13,118 fully vaccinated (on-campus vaccination campaign administered Pfizer-BioNTech, Moderna and Johnson & Johnson vaccines) persons (11,517 students, 916 faculty and 1,704 staff) on the UNH Durham campus, and by the end of the semester the fully vaccinated count increased to 14,697 (12,643 students, 1,073 faculty and 2,167 staff).

An average of 1607 daily total COVID-19 clinical tests were administered per day in Fall 2021. The incidence of COVID-19 increased from a 7-day average of 35 cases (positivity rate of 0.27%) on August 30 to 122 cases (positivity rate of 0.94%) by September 16. We observed a 7-day average of 94 cases (positivity rate of 0.79%) after Halloween activities, on November 4. After the Halloween weekend, measured SARS-CoV-2 RNA concentrations in wastewater liquids increased to the highest levels observed during the Fall 2021 semester (19,737 N1 copies/100 mL and 19,974 N2 copies/100 mL) in central campus wastewater and similarly in Durham WWTP (5660 N1 copies/100 mL and 5593 N2 copies/100 mL) (Figure 4.4A&B).

The incidence of COVID-19 fluctuated over time, influenced by the population mobility and seasonal holidays/activities (e.g. Halloween, Thanksgiving) even after the administration of the

booster dose of vaccines likely due to new variants (Delta) and waning vaccine doses in the broader population.

We assessed the relationship between clinical cases and SARS-CoV-2 biomarkers in the liquid fraction of Durham WWTP and central campus (Figure 4.4). During Fall 2021 semester and after the mass-scale vaccination campaign, the N1 SARS-CoV-2 biomarker concentration was positively correlated with current COVID-19 cases when wastewater data were lagged zero day ($\rho = 0.32$; $p > 0.05$) at sewershed level (Durham WWTP), however, the correlation was not statistically significant. N2 SARS-CoV-2 biomarker were also weakly correlated with same-day COVID-19 cases ($\rho = 0.334$; $p > 0.05$), although the statistically significant result were not observed.

The presence of SARS-CoV-2 RNA biomarkers (N1 and N2) in wastewater liquid samples collected from subsewershed level (central campus) were also measured. N1 and N2 SARS-CoV-2 biomarkers were positively correlated with the current COVID-19 cases when wastewater data were lagged zero day (N1: $\rho = 0.17$; $p > 0.05$; N2: $\rho = 0.16$; $p > 0.05$), however, the correlation was weak and not statistically significant. One of the possible explanations for this weak correlation could be that the average daily total COVID-19 clinical tests decreased during Fall 2021 semester since fully vaccinated students and staff were only required to participate in mandatory clinical testing twice a month and non-vaccinated individuals were required to test once a week (Figure S1). Therefore, the number of current COVID-19 cases were likely underestimates. It is important to mention that wastewater samples were collected 3× weekly, but the dates did not align to COVID-19 clinical testing and hence we were unable to calculate the lag for wastewater data during Fall 2021 semester.

Recent studies have suggested that testing wastewater solids for SARS-CoV-2 might be more sensitive than testing wastewater liquids for monitoring COVID-19 within communities (Graham

et al., 2020;Balboa et al., 2021). However, these studies most often report SARS-CoV-2 RNA concentration in either the liquid or the solid phase of wastewater. Accordingly, here we collected 24-hour composite samples from the primary influent of Durham WWTP and reported the presence of SARS-CoV-2 RNA in both liquid and solid phases of the wastewater.

Despite a few non-detects, SARS-CoV-2 N1 copies per gram of wastewater solids was positively correlated with current COVID-19 cases when wastewater data was lagged zero day ($\rho = 0.47$; $p<0.05$) (Figure 4.4B), and this correlation was statistically significant. Additionally, N2 copies per gram of wastewater solids was also significantly correlated with same-day COVID-19 cases ($\rho = 0.43$; $p<0.05$). These results indicated that N1 biomarker concentration in wastewater solids showed a slightly better correlation with current COVID-19 cases than the liquid phase of the samples. We observed a positivity rate of 0.64% in COVID-19 clinical cases on December 2 after the Thanksgiving holiday. Not surprisingly, the week after the Thanksgiving, SARS-CoV-2 biomarker concentrations in wastewater solids increased to the highest levels observed during the Fall 2021 semester (12,724.93 N1 copies/gram and 13,416.76 N2 copies/gram) in Durham WWTP (Figure 4.4B).

The result of our study highlighted that SARS-CoV-2 biomarker (N1 and N2) shedding rates may change during different stages of the pandemic, including the emergence of new variants. Interestingly, our results indicated that the average SARS-CoV-2 biomarker (N1 and N2) shedding per infected individual increased significantly ($p<0.001$) during Fall 2021 semester and after delta variant become dominant on the UNH campus (Figure C2). This significant increase is possibly due to longer duration of shedding related to Delta variant and higher viral loads (Prasek et al., 2022).

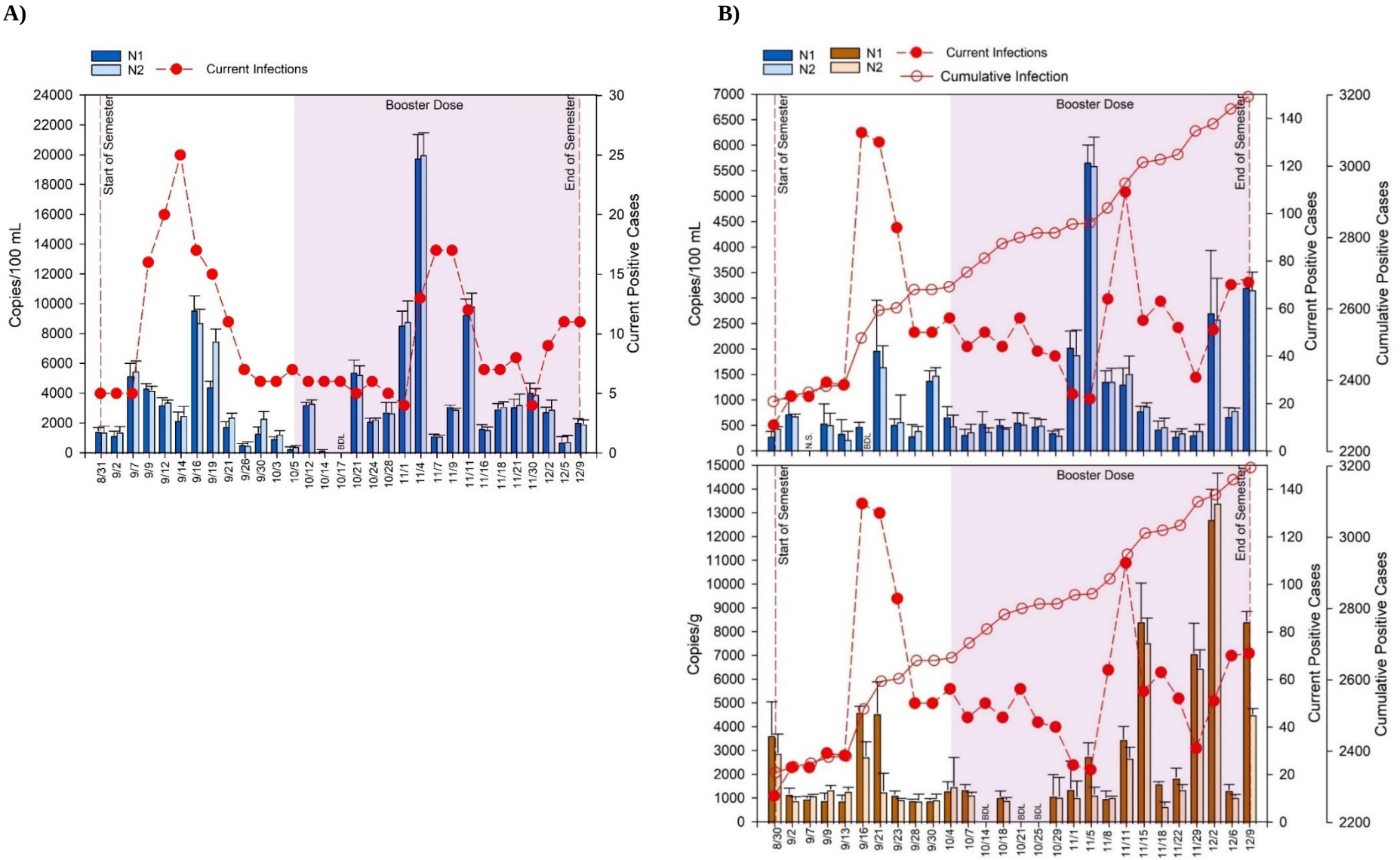

Figure 4.4 SARS-CoV-2 RNA in raw wastewater liquids (N1 & N2 copies per 100 mL) and solids (N1 & N2 copies per gram) as measured by RT-ddPCR after the administration of COVID-19 mass-scale vaccination campaign (Fall 2021 semester) at UNH central campus (A), and Durham WWTP (B). Liquid phase concentrations are shown as blue bars, while solid phase concentrations are shown in brown. BDL represents samples below limit of detection.

4.4 Discussion

Throughout the COVID-19 pandemic and as universities started reopening for the 2020-2021 academic year, wastewater surveillance was primarily used to monitor for COVID-19 prevalence at university campuses around the world. In this work, we sought to compare the SARS-CoV-2 biomarker concentrations in wastewater to the current COVID-19 cases at both sewershed and subsewershed levels. We also aimed to determine if mass-scale vaccination affected the signal of SARS-CoV-2 biomarkers in wastewater.

In prior studies (Bivins and Bibby, 2021;Corchis-Scott et al., 2021;Fahrenfeld et al., 2021;Sweetapple et al., 2022), measurements were made using wastewater solids or liquids from treatment plants, while in this study wastewater samples (both solids and liquids) were collected at both sewershed and subsewershed levels. Here, our comparison of SARS-CoV-2 biomarker concentration at community sewershed and central campus showed that the variability of detected SARS-CoV-2 levels could be associated with differences observed at the subsewer level, and using of different sampling methodology. We used the grab sampling of sewage manholes for collecting samples from campus during Spring 2021 semester. With the start of the Fall 2021 semester, we used a modified swab deployed into sewage manholes to collect representative samples of the subsewershed. Similar to recent studies (Rafiee et al., 2021;Liu et al., 2022), our results indicated that Moore swabs is a relatively simple, sensitive and sufficient sampling method for capturing the mean SARS-CoV-2 biomarker concentrations in wastewater flow over time, compared to grab sampling that may be less representative of community fecal shedding in subsewershed level. The findings of our study and others support the need for identification of these factors within community sewersheds and subsewersheds which may affect viral biomarker detection prior to employing surveillance efforts.

The availability of two mRNA vaccines (Pfizer-BioNTech and Moderna) for the broader young adult population, demonstrated approximately 95% efficacy against symptomatic COVID-19 in clinical trials (Kow and Hasan, 2021;Pilishvili et al., 2021). Similarly, our work showed that COVID-19 vaccine administration resulted in a significant decrease in SARS-CoV-2 RNA concentration in wastewater concurrent with decreasing number of COVID-19 infections in the community. Our findings are consistent with those of Levine-Tiefenbrun et al., (2021b), who reported the reduced viral load in breakthrough infection of vaccinated individuals (Levine-Tiefenbrun et al., 2021b). Moreover, we also observed that introduction of the delta variant (DHHS, 2021) resulted in a significant increase in SARS-CoV-2 RNA concentration in wastewater concurrent with increasing number of COVID-19 infections in the UNH community. Interestingly, our results indicated that the average SARS-CoV-2 biomarker (N1 and N2) shedding per infected individual increased significantly during Fall 2021 semester and after the delta variant become dominant on the UNH campus. This finding is consistent with related studies reporting the effectiveness of the COVID-19 vaccines in preventing infection. In these studies, decreasing viral load in breakthrough infections was diminished in parallel with the rise of the Delta variants in communities (Levine-Tiefenbrun et al., 2021a;Prasek et al., 2022).

Our analyses of the SARS-CoV-2 RNA concentration in the liquid and solid phases of the wastewater samples during Fall 2021 semester and after the mass-scale vaccination campaign, showed an enhanced biomarker equivalent concentration in the solid phase (200 to 2000×) than the liquid phase of the wastewater which is consistent with findings reported by other studies (Ye et al., 2016;Graham et al., 2020;Westhaus et al., 2021). Importantly, SARS-CoV-2 biomarker concentrations (N1 and N2) in wastewater solids were significantly correlated with current

COVID-19 cases when wastewater data was lagged zero day, while biomarkers in the liquid showed a weak correlation with current infections.

The result of this study demonstrated the efficacy and sensitivity of wastewater liquids and solids to evaluate SARS-CoV-2 RNA biomarker concentration at the sewershed level, even after mass-scale vaccinations. Our findings highlight the need to further evaluate the changes in SARS-CoV-2 RNA biomarker signal in response to vaccination and with the introduction of new COVID-19 variants to monitor and support public health. Furthermore, additional information on the duration and magnitude of viral RNA shedding via feces is required to better understand the effect of vaccines on reducing the viral load into the wastewater treatment facilities.

4.5 References

Ahmed, W., Angel, N., Edson, J., Bibby, K., Bivins, A., O'brien, J.W., Choi, P.M., Kitajima, M., Simpson, S.L., and Li, J. (2020a). First confirmed detection of SARS-CoV-2 in untreated wastewater in Australia: a proof of concept for the wastewater surveillance of COVID-19 in the community. *Science of the Total Environment* 728**,** 138764.

Ahmed, W., Bertsch, P.M., Bivins, A., Bibby, K., Farkas, K., Gathercole, A., Haramoto, E., Gyawali, P., Korajkic, A., and Mcminn, B.R. (2020b). Comparison of virus concentration methods for the RT-qPCR-based recovery of murine hepatitis virus, a surrogate for SARS-CoV-2 from untreated wastewater. *Science of the Total Environment* 739**,** 139960.

Amirian, E.S. (2020). Potential fecal transmission of SARS-CoV-2: current evidence and implications for public health. *International journal of infectious diseases* 95**,** 363-370.

Anderson-Coughlin, B.L., Shearer, A.E., Omar, A.N., Litt, P.K., Bernberg, E., Murphy, M., Anderson, A., Sauble, L., Ames, B., and Damminger Jr, O. (2022). Coordination of SARS-CoV-2 wastewater and clinical testing of university students demonstrates the importance of sampling duration and collection time. *Science of The Total Environment* 830**,** 154619.

Balboa, S., Mauricio-Iglesias, M., Rodriguez, S., Martínez-Lamas, L., Vasallo, F.J., Regueiro, B., and Lema, J.M. (2021). The fate of SARS-COV-2 in WWTPS points out the sludge line as a suitable spot for detection of COVID-19. *Science of The Total Environment* 772**,** 145268.

Battistone, A., Buttinelli, G., Fiore, S., Amato, C., Bonomo, P., Patti, A.M., Vulcano, A., Barbi, M., Binda, S., and Pellegrinelli, L. (2014). Sporadic isolation of Sabin-like polioviruses and high-level detection of non-polio enteroviruses during sewage surveillance in seven Italian cities, after several years of inactivated poliovirus vaccination. *Applied and environmental microbiology* 80**,** 4491-4501.

Betancourt, W.Q., Schmitz, B.W., Innes, G.K., Prasek, S.M., Brown, K.M.P., Stark, E.R., Foster, A.R., Sprissler, R.S., Harris, D.T., and Sherchan, S.P. (2021). COVID-19 containment on a college campus via wastewater-based epidemiology, targeted clinical testing and an intervention. *Science of The Total Environment* 779**,** 146408.

Bibby, K., and Peccia, J. (2013). Identification of viral pathogen diversity in sewage sludge by metagenome analysis. *Environmental science & technology* 47**,** 1945-1951.

Bivins, A., and Bibby, K. (2021). Wastewater surveillance during mass COVID-19 vaccination on a college campus. *Environmental Science & Technology Letters* 8**,** 792-798.

Blanco Fernández, M., Torres, C., Riviello-López, G., Poma, H., Rajal, V., Nates, S., Cisterna, D., Campos, R., and Mbayed, V. (2012). Analysis of the circulation of hepatitis A virus in Argentina since vaccine introduction. *Clinical Microbiology and Infection* 18**,** E548-E551.

Corchis-Scott, R., Geng, Q., Seth, R., Ray, R., Beg, M., Biswas, N., Charron, L., Drouillard, K.D., D'souza, R., and Heath, D.D. (2021). Averting an Outbreak of SARS-CoV-2 in a University Residence Hall through Wastewater Surveillance. *Microbiology spectrum* 9**,** e00792-00721.

Dhhs, N.H.D.O.H.a.H.S. (2021).).

Fahrenfeld, N., Medina, W.R.M., D'elia, S., Modica, M., Ruiz, A., and Mclane, M. (2021). Comparison of residential dormitory COVID-19 monitoring via weekly saliva testing and sewage monitoring. *Science of The Total Environment***,** 151947.

Gerrity, D., Papp, K., Stoker, M., Sims, A., and Frehner, W. (2021). Early-pandemic wastewater surveillance of SARS-CoV-2 in Southern Nevada: Methodology, occurrence, and incidence/prevalence considerations. *Water research X* 10**,** 100086.

Gibas, C., Lambirth, K., Mittal, N., Juel, M.a.I., Barua, V.B., Brazell, L.R., Hinton, K., Lontai, J., Stark, N., and Young, I. (2021). Implementing building-level SARS-CoV-2 wastewater surveillance on a university campus. *Science of The Total Environment* 782**,** 146749.

Gonzalez, R., Curtis, K., Bivins, A., Bibby, K., Weir, M.H., Yetka, K., Thompson, H., Keeling, D., Mitchell, J., and Gonzalez, D. (2020). COVID-19 surveillance in Southeastern Virginia using wastewater-based epidemiology. *Water research* 186**,** 116296.

Graham, K.E., Loeb, S.K., Wolfe, M.K., Catoe, D., Sinnott-Armstrong, N., Kim, S., Yamahara, K.M., Sassoubre, L.M., Mendoza Grijalva, L.M., and Roldan-Hernandez, L. (2020). SARS-CoV-2 RNA in wastewater settled solids is associated with COVID-19 cases in a large urban sewershed. *Environmental science & technology* 55**,** 488-498.

Harris-Lovett, S., Nelson, K.L., Beamer, P., Bischel, H.N., Bivins, A., Bruder, A., Butler, C., Camenisch, T.D., De Long, S.K., and Karthikeyan, S. (2021). Wastewater surveillance for SARS-CoV-2 on college campuses: initial efforts, lessons learned, and research needs. *International journal of environmental research and public health* 18**,** 4455.

Hovi, T., Shulman, L., Van Der Avoort, H., Deshpande, J., Roivainen, M., and De Gourville, E. (2012). Role of environmental poliovirus surveillance in global polio eradication and beyond. *Epidemiology & Infection* 140**,** 1-13.

Karthikeyan, S., Nguyen, A., Mcdonald, D., Zong, Y., Ronquillo, N., Ren, J., Zou, J., Farmer, S., Humphrey, G., and Henderson, D. (2021). Rapid, large-scale wastewater surveillance and automated reporting system enable early detection of nearly 85% of COVID-19 cases on a university campus. *Msystems* 6**,** e00793-00721.

Kow, C.S., and Hasan, S.S. (2021). Real-world effectiveness of BNT162b2 mRNA vaccine: a meta-analysis of large observational studies. *Inflammopharmacology* 29**,** 1075-1090.

Levine-Tiefenbrun, M., Yelin, I., Alapi, H., Katz, R., Herzel, E., Kuint, J., Chodick, G., Gazit, S., Patalon, T., and Kishony, R. (2021a). Viral loads of Delta-variant SARS-CoV-2 breakthrough infections after vaccination and booster with BNT162b2. *Nature medicine* 27**,** 2108-2110.

Levine-Tiefenbrun, M., Yelin, I., Katz, R., Herzel, E., Golan, Z., Schreiber, L., Wolf, T., Nadler, V., Ben-Tov, A., and Kuint, J. (2021b). Initial report of decreased SARS-CoV-2 viral load after inoculation with the BNT162b2 vaccine. *Nature medicine* 27**,** 790-792.

Liu, P., Ibaraki, M., Vantassell, J., Geith, K., Cavallo, M., Kann, R., Guo, L., and Moe, C.L. (2022). A sensitive, simple, and low-cost method for COVID-19 wastewater surveillance at an institutional level. *Science of The Total Environment* 807**,** 151047.

Lodder, W., Buisman, A., Rutjes, S., Heijne, J., Teunis, P., and De Roda Husman, A. (2012). Feasibility of quantitative environmental surveillance in poliovirus eradication strategies. *Applied and environmental microbiology* 78**,** 3800-3805.

Lu, X., Wang, L., Sakthivel, S.K., Whitaker, B., Murray, J., Kamili, S., Lynch, B., Malapati, L., Burke, S.A., and Harcourt, J. (2020). US CDC real-time reverse transcription PCR panel for detection of severe acute respiratory syndrome coronavirus 2. *Emerging infectious diseases* 26**,** 1654.

Majumdar, M., Klapsa, D., Wilton, T., Akello, J., Anscombe, C., Allen, D., Mee, E.T., Minor, P.D., and Martin, J. (2018). Isolation of vaccine-like poliovirus strains in sewage samples from the United Kingdom. *The Journal of Infectious Diseases* 217**,** 1222-1230.

Matthijnssens, J., Bilcke, J., Ciarlet, M., Martella, V., Bányai, K., Rahman, M., Zeller, M., Beutels, P., Van Damme, P., and Van Ranst, M. (2009). Rotavirus disease and vaccination: impact on genotype diversity. *Future microbiology* 4**,** 1303-1316.

Medema, G., Heijnen, L., Elsinga, G., Italiaander, R., and Brouwer, A. (2020). Presence of SARS-Coronavirus-2 RNA in sewage and correlation with reported COVID-19 prevalence in the early stage of the epidemic in the Netherlands. *Environmental Science & Technology Letters* 7**,** 511-516.

Mizumoto, K., Kagaya, K., Zarebski, A., and Chowell, G. (2020). Estimating the asymptomatic proportion of coronavirus disease 2019 (COVID-19) cases on board the Diamond Princess cruise ship, Yokohama, Japan, 2020. *Eurosurveillance* 25**,** 2000180.

Nishiura, H., Kobayashi, T., Miyama, T., Suzuki, A., Jung, S.-M., Hayashi, K., Kinoshita, R., Yang, Y., Yuan, B., and Akhmetzhanov, A.R. (2020). Estimation of the asymptomatic ratio of novel coronavirus infections (COVID-19). *International journal of infectious diseases* 94**,** 154-155.

Pilishvili, T., Gierke, R., Fleming-Dutra, K.E., Farrar, J.L., Mohr, N.M., Talan, D.A., Krishnadasan, A., Harland, K.K., Smithline, H.A., and Hou, P.C. (2021). Effectiveness of mRNA Covid-19 vaccine among US health care personnel. *New England Journal of Medicine* 385**,** e90.

Prasek, S.M., Pepper, I.L., Innes, G.K., Slinski, S., Ruedas, M., Sanchez, A., Brierley, P., Betancourt, W.Q., Stark, E.R., and Foster, A.R. (2022). Population level SARS-CoV-2 fecal shedding rates determined via wastewater-based epidemiology. *Science of The Total Environment***,** 156535.

Rafiee, M., Isazadeh, S., Mohseni-Bandpei, A., Mohebbi, S.R., Jahangiri-Rad, M., Eslami, A., Dabiri, H., Roostaei, K., Tanhaei, M., and Amereh, F. (2021). Moore swab performs equal to composite and outperforms grab sampling for SARS-CoV-2 monitoring in wastewater. *Science of The Total Environment* 790**,** 148205.

Scott, L.C., Aubee, A., Babahaji, L., Vigil, K., Tims, S., and Aw, T.G. (2021). Targeted wastewater surveillance of SARS-CoV-2 on a university campus for COVID-19 outbreak detection and mitigation. *Environmental research* 200**,** 111374.

Sweetapple, C., Melville-Shreeve, P., Chen, A.S., Grimsley, J.M., Bunce, J.T., Gaze, W., Fielding, S., and Wade, M.J. (2022). Building knowledge of university campus population dynamics

to enhance near-to-source sewage surveillance for SARS-CoV-2 detection. *Science of the Total Environment* 806**,** 150406.

Wang, H., Neyvaldt, J., Enache, L., Sikora, P., Mattsson, A., Johansson, A., Lindh, M., Bergstedt, O., and Norder, H. (2020). Variations among viruses in influent water and effluent water at a wastewater plant over one year as assessed by quantitative PCR and metagenomics. *Applied and environmental microbiology* 86**,** e02073-02020.

Westhaus, S., Weber, F.-A., Schiwy, S., Linnemann, V., Brinkmann, M., Widera, M., Greve, C., Janke, A., Hollert, H., and Wintgens, T. (2021). Detection of SARS-CoV-2 in raw and treated wastewater in Germany–suitability for COVID-19 surveillance and potential transmission risks. *Science of The Total Environment* 751**,** 141750.

Wurtzer, S., Marechal, V., Mouchel, J., and Moulin, L. (2020). "Time course quantitative detection of SARS-CoV-2 in Parisian wastewaters correlates with COVID-19 confirmed cases. medRxiv 2020.04. 12.20062679".).

Ye, Y., Ellenberg, R.M., Graham, K.E., and Wigginton, K.R. (2016). Survivability, partitioning, and recovery of enveloped viruses in untreated municipal wastewater. *Environmental science & technology* 50**,** 5077-5085.

Chapter 5. Implications and Future Work

This section summarizes the major findings from this dissertation research and recommends future research. My dissertation applied molecular tools to characterize water quality and pathogens for improved management of industrial and municipal wastewater. This research is a direct extension of my Master of Science graduate work in Iran, where I investigated the effectiveness of natural coagulants as an environmentally friendly alternative to synthetic chemical coagulants for treatment of wastewater from the steel industry. Chapter 2 of this dissertation focused on modifying two high-throughput molecular toxicity screening assays for application to high salinity industrial wastewaters derived from hydraulically fractured oil and gas wells. Chapters 3 and 4 involved application of molecular tools for quantification of viral biomarkers in municipal wastewater. Ultimately, I intend to utilize similar tools in a variety of environmental engineering problems during my career, including wastewater management, public health monitoring, and risk assessment.

5.1 Improved molecular tools for toxicity assessment of high salinity wastewater are needed

One of the major challenges in assessing toxicity of high salinity wastewater is the interaction of salt with other potentially harmful chemicals including oxidative radical initiators, biocides and surfactants. My work suggests acute toxicity is higher for the flowback fluid and produced water (FPW) samples when larger quantities of specific chemical additives are applied. I also observed that samples with the highest N-acetylcysteine (NAC) thiol reactivity, dominant predictor of additive mammalian toxicity, derived from shale well samples contained higher oxidative radical

chemicals. This finding is consistent with related studies quantifying NAC thiol reactivity in water and wastewater samples receiving higher oxidative inputs from disinfection processes which are thought to initiate the biological thiol-specific detoxification mechanism and suggests that similar reactions may occur in the fractured shale system (Dong et al., 2018;Dong et al., 2019).

These results support the need for careful management of wastewater from hydraulically fractured shale wells, particularly during the handling of injection and initial flowback fluids, when higher acute toxicity was measured, to mitigate their release to the environment.

Recommended future research to further expand this research include:

1. Additional testing of multiple toxicity end points to better characterize differences in FPW toxicity that vary through time and geologic formation as well as assess potential interactions between chemical additives.
2. Further studies on tracking temporal changes in toxicity for input media and produced fluid samples from multiple hydraulically fractured natural-gas wells across various shale formations. This advances our knowledge of the important role long-term studies will likely play on toxicity measurement of FPW samples from natural gas wells in different shale formations.
3. Expanded studies applying the NAC-based thiol reactivity toxicity assay on FPW samples which is a dominant predictor of additive mammalian toxicity. Employing this bioanalytical assay compared with other suite of organisms (e.g., Daphnia magna, zebrafish embryos, Oncorhynchus mykiss, Danio rerio) (Delompré et al., 2019;Folkerts et al., 2019) could enable direct comparison of composite toxicity of time series FPW samples.

5.2 Expanded studies on SARS-CoV-2 fate in wastewater are needed

Municipal sewage carries SARS-CoV-2 viral biomarkers shed in human stool by infected individuals, to sewer piping and eventually to wastewater treatment plants (WWTPs). Increasing prevalence of COVID-19 in the population therefore increases the viral load in WWTPs serving our communities. Appropriate wastewater treatment can prevent uncontrolled discharge of the viruses into the environment. A few studies have assessed viral RNA removal through the wastewater treatment process. However, it remains unclear the fate of the virus along the treatment train. Thus, there remains need to better understand how engineered facilities remove this novel coronavirus, and others like it, especially considering that a varied spectrum of removal efficiencies is expected depending on population infection rate, the treatment facility design, and the disinfection approach. Knowledge on potential sinks of the virus within the treatment train (e.g., sludge, liquids) is critical to minimize routes of exposure, and to inform public health responses.

Recommended future research in this field includes:

1. Measuring SARS-CoV-2 RNA concentrations in wastewater from a larger number of WWTPs to improve our ability to evaluate the effect of WWTP design on SARS-CoV-2 RNA distribution and fate. Furthermore, collecting more samples from different processes at each treatment plant might enhance our understanding of viral RNA fate within WWTPs.
2. Evaluating SARS-CoV-2 RNA concentrations in samples collected by composite samplers installed within different wastewater treatment trains would advance our understanding of viral RNA fate within WWTPs by capturing samples that are more representative.
3. Understanding the potential sinks of this new virus within the treatment train (e.g., sludge, liquids) to minimize routes of exposure, and to inform public health responses.

Specifically, studies that better characterize the liquid - solid partitioning of this new virus and removal mechanisms in various wastewater treatment processes are needed. Further investigation on whether the hydrophobic nature of the SARS-CoV-2 envelope makes solids a suitable phase for tracking COVID-19 biomarkers would improve our understanding of SARS-CoV-2 RNA fate within wastewater treatment plants.

4. Evaluating the influence of secondary treatment design (e.g., hydraulic retention time (HRT), and sludge retention time (SRT)) on SARS-CoV-2 RNA trends to improve prediction of viral RNA in the treatment plant. SARS-CoV-2 RNA accumulates in the sludge, therefore, understanding the conditions under which viral RNA adsorbs to the sludge is also important for predicting the fate of this virus within WWTPs.
5. Ascertaining the risk of viral transmission to wastewater treatment plant operators and surrounding residencies is negligible especially in light of new SARS-CoV-2 variants (e.g., B.1.1.7, B.1.351, P.1, B.1.617.2 and B.1.1.529) that are possibly more contagious compared to the original strain. Further studies are required to assess infectivity through viable virus estimation in the effluents from secondary treatments and after activated sludge and digestion processes to determine if additional treatment processes are needed to eliminate the COVID-19 virus and to prevent its spread via wastewater discharge or reuse schemes.

5.3 Understanding the influence of vaccination on SARS-CoV-2 biomarkers to improve surveillance of COVID-19

Studies around the world conducted during the pandemic demonstrated that tracking SARS-CoV-2 viral biomarkers in wastewater could provide early detection of outbreaks, elucidate the extent of the infection in under-tested communities, understand the impact of safety measures or lockdown procedures, and assess community prevalence. Recent studies showed that introduction of vaccines reduced the transmission of infectious viruses (e.g., rotavirus, norovirus, adenovirus, poliovirus, hepatitis A virus) and consequently diminished viral nucleic acid biomarker signals in wastewater (Matthijnssens et al., 2009;Blanco Fernández et al., 2012;Battistone et al., 2014;Yanez et al., 2014;Kiulia et al., 2021).

My work assessed temporal trends of SARS-CoV-2 biomarkers at a community WWTP, compared with a location upstream in the sewershed. I found COVID-19 vaccine administration resulted in a significant decrease in SARS-CoV-2 RNA concentration in wastewater concurrent with decreasing number of COVID-19 infections in the community when variants of concern were not likely to represent a large percentage of COVID-19 cases on UNH campus. Emergence of the new variants that might not be covered by existing vaccines resulted in a significant increase in SARS-CoV-2 RNA concentration in wastewater parallel with increasing number of COVID-19 infections in the UNH community. My analyses of the SARS-CoV-2 RNA concentration in the liquid and solid phase of the wastewater samples during Fall 2021 semester and after the mass-scale vaccination campaign, show elevated biomarker equivalent concentration in the solid phase (200 to 2000×) compared to the liquid phase of the wastewater suggesting the efficacy and sensitivity of wastewater solids to evaluate SARS-CoV-2 RNA biomarker concentration at the sewershed level.

Recommended future research projects include:

1. Evaluating changes in SARS-CoV-2 RNA biomarker signals and viral genomes in response to vaccination in the context of new variants. This would help explain the effectiveness of the current vaccines in preventing infection and decreasing the viral load in breakthrough infections in parallel with the rise of the new variants in the communities.
2. Designing and implementing long-term environmental surveillance plans for SARS CoV-2 on campuses and elsewhere to complement conventional public health interventions.
3. Characterizing the duration and magnitude of viral RNA shedding in feces would improve our understanding of the effect of vaccines on reducing the viral load in wastewater facilities.
4. Comparing sequencing data for SARS-CoV-2 in wastewater and clinical infection samples would improve our understanding of the diversity of SARS-CoV-2 circulating within a community.
5. Comparison of this study design to other study designs, based on indices of outcomes, cost and practicality (Harris-Lovett et al., 2021) will help synthesize insights to improve future surveillance efforts.

5.4 References

Battistone, A., Buttinelli, G., Fiore, S., Amato, C., Bonomo, P., Patti, A.M., Vulcano, A., Barbi, M., Binda, S., and Pellegrinelli, L. (2014). Sporadic isolation of Sabin-like polioviruses and high-level detection of non-polio enteroviruses during sewage surveillance in seven Italian cities, after several years of inactivated poliovirus vaccination. *Applied and environmental microbiology* 80**,** 4491-4501.

Blanco Fernández, M., Torres, C., Riviello-López, G., Poma, H., Rajal, V., Nates, S., Cisterna, D., Campos, R., and Mbayed, V. (2012). Analysis of the circulation of hepatitis A virus in Argentina since vaccine introduction. *Clinical Microbiology and Infection* 18**,** E548-E551.

Delompré, P., Blewett, T., Goss, G., and Glover, C. (2019). Shedding light on the effects of hydraulic fracturing flowback and produced water on phototactic behavior in Daphnia magna. *Ecotoxicology and environmental safety* 174**,** 315-323.

Dong, S., Page, M.A., Massalha, N., Hur, A., Hur, K., Bokenkamp, K., Wagner, E.D., and Plewa, M.J. (2019). Toxicological comparison of water, wastewaters, and processed wastewaters. *Environmental science & technology* 53**,** 9139-9147.

Dong, S., Page, M.A., Wagner, E.D., and Plewa, M.J. (2018). Thiol reactivity analyses to predict mammalian cell cytotoxicity of water samples. *Environmental science & technology* 52**,** 8822-8829.

Folkerts, E.J., Blewett, T.A., Delompré, P., Mehler, W.T., Flynn, S.L., Sun, C., Zhang, Y., Martin, J.W., Alessi, D.S., and Goss, G.G. (2019). Toxicity in aquatic model species exposed to a temporal series of three different flowback and produced water samples collected from a horizontal hydraulically fractured well. *Ecotoxicology and environmental safety* 180**,** 600-609.

Harris-Lovett, S., Nelson, K.L., Beamer, P., Bischel, H.N., Bivins, A., Bruder, A., Butler, C., Camenisch, T.D., De Long, S.K., and Karthikeyan, S. (2021). Wastewater surveillance for SARS-CoV-2 on college campuses: initial efforts, lessons learned, and research needs. *International journal of environmental research and public health* 18**,** 4455.

Kiulia, N.M., Gonzalez, R., Thompson, H., Aw, T.G., and Rose, J.B. (2021). Quantification and Trends of Rotavirus and Enterovirus in Untreated Sewage Using Reverse Transcription Droplet Digital PCR. *Food and Environmental Virology* 13**,** 154-169.

Matthijnssens, J., Bilcke, J., Ciarlet, M., Martella, V., Bányai, K., Rahman, M., Zeller, M., Beutels, P., Van Damme, P., and Van Ranst, M. (2009). Rotavirus disease and vaccination: impact on genotype diversity. *Future microbiology* 4**,** 1303-1316.

Yanez, L.A., Lucero, N.S., Barril, P.A., Díaz, M.D.P., Tenaglia, M.M., Spinsanti, L.I., Nates, S.V., Isa, M.B., and Ré, V.E. (2014). Evidence of hepatitis A virus circulation in central Argentina: seroprevalence and environmental surveillance. *Journal of Clinical Virology* 59**,** 38-43.

Appendix A. Supporting Information for Chapter 2

Supporting Tables

Table A1. Major ion concentrations (mg/L) of salt matched control that mimicked the chemistry of Appalachian shale FPW.

Constituents	Measured Conc. (mg/L)
Ca^{+2}	8000
Mg^{+2}	748.75
Na^{+}	20185
K^{+}	660
Cl^{-}	48113

Table A2. Bioluminescence Inhibition Assay Data

Type of sample	Well #	Approximate Time After Flowback Began (Days)	Sampling Date	Days after Fracturing	TDS (ppt)	DOC (mg/L)	Dilution Factor	pH	BLIA Inhibitory Effect (S)	BLIA Inhibitory Effect (SF)	TU_{50}
MARCELLUS SHALE											
M-4 fracture fluid (Kill fluid)	M-4	NA	3/3/2017	NA	19.1	NA	1	9.22	89.14	88.22	51.28
M-4 Drill mud	M-4	NA	8/28/2015	NA	124.9	NA	70	8.99	52.05	52.49	2.10
M-4 Sidewall mud	M-4	NA	9/3/2015	NA	104.0	NA	6	8.17	37.36	44.86	1.41
M-4 FPW	M-4	2	12/11/2015	25	17.50	312.2	4	6.4	5.25	0.37	0.030
M-4 FPW	M-4	13	12/22/2015	36	25.20	84.9	3	6.36	6.96	5.34	0.656
M-4 FPW	M-4	56	2/3/2016	79	55.30	98.5	5	5.99	8.06	0.8	0.006
M-4 FPW	M-4	70	2/17/2016	93	65.10	68.64	5	5.86	11.61	16.18	0.396
M-4 FPW	M-4	182	6/8/2016	205	143.50	59.67	5	6.35	6.73	4.43	0.002
M-4 FPW	M-4	280	9/14/2016	303	212.10	60.96	5	6.05	11.13	5.35	0.006
M-4 FPW	M-4	406	1/18/2017	429	300.30	416.15	6	5.42	-11.15	-22.36	-
M-4 FPW	M-4	490	4/12/2017	513	359.10	104.1	6	5.22	-15.78	-25.47	-
M-4 FPW	M-4	641	8/16/2017	664	464.80	NA	6	5.28	-17.21	-30.48	-
M-4 FPW	M-4	764	12/13/2017	787	550.90	NA	6	5.39	-24.98	-26.54	-
M-5 FPW	M-5	2	12/11/2015	36	25.20	68.91	3	6.3	33.61	30.76	3.68
M-5 FPW	M-5	9	12/18/2015	43	30.10	50.86	3	6.42	37.31	26.96	1.78
M-5 FPW	M-5	56	2/3/2016	90	63.00	159.9	4	6.21	29.11	20.24	0.43
M-5 FPW	M-5	70	2/17/2016	104	72.80	43.35	5	6.1	21.98	28.5	0.15
M-5 FPW	M-5	119	4/6/2016	153	107.10	41.96	5	6.27	26.69	10.24	1.16
M-5 FPW	M-5	182	6/8/2016	216	151.20	49.92	6	6.38	5.63	6.18	0.00
M-5 FPW	M-5	280	9/14/2016	314	219.80	50.2	6	6.25	-1.2	-30.88	0.00
M-5 FPW	M-5	764	12/13/2017	798	558.60	NA	4	5.72	6.08	-7.99	-
UTICA SHALE											
SW Fresh Water Tank	-	N/A	5/7/2015	N/A	0.14903	NA	-	8.541	-12.06	-28.62	-
SW Fresh Water Tank	-	N/A	5/14/2015	N/A	0.16387	NA	-	7.68	-9.88	-27.66	-

SW Produced Water Additive	-	N/A	5/14/2015	N/A	127.82	NA	7	6.323	4.52	-8.68	-
SW Produced Water Additive	-	N/A	5/29/2015	N/A	129.08	NA	7	5.71	1.54	13.18	-
U-6 FPW	U-6	1	7/14/2015	38	89.88	83.3	5	6.588	4.36	27.8	0.103
U-6 FPW	U-6	9	7/23/2015	46	109.27	64.06	6	6.33	9.72	16.78	0.067
U-6 FPW	U-6	16	7/30/2015	54	113.54	60.74	6	6.36	5.42	13.12	0.192
U-6 FPW	U-6	22	8/5/2015	60	117.6	83.82	6	6.32	21.87	12.31	0.531
U-6 FPW	U-6	30	8/13/2015	68	119.42	59.78	7	6.28	-24.87	-28.63	-
U-6 FPW	U-6	58	9/10/2015	96	130.55	48.62	7	6.22	-26.29	-25.16	-
U-6 FPW	U-6	87	10/8/2015	124	86.8	36.62	5	3.97	-26.17	-18.53	-
U-6 FPW	U-6	122	11/12/2015	159	111.3	50.29	7	4.5	-32.83	-32.14	-
U-6 FPW	U-6	392	8/8/2016	460	322	22.904	7	5.31	-18.05	-51.79	-
U-7 FPW	U-7	1	7/14/2015	38	128.73	153.9	7	5.97	-11.32	-39.14	-
U-7 FPW	U-7	9	7/23/2015	46	114.03	80.76	6	6.32	-19.73	-29.64	-
U-7 FPW	U-7	16	7/30/2015	54	120.05	61.41	7	6.2	-39.72	-46.68	-
U-7 FPW	U-7	30	8/13/2015	68	128.66	51.96	7	6.2	-47.79	-57.31	-
U-7 FPW	U-7	58	9/10/2015	96	135.87	55.23	7	6.15	-24.97	-17.72	-
U-7 FPW	U-7	87	10/8/2015	124	86.8	36.2	7	5.58	-26.58	-25.18	-
U-7 FPW	U-7	122	11/12/2015	159	111.3	40.46	7	5.03	-55.65	-62.91	-
U-7 FPW	U-7	392	8/8/2016	460	322	22.8	7	5.54	-59.28	-53.92	-

Table A3. NAC Thiol Reactivity Data

Type of sample	Well #	Approximate Time After Flowback Began (Days)	Sampling Date	Days after Fracturing	Concentration Factor	NAC-Thiol Assay: Response as the Mean Percent of the Negative Control (±SE)
MARCELLUS SHALE						
M-4 fracture fluid	M-4	NA	11/11/2015	NA	25	85.81
Input river	M-4	NA	11/11/2015	NA	200	89.75
M-4 FPW	M-4	4	12/13/2015	27	200	82.98
M-4 FPW	M-4	13	12/22/2015	36	200	80.5
M-4 FPW	M-4	56	2/3/2016	79	200	77.63
M-4 FPW	M-4	70	2/17/2016	93	200	78.27
M-4 FPW	M-4	182	6/8/2016	205	200	77.79
M-4 FPW	M-4	280	9/14/2016	303	200	89.67
M-4 FPW	M-4	406	1/18/2017	429	200	80.04
M-4 FPW	M-4	490	4/12/2017	513	200	91.28
M-4 FPW	M-4	641	8/16/2017	664	200	91.65
M-4 FPW	M-4	764	12/13/2017	787	200	96.08
M-5 fracture fluid	M-5	NA	11/5/2015	NA	25	90.45
Input river	M-5	NA	11/5/2015	NA	200	90.65
M-5 FPW	M-5	9	12/18/2015	43	200	78.97
M-5 FPW	M-5	36	1/14/2016	70	200	87.31
M-5 FPW	M-5	56	2/3/2016	90	200	85.5
M-5 FPW	M-5	70	2/17/2016	104	200	86.46
M-5 FPW	M-5	119	4/6/2016	153	200	92.3
M-5 FPW	M-5	182	6/8/2016	216	200	77.6
M-5 FPW	M-5	280	9/14/2016	314	200	99.09
M-5 FPW	M-5	764	12/13/2017	798	200	94.47

Table A4. Hydraulic fracturing fluid composition details for M-4 well in Marcellus Shale

Job Start Date:	11/6/2015
Job End Date:	11/15/2015
State:	West Virginia
County:	Monongalia
True Vertical Depth:	7,483
Total Base Water Volume (gal):	10,647,966
Total Base Non Water Volume:	0

Hydraulic Fracturing Fluid Composition:

Trade Name	Supplier	Purpose	Ingredients	Chemical Abstract Service Number (CAS #)	Maximum Ingredient Concentration in Additive (% by mass)**	Maximum Ingredient Concentration in HF Fluid (% by mass)**	Comments
Ingredients shown above are subject to 29 CFR 1910.1200(i) and appear on Material Safety Data Sheets (MSDS). Ingredients shown below are Non-MSDS.							
Proppant Transport	Schlumberger	Corrosion Inhibitor, Scale Inhibitor, Biocide, AntiFoam Agent, Acid, Breaker, Gelling Agent, Friction Reducer, Iron Control Agent, Fluid Loss Additive					
			Water (Including Mix Water Supplied by Client)*	NA		87.63568	
			Quartz, Crystalline silica	14808-60-7	99.06784	12.21724	
			Hydrochloric acid	7647-01-0	0.66726	0.08228	
			Ammonium sulfate	7783-20-2	0.06845	0.00844	
			Guar gum	9000-30-0	0.05865	0.00724	
			Acrylamide, 2-acrylamido-2-methylpropanesulfonic acid, sodium salt polymer	38193-60-1	0.05052	0.00623	
			Glutaraldehyde	111-30-8	0.02831	0.00349	
			Ethanol, 2,2',2"-nitrilotris-, 1,1',1"-tris(dihydrogen phosphate), sodium salt	68171-29-9	0.00971	0.00120	
			Diammonium peroxidisulphate	7727-54-0	0.00601	0.00074	

			Polymer of 2-acrylamido-2-methylpropanesulfonic acid sodium salt and methyl acrylate	136793-29-8	0.00541	0.00067	
			Alkyl(c12-16) dimethylbenzyl ammonium chloride	68424-85-1	0.00506	0.00062	
			Sodium erythorbate	6381-77-7	0.00436	0.00054	
			Trisodium ortho phosphate	7601-54-9	0.00427	0.00053	
			Urea	57-13-6	0.00332	0.00041	
			Polypropylene glycol	25322-69-4	0.00294	0.00036	
			Methanol	67-56-1	0.00252	0.00031	
			Fatty acids, tall-oil	61790-12-3	0.00156	0.00019	
			Thiourea, polymer with formaldehyde and 1-phenylethanone	68527-49-1	0.00129	0.00016	
			Ethylene Glycol	107-21-1	0.00121	0.00015	
			Non-crystalline silica (impurity)	7631-86-9	0.00084	0.00010	
			Vinylidene chloride/methylacrylate copolymer	25038-72-6	0.00080	0.00010	
			Sodium sulfate	7757-82-6	0.00078	0.00010	
			Alcohols, C14-15, ethoxylated (7EO)	68951-67-7	0.00061	0.00008	
			Ethanol	64-17-5	0.00061	0.00007	
			Propargyl alcohol	107-19-7	0.00041	0.00005	
			2-Propenamid (impurity)	79-06-1	0.00017	0.00002	
			Hexadec-1-ene	629-73-2	0.00014	0.00002	
			1-Octadecene (C18)	112-88-9	0.00007	0.00001	
			Dimethyl siloxanes and silicones	63148-62-9	0.00005	0.00001	
			Tetrasodium ethylenediaminetetraacetate	64-02-8	0.00009	0.00001	
			Dodecamethylcyclohexasiloxane	540-97-6			
			Siloxanes and silicones, dimethyl, reaction products with silica	67762-90-7	0.00001		
			Octamethylcyclotetrasiloxane	556-67-2			
			poly(tetrafluoroethylene)	9002-84-0	0.00001		
			Formaldehyde	50-00-0	0.00001		
			Copper(II) sulfate	7758-98-7			
			Decamethyl cyclopentasiloxane	541-02-6			
			Magnesium silicate hydrate (talc)	14807-96-6	0.00002		
FR Pro 150	ECM	Friction Reduction					
			Water	7732-18-5	50.00000	0.01575	
			Polyacrylamide-co-acrylic acid	9003-06-9	32.00000	0.01008	
			Sodium Chloride	7647-14-5	15.00000	0.00472	
			Alcohol Ethoxylate Surfactants	Trade	5.00000	0.00157	
			Petroleum Distillate	64742-47-8	25.00000		

* Total Water Volume sources may include fresh water, produced water, and/or recycled water
** Information is based on the maximum potential for concentration and thus the total may be over 100%

Note: For Field Development Products (products that begin with FDP), MSDS level only information has been provided.
Ingredient information for chemicals subject to 29 CFR 1910.1200(i) and Appendix D are obtained from suppliers Material Safety Data Sheets (MSDS)

Table A5. Hydraulic fracturing fluid composition details for M-5 well in Marcellus Shale

Job Start Date:	10/28/2015
Job End Date:	11/5/2015
State:	West Virginia
County:	Monongalia
True Vertical Depth:	7,530
Total Base Water Volume (gal):	9,961,350
Total Base Non Water Volume:	0

Hydraulic Fracturing Fluid Composition:

Trade Name	Supplier	Purpose	Ingredients	Chemical Abstract Service Number (CAS #)	Maximum Ingredient Concentration in Additive (% by mass)**	Maximum Ingredient Concentration in HF Fluid (% by mass)**	Comments
Ingredients shown above are subject to 29 CFR 1910.1200(i) and appear on Material Safety Data Sheets (MSDS). Ingredients shown below are Non-MSDS.							
Proppant Transport	Schlumberger	Corrosion Inhibitor, Scale Inhibitor, Biocide, Acid, Breaker, Gelling Agent, Friction Reducer, Iron Control Agent, Fluid Loss Additive , Propping Age					
			Water (Including Mix Water Supplied by Client)*	NA		87.58016	
			Quartz, Crystalline silica	14808-60-7	98.77034	12.26228	
			Hydrochloric acid	7647-01-0	0.90405	0.11223	
			Ammonium sulfate	7783-20-2	0.12127	0.01506	
			Acrylamide, 2-acrylamido-2-methylpropanesulfonic acid, sodium salt polymer	38193-60-1	0.08951	0.01111	
			Glutaraldehyde	111-30-8	0.03083	0.00383	
			Guar gum	9000-30-0	0.02213	0.00275	
			Polymer of 2-acrylamido-2-methylpropanesulfonic acid sodium salt and methyl acrylate	136793-29-8	0.00959	0.00119	

			Ethanol, 2,2',2"-nitrilotris-, 1,1',1"-tris(dihydrogen phosphate), sodium salt	68171-29-9	0.00943	0.00117	
			Sodium erythorbate	6381-77-7	0.00589	0.00073	
			Urea	57-13-6	0.00589	0.00073	
			Alkyl(c12-16) dimethylbenzyl ammonium chloride	68424-85-1	0.00551	0.00068	
			Trisodium ortho phosphate	7601-54-9	0.00415	0.00051	
			Methanol	67-56-1	0.00332	0.00041	
			Fatty acids, tall-oil	61790-12-3	0.00210	0.00026	
			Thiourea, polymer with formaldehyde and 1-phenylethanone	68527-49-1	0.00174	0.00022	
			Sodium sulfate	7757-82-6	0.00137	0.00017	
			Non-crystalline silica (impurity)	7631-86-9	0.00128	0.00016	
			Ethylene Glycol	107-21-1	0.00118	0.00015	
			Alcohols, C14-15, ethoxylated (7EO)	68951-67-7	0.00082	0.00010	
			Ethanol	64-17-5	0.00066	0.00008	
			Propargyl alcohol	107-19-7	0.00055	0.00007	
			2-Propenamid (impurity)	79-06-1	0.00029	0.00004	
			Hexadec-1-ene	629-73-2	0.00018	0.00002	
			Tetrasodium ethylenediaminetetraacetate	64-02-8	0.00015	0.00002	
			Diammonium peroxidisulphate	7727-54-0	0.00008	0.00001	
			1-Octadecene (C18)	112-88-9	0.00009	0.00001	
			Dimethyl siloxanes and silicones	63148-62-9	0.00008	0.00001	
			Decamethyl cyclopentasiloxane	541-02-6	0.00001		
			Siloxanes and silicones, dimethyl, reaction products with silica	67762-90-7	0.00001		
			Octamethylcyclotetrasiloxane	556-67-2	0.00001		
			Formaldehyde	50-00-0	0.00001		
			Dodecamethylcyclohexasiloxane	540-97-6			
			Copper(II) sulfate	7758-98-7			
FR Pro 150	ECM	Friction Reduction					
			Water	7732-18-5	50.00000	0.00240	
			Polyacrylamide-co-acrylic acid	9003-06-9	32.00000	0.00154	
			Sodium Chloride	7647-14-5	15.00000	0.00072	
			Alcohol Ethoxylate Surfactants	Trade	5.00000	0.00024	
			Hydrotreated Petroleum Distillate	64742-47-8	25.00000		

* Total Water Volume sources may include fresh water, produced water, and/or recycled water
** Information is based on the maximum potential for concentration and thus the total may be over 100%

Note: For Field Development Products (products that begin with FDP), MSDS level only information has been provided.
Ingredient information for chemicals subject to 29 CFR 1910.1200(i) and Appendix D are obtained from suppliers Material Safety Data Sheets (MSDS)

Table A6. Hydraulic fracturing fluid composition details for U-6 well in the Utica-Point Pleasant Formation

Job Start Date:	4/30/2015
Job End Date:	5/30/2015
State:	Ohio
County:	Monroe
True Vertical Depth:	9,619
Total Base Water Volume (gal):	7,519,974
Total Base Non Water Volume:	0

Hydraulic Fracturing Fluid Composition:

Trade Name	Supplier	Purpose	Ingredients	Chemical Abstract Service Number (CAS #)	Maximum Ingredient Concentration in Additive (% by mass)**	Maximum Ingredient Concentration in HF Fluid (% by mass)**	Comments
Fresh water	Stingray	Carrier					
			Water	7732-18-5	100.00000	87.27337	
40/70 White	Steubenville/Cadiz	Proppant					
			Sand	14808-60-7	100.00000	11.93720	
Muriatic Acid	Axiall, LLC	Acid					
			Water	7732-18-5	60.00000	0.21773	
			Hydrogen chloride	7647-01-0	40.00000	0.14516	
100 mesh	Minerva/Cadiz	Proppant					
			Sand	14808-60-7	100.00000	0.23238	
FRA 409	Weatherford	Friction Reducer					
			Ethanaminium, N,N,N-trimethyl-2-[(1-oxo-2-propenyl)oxy]-, chloride, polymer with 2-propenamide	69418-26-4	70.00000	0.07463	
			Proprietary	Proprietary	30.00000	0.03198	
			Petroleum Distillate	64742-47-8	10.00000	0.01066	
			Alcohols, C12-14-secondary, ethoxylated	84133-50-6	5.00000	0.00533	
			Adipic acid	124-04-9	3.00000	0.00320	
B-84	X-Chem, LLC	Biocide					
			Water	7732-18-5	55.50000	0.01738	

			Glutaraldehyde	111-30-8	27.00000	0.00846	
			Didecyl dimethyl ammonium chloride	7173-51-5	8.00000	0.00251	
			n-Alkyl dimethyl benzyl ammonium chloride	68424-85-1	5.50000	0.00172	
			Ethanol	64-17-5	4.00000	0.00125	
VBL-29	X-Chem, LLC	Breaker					
			Water	7732-18-5	90.00000	0.02785	
			Hydrogen Peroxide	7722-84-1	10.00000	0.00309	
Plexgel 907L-EB	Chemplex SOLVAY	Viscosifier					
			Guar Gum	9000-30-0	50.00000	0.00638	
			Distillate(petroleum), hydrotreated light	64742-47-8	50.00000	0.00638	
			Organophylic Clay	Proprietary	2.00000	0.00026	
			Alcohol ethoxylate	34398-01-1	0.99000	0.00013	
			Cyrstalline Silica	14808-60-7	0.06000	0.00001	
SC-30	X-Chem, LLC	Scale Inhibitor					
			Water	7732-18-5	70.00000	0.00729	
			Sodium Polyacrylate	Proprietary	30.00000	0.00312	
TCA 6038F	X-Chem, LLC	Corrosion Inhibitor					
			Water	7732-18-5	80.00000	0.00169	
			Methanol	67-56-1	20.00000	0.00042	
Ingredients shown above are subject to 29 CFR 1910.1200(i) and appear on Material Safety Data Sheets (MSDS). Ingredients shown below are Non-MSDS.							

* Total Water Volume sources may include fresh water, produced water, and/or recycled water
** Information is based on the maximum potential for concentration and thus the total may be over 100%

Note: For Field Development Products (products that begin with FDP), MSDS level only information has been provided.
Ingredient information for chemicals subject to 29 CFR 1910.1200(i) and Appendix D are obtained from suppliers Material Safety Data Sheets (MSDS)

Table A7. Hydraulic fracturing fluid composition details for U-7 well in the Utica-Point Pleasant Formation

Job Start Date:	4/30/2015
Job End Date:	5/30/2015
State:	Ohio
County:	Monroe
True Vertical Depth:	9,643
Total Base Water Volume (gal):	7,485,366
Total Base Non Water Volume:	0

Hydraulic Fracturing Fluid Composition:

Trade Name	Supplier	Purpose	Ingredients	Chemical Abstract Service Number (CAS #)	Maximum Ingredient Concentration in Additive (% by mass)**	Maximum Ingredient Concentration in HF Fluid (% by mass)**	Comments
Fresh water	Stingray	Carrier					
			Water	7732-18-5	100.00000	87.34324	
40/70 White	Steubenville/Cadiz	Proppant					
			Sand	14808-60-7	100.00000	11.90548	
Muriatic Acid	Axiall, LLC	Acid					
			Water	7732-18-5	60.00000	0.19527	
			Hydrogen chloride	7647-01-0	40.00000	0.13018	
100 mesh	Minerva/Cadiz	Proppant					
			Sand	14808-60-7	100.00000	0.23254	
FRA 409	Weatherford	Friction Reducer					
			Ethanaminium, N,N,N-trimethyl-2-[(1-oxo-2-propenyl)oxy]-, chloride, polymer with 2-propenamide	69418-26-4	70.00000	0.07695	
			Proprietary	Proprietary	30.00000	0.03298	
			Petroleum Distillate	64742-47-8	10.00000	0.01099	
			Alcohols, C12-14-secondary, ethoxylated	84133-50-6	5.00000	0.00550	
			Adipic acid	124-04-9	3.00000	0.00330	
B-84	X-Chem, LLC	Biocide					
			Water	7732-18-5	55.50000	0.01766	

			Glutaraldehyde	111-30-8	27.00000	0.00859	
			Didecyl dimethyl ammonium chloride	7173-51-5	8.00000	0.00255	
			n-Alkyl dimethyl benzyl ammonium chloride	68424-85-1	5.50000	0.00175	
			Ethanol	64-17-5	4.00000	0.00127	
VBL-29	X-Chem, LLC	Breaker					
			Water	7732-18-5	90.00000	0.02733	
			Hydrogen Peroxide	7722-84-1	10.00000	0.00304	
SC-30	X-Chem, LLC	Scale Inhibitor					
			Water	7732-18-5	70.00000	0.00771	
			Sodium Polyacrylate	Proprietary	30.00000	0.00330	
Plexgel 907L-EB	Chemplex SOLVAY	Viscosifier					
			Guar Gum	9000-30-0	50.00000	0.00435	
			Distillate(petroleum), hydrotreated light	64742-47-8	50.00000	0.00435	
			Organophylic Clay	Proprietary	2.00000	0.00017	
			Alcohol ethoxylate	34398-01-1	0.99000	0.00009	
			Cyrstalline Silica	14808-60-7	0.06000	0.00001	
TCA 6038F	X-Chem, LLC	Corossion Inhibitor					
			Water	7732-18-5	80.00000	0.00117	
			Methanol	67-56-1	20.00000	0.00029	

Ingredients shown above are subject to 29 CFR 1910.1200(i) and appear on Material Safety Data Sheets (MSDS). Ingredients shown below are Non-MSDS.

* Total Water Volume sources may include fresh water, produced water, and/or recycled water
** Information is based on the maximum potential for concentration and thus the total may be over 100%

Note: For Field Development Products (products that begin with FDP), MSDS level only information has been provided.
Ingredient information for chemicals subject to 29 CFR 1910.1200(i) and Appendix D are obtained from suppliers Material Safety Data Sheets (MSDS)

Table A8. Organic Chemistry Data

Type of sample	Well #	Approximate Time After Flowback Began (Days)	Sampling Date	Benzene (µg/L)	Toluene (µg/L)	Ethylbenzene (µg/L)	Xylene t (µg/L)	m,p-xylene (µg/L)	o-Xylene (µg/L)	MBAS (mg/L)	O&G (mg/L)
MARCELLUS SHALE											
M-4 FPW	M-4	1	12/10/2015	3	7.2	0.34	5	4	1.1	0.08	4
M-4 FPW	M-4	13	12/22/2015	2.2	2.7	0.11	1.2	0.71	0.53	0.48	36
M-4 FPW	M-4	42	1/20/2016	10	13	1.1	3.2	2.1	2.3	0.38	32
M-4 FPW	M-4	56	2/3/2016	12	10	11	31	20	10.5	0.55	88
M-4 FPW	M-4	133	4/20/2016	2.8	3.4	0.11	1	0.62	0.41	0.91	2
M-4 FPW	M-4	206	7/2/2016	1.4	1.6	0	0.31	0.2	0.11	0.38	250
M-4 FPW	M-4	287	9/21/2016	9.3	13	0.56	3	1.6	1.3	0.53	8
M-4 FPW	M-4	401	1/13/2017	2.1	2.3	0.11	0.31	0.2	0.11	0.84	2
M-4 FPW	M-4	485	4/7/2017	1.2	0.98	0.11	0.31	0.2	0.11	1.5	1
M-4 FPW	M-4	675	9/20/2017	0.67	0.37	0.2	0.65	0.49	0.18	1.2	2
M-4 FPW	M-4	771	12/20/2017	0.15	0.37	0.2	0.65	0.49	0.18	0.11	1
M-5 FPW	M-5	1	12/10/2015	4.3	18	1.4	16	12	4	0.56	41
M-5 FPW	M-5	8	12/17/2015	14	22	1.1	13	8.1	4.7	0.34	140
M-5 FPW	M-5	13	12/22/2015	12	10	11	31	20	10.5	0.22	41
M-5 FPW	M-5	42	1/20/2016	27	53	4	23	14	9.2	0.26	28
M-5 FPW	M-5	56	2/3/2016	12	10	11	31	20	10.5	0.27	500
M-5 FPW	M-5	133	4/20/2016	5.6	12	1.1	10	7.2	3.2	0.88	4
M-5 FPW	M-5	203	6/29/2016	8.8	15	0.83	3.6	2.1	1.6	0.89	12
M-5 FPW	M-5	287	9/21/2016	1.4	3.2	0.5	0.85	0.46	0.39	0.67	190
M-5 FPW	M-5	402	2/14/2017	2.2	7	0.48	2.1	1.4	0.72	3	16
M-5 FPW	M-5	771	12/20/2017	1.7	1.5	0.2	0.65	0.49	0.18	0.02	7

Table A9. Iodinated Organic Ions Data

Type of sample	Well #	Approximate Time After Flowback Began (Days)	Sampling Date	Number of Iodinated Ions	cumulative iodinated intensity
MARCELLUS SHALE					
M-4 FPW	M-4	1	12/10/2015	24	365771652
M-4 FPW	M-4	2	12/11/2015	4	53009405
M-4 FPW	M-4	3	12/12/2015	23	247156272
M-4 FPW	M-4	4	12/13/2015	25	335868550
M-4 FPW	M-4	7	12/16/2015	9	84575542
M-4 FPW	M-4	32	1/10/2016	55	1589292678
M-4 FPW	M-4	52	1/30/2016	54	1232849252
M-4 FPW	M-4	66	2/13/2016	42	701786850
M-4 FPW	M-4	80	2/27/2016	47	1131320476
M-4 FPW	M-4	115	4/2/2016	34	449540466
M-4 FPW	M-4	178	6/4/2016	21	249839235
M-4 FPW	M-4	213	7/9/2016	59	1536697731
M-4 FPW	M-4	276	9/10/2016	28	176118846
M-5 FPW	M-5	1	12/10/2015	38	655626375
M-5 FPW	M-5	5	12/14/2015	12	202148089
M-5 FPW	M-5	27	1/5/2016	27	412030329
M-5 FPW	M-5	47	1/25/2016	36	565581406
M-5 FPW	M-5	61	2/8/2016	31	508076506
M-5 FPW	M-5	110	3/28/2016	43	759333756
M-5 FPW	M-5	271	9/5/2016	34	462125872

Data from J. L. Luek, M. Harir, P. Schmitt-Kopplin, P. J. Mouser and M. Gonsior, Temporal dynamics of halogenated organic compounds in Marcellus Shale flowback, *Water research*, 2018, **136**, 200-206.

Supporting Figures

Figure A1. Experimental factors considered in this paper.

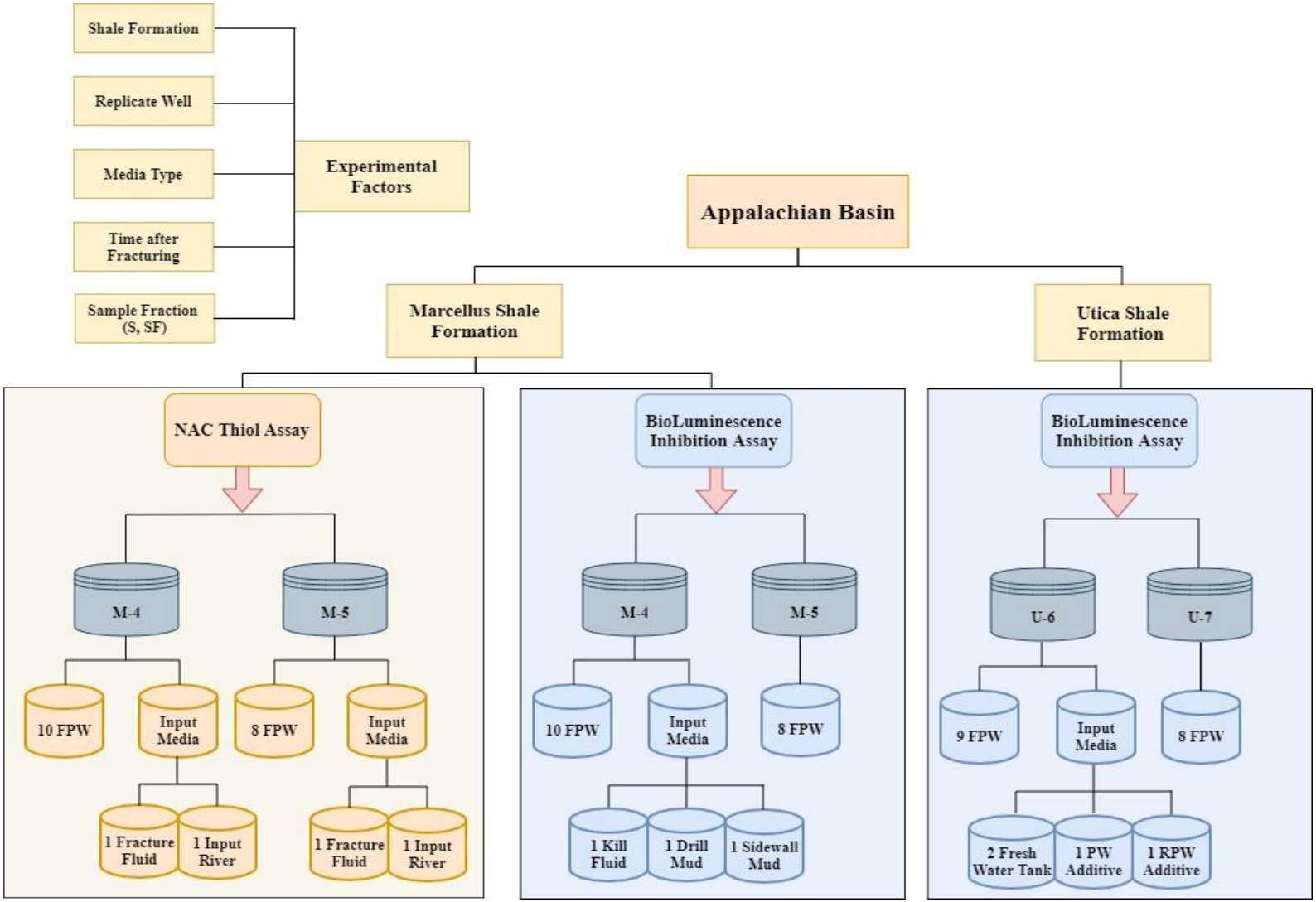

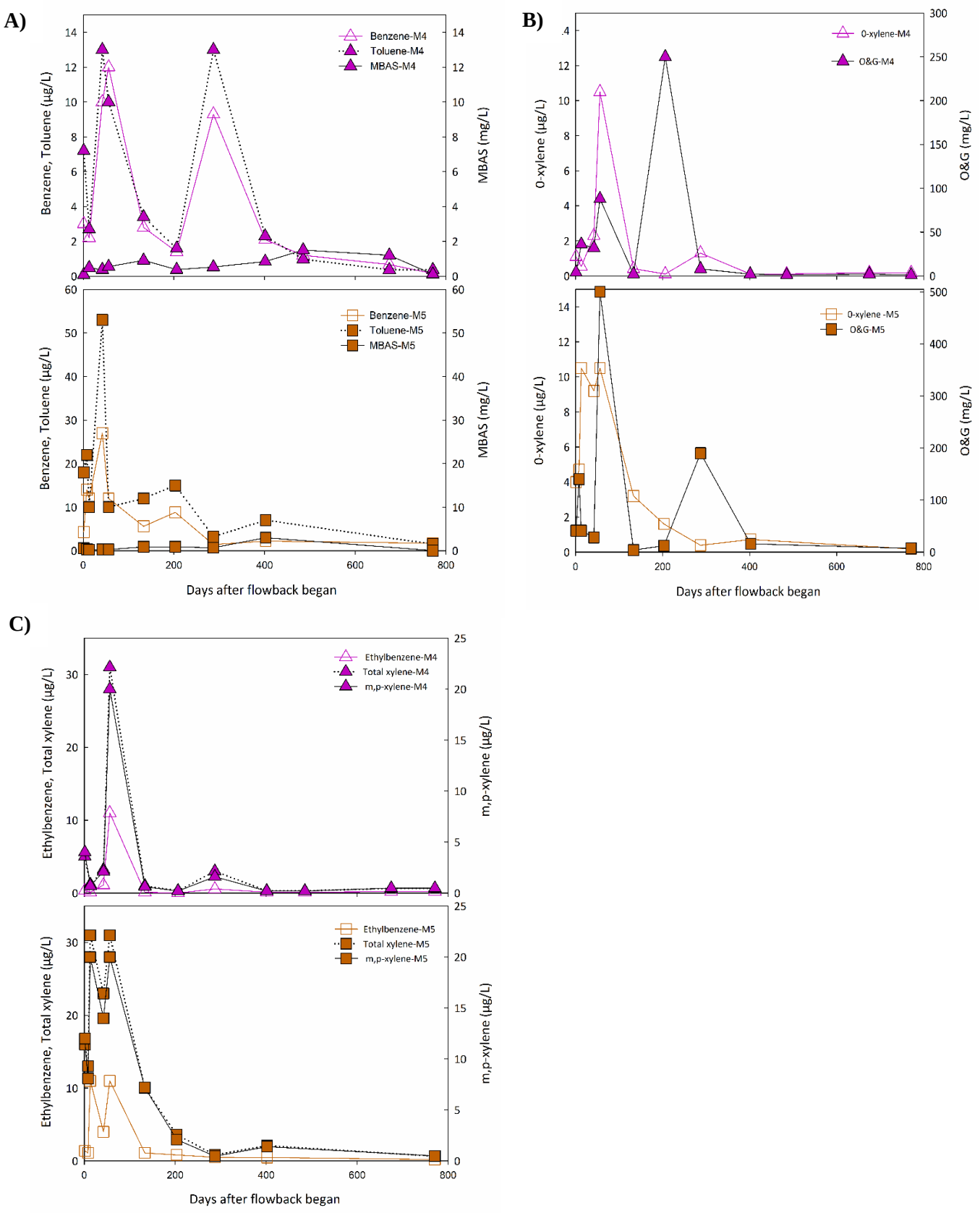

Figure A2. (A) Benzene, Toluene and MBAS trends, (days 1-771) (B) o-xylene and O&G trends, (days 1-771) and (C) Ethylbenzene, total xylene and m,p-xylene trends in Marcellus shale formation, (days 1-771).

Appendix B. Supporting Information for Chapter 3

Materials and Methods

Viral RNA precipitation, extraction, and quantification

Each RT-ddPCR reaction was performed in 22 μL final volume containing 5.5 μL 1×one-step RT-ddPCR Supermix (Bio-Rad), 2.2 μL reverse transcriptase (Bio-Rad), 1.1 μL 300 mM DTT (BioRad), 1.1 μL forward and reverse primer and probe mixture (2019-nCoV CDC ddPCR Triplex Probe Assay (20x); BioRad), 6.6 μL RNase-free water, and 5.5 μL eluted template RNA. See Table S2 for primer and probes used in this study. Droplets were generated by adding 70 μL of droplet generation oil to the PCR mixture on a QX200 AutoDG Droplet Digital PCR System (Bio-Rad Laboratories, Hercules, CA). RT-ddPCR was performed using a Bio-RadC1000Touch Thermal Cycler with the following settings: 60-min reverse transcription at 50°C (1 cycle), 10-minenzyme activation at 95°C (1 cycle), 30-s denaturation at 94°C (40 cycles), 1-min annealing/extension cycle at 55°C (40 cycles; ramp rate of 2°C/s), 10-min enzyme deactivation at 98°C (1 cycle) and 30-min droplet stabilization at 4°C. Droplets were read using a QX200 droplet reader with positive droplets called manually and quantification performed using QX Manager Standard Edition software (Bio-Rad, Hercules, CA). All RT-ddPCR reactions were performed in triplicate, and each plate include a no template control and a positive control (catalog no. COV019; Exact Diagnostics, Fort Worth, TX).

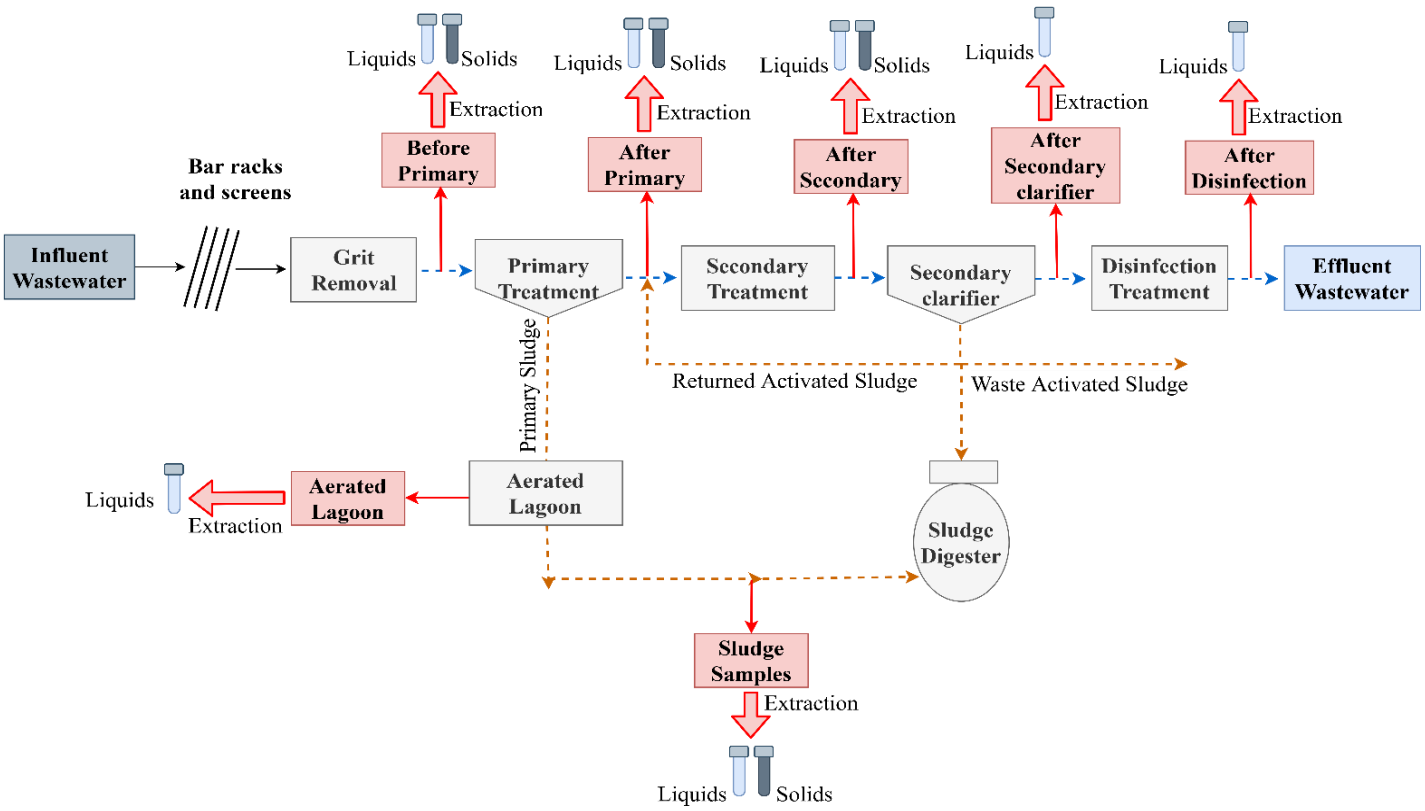

Figure B1. Sampling locations in the selected wastewater treatment plants

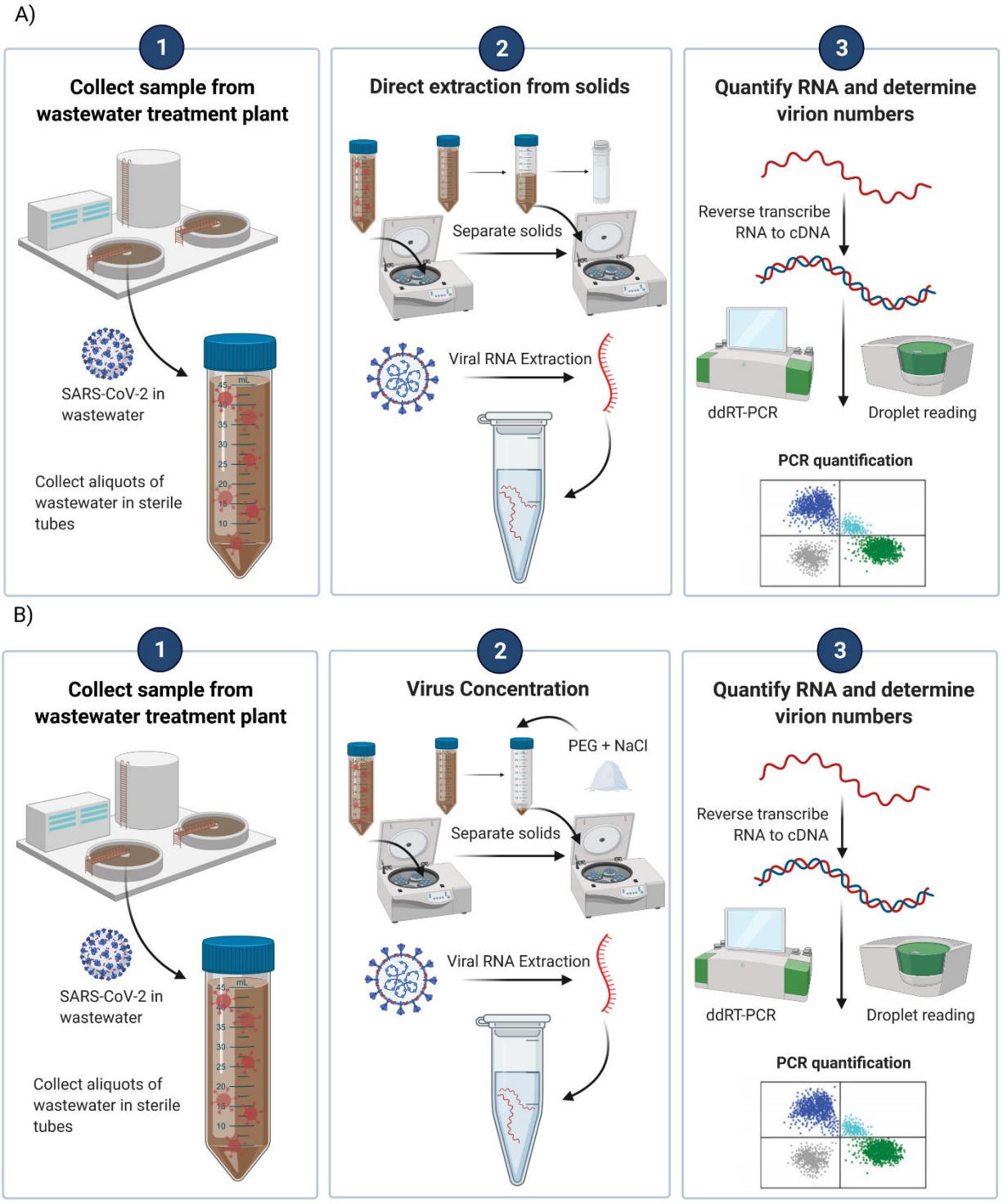

Figure B2. Methods used in quantifying SARS-CoV-2 RNA in wastewater samples (solid (A) and liquid phase (B)). All components of the figure have been made using BioRender.com. We have quantified two biomarker regions of the viral nucleocapside (N) protein (N1 and N2), using a reverse transcriptase digital droplet polymerase chain reaction (ddPCR) assay optimized in our lab for wastewater matrices. Our approach separates solids and liquids using high speed centrifugation coupled to a chemical precipitation step (PEG-Na). Extraction of RNA is conducted using an automated Qiagen Qiacube using the commercially-available Allprep PowerViral DNA/RNA Kit.

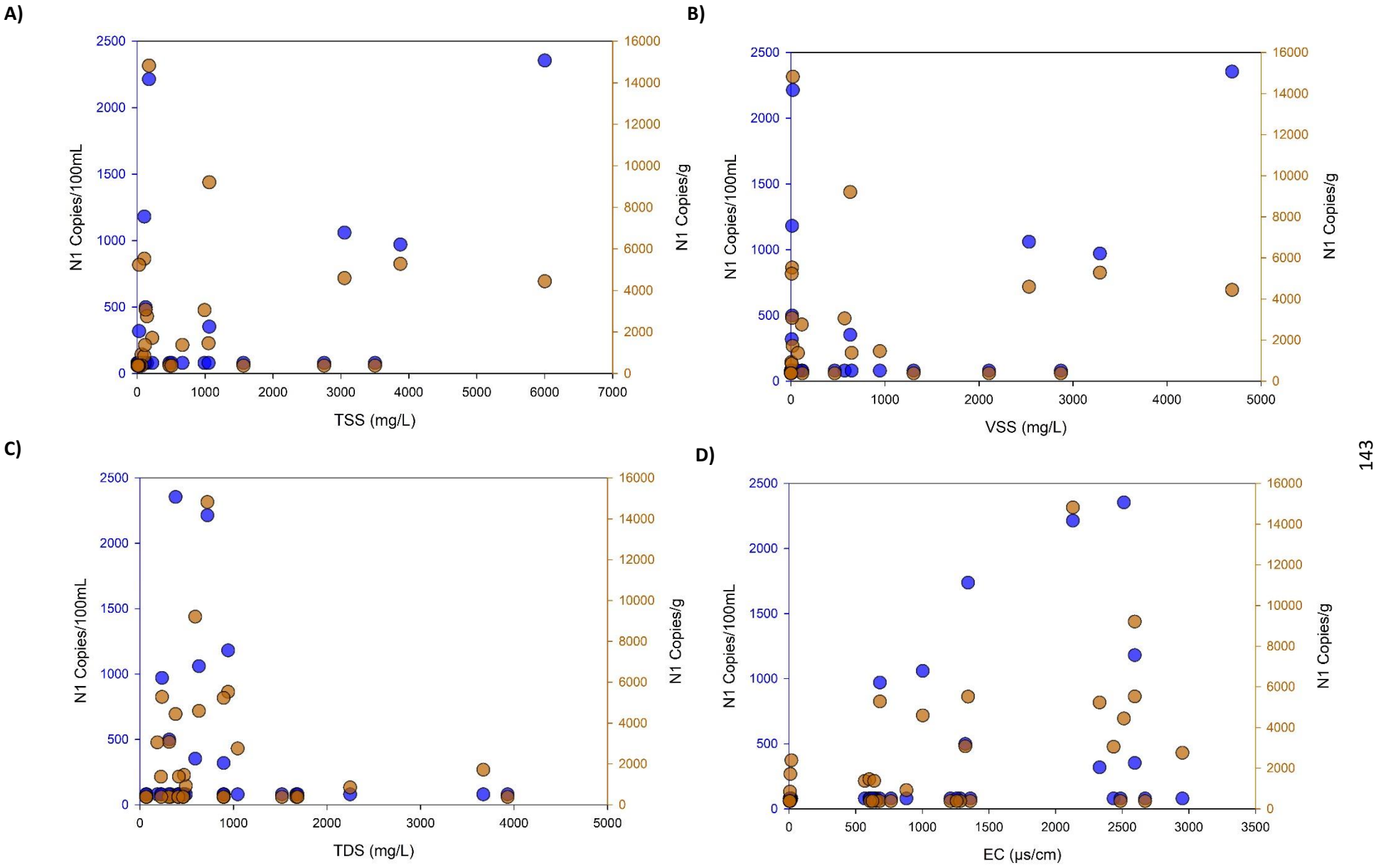
A)
N1 Copies/100mL
N1 Copies/g
TSS (mg/L)
B)
N1 Copies/100mL
N1 Copies/g
VSS (mg/L)
C)
N1 Copies/100mL
N1 Copies/g
TDS (mg/L)
D)
N1 Copies/100mL
N1 Copies/g
EC (µs/cm)

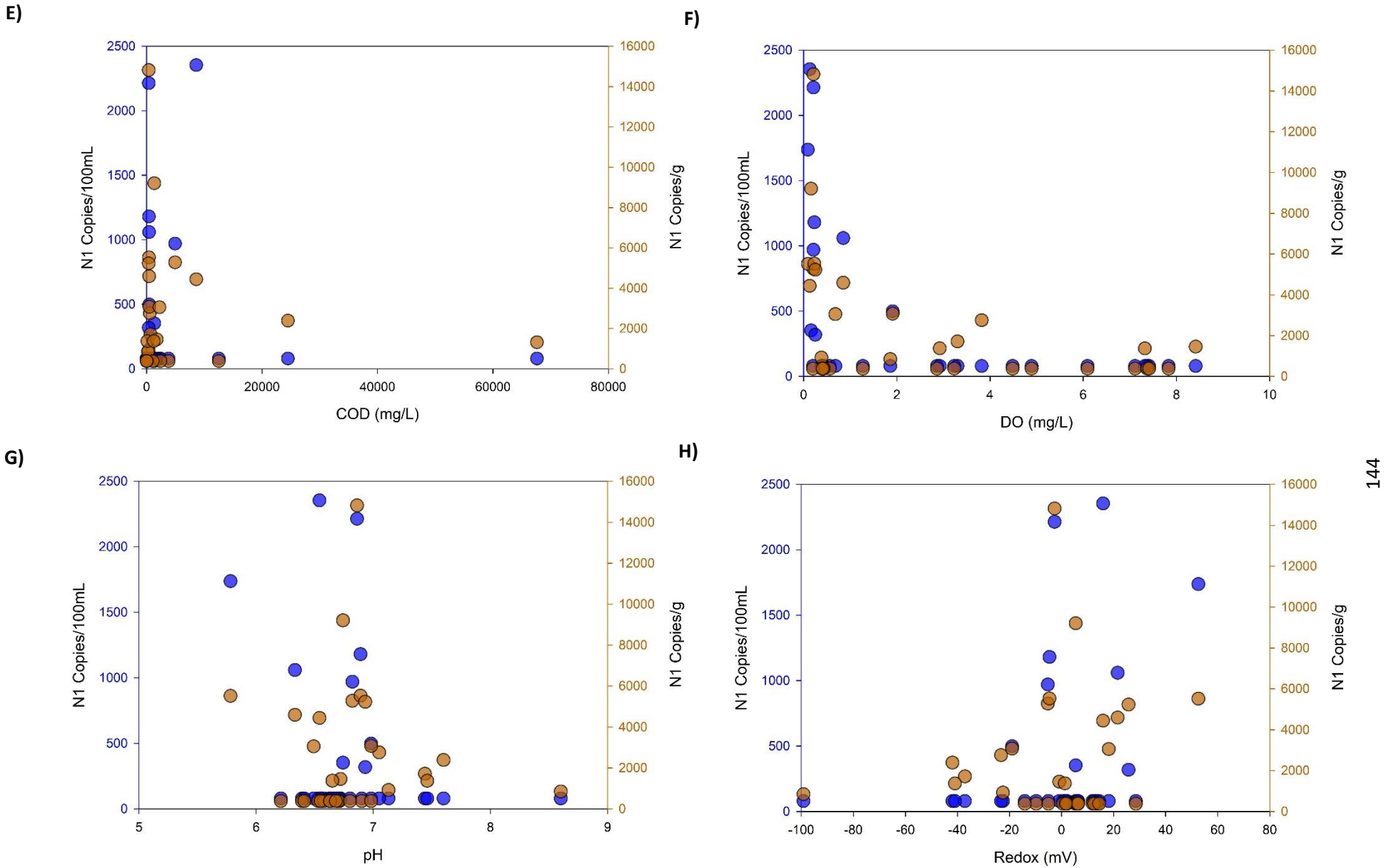

Figure B3. Estimates of correlation between SARS-CoV-2 RNA concentration in the liquid and solid samples and A) TSS, B) VSS, C) TDS, D) EC, E) COD, F) DO, G) pH and H) Redox across coastal New England WWTPs. To highlight the effect of physicochemical parameters on SARS-CoV-2 RNA concentration, sampling locations are not differentiated. Liquid phase concentrations are displayed as blue symbol, while solid phase concentrations are shown in brown.

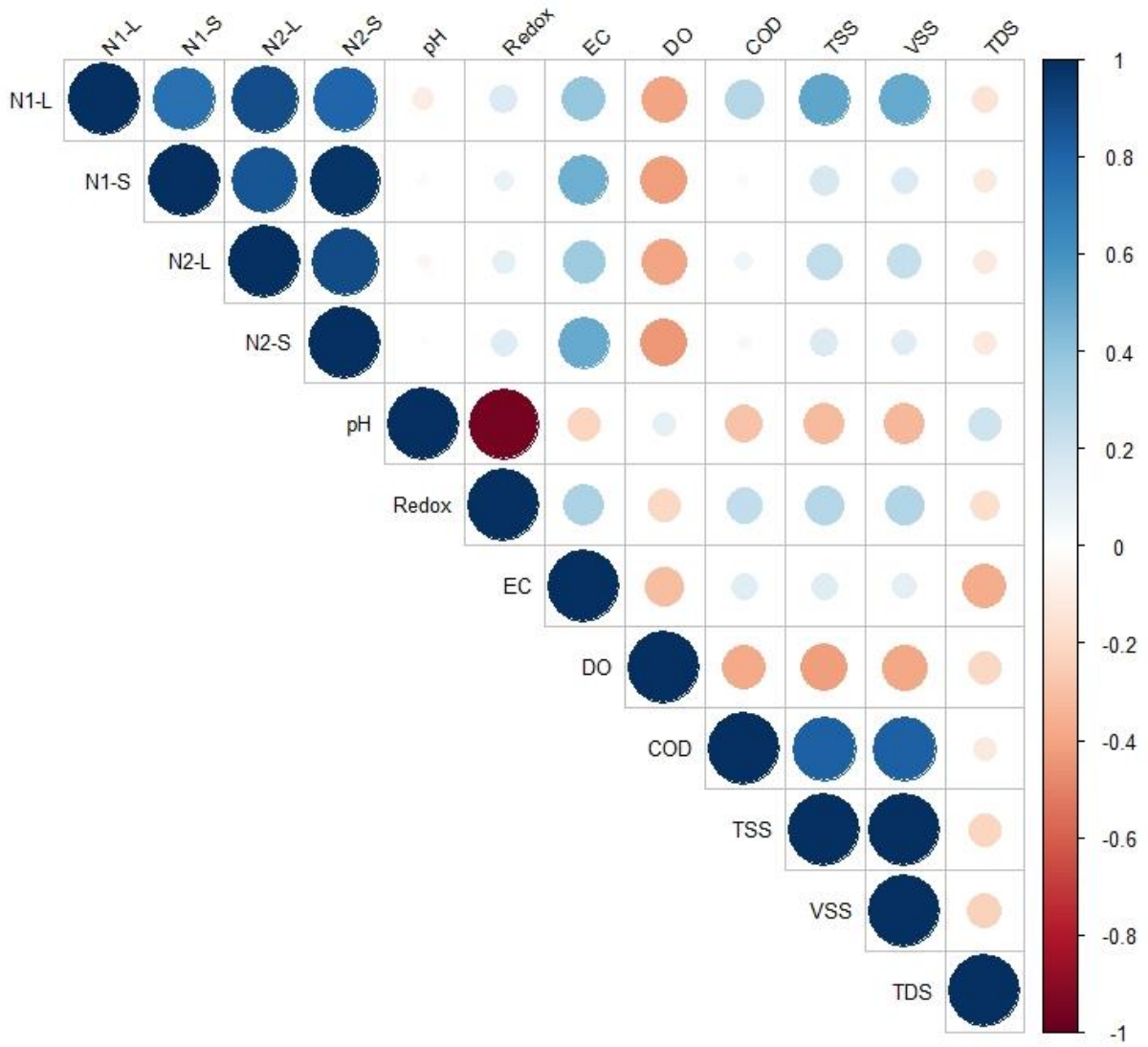

Figure B4. Estimates of correlation between SARS-CoV-2 RNA concentration in the liquid and solid samples and physicochemical parameters across coastal New England WWTPs.

Table B1. Characteristics of surveyed WWTPs.

Facility Parameter	NH-1 Bar + CD	NH-2 Bar + UV	NH-3 AS + UV (1)	NH-4 AS + UV (2)	NH-5 AS + CD (2)	ME AS + CD (3)	MA AS + CD (1)
Sampling Date	11/13/2020	1/14/2021	12/21/2020	1/25/2021	1/25/2021	12/30/2020	2/18/2021
Population Served	16000	11000	28972	16418	21063	1062	3,100,000
7-day percent positivity reported at the state level (CDC 2021)	3.6-4.2%	7.8%	7.5-8.5%	5-5.5%	5-5.5%	6-6.5%	8-9.9%
Average daily flow (MGD)	1	1.2-2.4	4.7	5	3.5	0.563	North System: 910 South System: 360
Treatment level	Secondary	Secondary	Secondary	Secondary	Secondary	Secondary	Secondary
Preliminary treatment	Coarse screens, fine screens, grit chamber	Coarse screens, fine screens, grit chamber	Coarse screens, fine screens, grit chamber	Coarse screens, fine screens, grit chamber	Coarse screens, fine screens, grit chamber	-	Coarse screens, fine screens, grit chamber
Primary treatment	Open-air rectangular primary clarifiers	-	Open-air rectangular primary clarifiers	-	Open-air rectangular primary clarifiers	-	Open-air rectangular primary clarifiers
Secondary treatment	Bardenpho-4	Bardenpho-4	Conventional activated sludge	Conventional activated sludge	Two stage biological aerated filter (BAF)	Conventional activated sludge	Conventional activated sludge
Disinfection prior to discharge	Chlorination/ De Chlorination	Ultraviolet	Ultraviolet	Ultraviolet	Chlorination/ De Chlorination	Chlorination/ De Chlorination	Chlorination/ De Chlorination

Table B2. List of PCR primers and probes used in this study (Control and Prevention 2020).

Primer/probe & supplier	Sequence
2019-nCoV_N1 forward primer	GAC CCC AAA ATC AGC GAA AT
2019-nCoV_N1 reverse primer	TCT GGT TAC TGC CAG TTG AAT CTG
2019-nCoV_N1 probe	FAM-ACC CCG CAT TAC GTT TGG TGG ACC-BHQ1
2019-nCoV_N2 forward primer	TTA CAA ACA TTG GCC GCA AA
2019-nCoV_N2 reverse primer	GCG CGA CAT TCC GAA GAA
2019-nCoV_N2 probe	FAM-ACA ATT TGC CCC CAG CGC TTC AG-BHQ1
RNAse P Forward Primer	AGA TTT GGA CCT GCG AGC G
RNAse P Reverse Primer	GAG CGG CTG TCT CCA CAA GT
RNAse P Probe	FAM – TTC TGA CCT GAA GGC TCT GCG CG – BHQ-1

Table B3. Variation in SARS-CoV-2 biomarker loading found in the liquid and solid samples collected from four different wastewater treatment plants in coastal New England area. BDL represents values below the limit of detection which represents the instrument quantification detection limit of 182 copies/100 ml wastewater for liquid samples and limit of 913 cp/g for solid samples. N.S. indicates no sample was analyzed at a given time point; BDL* represents samples that SARS-CoV-2 biomarker detected but values were below limit of detection of method.

		Treatment Stage	Replicate 1				Replicate 2			
			Liquids		Solids		Liquids		Solids	
			N1 copies/100mL	N2 copies/100mL	N1 copies/g	N2 copies/g	N1 copies/100mL	N2 copies/100mL	N1 copies/g	N2 copies/g
MA	AS + CD (1)	Wastewater Influent: North System	1099	1114	5232	4883	1281	1525	5948	5503
		Wastewater Influent: South System	2073	1925	15158	15500	2369	2257	14568	14096
		After Primary Sedimentation	317	302	12999	6832	409	346	5528	5412
		After Primary	269	292	5151	5049	390	458	5430	5748
		After Secondary	BDL*	BDL*	3632	3487	BDL*	BDL*	2606	2496
		Return Activated Sludge	550	385	4631	5089	4172	1201	4375	4656
		After Sludge Digester	BDL	BDL	2285	2122	BDL	BDL*	2626	2582
		After Secondary Clarifier	BDL*	BDL*	N.S.	N.S.	BDL*	BDL*	N.S.	N.S.
		After Disinfection	BDL*	BDL*	N.S.	N.S.	BDL*	BDL*	N.S.	N.S.
		Treatment Stage	Replicate 1				Replicate 2			
			Liquids		Solids		Liquids		Solids	
			N1 copies/100mL	N2 copies/100mL	N1 copies/g	N2 copies/g	N1 copies/100mL	N2 copies/100mL	N1 copies/g	N2 copies/g
NH-1	Bar + CD	Before Primary	1138	850	4541	3805	1000	970	4767	3606
		After Primary	BDL*	BDL*	1013	1051	BDL*	BDL*	976	BDL*
		After Secondary	BDL*	BDL*	BDL*	BDL*	BDL*	BDL*	BDL*	BDL*
		Return Activated Sludge	977	776	4840	3746	982	936	5843	3503
		After Secondary Clarifier	BDL*	BDL*	N.S.	N.S.	BDL*	BDL*	N.S.	N.S.
		After Disinfection	BDL*	BDL*	N.S.	N.S.	BDL*	BDL*	N.S.	N.S.
		Waste Activated Sludge	1958	1615	5808	4941	1533	1445	5355	3912

Table B3 continued.

		Treatment Stage	Replicate 1				Replicate 2			
			Liquids		Solids		Liquids		Solids	
			N1 copies/100mL	N2 copies/100mL	N1 copies/g	N2 copies/g	N1 copies/100mL	N2 copies/100mL	N1 copies/g	N2 copies/g
NH-2	Bar + UV	Before Primary	BDL*	BDL*	BDL*	BDL*	BDL*	BDL*	BDL*	BDL*
		After Secondary	BDL*	BDL*	BDL*	BDL*	BDL*	BDL*	BDL*	BDL*
		Return Activated Sludge	BDL*	BDL*	BDL	BDL*	BDL*	BDL*	BDL*	BDL*
		After Secondary Clarifier	BDL	BDL	N.S.	N.S.	BDL	BDL	N.S.	N.S.
		After Disinfection	BDL*	BDL*	BDL*	BDL*	BDL*	BDL*	BDL*	BDL*
		Waste Activated Sludge	N.S.	N.S.	N.S.	N.S.	N.S.	N.S.	N.S.	N.S.
		Treatment Stage	Replicate 1				Replicate 2			
			Liquids		Solids		Liquids		Solids	
			N1 copies/100mL	N2 copies/100mL	N1 copies/g	N2 copies/g	N1 copies/100mL	N2 copies/100mL	N1 copies/g	N2 copies/g
NH-3	AS + UV (1)	Before Primary	BDL*	BDL*	2190	1533	BDL*	BDL*	3452	3061
		After Primary	523	439	3432	2694	494	435	2851	2387
		After Secondary	BDL*	BDL*	BDL*	BDL*	BDL*	BDL*	BDL*	BDL*
		Return Activated Sludge	BDL*	BDL*	BDL*	BDL*	BDL*	BDL	BDL*	BDL*
		After Secondary Clarifier	BDL*	BDL*	N.S.	N.S.	BDL*	BDL*	N.S.	N.S.
		After Disinfection	BDL	BDL*	N.S.	N.S.	BDL*	BDL*	N.S.	N.S.
		Waste Activated Sludge	N.S.	N.S.	N.S.	N.S.	N.S.	N.S.	N.S.	N.S.
		Treatment Stage	Replicate 1				Replicate 2			
			Liquids		Solids		Liquids		Solids	
			N1 copies/100mL	N2 copies/100mL	N1 copies/g	N2 copies/g	N1 copies/100mL	N2 copies/100mL	N1 copies/g	N2 copies/g
NH-4	AS + UV (2)	Before Secondary	BDL	BDL*	BDL	BDL*	BDL*	BDL*	BDL*	BDL*
		Aerated Lagoon	347	285	N.S.	N.S.	567	445	N.S.	N.S.
		After Secondary	BDL*	BDL*	BDL*	BDL*	BDL	BDL	BDL*	BDL*
		Return Activated Sludge	BDL	BDL*	BDL*	BDL*	BDL*	BDL*	BDL*	BDL*
		After Secondary Clarifier	BDL*	BDL*	N.S.	N.S.	BDL*	BDL*	N.S.	N.S.
		After Disinfection	BDL*	BDL	N.S.	N.S.	BDL	BDL*	N.S.	N.S.
		Waste Activated Sludge	BDL*	BDL*	BDL*	BDL*	BDL	BDL	BDL*	BDL*

Table B3 continued.

		Treatment Stage	Replicate 1				Replicate 2			
			Liquids		Solids		Liquids		Solids	
			N1 copies/100mL	N2 copies/100mL	N1 copies/g	N2 copies/g	N1 copies/100mL	N2 copies/100mL	N1 copies/g	N2 copies/g
NH-5	AS + CD (2)	Before Primary (Before Grit)	BDL*	BDL*	BDL*	BDL*	BDL*	BDL*	BDL*	BDL*
		Before Primary (After Grit)	BDL*	BDL*	1786	922	BDL*	BDL*	BDL*	BDL*
		After Primary	188	BDL*	922	BDL*	BDL*	BDL*	BDL*	BDL*
		Return Activated Sludge	BDL*	BDL*	BDL*	BDL*	BDL*	BDL*	BDL*	BDL*
		After Secondary Clarifier	BDL*	BDL*	N.S.	N.S.	BDL*	BDL*	N.S.	N.S.
		After Disinfection	BDL*	BDL*	N.S.	N.S.	BDL*	BDL*	N.S.	N.S.
		Waste Activated Sludge	BDL	BDL	1339	917	BDL	BDL	1433	940
		Treatment Stage	Replicate 1				Replicate 2			
			Liquids		Solids		Liquids		Solids	
			N1 copies/100mL	N2 copies/100mL	N1 copies/g	N2 copies/g	N1 copies/100mL	N2 copies/100mL	N1 copies/g	N2 copies/g
ME	AS + CD (3)	Before Secondary	BDL*	BDL*	1456	BDL*	BDL*	BDL*	1430	BDL*
		After Secondary	BDL*	BDL*	1601	BDL*	BDL*	BDL*	1462	929
		Return Activated Sludge	BDL*	BDL*	1331	BDL*	BDL*	BDL*	1562	BDL*
		After Secondary Clarifier	BDL*	BDL*	N.S.	N.S.	BDL*	BDL*	N.S.	N.S.
		After Disinfection	BDL*	BDL*	N.S.	N.S.	BDL*	BDL*	N.S.	N.S.
		Waste Activated Sludge	N.S.	N.S.	N.S.	N.S.	N.S.	N.S.	N.S.	N.S.

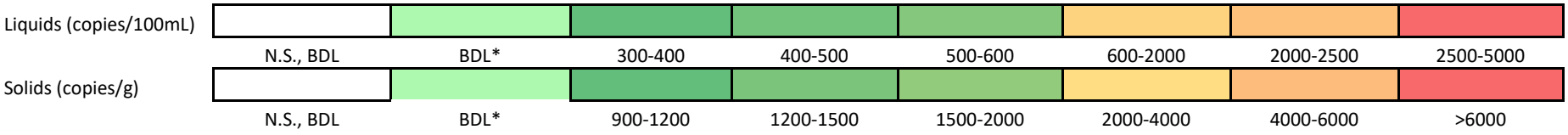

Table B4. SARS-CoV-2 RNA log removal for the different water and sludge treatment processes. Log removal is provided for each treatment stage.

			Liquids	
			N1 log removal	N2 log removal
MA	AS + CD (1)	After Primary (North)	0.56	0.55
		After Primary (South)	0.83	0.75
		After Secondary	1.39	1.36
		After Secondary + Secondary Clarifier	1.39	1.36
		After Disinfection	1.39	1.36
			Liquids	
			N1 log removal	N2 log removal
NH-1	Bar + CD	After Primary	1.07	1.00
		After Secondary	1.07	1.00
		After Secondary + Secondary Clarifier	1.07	1.00
		After Disinfection	1.07	1.00
			Liquids	
			N1 log removal	N2 log removal
NH-2	Bar + UV	After Primary	0	0
		After Secondary	0	0
		After Secondary + Secondary Clarifier	0	0
		After Disinfection	0	0
			Liquids	
			N1 log removal	N2 log removal
NH-3	AS + UV (1)	After Primary	-0.75	-0.68
		After Secondary	0.00	0.00
		After Secondary + Secondary Clarifier	0.00	0.00
		After Disinfection	0.00	0.00
			Liquids	
			N1 log removal	N2 log removal
NH-4	AS + UV (2)	After Primary	0.0	0.0
		After Secondary	-0.7	-0.6
		After Secondary + Secondary Clarifier	0.0	0.0
		After Disinfection	0.0	0.0
			Liquids	
			N1 log removal	N2 log removal
NH-5	AS + CD (2)	After Primary	-0.19	0.00
		After Secondary	0.00	0.00
		After Secondary + Secondary Clarifier	0.00	0.00
		After Disinfection	0.00	0.00
			Liquids	
			N1 log removal	N2 log removal
ME	AS + CD (3)	After Primary	0	0
		After Secondary	0	0
		After Secondary + Secondary Clarifier	0	0
		After Disinfection	0	0

Table B4 continued.

			Solids	
			N1 log removal	N2 log removal
MA	AS + CD (1)	After Primary (North)	0.02	-0.02
		After Primary (South)	0.45	0.44
		After Primary Sludge (North)	-0.22	-0.07
		After Primary Sludge (South)	0.21	0.38
		After Return Activated Sludge (North)	0.09	0.03
		After Return Activated Sludge (South)	0.52	0.48
		After Sludge Digester (North)	0.36	0.34
		After Sludge Digester (South)	0.78	0.80
			Solids	
			N1 log removal	N2 log removal
NH-1	Bar + CD	After Primary	0.67	0.69
		After Bar	1.01	0.91
			Solids	
			N1 log removal	N2 log removal
NH-2	Bar + UV	After Primary	0.0	0.0
		After Bar	0.0	0.0
			Solids	
			N1 log removal	N2 log removal
NH-3	AS + UV (1)	After Primary	-0.05	-0.04
		After Return Activated Sludge	0.79	0.70
			Solids	
			N1 log removal	N2 log removal
NH-4	AS + UV (2)	After Secondary	0.0	0.0
		After Return Activated Sludge	0.0	0.0
			Solids	
			N1 log removal	N2 log removal
NH-5	AS + CD (2)	After Primary	0.21	0.18
		After Secondary	0.00	0.00
			Solids	
			N1 log removal	N2 log removal
ME	AS + CD (3)	After Secondary	0.0	0.0
		After Return Activated Sludge	0.0	0.0

Table B5. The sorption coefficient, Log KD, for SARS-CoV-2 virus based on the N1 and N2 biomarker counts.

		Treatment Stage	Log KD (N1 biomarker counts)	Log KD (N2 biomarker counts)
MA	AS + CD (1)	Wastewater Influent: North System	2.67	2.6
		Wastewater Influent: South System	2.83	2.85
		After Primary Sedimentation	3.37	3.27
		After Primary	3.21	3.17
		After Secondary	3.57	3.71
		Return Activated Sludge	2.47	2.86
		After Sludge Digester	N.C.	N.C.
		After Secondary Clarifier	N.C.	N.C.
		After Disinfection	N.C.	N.C.
		Treatment Stage	Log KD (N1 biomarker counts)	Log KD (N2 biomarker counts)
NH-1	Bar + CD	Before Primary	2.63	2.6
		After Primary	N.C.	N.C.
		After Secondary	N.C.	N.C.
		Return Activated Sludge	2.73	2.6
		After Secondary Clarifier	N.C.	N.C.
		After Disinfection	N.C.	N.C.
		Waste Activated Sludge	2.92	2.88
		Treatment Stage	Log KD (N1 biomarker counts)	Log KD (N2 biomarker counts)
NH-3	AS + UV (1)	Before Primary	N.C.	N.C.
		After Primary	2.79	2.76
		After Secondary	N.C.	N.C.
		Return Activated Sludge	N.C.	N.C.
		After Secondary Clarifier	N.C.	N.C.
		After Disinfection	N.C.	N.C.
		Waste Activated Sludge	N.S.	N.S.

Note: KD Values were not calculated for other 4 WWTP sicne the the liquid and/or solid SARS-CoV-2 viral biomarker concentrations were below detection limit.

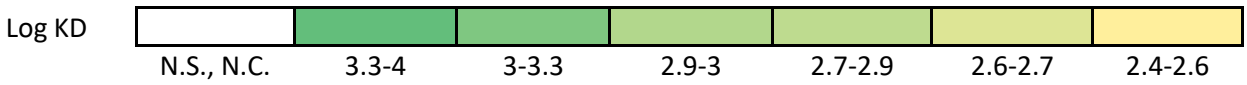

Table B6. Wastewater quality characteristics of the samples across the study locations.

			pH	Redox (mV)	EC (µs/cm)	DO (%Sat)	DO (mg/L)	COD (mg/L)	TSS (mg/L)	VSS (mg/L)	TDS (mg/L)
MA	AS + CD (1)	Wastewater Influent: North System	6.89	-4.7	2593	2.1	0.23	384.8	104	12	942
		Wastewater Influent: South System	6.86	-2.7	2129	2	0.21	354.8	172.5	20	720
		After Primary Sedimentation	6.74	5.4	2593	1.4	0.16	1320	1060	630	590
		After Primary	6.93	25.7	2329	1.4	0.25	356	28	8	894
		After Secondary	6.49	18.1	2434	5.7	0.68	2224	990	570	185
		Return Activated Sludge	6.54	15.9	2512	1.3	0.13	8590	6000	4690	380
		After Sludge Digester	7.6	-42	16.15	N.A.	N.A.	24462	N.A.	N.A.	N.A.
		After Secondary Clarifier	6.58	12.5	2671	23	2.86	21.5	12	0	896
		After Disinfection	6.55	14.4	2486	10.2	1.27	29.2	8	0	892
NH-1	Bar + CD		pH	Redox (mV)	EC (µs/cm)	DO (%Sat)	DO (mg/L)	COD (mg/L)	TSS (mg/L)	VSS (mg/L)	TDS (mg/L)
		Before Primary	6.33	21.5	1002	9	0.85	420	3050	2531.5	630
		After Primary	7.13	-22.6	879.6	3.9	0.382	358	64	4	490
		After Secondary	6.71	0.5	651.1	5.6	0.56	1348	1563.33	1303.33	326.66
		Return Activated Sludge	6.82	-5.3	680.5	1.8	0.21	4915	3875	3285	235
		After Secondary Clarifier	6.9	-9.8	678.2	43.7	4.48	25.1	16	0	306
		After Disinfection	6.98	-14.2	763.5	71	7.11	30.2	3	0	70
		Waste Activated Sludge	5.78	52.5	1342	1.2	0.09	N.A.	N.A.	N.A.	N.A.
NH-2	Bar + UV		pH	Redox (mV)	EC (µs/cm)	DO (%Sat)	DO (mg/L)	COD (mg/L)	TSS (mg/L)	VSS (mg/L)	TDS (mg/L)
		Before Secondary	7.2	-24	983.4	70.5	8.05	305	307.5	72.5	210
		After Secondary	6.64	6.2	873.2	31.6	7.67	2572	2053.33	1556.66	150
		Return Activated Sludge	6.61	87.8	853.9	3.6	0.3	6750	4703.33	3716.66	683.33
		After Secondary Clarifier	6.78	-1.6	860.6	47.4	5.67	6	120	0	360
		After Disinfection	6.85	5.7	867.7	74.7	8.85	5.28	132	0	340
		Waste Activated Sludge	N.S.	N.S.	N.S.	N.S.	N.S.	N.S.	N.S.	N.S.	N.S.
NH-3	AS + UV (1)		pH	Redox (mV)	EC (µs/cm)	DO (%Sat)	DO (mg/L)	COD (mg/L)	TSS (mg/L)	VSS (mg/L)	TDS (mg/L)

		Before Primary	7.05	-23.3	2951	30.8	3.82	540	143.33	114.664	1043.33
		After Primary	6.98	-19.1	1321	16.7	1.91	454	124	12	312
		After Secondary	6.39	13.5	1210	3.6	0.43	3780	2750	2105	460
		Return Activated Sludge	6.41	11.9	1359	3.6	0.39	12496	3500	2870	410
		After Secondary Clarifier	6.55	5.3	1283	65.8	7.37	8.92	26	0	408
		After Disinfection	6.53	5.8	1256	66.7	7.41	5.21	10	0	460
		Waste Activated Sludge	N.S.	N.S.	N.S.	N.S.	N.S.	N.S.	N.S.	N.S.	N.S.
NH-4	**AS + UV (2)**		**pH**	**Redox (mV)**	**EC (µs/cm)**	**DO (%Sat)**	**DO (mg/L)**	**COD (mg/L)**	**TSS (mg/L)**	**VSS (mg/L)**	**TDS (mg/L)**
		Before Secondary	6.99	-13.7	1219	20.9	2.55	318.5	190	8	408
		Aerated Lagoon	7.06	-17.7	932.6	27.2	3.35	328	182	32	182
		After Secondary	6.24	27.1	870.5	30.4	3.94	5976	2660	1815	250
		Return Activated Sludge	6.15	31.9	850.6	7.3	0.9	6138	4775	3635	145
		After Secondary Clarifier	6.25	25.9	856.8	52.9	6.49	17.7	160	0	402
		After Disinfection	6.57	9	872.8	86.7	10.87	2.2	140	0	172
		Waste Activated Sludge	6.18	30.6	869	10.7	1.33	6650	N.A.	N.A.	N.A.
NH-5	**AS + CD (2)**		**pH**	**Redox (mV)**	**EC (µs/cm)**	**DO (%Sat)**	**DO (mg/L)**	**COD (mg/L)**	**TSS (mg/L)**	**VSS (mg/L)**	**TDS (mg/L)**
		Before Primary (Before Grit)	6.21	28.5	8.36	3.7	0.2	2372	475	465	3930
		Before Primary (After Grit)	7.44	-37.2	9.08	23.2	3.3	660	220	16.66	3670
		After Primary	8.6	-99.2	5.75	16.5	1.86	224	104	7.5	2246
		Return Activated Sludge	6.7	2	3.87	3.7	0.41	1040	505	120	1670
		After Secondary Clarifier	6.63	6.3	3.56	26.9	3.23	20.3	64	0	1516
		After Disinfection	6.63	6.3	3.54	40.8	4.89	3.6	32	0	1684
		Waste Activated Sludge	N.A.	N.A.	N.A.	N.A.	N.A.	67600	N.A.	N.A.	N.A.
ME	**AS + CD (3)**		**pH**	**Redox (mV)**	**EC (µs/cm)**	**DO (%Sat)**	**DO (mg/L)**	**COD (mg/L)**	**TSS (mg/L)**	**VSS (mg/L)**	**TDS (mg/L)**
		Before Secondary	7.46	-41	567.2	59.7	7.32	127	114	74	224
		After Secondary	6.72	-0.9	600.7	68.7	8.41	1756	1050	945	470
		Return Activated Sludge	6.65	1.2	637.6	23.6	2.92	1225	665	645	415
		After Secondary Clarifier	6.8	-5.1	607.5	63.9	7.83	13.1	21	0	226
		After Disinfection	6.68	1.6	624.8	49.8	6.09	2.31	12	0	65
		Waste Activated Sludge	N.S.	N.S.	N.S.	N.S.	N.S.	N.S.	N.S.	N.S.	N.S.

Table B7. Liquid-solid partitioning of SARS-CoV-2 biomarkers across treatment stages in three different wastewater treatment plants in coastal New England area.

AS + CD (1)-Influent-North					
N1					
Sample	Volume Processed (mL)/Mass Solids Processed (1g=1mL)	Copies per extraction	Average copies per mL	Average copies per mL (Average)	Ratio
Influent North R1 1	105	1246.75	1154.01	1249.74	0.47
Influent North R1 2	105	1174.07			
Influent North R1 3	105	1041.21			
Influent North R2 1	105	1036.79	1345.47		
Influent North R2 2	105	1615.67			
Influent North R2 3	105	1383.93			
Influent North Solid R1 1	0.25	1302.69	1307.92	1397.50	0.53
Influent North Solid R1 2	0.25	1294.75			
Influent North Solid R1 3	0.25	1326.32			
Influent North Solid R2 1	0.25	1189.88	1487.07		
Influent North Solid R2 2	0.25	1716.23			
Influent North Solid R2 3	0.25	1555.11			
N2					
Sample	Volume Processed (mL)/Mass Solids Processed (1g=1mL)	Copies per extraction	Average copies per mL	Average copies per mL (Average)	Ratio
Influent North R1 1	105	1045.22	1169.35	1385.21	0.52
Influent North R1 2	105	1281.10			
Influent North R1 3	105	1181.73			
Influent North R2 1	105	1591.62	1601.07		
Influent North R2 2	105	1599.13			
Influent North R2 3	105	1612.45			
Influent North Solid R1 1	0.25	1408.63	1220.83	1298.35	0.48
Influent North Solid R1 2	0.25	1273.47			
Influent North Solid R1 3	0.25	980.39			
Influent North Solid R2 1	0.25	1131.22	1375.87		
Influent North Solid R2 2	0.25	1475.20			
Influent North Solid R2 3	0.25	1521.19			

Table B7 continued.

AS + CD (1)-Influent-South					
N1					
Sample	Volume Processed (mL)/Mass Solids Processed (1g=1mL)	Copies per extraction	Average copies per mL	Average copies per mL (Average)	Ratio
Influent South R1 1	105	2068.29	2176.71	2332.05	0.39
Influent South R1 2	105	2361.47			
Influent South R1 3	105	2100.37			
Influent South R2 1	105	2833.68	2487.40		
Influent South R2 2	105	2585.26			
Influent South R2 3	105	2043.26			
Influent South Solid R1 1	0.25	3787.05	3789.59	3715.80	0.61
Influent South Solid R1 2	0.25	3611.78			
Influent South Solid R1 3	0.25	3969.94			
Influent South Solid R2 1	0.25	4728.08	3642.02		
Influent South Solid R2 2	0.25	3476.74			
Influent South Solid R2 3	0.25	2721.25			
N2					
Sample	Volume Processed (mL)/Mass Solids Processed (1g=1mL)	Copies per extraction	Average copies per mL	Average copies per mL (Average)	Ratio
Influent South R1 1	105	1776.91	2021.38	2195.66	0.37
Influent South R1 2	105	2477.67			
Influent South R1 3	105	1809.55			
Influent South R2 1	105	2731.89	2369.95		
Influent South R2 2	105	2432.39			
Influent South R2 3	105	1945.56			
Influent South Solid R1 1	0.25	3787.05	3874.99	3699.50	0.63
Influent South Solid R1 2	0.25	3724.95			
Influent South Solid R1 3	0.25	4112.97			
Influent South Solid R2 1	0.25	4781.95	3524.01		
Influent South Solid R2 2	0.25	3068.82			
Influent South Solid R2 3	0.25	2721.25			

Table B7 continued.

AS + CD (1)- After Primary Sedimentation					
N1					
Sample	Volume Processed (mL)/Mass Solids Processed (1g=1mL)	Copies per extraction	Average copies per mL	Average copies per mL (Average)	Ratio
After Primary Sediment R1 1	105	414.95	333.33	381.27	0.14
After Primary Sediment R1 2	105	283.63			
After Primary Sediment R1 3	105	301.41			
After Primary Sediment R2 1	105	352.79	429.21		
After Primary Sediment R2 2	105	490.82			
After Primary Sediment R2 3	105	444.01			
After Primary Sediment Solid R1 1	0.25	3049.21	3249.73	2315.82	0.86
After Primary Sediment Solid R1 2	0.25	3767.22			
After Primary Sediment Solid R1 3	0.25	2932.77			
After Primary Sediment Solid R2 1	0.25	1313.85	1381.90		
After Primary Sediment Solid R2 2	0.25	1615.21			
After Primary Sediment Solid R2 3	0.25	1216.64			
N2					
Sample	Volume Processed (mL)/Mass Solids Processed (1g=1mL)	Copies per extraction	Average copies per mL	Average copies per mL (Average)	Ratio
After Primary Sediment R1 1	105	301.71	317.13	340.22	0.18
After Primary Sediment R1 2	105	283.63			
After Primary Sediment R1 3	105	366.05			
After Primary Sediment R2 1	105	392.03	363.31		
After Primary Sediment R2 2	105	350.48			
After Primary Sediment R2 3	105	347.41			
After Primary Sediment Solid R1 1	0.25	1712.51	1707.99	1530.44	0.82
After Primary Sediment Solid R1 2	0.25	1833.84			
After Primary Sediment Solid R1 3	0.25	1577.61			
After Primary Sediment Solid R2 1	0.25	1439.37	1352.90		
After Primary Sediment Solid R2 2	0.25	1295.05			
After Primary Sediment Solid R2 3	0.25	1324.29			

Table B7 continued.

AS + CD (1)- After Primary					
N1					
Sample	Volume Processed (mL)/Mass Solids Processed (1g=1mL)	Copies per extraction	Average copies per mL	Average copies per mL (Average)	Ratio
After Primary R1 1	105	319.40	282.80	346.32	0.21
After Primary R1 2	105	310.48			
After Primary R1 3	105	218.51			
After Primary R2 1	105	374.59	409.84		
After Primary R2 2	105	352.38			
After Primary R2 3	105	502.55			
After Primary Solid R1 1	0.25	1155.48	1287.64	1322.60	0.79
After Primary Solid R1 2	0.25	1294.82			
After Primary Solid R1 3	0.25	1412.61			
After Primary Solid R2 1	0.25	1365.74	1357.57		
After Primary Solid R2 2	0.25	1399.14			
After Primary Solid R2 3	0.25	1307.82			
N2					
Sample	Volume Processed (mL)/Mass Solids Processed (1g=1mL)	Copies per extraction	Average copies per mL	Average copies per mL (Average)	Ratio
After Primary R1 1	105	283.89	307.08	393.75	0.23
After Primary R1 2	105	327.74			
After Primary R1 3	105	309.61			
After Primary R2 1	105	374.59	480.41		
After Primary R2 2	105	489.56			
After Primary R2 3	105	577.09			
After Primary Solid R1 1	0.25	1155.48	1262.13	1349.62	0.77
After Primary Solid R1 2	0.25	1275.72			
After Primary Solid R1 3	0.25	1355.18			
After Primary Solid R2 1	0.25	1548.44	1437.11		
After Primary Solid R2 2	0.25	1437.59			
After Primary Solid R2 3	0.25	1325.31			

Table B7 continued.

AS + CD (1)- After Secondary					
N1					
Sample	Volume Processed (mL)/Mass Solids Processed (1g=1mL)	Copies per extraction	Average copies per mL	Average copies per mL (Average)	Ratio
After Secondary R1 1	105	90.79	84.66	86.66	0.10
After Secondary R1 2	105	65.58			
After Secondary R1 3	105	97.62			
After Secondary R2 1	105	77.63	88.65		
After Secondary R2 2	105	116.43			
After Secondary R2 3	105	71.89			
After Secondary Solid R1 1	0.25	930.88	907.95	779.77	0.90
After Secondary Solid R1 2	0.25	912.03			
After Secondary Solid R1 3	0.25	880.94			
After Secondary Solid R2 1	0.25	639.42	651.59		
After Secondary Solid R2 2	0.25	673.43			
After Secondary Solid R2 3	0.25	641.92			
N2					
Sample	Volume Processed (mL)/Mass Solids Processed (1g=1mL)	Copies per extraction	Average copies per mL	Average copies per mL (Average)	Ratio
After Secondary R1 1	105	45.39	83.26	63.09	0.08
After Secondary R1 2	105	131.17			
After Secondary R1 3	105	73.21			
After Secondary R2 1	105	58.22	42.92		
After Secondary R2 2	105	46.57			
After Secondary R2 3	105	23.96			
After Secondary Solid R1 1	0.25	778.65	871.74	747.92	0.92
After Secondary Solid R1 2	0.25	892.59			
After Secondary Solid R1 3	0.25	943.99			
After Secondary Solid R2 1	0.25	472.45	624.09		
After Secondary Solid R2 2	0.25	696.69			
After Secondary Solid R2 3	0.25	703.15			

Table B7 continued.

AS + CD (1)- RAS					
N1					
Sample	Volume Processed (mL)/Mass Solids Processed (1g=1mL)	Copies per extraction	Average copies per mL	Average copies per mL (Average)	Ratio
RAS R1 1	105	527.43	577.51	517.06	0.31
RAS R1 2	105	601.88			
RAS R1 3	105	603.21			
RAS R2 1	105	12227.92	456.62		
RAS R2 2	105	527.74			
RAS R2 3	105	385.49			
RAS Solid R1 1	0.25	994.09	1157.67	1125.74	0.69
RAS Solid R1 2	0.25	1237.26			
RAS Solid R1 3	0.25	1241.66			
RAS Solid R2 1	0.25	1235.77	1093.82		
RAS Solid R2 2	0.25	1317.38			
RAS Solid R2 3	0.25	728.32			
N2					
Sample	Volume Processed (mL)/Mass Solids Processed (1g=1mL)	Copies per extraction	Average copies per mL	Average copies per mL (Average)	Ratio
RAS R1 1	105	234.27	403.97	372.03	0.23
RAS R1 2	105	575.68			
RAS R1 3	105	401.97			
RAS R2 1	105	3101.43	340.08		
RAS R2 2	105	342.90			
RAS R2 3	105	337.27			
RAS Solid R1 1	0.25	1154.82	1272.30	1218.20	0.77
RAS Solid R1 2	0.25	1208.41			
RAS Solid R1 3	0.25	1453.66			
RAS Solid R2 1	0.25	997.61	1164.10		
RAS Solid R2 2	0.25	1575.99			
RAS Solid R2 3	0.25	918.69			

Table B7 continued.

AS + CD (1)- After Sludge Digester					
N1					
Sample	Volume Processed (mL)/Mass Solids Processed (1g=1mL)	Copies per extraction	Average copies per mL	Average copies per mL (Average)	Ratio
After Sludge Digester R1 1	105	0	0	0	0
After Sludge Digester R1 2	105	0			
After Sludge Digester R1 3	105	0			
After Sludge Digester R2 1	105	0	0		
After Sludge Digester R2 2	105	0			
After Sludge Digester R2 3	105	0			
After Sludge Digester Solid R1 1	0.25	552.13	571.25	613.91	1
After Sludge Digester Solid R1 2	0.25	618.69			
After Sludge Digester Solid R1 3	0.25	542.93			
After Sludge Digester Solid R2 1	0.25	769.30	656.57		
After Sludge Digester Solid R2 2	0.25	643.38			
After Sludge Digester Solid R2 3	0.25	557.03			
N2					
Sample	Volume Processed (mL)/Mass Solids Processed (1g=1mL)	Copies per extraction	Average copies per mL	Average copies per mL (Average)	Ratio
After Sludge Digester R1 1	105	0	0	5.63	0.01
After Sludge Digester R1 2	105	0			
After Sludge Digester R1 3	105	0			
After Sludge Digester R2 1	105	0	11.26		
After Sludge Digester R2 2	105	0			
After Sludge Digester R2 3	105	33.78			
After Sludge Digester Solid R1 1	0.25	552.13	530.52	587.96	0.99
After Sludge Digester Solid R1 2	0.25	518.25			
After Sludge Digester Solid R1 3	0.25	521.19			
After Sludge Digester Solid R2 1	0.25	595.37	645.40		
After Sludge Digester Solid R2 2	0.25	758.46			
After Sludge Digester Solid R2 3	0.25	582.38			

Table B7 continued.

Bar + CD- Before Primary					
N1					
Sample	Volume Processed (mL)/Mass Solids Processed (1g=1mL)	Copies per extraction	Average copies per mL	Average copies per mL (Average)	Ratio
Before Primary R1 1	105	1292.02	1195.38	1136.25	0.49
Before Primary R1 2	105	1207.01			
Before Primary R1 3	105	1087.12			
Before Primary R2 1	105	978.90	1049.77		
Before Primary R2 2	105	1091.03			
Before Primary R2 3	105	1079.37			
Before Primary R3 1	105	1182.61	1163.59		
Before Primary R3 2	105	1111.58			
Before Primary R3 3	105	1196.58			
Before Primary Solid R1 1	0.25	1164.33	1135.26	1161.87	0.51
Before Primary Solid R1 2	0.25	967.87			
Before Primary Solid R1 3	0.25	1273.58			
Before Primary Solid R2 1	0.25	1041.31	1191.68		
Before Primary Solid R2 2	0.25	1544.48			
Before Primary Solid R2 3	0.25	989.26			
Before Primary Solid R3 1	0.25	1286.12	1158.68		
Before Primary Solid R3 2	0.25	1050.22			
Before Primary Solid R3 3	0.25	1139.69			
N2					
Sample	Volume Processed (mL)/Mass Solids Processed (1g=1mL)	Copies per extraction	Average copies per mL	Average copies per mL (Average)	Ratio
Before Primary R1 1	105	922.1446991	922.14	892.10	937.05
Before Primary R1 2	105	1013.472271	1013.47		
Before Primary R1 3	105	740.6697273	740.67		
Before Primary R2 1	105	1011.598206	1011.60	1018.10	
Before Primary R2 2	105	913.3940697	913.39		
Before Primary R2 3	105	1129.307652	1129.31		
Before Primary R3 1	105	893.9929962	893.99	900.96	
Before Primary R3 2	105	930.9671402	930.97		
Before Primary R3 3	105	877.9076576	877.91		
Before Primary Solid R1 1	0.25	930.9988022	931.00	951.27	885.93
Before Primary Solid R1 2	0.25	840.7052994	840.71		
Before Primary Solid R1 3	0.25	1082.106495	1082.11		
Before Primary Solid R2 1	0.25	743.3215618	743.32	901.37	
Before Primary Solid R2 2	0.25	1081.667614	1081.67		
Before Primary Solid R2 3	0.25	879.135704	879.14		
Before Primary Solid R3 1	0.25	757.6325417	757.63	805.15	
Before Primary Solid R3 2	0.25	961.039257	961.04		
Before Primary Solid R3 3	0.25	696.7654228	696.77		

Table B7 continued.

Bar + CD- After Primary					
N1					
Sample	Volume Processed (mL)/Mass Solids Processed (1g=1mL)	Copies per extraction	Average copies per mL	Average copies per mL (Average)	Ratio
After Primary R1 1	105	72.45	29.24	26.67	0.11
After Primary R1 2	105	0.00			
After Primary R1 3	105	15.26			
After Primary R2 1	105	38.63	34.06		
After Primary R2 2	105	31.93			
After Primary R2 3	105	31.62			
After Primary R3 1	105	0.00	16.71		
After Primary R3 2	105	33.50			
After Primary R3 3	105	16.63			
After Primary Solid R1 1	0.25	183.53	253.23	215.40	0.89
After Primary Solid R1 2	0.25	342.67			
After Primary Solid R1 3	0.25	233.50			
After Primary Solid R2 1	0.25	226.30	243.94		
After Primary Solid R2 2	0.25	239.54			
After Primary Solid R2 3	0.25	265.98			
After Primary Solid R3 1	0.25	201.94	149.03		
After Primary Solid R3 2	0.25	102.35			
After Primary Solid R3 3	0.25	142.81			
N2					
Sample	Volume Processed (mL)/Mass Solids Processed (1g=1mL)	Copies per extraction	Average copies per mL	Average copies per mL (Average)	Ratio
After Primary R1 1	105	14.49	14.56	16.07	0.08
After Primary R1 2	105	29.18			
After Primary R1 3	105	0.00			
After Primary R2 1	105	19.32	17.03		
After Primary R2 2	105	15.97			
After Primary R2 3	105	15.81			
After Primary R3 1	105	0.00	16.63		
After Primary R3 2	105	0.00			
After Primary R3 3	105	49.90			
After Primary Solid R1 1	0.25	216.91	262.65	195.38	0.92
After Primary Solid R1 2	0.25	378.76			
After Primary Solid R1 3	0.25	192.28			
After Primary Solid R2 1	0.25	226.30	200.36		
After Primary Solid R2 2	0.25	165.81			
After Primary Solid R2 3	0.25	208.96			
After Primary Solid R3 1	0.25	124.25	123.13		
After Primary Solid R3 2	0.25	102.35			
After Primary Solid R3 3	0.25	142.81			

Table B7 continued.

Bar + CD- After Secondary					
N1					
Sample	Volume Processed (mL)/Mass Solids Processed (1g=1mL)	Copies per extraction	Average copies per mL	Average copies per mL (Average)	Ratio
After Secondary R1 1	105	28.52	38.14	29.85	0.34
After Secondary R1 2	105	27.65			
After Secondary R1 3	105	58.24			
After Secondary R2 1	105	33.65	21.57		
After Secondary R2 2	105	0.00			
After Secondary R2 3	105	31.05			
After Secondary R3 1	105	12330.16	12841.99		
After Secondary R3 2	105	13290.69			
After Secondary R3 3	105	12905.12			
After Secondary Solid R1 1	0.25	14.80	75.59	57.74	0.66
After Secondary Solid R1 2	0.25	89.53			
After Secondary Solid R1 3	0.25	122.44			
After Secondary Solid R2 1	0.25	34.96	45.78		
After Secondary Solid R2 2	0.25	85.65			
After Secondary Solid R2 3	0.25	16.72			
After Secondary Solid R3 1	0.25	34.58	51.84		
After Secondary Solid R3 2	0.25	71.53			
After Secondary Solid R3 3	0.25	49.42			
N2					
Sample	Volume Processed (mL)/Mass Solids Processed (1g=1mL)	Copies per extraction	Average copies per mL	Average copies per mL (Average)	Ratio
After Secondary R1 1	105	42.78	23.97	16.87	0.21
After Secondary R1 2	105	0.00			
After Secondary R1 3	105	29.12			
After Secondary R2 1	105	33.65	26.65		
After Secondary R2 2	105	30.77			
After Secondary R2 3	105	15.52			
After Secondary R3 1	105	27244.18	27505.80		
After Secondary R3 2	105	27491.47			
After Secondary R3 3	105	27781.73			
After Secondary Solid R1 1	0.25	59.19	96.50	61.67	0.79
After Secondary Solid R1 2	0.25	125.35			
After Secondary Solid R1 3	0.25	104.95			
After Secondary Solid R2 1	0.25	87.41	54.56		
After Secondary Solid R2 2	0.25	42.82			
After Secondary Solid R2 3	0.25	33.45			
After Secondary Solid R3 1	0.25	34.58	33.96		
After Secondary Solid R3 2	0.25	17.88			
After Secondary Solid R3 3	0.25	49.42			

Table B7 continued.

Bar + CD- RAS					
N1					
Sample	Volume Processed (mL)/Mass Solids Processed (1g=1mL)	Copies per extraction	Average copies per mL	Average copies per mL (Average)	Ratio
RAS R1 1	105	1029.26	1026.21	1028.61	0.44
RAS R1 2	105	994.90			
RAS R1 3	105	1054.47			
RAS R2 1	105	971.02	1031.02		
RAS R2 2	105	1043.57			
RAS R2 3	105	1078.46			
RAS R3 1	105	834.08	982.76		
RAS R3 2	105	1076.20			
RAS R3 3	105	1037.99			
RAS Solid R1 1	0.25	1175.24	1209.99	1297.12	0.56
RAS Solid R1 2	0.25	1322.55			
RAS Solid R1 3	0.25	1132.18			
RAS Solid R2 1	0.25	1513.15	1460.85		
RAS Solid R2 2	0.25	1610.44			
RAS Solid R2 3	0.25	1258.98			
RAS Solid R3 1	0.25	1166.15	1220.50		
RAS Solid R3 2	0.25	1127.68			
RAS Solid R3 3	0.25	1367.68			
N2					
Sample	Volume Processed (mL)/Mass Solids Processed (1g=1mL)	Copies per extraction	Average copies per mL	Average copies per mL (Average)	Ratio
RAS R1 1	105	721.55	814.38	599.04	0.40
RAS R1 2	105	832.18			
RAS R1 3	105	889.40			
RAS R2 1	105	954.80	982.74		
RAS R2 2	105	998.10			
RAS R2 3	105	995.32			
RAS R3 1	105	894.86	982.49		
RAS R3 2	105	995.72			
RAS R3 3	105	1056.91			
RAS Solid R1 1	0.25	987.49	936.51	883.19	0.60
RAS Solid R1 2	0.25	923.41			
RAS Solid R1 3	0.25	898.64			
RAS Solid R2 1	0.25	1019.85	875.80		
RAS Solid R2 2	0.25	906.66			
RAS Solid R2 3	0.25	700.89			
RAS Solid R3 1	0.25	987.89	837.25		
RAS Solid R3 2	0.25	715.02			
RAS Solid R3 3	0.25	808.85			

Table B7 continued.

Bar + CD- WAS					
N1					
Sample	Volume Processed (mL)/Mass Solids Processed (1g=1mL)	Copies per extraction	Average copies per mL	Average copies per mL (Average)	Ratio
WAS R1 1	105	0.00	824.00	1496.67	0.46
WAS R1 2	105	824.00			
WAS R1 3	105	0.00			
WAS R2 1	105	2008.00	2056.00		
WAS R2 2	105	1944.00			
WAS R2 3	105	2216.00			
WAS R3 1	105	0.00	1610.00		
WAS R3 2	105	1330.00			
WAS R3 3	105	1890.00			
WAS Solid R1 1	0.25	1980.00	2410.00	1733.56	0.54
WAS Solid R1 2	0.25	2720.00			
WAS Solid R1 3	0.25	2530.00			
WAS Solid R2 1	0.25	1526.00	1452.00		
WAS Solid R2 2	0.25	1424.00			
WAS Solid R2 3	0.25	1406.00			
WAS Solid R3 1	0.25	1208.00	1338.67		
WAS Solid R3 2	0.25	1342.00			
WAS Solid R3 3	0.25	1466.00			
N2					
Sample	Volume Processed (mL)/Mass Solids Processed (1g=1mL)	Copies per extraction	Average copies per mL	Average copies per mL (Average)	Ratio
WAS R1 1	105	0.00	760.00	1324.33	0.48
WAS R1 2	105	760.00			
WAS R1 3	105	0.00			
WAS R2 1	105	1374.00	1696.00		
WAS R2 2	105	1796.00			
WAS R2 3	105	1918.00			
WAS R3 1	105	0.00	1517.00		
WAS R3 2	105	1448.00			
WAS R3 3	105	1586.00			
WAS Solid R1 1	0.25	1940.00	2136.00	1449.78	0.52
WAS Solid R1 2	0.25	2254.00			
WAS Solid R1 3	0.25	2214.00			
WAS Solid R2 1	0.25	1340.00	1235.33		
WAS Solid R2 2	0.25	1182.00			
WAS Solid R2 3	0.25	1184.00			
WAS Solid R3 1	0.25	918.00	978.00		
WAS Solid R3 2	0.25	1170.00			
WAS Solid R3 3	0.25	846.00			

Table B7 continued.

AS + UV (1)- Before Primary					
N1					
Sample	Volume Processed (mL)/Mass Solids Processed (1g=1mL)	Copies per extraction	Average copies per mL	Average copies per mL (Average)	Ratio
Before Primary R1 1	105	110.35	148.72	169.38	0.19
Before Primary R1 2	105	160.90			
Before Primary R1 3	105	174.91			
Before Primary R2 1	105	244.10	190.04		
Before Primary R2 2	105	112.22			
Before Primary R2 3	105	213.81			
Before Primary Solid R1 1	0.25	589.65	547.48	705.26	0.81
Before Primary Solid R1 2	0.25	524.62			
Before Primary Solid R1 3	0.25	528.16			
Before Primary Solid R2 1	0.25	801.86	863.04		
Before Primary Solid R2 2	0.25	795.65			
Before Primary Solid R2 3	0.25	991.63			
N2					
Sample	Volume Processed (mL)/Mass Solids Processed (1g=1mL)	Copies per extraction	Average copies per mL	Average copies per mL (Average)	Ratio
Before Primary R1 1	105	202.34	141.37	152.51	0.21
Before Primary R1 2	105	64.35			
Before Primary R1 3	105	157.42			
Before Primary R2 1	105	209.21	163.65		
Before Primary R2 2	105	144.30			
Before Primary R2 3	105	137.42			
Before Primary Solid R1 1	0.25	471.60	383.37	574.31	0.79
Before Primary Solid R1 2	0.25	291.31			
Before Primary Solid R1 3	0.25	387.20			
Before Primary Solid R2 1	0.25	733.51	765.24		
Before Primary Solid R2 2	0.25	632.68			
Before Primary Solid R2 3	0.25	929.53			

Table B7 continued.

AS + UV (1)- After Primary					
N1					
Sample	Volume Processed (mL)/Mass Solids Processed (1g=1mL)	Copies per extraction	Average copies per mL	Average copies per mL (Average)	Ratio
After Primary R1 1	105	568.08	549.22	534.14	0.40
After Primary R1 2	105	513.44			
After Primary R1 3	105	566.14			
After Primary R2 1	105	516.64	519.05		
After Primary R2 2	105	670.41			
After Primary R2 3	105	370.09			
After Primary Solid R1 1	0.25	1029.11	857.89	785.35	0.60
After Primary Solid R1 2	0.25	829.64			
After Primary Solid R1 3	0.25	714.92			
After Primary Solid R2 1	0.25	762.09	712.82		
After Primary Solid R2 2	0.25	695.23			
After Primary Solid R2 3	0.25	681.13			
N2					
Sample	Volume Processed (mL)/Mass Solids Processed (1g=1mL)	Copies per extraction	Average copies per mL	Average copies per mL (Average)	Ratio
After Primary R1 1	105	372.04	461.03	458.78	0.42
After Primary R1 2	105	444.92			
After Primary R1 3	105	566.14			
After Primary R2 1	105	442.77	456.53		
After Primary R2 2	105	539.90			
After Primary R2 3	105	386.93			
After Primary Solid R1 1	0.25	691.49	673.39	635.04	0.58
After Primary Solid R1 2	0.25	691.16			
After Primary Solid R1 3	0.25	637.52			
After Primary Solid R2 1	0.25	704.84	596.69		
After Primary Solid R2 2	0.25	526.50			
After Primary Solid R2 3	0.25	558.73			

Table B7 continued.

AS + UV (1)- After Secondary					
N1					
Sample	Volume Processed (mL)/Mass Solids Processed (1g=1mL)	Copies per extraction	Average copies per mL	Average copies per mL (Average)	Ratio
After Secondary R1 1	105	18.39	17.45	11.62	0.14
After Secondary R1 2	105	0.00			
After Secondary R1 3	105	33.96			
After Secondary R2 1	105	0.00	5.80		
After Secondary R2 2	105	0.00			
After Secondary R2 3	105	17.40			
After Secondary Solid R1 1	0.25	91.96	79.26	74.31	0.86
After Secondary Solid R1 2	0.25	112.00			
After Secondary Solid R1 3	0.25	33.83			
After Secondary Solid R2 1	0.25	73.31	69.35		
After Secondary Solid R2 2	0.25	22.54			
After Secondary Solid R2 3	0.25	112.21			
N2					
Sample	Volume Processed (mL)/Mass Solids Processed (1g=1mL)	Copies per extraction	Average copies per mL	Average copies per mL (Average)	Ratio
After Secondary R1 1	105	18.39	11.79	11.20	0.13
After Secondary R1 2	105	0.00			
After Secondary R1 3	105	16.98			
After Secondary R2 1	105	0.00	10.62		
After Secondary R2 2	105	14.45			
After Secondary R2 3	105	17.40			
After Secondary Solid R1 1	0.25	110.35	79.76	72.08	0.87
After Secondary Solid R1 2	0.25	112.00			
After Secondary Solid R1 3	0.25	16.91			
After Secondary Solid R2 1	0.25	73.31	64.40		
After Secondary Solid R2 2	0.25	45.08			
After Secondary Solid R2 3	0.25	74.80			

Table B7 continued.

AS + UV (1)- RAS					
N1					
Sample	Volume Processed (mL)/Mass Solids Processed (1g=1mL)	Copies per extraction	Average copies per mL	Average copies per mL (Average)	Ratio
RAS R1 1	105	20.05	6.68	8.70	0.08
RAS R1 2	105	0.00			
RAS R1 3	105	0.00			
RAS R2 1	105	0.00	10.71		
RAS R2 2	105	0.00			
RAS R2 3	105	32.13			
RAS Solid R1 1	0.25	134.20	119.44	105.18	0.92
RAS Solid R1 2	0.25	57.81			
RAS Solid R1 3	0.25	166.31			
RAS Solid R2 1	0.25	102.51	90.92		
RAS Solid R2 2	0.25	78.44			
RAS Solid R2 3	0.25	91.80			
N2					
Sample	Volume Processed (mL)/Mass Solids Processed (1g=1mL)	Copies per extraction	Average copies per mL	Average copies per mL (Average)	Ratio
RAS R1 1	105	20.05	6.68	3.34	0.04
RAS R1 2	105	0.00			
RAS R1 3	105	0.00			
RAS R2 1	105	0.00	0.00		
RAS R2 2	105	0.00			
RAS R2 3	105	0.00			
RAS Solid R1 1	0.25	57.50	98.28	81.79	0.96
RAS Solid R1 2	0.25	154.20			
RAS Solid R1 3	0.25	83.14			
RAS Solid R2 1	0.25	82.01	65.30		
RAS Solid R2 2	0.25	58.83			
RAS Solid R2 3	0.25	55.08			

Table B8. Estimates of correlation between SARS-CoV-2 RNA concentration in the liquid and solid samples and physicochemical parameters in coastal New England WWTPs.

		Treatment Stage	pH	Redox (mV)	EC (µs/cm)	DO (mg/L)	COD (mg/L)	TSS (mg/L)	VSS (mg/L)	TDS (mg/L)	N1-L	N1-S	N2-L	N2-S
MA	AS + CD (1)	Wastewater Influent: North System	6.89	-4.7	2593	0.23	384.8	104	12	942	1190	5590	1319.5	5193
		Wastewater Influent: South System	6.86	-2.7	2129	0.21	354.8	172.5	20	720	2220.975	14863	2091.045	14798
		After Primary Sedimentation	6.74	5.4	2593	0.16	1320	1060	630	590	363	9263.5	324	6122
		After Primary	6.93	25.7	2329	0.25	356	28	8	894	329.5	5290.5	375	5398.5
		After Secondary	6.49	18.1	2434	0.68	2224	990	570	185	91	3119	91	2991.5
		Return Activated Sludge	6.54	15.9	2512	0.13	8590	6000	4690	380	2361	4503	793	4872.5
		After Sludge Digester	7.6	-42	16.15	N.S.	24462	N.S.	N.S.	N.S.	91	2455.5	91	2352
		After Secondary Clarifier	6.58	12.5	2671	2.86	21.5	12	0	896	91	456.5	91	456.5
		After Disinfection	6.55	14.4	2486	1.27	29.2	8	0	892	91	456.5	91	456.5
		Treatment Stage	pH	Redox (mV)	EC (µs/cm)	DO (mg/L)	COD (mg/L)	TSS (mg/L)	VSS (mg/L)	TDS (mg/L)	N1-L	N1-S	N2-L	N2-S
NH-1	Bar + CD	Before Primary	6.33	21.5	1002	0.85	420	3050	2531.5	630	1069.12	4653.885	909.615	3705.29
		After Primary	7.13	-22.6	879.6	0.382	358	64	4	490	91	994.345	91	1050.61
		After Secondary	6.71	0.5	651.1	0.56	1348	1563.33	1303.33	326.66	91	456.5	91	456.5
		Return Activated Sludge	6.82	-5.3	680.5	0.21	4915	3875	3285	235	979.63	5341.695	855.775	3624.625
		After Secondary Clarifier	6.9	-9.8	678.2	4.48	25.1	16	0	306	91	456.5	91	456.5
		After Disinfection	6.98	-14.2	763.5	7.11	30.2	3	0	70	91	456.5	91	456.5
		Waste Activated Sludge	5.78	52.5	1342	0.09	N.S.	N.S.	N.S.	N.S.	1745.715	5581.335	1530	4426.665
		Treatment Stage	pH	Redox (mV)	EC (µs/cm)	DO (mg/L)	COD (mg/L)	TSS (mg/L)	VSS (mg/L)	TDS (mg/L)	N1-L	N1-S	N2-L	N2-S
NH-3	AS + UV (1)	Before Primary	7.05	-23.3	2951	3.82	540	143.33	114.664	1043.33	91	2821.045	91	2297.22
		After Primary	6.98	-19.1	1321	1.91	454	124	12	312	508.7	3141.41	436.935	2540.17
		After Secondary	6.39	13.5	1210	0.43	3780	2750	2105	460	91	456.5	91	456.5
		Return Activated Sludge	6.41	11.9	1359	0.39	12496	3500	2870	410	91	456.5	91	456.5
		After Secondary Clarifier	6.55	5.3	1283	7.37	8.92	26	0	408	91	456.5	91	456.5
		After Disinfection	6.53	5.8	1256	7.41	5.21	10	0	460	91	456.5	91	456.5
		Waste Activated Sludge	N.S.	N.S.	N.S.	N.S.	N.S.	N.S.	N.S.	N.S.	91	456.5	91	456.5

		Treatment Stage	pH	Redox (mV)	EC (ms/cm)	DO (mg/L)	COD (mg/L)	TSS (mg/L)	VSS (mg/L)	TDS (mg/L)	N1-L	N1-S	N2-L	N2-S
NH-5	AS + CD (2)	Before Primary (Before Grit)	6.21	28.5	8.36	0.2	2372	475	465	3930	91	456.5	91	456.5
		Before Primary (After Grit)	7.44	-37.2	9.08	3.3	660	220	16.66	3670	91	1786.22	91	922.33
		After Primary	8.6	-99.2	5.75	1.86	224	104	7.5	2246	91	921.72	91	456.5
		Return Activated Sludge	6.7	2	3.87	0.41	1040	505	120	1670	91	456.5	91	456.5
		After Secondary Clarifier	6.63	6.3	3.56	3.23	20.3	64	0	1516	91	456.5	91	456.5
		After Disinfection	6.63	6.3	3.54	4.89	3.6	32	0	1684	91	456.5	91	456.5
		Waste Activated Sludge	N.S.	N.S.	N.S.	N.S.	67600	N.S.	N.S.	N.S.	91	1385.76	91	928.555

		Treatment Stage	pH	Redox (mV)	EC (µs/cm)	DO (mg/L)	COD (mg/L)	TSS (mg/L)	VSS (mg/L)	TDS (mg/L)	N1-L	N1-S	N2-L	N2-S
ME	AS + CD (3)	Before Secondary	7.46	-41	567.2	7.32	127	114	74	224	91	1442.79	91	456.5
		After Secondary	6.72	-0.9	600.7	8.41	1756	1050	945	470	91	1531.345	91	456.5
		Return Activated Sludge	6.65	1.2	637.6	2.92	1225	665	645	415	91	1446.8	91	456.5
		After Secondary Clarifier	6.8	-5.1	607.5	7.83	13.1	21	0	226	91	456.5	91	456.5
		After Disinfection	6.68	1.6	624.8	6.09	2.31	12	0	65	91	456.5	91	456.5
		Waste Activated Sludge	N.S.	N.S.	N.S.	N.S.	N.S.	N.S.	N.S.	N.S.	91	456.5	91	456.5

	SARS-CoV-2 biomarkers	pH	Redox (mV)	EC (µs/cm)	DO (mg/L)	COD (mg/L)	TSS (mg/L)	VSS (mg/L)	TDS (mg/L)
Correlation	N1-L	-0.243	0.248	*0.374	*-0.427	-0.0364	*0.524	*0.507	*-0.143
	N1-S	-0.0478	0.141	*0.471	*-0.437	-0.0439	0.164	0.141	-0.113
	N2-L	-0.22	0.263	*0.344	*-0.426	-0.0835	0.248	0.24	-0.113
	N2-S	-0.0619	0.166	*0.489	-0.447	-0.0457	0.15	0.126	-0.113

*indicates statistical significance at $p<0.05$

N.S. indicates no sample was analyzed at a given sampling point.

Supplemental References

CDC (2021). "United States COVID-19 Cases, Deaths, and Laboratory Testing (NAATs) by State, Territory, and Jurisdiction."

Control, C. f. D. and Prevention (2020). "CDC 2019-novel coronavirus (2019-nCoV) real-time RT-PCR diagnostic panel."

Appendix C. Supporting Information for Chapter 4

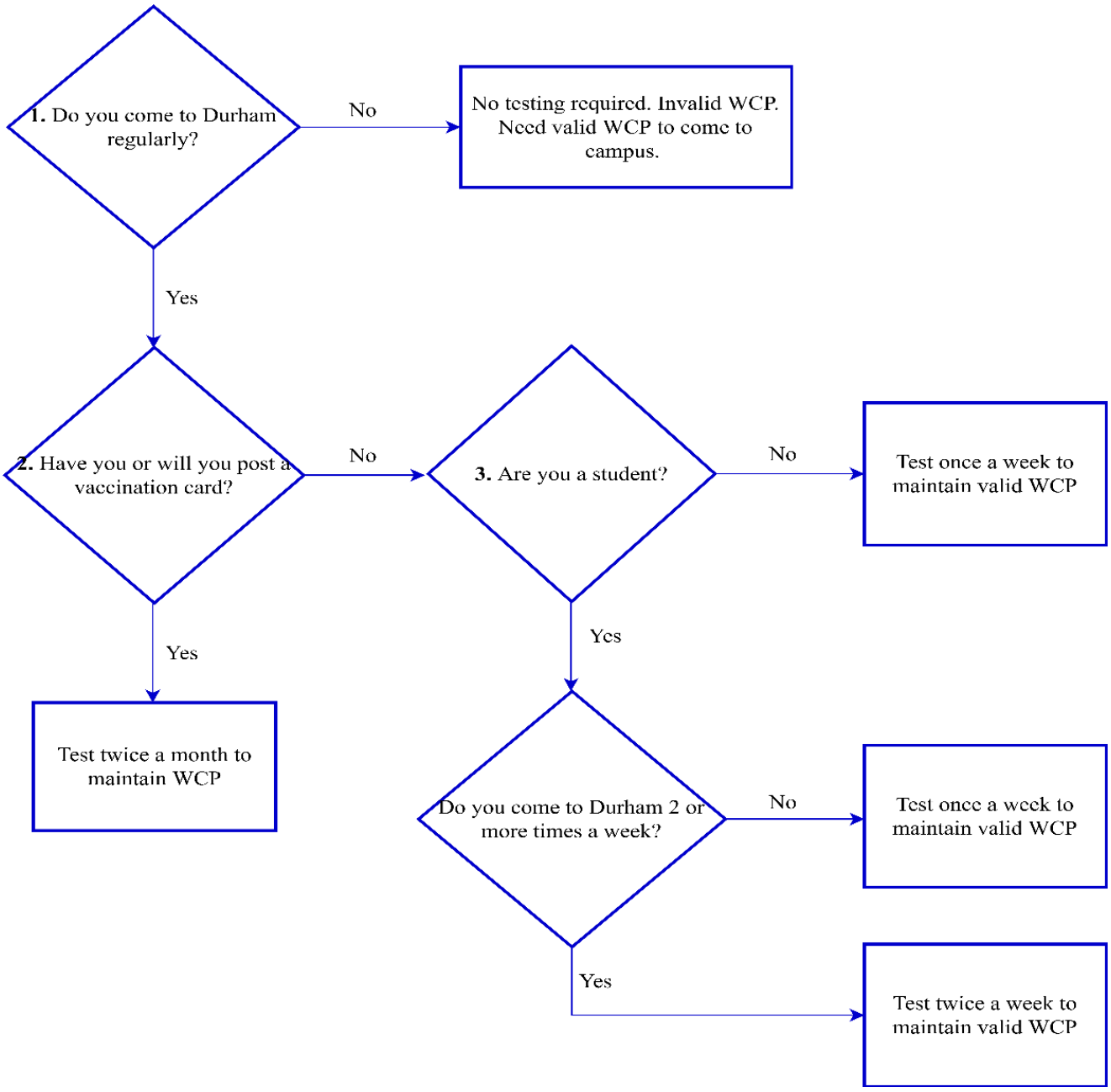

Figure C1. Student testing frequency at UNH Durham campus during Fall 2021. WCP indicates the Wildcat Pass (Adapted from UNH COVID-19 Dashboard).

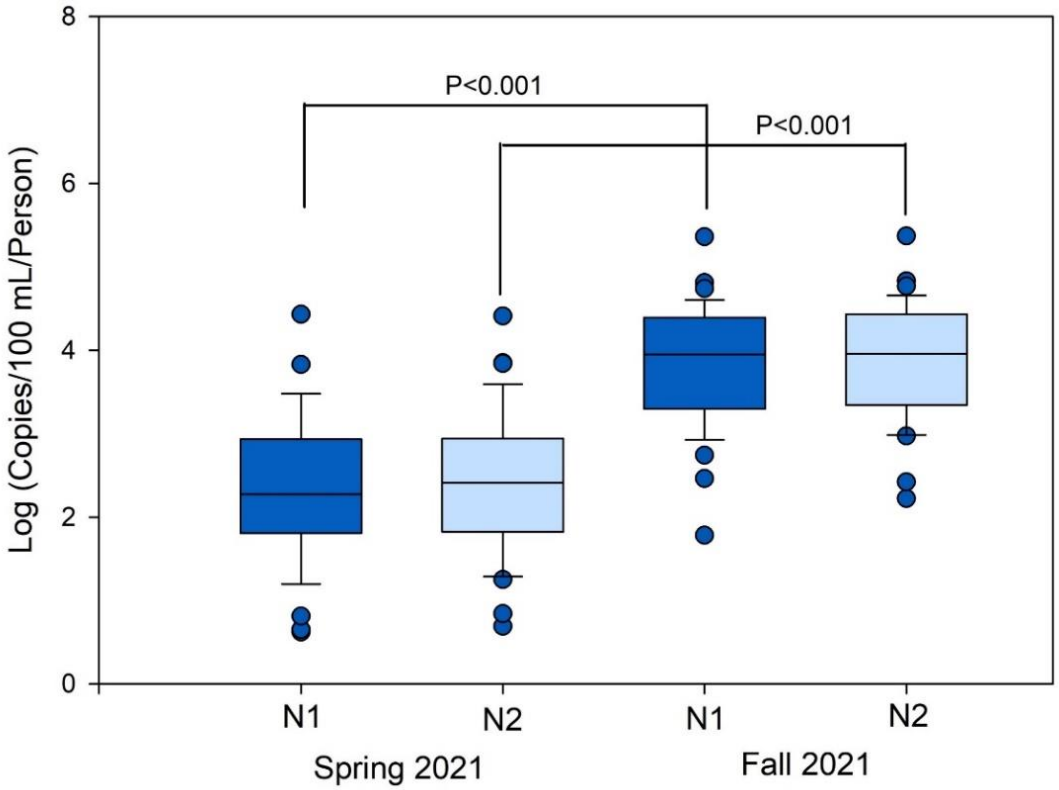

Figure C2. Average SARS-CoV-2 RNA shedding per infected individual isolating on UNH campus before, during and after mass-scale vaccination campaign.

Table C1. List of PCR primers and probes used in this study (Control and Prevention, 2020).

Primer/probe & supplier	Sequence
2019-nCoV_N1 forward primer	GAC CCC AAA ATC AGC GAA AT
2019-nCoV_N1 reverse primer	TCT GGT TAC TGC CAG TTG AAT CTG
2019-nCoV_N1 probe	FAM-ACC CCG CAT TAC GTT TGG TGG ACC-BHQ1
2019-nCoV_N2 forward primer	TTA CAA ACA TTG GCC GCA AA
2019-nCoV_N2 reverse primer	GCG CGA CAT TCC GAA GAA
2019-nCoV_N2 probe	FAM-ACA ATT TGC CCC CAG CGC TTC AG-BHQ1
RNAse P Forward Primer	AGA TTT GGA CCT GCG AGC G
RNAse P Reverse Primer	GAG CGG CTG TCT CCA CAA GT
RNAse P Probe	FAM – TTC TGA CCT GAA GGC TCT GCG CG – BHQ-1

Table C2. Data pairings for COVID-19 cases and N1 copies per 100 mL of wastewater liquids with no lag, 2-day lag, 4-day lag, 6-day lag, 8-day lag and 10-day lag of the wastewater data from Durham WWTP during Spring 2021 semester. The first data pair for the Pearson calculation in each case is highlighted. BDL indicates samples below detection limit of device.

Sample Date	COVID-19 Cases	No lag	2-day lag	4-day lag	6-day lag	8-day lag	10-day lag
		N1 (copies/100 ml)	N1 (copies/100 ml)	N1 (copies/100 ml)	N1 (copies/100 ml)	N1 (copies/100 ml)	N1 (copies/100 ml)
1/4/2021	52	421.92					
1/6/2021	58	928	421.92				
1/8/2021	57	484	928	421.92			
1/11/2021	62	264	484	928	421.92		
1/13/2021	50	1439	264	484	928	421.92	
1/15/2021	42	196	1439	264	484	928	421.92
1/19/2021	38	655	196	1439	264	484	928
1/20/2021	29	2876	655	196	1439	264	484
1/22/2021	35	452	2876	655	196	1439	264
1/25/2021	30	207	452	2876	655	196	1439
1/28/2021	34	586	207	452	2876	655	196
1/29/2021	34	397	586	207	452	2876	655
2/1/2021	49	264	397	586	207	452	2876
2/3/2021	49	526	264	397	586	207	452
2/5/2021	46	498	526	264	397	586	207
2/8/2021	78	442	498	526	264	397	586
2/10/2021	102	2495	442	498	526	264	397
2/12/2021	232	3890	2495	442	498	526	264
2/15/2021	361	3290	3890	2495	442	498	526
2/17/2021	398	3055	3290	3890	2495	442	498
2/19/2021	379	2261	3055	3290	3890	2495	442
2/22/2021	317	728	2261	3055	3290	3890	2495
2/24/2021	238	1068	728	2261	3055	3290	3890
2/26/2021	214	1446	1068	728	2261	3055	3290
3/1/2021	86	615	1446	1068	728	2261	3055
3/3/2021	81	552	615	1446	1068	728	2261
3/5/2021	93	753	552	615	1446	1068	728
3/8/2021	81	274	753	552	615	1446	1068
3/10/2021	81	2063	274	753	552	615	1446

3/12/2021	84	1569	2063	274	753	552	615
3/15/2021	75	640	1569	2063	274	753	552
3/17/2021	71	698	640	1569	2063	274	753
3/19/2021	71	1145	698	640	1569	2063	274
3/22/2021	110	191	1145	698	640	1569	2063
3/24/2021	118	574	191	1145	698	640	1569
3/26/2021	109	464	574	191	1145	698	640
3/29/2021	104	750	464	574	191	1145	698
3/31/2021	94	639	750	464	574	191	1145
4/2/2021	94	1622	639	750	464	574	191
4/5/2021	94	673	1622	639	750	464	574
4/7/2021	94	1786	673	1622	639	750	464
4/9/2021	111	1468	1786	673	1622	639	750
4/12/2021	89	482	1468	1786	673	1622	639
4/14/2021	98	539	482	1468	1786	673	1622
4/16/2021	98	BDL	539	482	1468	1786	673
4/19/2021	66	334	BDL	539	482	1468	1786
4/21/2021	60	651	334	BDL	539	482	1468
4/23/2021	43	BDL	651	334	BDL	539	482
4/26/2021	33	227	BDL	651	334	BDL	539
4/28/2021	28	297	227	BDL	651	334	BDL
4/30/2021	28	BDL	297	227	BDL	651	334
5/3/2021	28	BDL	BDL	297	227	BDL	651
5/5/2021	25	BDL	BDL	BDL	297	227	BDL
5/7/2021	24	BDL	BDL	BDL	BDL	297	227
5/10/2021	12	BDL	BDL	BDL	BDL	BDL	297
5/12/2021	11	BDL	BDL	BDL	BDL	BDL	BDL
5/16/2021	14	195	BDL	BDL	BDL	BDL	BDL
5/17/2021	14	197	195	BDL	BDL	BDL	BDL
5/19/2021	14	BDL	197	195	BDL	BDL	BDL
5/21/2021	14	1012	BDL	197	195	BDL	BDL
5/24/2021	6	345	1012	BDL	197	195	BDL
5/27/2021	5	234	345	1012	BDL	197	195
5/31/2021	5	BDL	234	345	1012	BDL	197

Table C3. Data pairings for COVID-19 cases and N2 copies per 100 mL of wastewater liquids with no lag, 2-day lag, 4-day lag, 6-day lag, 8-day lag and 10-day lag of the wastewater data from Durham WWTP during Spring 2021 semester. The first data pair for the Pearson calculation in each case is highlighted. BDL indicates samples below detection limit of device.

Sample Date	COVID-19 Cases	No lag	2-day lag	4-day lag	6-day lag	8-day lag	10-day lag
		N2 (copies/100 ml)	N2 (copies/100 ml)	N2 (copies/100 ml)	N2 (copies/100 ml)	N2 (copies/100 ml)	N2 (copies/100 ml)
1/4/2021	52	192.05					
1/6/2021	58	789	192.05				
1/8/2021	57	590	789	192.05			
1/11/2021	62	344	590	789	192.05		
1/13/2021	50	1350	344	590	789	192.05	
1/15/2021	42	240	1350	344	590	789	192.05
1/19/2021	38	657	240	1350	344	590	789
1/20/2021	29	1390	657	240	1350	344	590
1/22/2021	35	357	1390	657	240	1350	344
1/25/2021	30	BDL	357	1390	657	240	1350
1/28/2021	34	548	BDL	357	1390	657	240
1/29/2021	34	371	548	BDL	357	1390	657
2/1/2021	49	204	371	548	BDL	357	1390
2/3/2021	49	455	204	371	548	BDL	357
2/5/2021	46	451	455	204	371	548	BDL
2/8/2021	78	505	451	455	204	371	548
2/10/2021	102	2571	505	451	455	204	371
2/12/2021	232	3523	2571	505	451	455	204
2/15/2021	361	2948	3523	2571	505	451	455
2/17/2021	398	2855	2948	3523	2571	505	451
2/19/2021	379	2319	2855	2948	3523	2571	505
2/22/2021	317	702	2319	2855	2948	3523	2571
2/24/2021	238	972	702	2319	2855	2948	3523
2/26/2021	214	1498	972	702	2319	2855	2948
3/1/2021	86	584	1498	972	702	2319	2855
3/3/2021	81	523	584	1498	972	702	2319
3/5/2021	93	813	523	584	1498	972	702
3/8/2021	81	238	813	523	584	1498	972
3/10/2021	81	1924	238	813	523	584	1498

3/12/2021	84	1630	1924	238	813	523	584
3/15/2021	75	578	1630	1924	238	813	523
3/17/2021	71	676	578	1630	1924	238	813
3/19/2021	71	1161	676	578	1630	1924	238
3/22/2021	110	210	1161	676	578	1630	1924
3/24/2021	118	660	210	1161	676	578	1630
3/26/2021	109	445	660	210	1161	676	578
3/29/2021	104	606	445	660	210	1161	676
3/31/2021	94	597	606	445	660	210	1161
4/2/2021	94	1721	597	606	445	660	210
4/5/2021	94	676	1721	597	606	445	660
4/7/2021	94	1671	676	1721	597	606	445
4/9/2021	111	1347	1671	676	1721	597	606
4/12/2021	89	416	1347	1671	676	1721	597
4/14/2021	98	444	416	1347	1671	676	1721
4/16/2021	98	BDL	444	416	1347	1671	676
4/19/2021	66	330	BDL	444	416	1347	1671
4/21/2021	60	511	330	BDL	444	416	1347
4/23/2021	43	BDL	511	330	BDL	444	416
4/26/2021	33	245	BDL	511	330	BDL	444
4/28/2021	28	296	245	BDL	511	330	BDL
4/30/2021	28	BDL	296	245	BDL	511	330
5/3/2021	28	BDL	BDL	296	245	BDL	511
5/5/2021	25	BDL	BDL	BDL	296	245	BDL
5/7/2021	24	BDL	BDL	BDL	BDL	296	245
5/10/2021	12	BDL	BDL	BDL	BDL	BDL	296
5/12/2021	11	BDL	BDL	BDL	BDL	BDL	BDL
5/16/2021	14	BDL	BDL	BDL	BDL	BDL	BDL
5/17/2021	14	BDL	BDL	BDL	BDL	BDL	BDL
5/19/2021	14	BDL	BDL	BDL	BDL	BDL	BDL
5/21/2021	14	662	BDL	BDL	BDL	BDL	BDL
5/24/2021	6	BDL	662	BDL	BDL	BDL	BDL
5/27/2021	5	175	BDL	662	BDL	BDL	BDL
5/31/2021	5	BDL	175	BDL	662	BDL	BDL

Table C4. Data pairings for COVID-19 cases and N1 copies per 100 mL of wastewater liquids with no lag, 2-day lag, 4-day lag, 6-day lag, 8-day lag and 10-day lag of the wastewater data from UNH Central campus during Spring 2021 semester. The first data pair for the Pearson calculation in each case is highlighted. BDL indicates samples below detection limit of device.

Sample Date	COVID-19 Cases	No lag	2-day lag	4-day lag	6-day lag	8-day lag	10-day lag
		N1 (copies/100 ml)	N1 (copies/100 ml)	N1 (copies/100 ml)	N1 (copies/100 ml)	N1 (copies/100 ml)	N1 (copies/100 ml)
1/24/2021	6	BDL					
1/28/2021	6	BDL	BDL				
1/31/2021	5	BDL	BDL	BDL			
2/4/2021	9	BDL	BDL	BDL	BDL		
2/7/2021	12	1227	BDL	BDL	BDL	BDL	
2/9/2021	26	537	1227	BDL	BDL	BDL	BDL
2/11/2021	43	1146	537	1227	BDL	BDL	BDL
2/14/2021	55	722	1146	537	1227	BDL	BDL
2/16/2021	54	527	722	1146	537	1227	BDL
2/18/2021	43	1998	527	722	1146	537	1227
2/21/2021	34	446	1998	527	722	1146	537
2/23/2021	24	941	446	1998	527	722	1146
2/25/2021	17	248	941	446	1998	527	722
2/28/2021	10	817	248	941	446	1998	527
3/2/2021	11	BDL	817	248	941	446	1998
3/4/2021	11	504	BDL	817	248	941	446
3/7/2021	13	BDL	504	BDL	817	248	941
3/9/2021	11	251	BDL	504	BDL	817	248
3/11/2021	10	307	251	BDL	504	BDL	817
3/14/2021	11	BDL	307	251	BDL	504	BDL
3/16/2021	12	BDL	BDL	307	251	BDL	504
3/18/2021	16	706	BDL	BDL	307	251	BDL
3/21/2021	17	BDL	706	BDL	BDL	307	251
3/23/2021	18	BDL	BDL	706	BDL	BDL	307

3/25/2021	15	895	BDL	BDL	706	BDL	BDL
3/28/2021	15	BDL	895	BDL	BDL	706	BDL
3/30/2021	14	BDL	BDL	895	BDL	BDL	706
4/1/2021	15	381	BDL	BDL	895	BDL	BDL
4/4/2021	13	BDL	381	BDL	BDL	895	BDL
4/6/2021	14	2989	BDL	381	BDL	BDL	895
4/8/2021	15	604	2989	BDL	381	BDL	BDL
4/11/2021	15	2460	604	2989	BDL	381	BDL
4/13/2021	13	BDL	2460	604	2989	BDL	381
4/15/2021	10	229	BDL	2460	604	2989	BDL
4/18/2021	8	BDL	229	BDL	2460	604	2989
4/20/2021	7	900	BDL	229	BDL	2460	604
4/22/2021	6	BDL	900	BDL	229	BDL	2460
4/25/2021	5	331	BDL	900	BDL	229	BDL
4/27/2021	4	BDL	331	BDL	900	BDL	229
4/29/2021	5	BDL	BDL	331	BDL	900	BDL
5/2/2021	4	BDL	BDL	BDL	331	BDL	900
5/4/2021	4	BDL	BDL	BDL	BDL	331	BDL
5/6/2021	2	BDL	BDL	BDL	BDL	BDL	331
5/9/2021	1	BDL	BDL	BDL	BDL	BDL	BDL
5/11/2021	1	BDL	BDL	BDL	BDL	BDL	BDL
5/13/2021	2	BDL	BDL	BDL	BDL	BDL	BDL
5/16/2021	3	BDL	BDL	BDL	BDL	BDL	BDL
5/18/2021	2	BDL	BDL	BDL	BDL	BDL	BDL
5/20/2021	1	BDL	BDL	BDL	BDL	BDL	BDL
5/24/2021	1	BDL	BDL	BDL	BDL	BDL	BDL
5/27/2021	1	BDL	BDL	BDL	BDL	BDL	BDL

Table C5. Data pairings for COVID-19 cases and N2 copies per 100 mL of wastewater liquids with no lag, 2-day lag, 4-day lag, 6-day lag, 8-day lag and 10-day lag of the wastewater data from UNH Central campus during Spring 2021 semester. The first data pair for the Pearson calculation in each case is highlighted. BDL indicates samples below detection limit of device.

Sample Date	COVID-19 Cases	No lag	2-day lag	4-day lag	6-day lag	8-day lag	10-day lag
		N2 (copies/100 ml)	N2 (copies/100 ml)	N2 (copies/100 ml)	N2 (copies/100 ml)	N2 (copies/100 ml)	N2 (copies/100 ml)
1/24/2021	6	BDL					
1/28/2021	6	BDL	BDL				
1/31/2021	5	BDL	BDL	BDL			
2/4/2021	9	BDL	BDL	BDL	BDL		
2/7/2021	12	927	BDL	BDL	BDL	BDL	
2/9/2021	26	498	927	BDL	BDL	BDL	BDL
2/11/2021	43	820	498	927	BDL	BDL	BDL
2/14/2021	55	418	820	498	927	BDL	BDL
2/16/2021	54	349	418	820	498	927	BDL
2/18/2021	43	1757	349	418	820	498	927
2/21/2021	34	412	1757	349	418	820	498
2/23/2021	24	784	412	1757	349	418	820
2/25/2021	17	BDL	784	412	1757	349	418
2/28/2021	10	789	BDL	784	412	1757	349
3/2/2021	11	BDL	789	BDL	784	412	1757
3/4/2021	11	459	BDL	789	BDL	784	412
3/7/2021	13	BDL	459	BDL	789	BDL	784
3/9/2021	11	241	BDL	459	BDL	789	BDL
3/11/2021	10	269	241	BDL	459	BDL	789
3/14/2021	11	BDL	269	241	BDL	459	BDL
3/16/2021	12	BDL	BDL	269	241	BDL	459
3/18/2021	16	549	BDL	BDL	269	241	BDL
3/21/2021	17	BDL	549	BDL	BDL	269	241

3/23/2021	18	BDL	BDL	549	BDL	BDL	269
3/25/2021	15	1034	BDL	BDL	549	BDL	BDL
3/28/2021	15	BDL	1034	BDL	BDL	549	BDL
3/30/2021	14	BDL	BDL	1034	BDL	BDL	549
4/1/2021	15	BDL	BDL	BDL	1034	BDL	BDL
4/4/2021	13	BDL	BDL	BDL	BDL	1034	BDL
4/6/2021	14	2657	BDL	BDL	BDL	BDL	1034
4/8/2021	15	358	2657	BDL	BDL	BDL	BDL
4/11/2021	15	2579	358	2657	BDL	BDL	BDL
4/13/2021	13	BDL	2579	358	2657	BDL	BDL
4/15/2021	10	BDL	BDL	2579	358	2657	BDL
4/18/2021	8	BDL	BDL	BDL	2579	358	2657
4/20/2021	7	791	BDL	BDL	BDL	2579	358
4/22/2021	6	BDL	791	BDL	BDL	BDL	2579
4/25/2021	5	269	BDL	791	BDL	BDL	BDL
4/27/2021	4	BDL	269	BDL	791	BDL	BDL
4/29/2021	5	BDL	BDL	269	BDL	791	BDL
5/2/2021	4	BDL	BDL	BDL	269	BDL	791
5/4/2021	4	BDL	BDL	BDL	BDL	269	BDL
5/6/2021	2	BDL	BDL	BDL	BDL	BDL	269
5/9/2021	1	BDL	BDL	BDL	BDL	BDL	BDL
5/11/2021	1	BDL	BDL	BDL	BDL	BDL	BDL
5/13/2021	2	BDL	BDL	BDL	BDL	BDL	BDL
5/16/2021	3	BDL	BDL	BDL	BDL	BDL	BDL
5/18/2021	2	BDL	BDL	BDL	BDL	BDL	BDL
5/20/2021	1	BDL	BDL	BDL	BDL	BDL	BDL
5/24/2021	1	BDL	BDL	BDL	BDL	BDL	BDL
5/27/2021	1	BDL	BDL	BDL	BDL	BDL	BDL

Table C6. Data pairings for COVID-19 cases and N1 and N2 copies per 100 mL of wastewater liquids with no lag of the wastewater data from Durham WWTP during Summer 2021 semester. BDL indicates samples below detection limit of device.

Sample Date	COVID-19 Cases	No lag N1 (copies/100 ml)		Sample Date	COVID-19 Cases	No lag N2 (copies/100 ml)
6/2/2021	5	BDL		6/2/2021	5	BDL
6/6/2021	1	BDL		6/6/2021	1	BDL
6/9/2021	1	BDL		6/9/2021	1	BDL
6/13/2021	1	BDL		6/13/2021	1	BDL
6/16/2021	1	BDL		6/16/2021	1	BDL
6/20/2021	1	BDL		6/20/2021	1	BDL
6/23/2021	1	BDL		6/23/2021	1	BDL
6/27/2021	1	BDL		6/27/2021	1	BDL
6/30/2021	1	BDL		6/30/2021	1	BDL
7/5/2021	1	BDL		7/5/2021	1	BDL
7/7/2021	1	BDL		7/7/2021	1	BDL
7/11/2021	1	BDL		7/11/2021	1	BDL
7/14/2021	1	BDL		7/14/2021	1	BDL
7/18/2021	1	BDL		7/18/2021	1	BDL
7/21/2021	1	BDL		7/21/2021	1	BDL
7/25/2021	1	383		7/25/2021	1	314
7/28/2021	5	BDL		7/28/2021	5	BDL
8/1/2021	5	BDL		8/1/2021	5	BDL
8/4/2021	9	292		8/4/2021	9	226
8/8/2021	8	BDL		8/8/2021	8	BDL
8/11/2021	9	BDL		8/11/2021	9	BDL
8/15/2021	7	BDL		8/15/2021	7	BDL
8/18/2021	7	BDL		8/18/2021	7	BDL
8/22/2021	10	BDL		8/22/2021	10	BDL
8/25/2021	14	196		8/25/2021	14	333

Table C7. Data pairings for COVID-19 cases and N1 and N2 copies per 100 mL of wastewater liquids with no lag of the wastewater data from UNH Central campus during Summer 2021 semester. BDL indicates samples below detection limit of device.

Sample Date	COVID-19 Cases	No lag		Sample Date	COVID-19 Cases	No lag
		N1 (copies/100 ml)				N2 (copies/100 ml)
6/1/2021	0	BDL		6/1/2021	0	BDL
6/3/2021	0	BDL		6/3/2021	0	BDL
6/7/2021	0	209		6/7/2021	0	BDL
6/10/2021	0	BDL		6/10/2021	0	BDL
6/14/2021	0	BDL		6/14/2021	0	BDL
6/17/2021	0	BDL		6/17/2021	0	BDL
6/21/2021	0	BDL		6/21/2021	0	BDL
6/24/2021	0	BDL		6/24/2021	0	BDL
6/28/2021	0	BDL		6/28/2021	0	BDL
7/1/2021	0	BDL		7/1/2021	0	BDL
7/6/2021	0	BDL		7/6/2021	0	BDL
7/8/2021	0	BDL		7/8/2021	0	BDL
7/12/2021	0	BDL		7/12/2021	0	BDL
7/15/2021	0	BDL		7/15/2021	0	BDL
7/19/2021	0	BDL		7/19/2021	0	BDL
7/22/2021	0	243		7/22/2021	0	145
7/26/2021	0	BDL		7/26/2021	0	BDL
7/29/2021	0	BDL		7/29/2021	0	BDL
8/2/2021	1	BDL		8/2/2021	1	BDL
8/5/2021	0	236		8/5/2021	0	BDL
8/9/2021	0	678		8/9/2021	0	787
8/12/2021	1	BDL		8/12/2021	1	BDL
8/16/2021	1	BDL		8/16/2021	1	BDL
8/19/2021	0	BDL		8/19/2021	0	BDL
8/23/2021	1	BDL		8/23/2021	1	BDL

Table C8. Data pairings for COVID-19 cases and N1 and N2 copies per 100 mL of wastewater liquids with no lag of the wastewater data from Durham WWTP during Fall 2021 semester. BDL indicates samples below detection limit of device.

Sample Date	COVID-19 Cases	No lag N1 (copies/100 ml)		Sample Date	COVID-19 Cases	No lag N2 (copies/100 ml)
8/30/2021	1	291.59		8/30/2021	1	451.01
9/2/2021	2	727		9/2/2021	2	690
9/7/2021	3	BDL		9/7/2021	3	BDL
9/9/2021	4	551		9/9/2021	4	517
9/13/2021	5	347.68		9/13/2021	5	227.69
9/16/2021	6	484		9/16/2021	6	BDL
9/21/2021	7	1977.7		9/21/2021	7	1655.42
9/23/2021	8	521.42		9/23/2021	8	579.3
9/28/2021	9	298.6		9/28/2021	9	405.38
9/30/2021	10	1387.66		9/30/2021	10	1488.7
10/4/2021	11	673		10/4/2021	11	495
10/7/2021	12	326.98		10/7/2021	12	377.24
10/14/2021	13	542		10/14/2021	13	389
10/18/2021	14	516		10/18/2021	14	450
10/21/2021	15	569		10/21/2021	15	528
10/25/2021	16	489		10/25/2021	16	507
10/29/2021	17	362		10/29/2021	17	312
11/1/2021	18	2032		11/1/2021	18	1889
11/5/2021	19	5659.56		11/5/2021	19	5592.59
11/8/2021	20	1364		11/8/2021	20	1367
11/11/2021	21	1313.6		11/11/2021	21	1520.83
11/15/2021	22	789		11/15/2021	22	883
11/18/2021	23	431		11/18/2021	23	476
11/22/2021	24	288		11/22/2021	24	359
11/29/2021	25	317		11/29/2021	25	402
12/2/2021	26	2708.44		12/2/2021	26	2588.95
12/6/2021	27	677		12/6/2021	27	799
12/9/2021	28	3207.29		12/9/2021	28	3162.52

Table C9. Data pairings for COVID-19 cases and N1 and N2 copies per 100 mL of wastewater solids with no lag of the wastewater data from Durham WWTP during Fall 2021 semester. BDL indicates samples below detection limit of device.

Sample Date	COVID-19 Cases	No lag		Sample Date	COVID-19 Cases	No lag
		N1 (copies/g)				N2 (copies/g)
8/30/2021	1	3659.4		8/30/2021	1	2919.15
9/2/2021	2	1189.9		9/2/2021	2	922.3
9/7/2021	3	998.9		9/7/2021	3	1139.22
9/9/2021	4	935.13		9/9/2021	4	1384.83
9/13/2021	5	919.68		9/13/2021	5	1319.55
9/16/2021	6	4634.2		9/16/2021	6	2772.74
9/21/2021	7	4579.38		9/21/2021	7	1302.37
9/23/2021	8	1160.49		9/23/2021	8	980.33
9/28/2021	9	930.61		9/28/2021	9	919.58
9/30/2021	10	927.69		9/30/2021	10	964.76
10/4/2021	11	1344.53		10/4/2021	11	1520.48
10/7/2021	12	1392.53		10/7/2021	12	1168.16
10/14/2021	13	BDL		10/14/2021	13	BDL
10/18/2021	14	1066.04		10/18/2021	14	944.49
10/21/2021	15	BDL		10/21/2021	15	BDL
10/25/2021	16	BDL		10/25/2021	16	BDL
10/29/2021	17	1115.94		10/29/2021	17	1075.89
11/1/2021	18	1393.57		11/1/2021	18	1057.07
11/5/2021	19	2787.17		11/5/2021	19	1162.41
11/8/2021	20	1008.97		11/8/2021	20	1061.77
11/11/2021	21	3495.76		11/11/2021	21	2709.1
11/15/2021	22	8430.04		11/15/2021	22	7566.18
11/18/2021	23	1629.41		11/18/2021	23	682.91
11/22/2021	24	1884.67		11/22/2021	24	1390.62
11/29/2021	25	7104.83		11/29/2021	25	6482.05
12/2/2021	26	12724.93		12/2/2021	26	13416.76
12/6/2021	27	1356.85		12/6/2021	27	1062.38

12/9/2021	28	8437.04		12/9/2021	28	4532.54

Table C10. Data pairings for COVID-19 cases and N1 and N2 copies per 100 mL of wastewater liquids with no lag of the wastewater data from UNH Central campus during Fall 2021 semester. BDL indicates samples below detection limit of device.

Sample Date	COVID-19 Cases	No lag		Sample Date	COVID-19 Cases	No lag
		N1 (copies/100 ml)				N2 (copies/100 ml)
8/31/2021	5	1458		8/31/2021	5	1418
9/2/2021	5	1159		9/2/2021	5	1413
9/7/2021	5	5172		9/7/2021	5	5488
9/9/2021	16	4334		9/9/2021	16	4200
9/12/2021	20	3223.27		9/12/2021	20	3421.08
9/14/2021	25	2176.69		9/14/2021	25	2512.97
9/16/2021	17	9573.79		9/16/2021	17	8738.09
9/19/2021	15	4426.56		9/19/2021	15	7497.90
9/21/2021	11	1779.80		9/21/2021	11	2417.28
9/26/2021	7	558.79		9/26/2021	7	502.44
9/30/2021	6	1335.74		9/30/2021	6	2335
10/3/2021	6	973.17		10/3/2021	6	1255
10/5/2021	7	293		10/5/2021	7	437
10/12/2021	6	3243		10/12/2021	6	3326
10/14/2021	6	195		10/14/2021	6	BDL
10/17/2021	6	BDL		10/17/2021	6	BDL
10/21/2021	5	5413.77		10/21/2021	5	5269.50
10/24/2021	6	2116.42		10/24/2021	6	2263.72
10/28/2021	5	2749		10/28/2021	5	2687
11/1/2021	4	8550.98		11/1/2021	4	8806.99
11/4/2021	13	19736.83		11/4/2021	13	19974.20
11/7/2021	17	1147.38		11/7/2021	17	1133.85
11/9/2021	17	3115		11/9/2021	17	2946

11/11/2021	12	9276.91		11/11/2021	12	9859.77
11/16/2021	7	1635		11/16/2021	7	1562
11/18/2021	7	2957		11/18/2021	7	3114
11/21/2021	8	3089.45		11/21/2021	8	3246.22
11/30/2021	4	4060		11/30/2021	4	3933
12/2/2021	9	2764.13		12/2/2021	9	2939.76
12/5/2021	11	739.63		12/5/2021	11	749.32
12/9/2021	11	2050.43		12/9/2021	11	1949.36

Supplemental References

Control, C.F.D., and Prevention (2020). CDC 2019-novel coronavirus (2019-nCoV) real-time RT-PCR diagnostic panel.

Dashboard, U.C.-L.T. UNH. Available: https://www.unh.edu/coronavirus/dashboard [Accessed].